CEWQO'17

24th Central European Workshop on Quantum Optics

26-30 June, 2017

at the Technical University of Denmark, Lyngby

DTU

Dear Attendees,

It is our great pleasure to welcome you to CEWQO'2017, the 24th Central European Workshop on Quantum Optics and the first time in Denmark. We are indeed very happy to see you all here at DTU.

Quantum technology is booming these years. The EU has decided to launch a new flagship program within the field and we see a growing number of scientific groups embarking on this exciting field of study. The industry is also showing an increasing interest in quantum technology. We have therefore decided to have a slightly stronger emphasis in this direction for this year's version of CEWQO, in particular with the organization of a dedicated session on commercializing quantum technology.

This conference is the result of many people's efforts, and we would like to thank them all. All members of the advisory board have provided us with invaluable guidance and we owe them our greatest gratitude. In particular, we would like to thank Prof. Gunnar Björk from KTH for numerous and extremely detailed advices and Prof. Luis Sanchez-Soto from University of Madrid for his strong support in getting CEWQO to DTU. The work of the program committee in reviewing the very high number of high-quality contributed submissions has also been indispensable. We would like to thank them for this important work.

Finally, we would like to thank the staff and students of the Quantum Physics and Information Technology (QPIT) section at the Department of Physics, DTU. Their contributions were simply essential for making this event successful.

We hope you will all enjoy the workshop!

Sincerely,

The organizing committee for CEWQO'2017

Advisory board

Konrad Banaszek
Gunnar Björk
Nicolas Cerf
Aurelian Isar
Natalia Korolkova
Margarita Man'ko
Ninni Messina
Luis Sanchez-Soto

Program committee

Antonio Acín (Barcelona, Spain)
Jonatan Bohr Brask (Genéve, Switzerland)
Jaromír Fiurášek (Olomouc, Czech Republic)
Barry Garraway (Sussex, UK)
Ilja Gerhardt (Stuttgart, Germany)
Frédéric Grosshans (Paris, France)
Kasper Jensen (Copenhagen, Denmark)
Anthony Leverrier (Paris, France)
Paulina Marian (Bucharest, Romania)
Dmitry Mogilevtsev (Minsk, Belarus)
Jonas Neergaard-Nielsen - Chair (DTU)
Elke Neu (Saarbrücken, Germany)
Tracy E. Northup (Innsbruck, Austria)
Matteo G. A. Paris (Milan, Italy)
Ana Predojević (Ulm, Germany)
Friedemann Reinhard (Munich, Germany)
Magdalena Stobińska (Warsaw, Poland)
Michael Vanner (Oxford, UK)
Denis Vasilyev (Innsbruck, Austria)
Patrick Windpassinger (Mainz, Germany)
Alessandro Zavatta (Florence, Italy)

Local organizers

Ulrik Lund Andersen
Tobias Gehring
Alexander Huck
Tine Hougaard Klitmøller
Jonas S. Neergaard-Nielsen

Practical information

The **emergency** number in Denmark is 112. Defibrillators can be found in the neighbouring buildings 301 and 306.

Smoking is not allowed inside all buildings at DTU.

Toilets are in the basement of building 303, access through the stairs at the east side.

For **WiFi** you can use the eduroam network or the personal login handed out at the registration.

The **wardrobe** is on your own responsibility. Please don't leave any personal items lying around since this is a public institution with open access.

Lunch will be served every day in the DTU canteen in the main building 101. The canteen is within 5 min walking distance from the conference, please see the DTU map for details.

You can get in touch with the **industry exhibitors** all Tuesday and Wednesday.

A **conference group picture** with all participants will be taken on Thursday before lunch.

You can find an online version of the program as well as a download of the full length version of this leaflet, containing all abstracts, at the conference website *https://cewqo2017.dk*.

Announcements during the conference will primarily be given via the official Twitter account, *https://twitter.com/cewqo2017*.

You can access a conference **live-stream** at *http://www.ustream.tv/channel/dtu-auditorie-42*.

Getting **from Copenhagen to DTU (and back)**: Take the train to Lyngby St. from any of the stations in central Copenhagen and switch to bus from there. Alternatively, catch the highway buses 150S or 15E to/from Nørreport St. and get on/off at the "Rævehøjvej (DTU)" stop. From there it's a 5-10 minutes walk to the conference venue.

Getting **from Lyngby Station to DTU**: Take bus 180, 190 (parked just on the right when exiting the station's north exit) or 300S (towards Holte St, parked just on the left when exiting) and get off at the stop named "DTU" (sometimes "DTU, Anker Engelunds Vej)".

Getting **from DTU to Lyngby**: Take bus 181 or 300S (towards Ishøj St) from the bus stop across the street from the conference venue or bus 190 from the bus stop on the same side as the venue. 30E from the opposite side is also an option, but this line does not stop at Lyngby Station, so you would have to get off at Lyngby Storcenter and walk to the station.

Please study the maps below or consult *https://www.rejseplanen.dk* for planning your public transport.

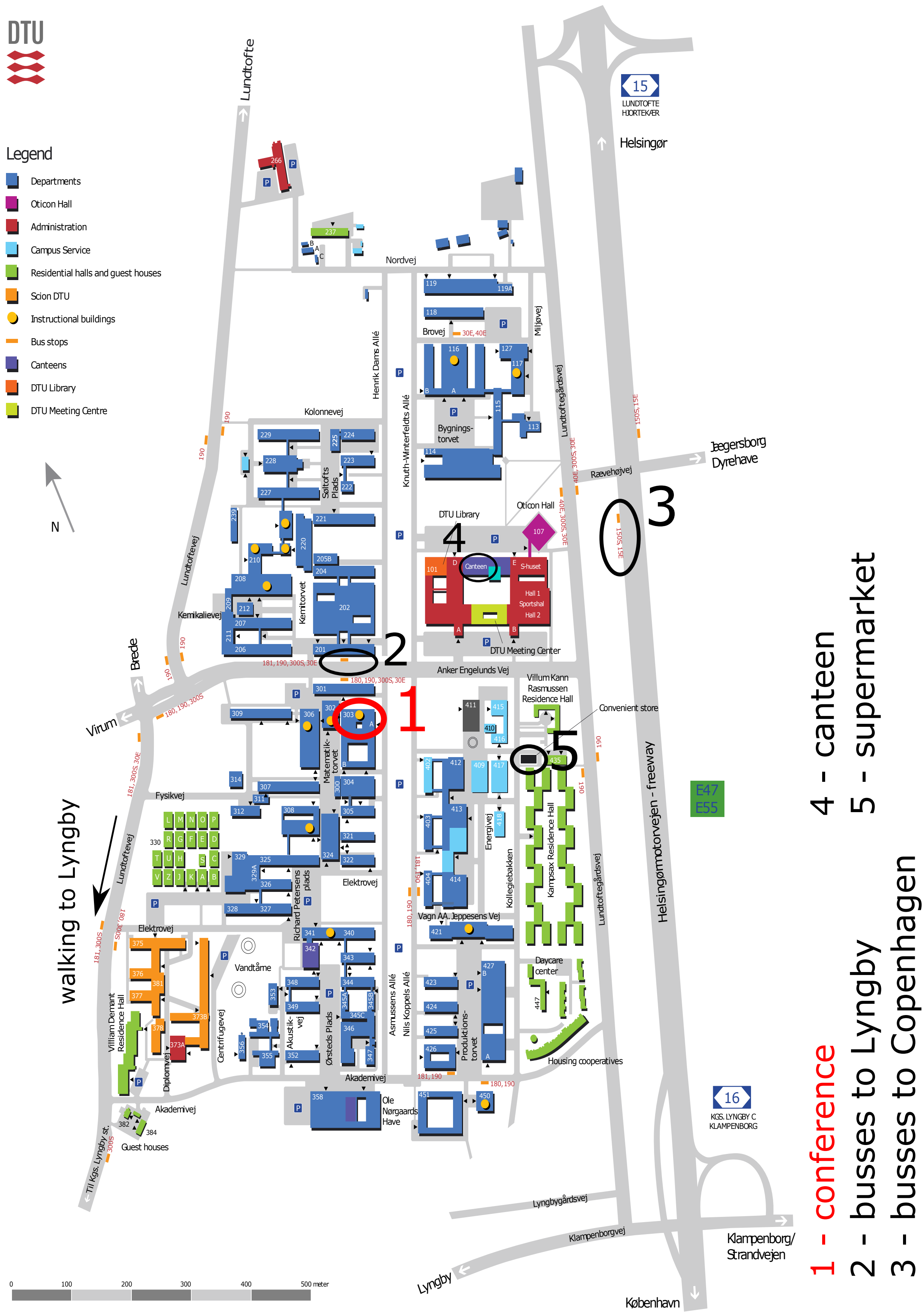
DTU
Legend
Departments
Oticon Hall
Administration
Campus Service
Residential halls and guest houses
Scion DTU
Instructional buildings
Bus stops
Canteens
DTU Library
DTU Meeting Centre
N
Lundtofte
Helsingør
15
LUNDTOFTE
HJORTEKÆR
Nordvej
Brovej
Miljøvej
Henrik Dams Allé
Knuth-Winterfeldts Allé
Bygnings-torvet
Lundtoftegårdsvej
Kolonnevej
Jægersborg Dyrehave
Rævehøjvej
DTU Library
Oticon Hall
Canteen
S-huset
Hall 1
Sportshal
Hall 2
DTU Meeting Center
Anker Engelunds Vej
Kemitorvet
Kemikalievej
Lundtoftevej
Brede
Virum
Villum Kann Rasmussen Residence Hall
Convenient store
Matematiktorvet
Fysikvej
Elektrovej
Energivej
Kollegiebakken
Kampsax Residence Hall
Helsingørmotorvejen - freeway
E47
E55
Vagn Aa. Jeppesens Vej
Richard Petersens plads
Vandtårne
Akustikvej
Ørsteds Plads
Asmussens Allé
Nils Koppels Allé
Produktionstorvet
Daycare center
Housing cooperatives
Centrifugevej
Diplomvej
Villiam Demant Residence Hall
Akademivej
Ole Nørgaards Have
Guest houses
Til Kgs. Lyngby st.
walking to Lyngby
16
KGS. LYNGBY C
KLAMPENBORG
Lyngbygårdsvej
Klampenborgvej
Klampenborg/ Strandvejen
Lyngby
København
0
100
200
300
400
500 meter
1 - conference
2 - busses to Lyngby
3 - busses to Copenhagen
4 - canteen
5 - supermarket

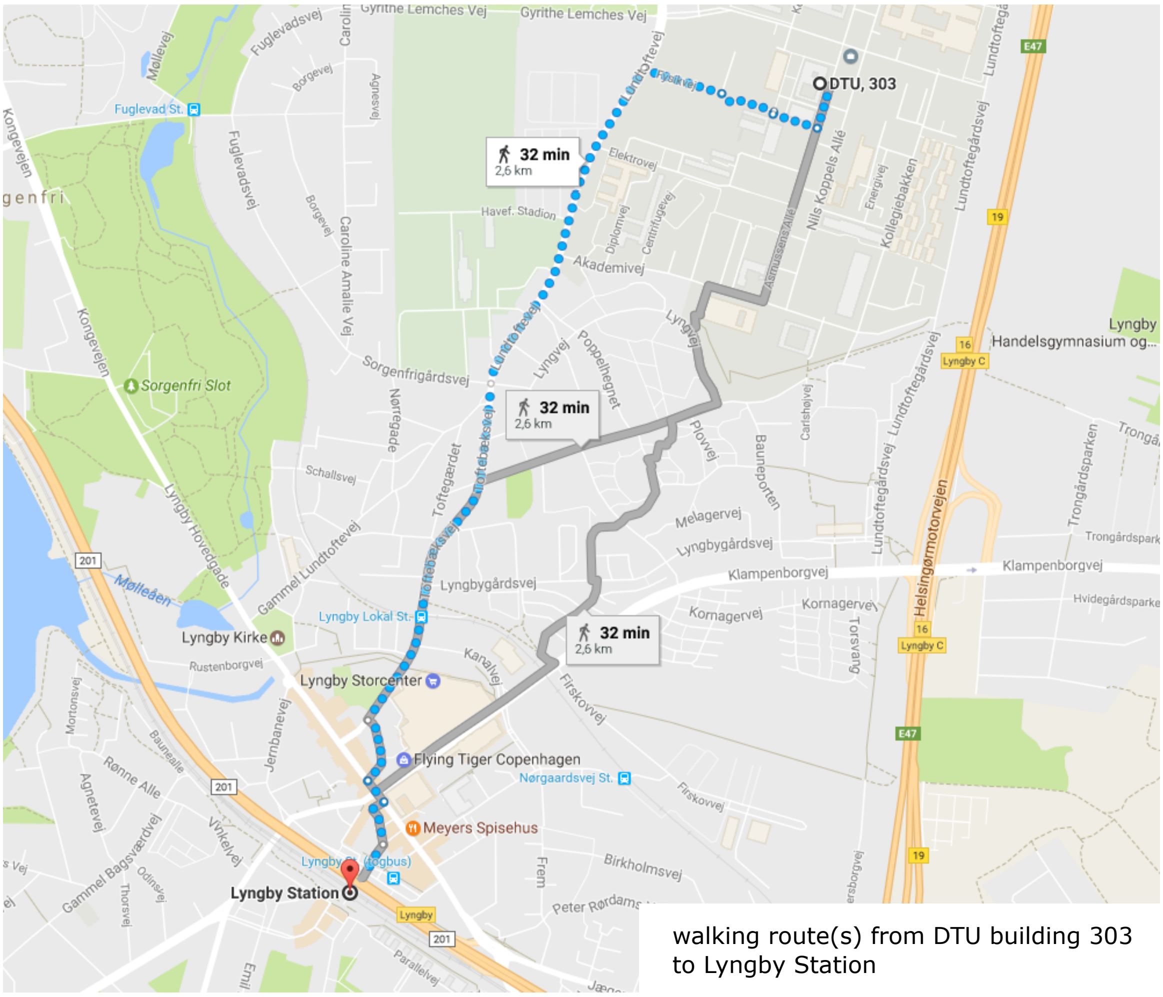

walking route(s) from DTU building 303 to Lyngby Station

Areas with restaurants in Lyngby

Meyers Spisehus - Conference dinner

Bus stops

	Monday	Tuesday	Wednesday	Thursday	Friday
08:00	Registration				
	Welcome	Coffee	Coffee	Coffee	Coffee
09:00	Tim Ralph	Andrew Shields	Ronald Hanson	Akira Furusawa	Klemens Hammerer
	Patrick Maletinsky	Dirk Englund	Simon Gröblacher	Gerd Leuchs	Eleni Diamanti
10:00	David Hunger	Warwick Bowen	Marco Bellini	Marco Genovese	Cosmo Lupo Stefano Pironio Jonatan Bohr Brask
	Coffee break	Coffee break	Coffee break	Coffee break	Coffee break
11:00	Stefano Pirandola	Norbert Lütkenhaus	Stephanie Wehner	Julien Laurat	Hyunseok Jeong
	Robert Sewell	Giacomo De Palma	Sebastian Steinlechner	Pau Farrera	Ulrich Hoff
12:00	Lambert Giner	Nathan Walk	Milena D'Angelo	Jaromír Fiurášek	Farid Shahandeh
	Anaelle Hertz	Raj Patel	Ivano Ruo-Berchera	Oleksandr Kyriienko	Giulia Ferrini
13:00	Lunch break	Lunch break	Lunch break	Lunch break	Lunch break
14:00	Konrad Banaszek	Industry forum: Romain Alléaume Mathieu Munsch Søren Stobbe	Excursion	Radim Filip	Matthias Christandl
	Stephan Götzinger			Joshua Nunn	Hyang-Tag Lim
15:00	Jake Iles-Smith			Alexander Ulanov	Ali Elshaari
	Thomas Kauten	Speed talks		Valentina Parigi	Goodbye
	Coffee break			Coffee break	
16:00	Kasper Jensen	Poster session		Andrea Smirne	
	Fedor Jelezko			Jaehak Lee	
17:00				Eugene Polzik	
	Speed talks			Roberta Zambrini	
18:00					
19:00				Conference dinner	


17

Events

Industry session

There are clear indications that there is increased interest from both commercial and governmental entities in investing heavily in research and development activities that will bring the technologies of the second quantum revolution into a commercial context. While many of these technologies have the potential to be paradigm-shattering, there are still many technological and commercial challenges to be addressed, some of which are unique to Quantum Technologies.

Cathal Mahon, CEO of Qubiz - Quantum Innovation Center

The industry session on Tuesday afternoon includes a panel discussion on the subject “Is now the time to tunnel to market?” The context for the discussion will be provided by the 3 speakers, each with their own unique and first hand, hands-on experience of these challenges.

14:00-14:20 Mathieu Munsch, Qnami (Switzerland)

14:20-14:40 Romain Alléaume, SeQureNet (France)

14:40-15:00 Søren Stobbe, Sparrow Quantum (Denmark)

15:00-15:30 Panel discussion, facilitated by Cathal Mahon, Qubiz (Denmark)

Poster session

More than 150 poster presentations have been registered for the conference. To let everyone have time to explore them, the poster session on Tuesday will be split into 3 sub-sessions lasting 1h each:

16:15–17:15 Poster numbers $\equiv 1 \pmod 3$: 1, 4, 7, ...

17:15–18:15 Poster numbers $\equiv 2 \pmod 3$: 2, 5, 8, ...

18:15–19:15 Poster numbers $\equiv 0 \pmod 3$: 3, 6, 9, ...

You are expected to be near your poster during its designated slot but can spend the remaining two hours on visiting other posters.

The two best posters will be awarded a prize.

During the poster session, beverages and traditional hotdogs will be served outside in the courtyard from authentic cars (in Danish: *pølsevogn*).

Some of the posters will be introduced in 30 second speed talks on Monday and Tuesday.

You can hang your poster on Monday and leave it up for the duration of the conference (although, please take it down at latest during the lunch break on Friday).

Excursion

On Wednesday, a boat trip with guide through the Copenhagen channels is planned. At the end of the tour you will be dropped off near Nyhavn from where you are free to explore Copenhagen on your own.

14:00 Pick-up in buses from building 101A (where we have lunch)

15:00 Boats depart from Ofelia Plads / Kvæsthusbroen

16:00 End of tour at same location as departure

Conference dinner

The conference dinner will be served in *Meyers Spisehus* (*www.meyersspisehus.dk*) on Thursday evening, beginning at 19:00. Meyers Spisehus is located in the center of Lyngby (see the map of Lyngby for details). From DTU it takes about 25 min to walk there, or you may take a bus towards Lyngby, getting off at Lyngby Storcenter or Lyngby Station.

We thank our sponsors

CARLSBERG FOUNDATION

SPARROW QUANTUM

attocube
pioneers of precision

Qubiz
Quantum Innovation Center

LOT
QuantumDesign

SINGLE QUANTUM
Excellence in photon detection

NKT Photonics

DET FRIE FORSKNINGSRÅD
DANISH COUNCIL FOR
INDEPENDENT RESEARCH

CRYPTOMAThIC

Scientific program

Monday

Tuesday

Wednesday

Thursday

Friday

Posters

Entanglement and relativistic effects for Gaussian states

Tim Ralph, Spyridon Tserkis, Daiqin Su
University of Queensland

We present for the first time an analytic formula for the entanglement of formation (EoF) of general bipartite Gaussian states. We show through physical examples that EoF is a superior measure of entanglement than Negativity. We also discuss an unexpected decoherence effect when detecting the radiation from accelerated quantum sources.

Single spin quantum sensing and imaging

Patrick Maletinsky

Electronic spins yield excellent quantum sensors, offering quantitative, nanoscale sensing down to single spin levels. I will present our recent achievements in employing electronic spins for nanoscale magnetometry of solid-state systems. I will focus on quantitative quantum sensing of antiferromagnets and superconductors and how it competes with state-of-the-art magnetic imaging.

Purcell-enhanced single-photon emission from colour centers in diamond coupled to tunable microcavities

D. Hunger[1], H. Kaupp[2], J. Benedikter[2], T. Hümmer[2], H. Fedder[3], H.-C. Chang[4], A. Bommer[5], C. Becher[5], J. Liang[6], A. Krueger[6], J. Smith[7], T. W. Hänsch[2]

[1]*Karlsruhe Institute of Technology, Wolfgang Gaede Str. 1, 76131 Karlsruhe, Germany*
[2]*Ludwig-Maximilians University Munich, Schellingstr. 4, 80799 Munich, Germany*
[3]*3. Physikalisches Institut, Universität Stuttgart, Pfaffenwaldring 57, 70569 Stuttgart, Germany*
[4]*Inst. of Atomic and Molecular Sciences, Academia Sinica, Taipei 106, Taiwan,*
[5]*Universität des Saarlandes, Campus E2.6, 66123 Saarbrücken, Germany*
[6]*University of Oxford, 16 Parks Road Oxford OX1 3PH, United Kingdom*

Optical microcavities are a powerful tool to control spontaneous emission of individual quantum emitters. Fabry-Perot cavities built from laser-machined and mirror-coated optical fibers are particularly promising in this context, since they offer small mode volumes and large quality factors combined with full tunability and direct access to the cavity field [1]. For quantum emitters coupled to the cavity, this gives rise to the Purcell effect, which enables enhancement of fluorescence emission and high collection efficiency. This offers a route for bright and narrow-band single photon sources as well as efficient spin state readout.

In our experiment, we couple colour centers in diamond such as the nitrogen vacancy center to a cavity with a mode volume as small as 1 λ^3 [2]. We record cavity-enhanced fluorescence images and study several single emitters with one cavity. We observe lifetime changes by more than a factor of two and obtain cavity-enhanced single photon emission rates exceeding 10^6 photons per second.

Alternatively, we study silicon vacancy centers in diamond, which offer a dominant zero phonon line with narrow linewidth also under ambient conditions. Coupled to a cavity, this offers the potential for Purcell factors beyond 10 and up to GHz single photon rates [3].

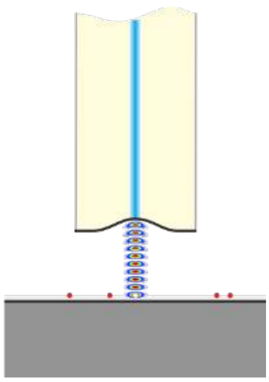

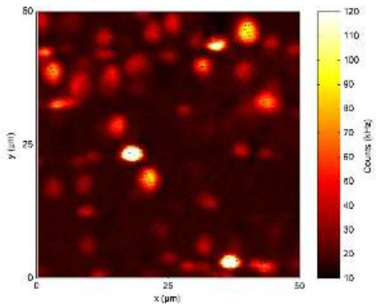

Figure 1 Left: Schematic setup of a tunable Fabry-Perot microcavity formed by a lasermachined endfacet of an optical fiber and a macroscopic mirror. The sample is placed on the planar mirror and can be raster scanned through the cavity mode to achieve optimal spatial and spectral overlap. Right: Scanning-cavity fluorescence image of NV centers in nanodiamonds

[1] D. Hunger, T. Steinmetz, Y. Colombe, C. Deutsch, T. W. Hänsch, J. Reichel, “Fiber Fabry-Perot cavity with high Finesse”, New Journal of Physics **12** (2010), 065038.

[2] H. Kaupp, T. Hümmer, M. Mader, B. Schlederer, J. Benedikter, P. Haeusser, H.-Ch. Chang, H. Fedder, T. W. Hänsch, D. Hunger, “Purcell-enhanced single-photon emission from nitrogen-vacancy centers coupled to a tunable microcavity”, arXiv:1606.00167 (2016)

[3] J. Benedikter, H. Kaupp, T. Hümmer, J. Liang, A. Bommer, C. Becher, A. Krueger, J. M. Smith, T. W. Hänsch, D. Hunger, „Cavity-enhanced single photon source based on the silicon vacancy center in diamond“, Phys. Rev. Appl. 7, 024031 (2017)

Capacities of repeater-assisted quantum communications

Stefano Pirandola

We bound the ultimate rates for distributing secret keys via quantum repeaters, from the basic scenario of a single repeater chain to an arbitrarily-complex quantum network, where systems may be routed through single or multiple paths. We establish the end-to-end capacities under fundamental noise models, including optical loss.

Simultaneous tracking of spin angle and amplitude beyond classical limits

Giorgio Colangelo,[1,*] Ferran Martin Ciurana,[1] Lorena C. Bianchet,[1] Robert J. Sewell,[1] and Morgan W. Mitchell[1,2]
[1] *ICFO-Institut de Ciencies Fotoniques, The Barcelona Institute of Science and Technology, 08860 Castelldefels, Barcelona, Spain*
[2] *ICREA – Institució Catalana de Recerca i Estudis Avançats, 08015 Barcelona, Spain*
(Dated: April 1, 2017)

Measurement of spin precession is central to extreme sensing in physics,geophysics,chemistry,nanotechnologyand underlies powerful magnetic resonance spectroscopies.Because there is no spin-angle operator, any measurement of spin precession is necessarily indirect, e.g., inferred from spin projectors F_α at different times. Such projectors do not commute, and thus quantum measurement back-action (QMBA) necessarily enters the spin measurement record, introducing errors and limiting sensitivity. Here [1] we show how to reduce this disturbance below $\delta F_\alpha \sim \sqrt{N}$, the classical limit for N spins, by directing the QMBA almost entirely into an unmeasured spin component. This generates a planar squeezed state[2] which, because spins obey non-Heisenberg uncertainty relations [3], allows simultaneous precise knowledge of spin angle and amplitude. We use high-dynamic-range optical quantum non-demolition measurements[4–6] applied to a precessing magnetic spin ensemble, to demonstrate spin tracking with steady-state angular sensitivity **2.9 dB** beyond the standard quantum limit, simultaneous with amplitude sensitivity **7.0 dB** beyond Poisson statistics. This method for the first time surpasses classical limits in non-commuting observables, and enables orders-of-magnitude sensitivity boosts for state-of-the-art sensing[7] and spectroscopy.

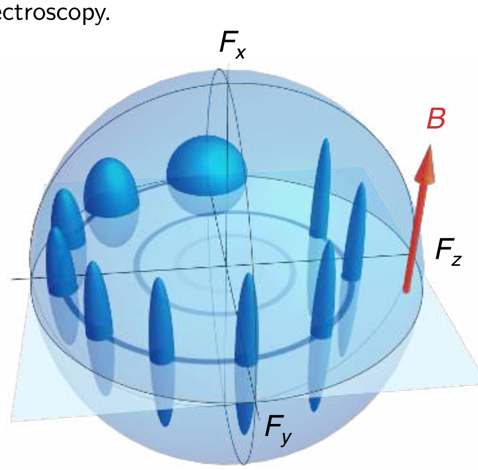

FIG. 1. Simultaneous, precise tracking of spin angle and amplitude. Bloch-sphere representation of the atomic state evolution. Ellipsoids show uncertainty volumes (not to scale) as the state evolves anti-clockwise from an initial, F_y-polarized state with isotropic uncertainty. An x-oriented magnetic field $\mathbf{B}$ drives a coherent spin precession in the F_y–F_z plane. Quasi-continuous measurement of F_z produces a reduction in F_z and F_y variances, with a corresponding increase in var(F_x).

[1] G. Colangelo, F. Martin Ciurana, L. C. Bianchet, R.J. Sewell, Simultaneous tracking of spin angle and amplitude beyond classical limits, *Nature* **543**, 525 (2017).
[2] Q. Y. He, S.-G. Peng, P. D. Drummond, M. D. Reid, Planar quantum squeezing and atom interferometry, *Phys. Rev. A* **84**, 022107 (2011).
[3] H. P. Robertson, The uncertainty principle, *Phys. Rev.* **34**, 163 (1929).
[4] M. Koschorreck, M. Napolitano, B. Dubost, M. W. Mitchell, Quantum nondemolition measurement of large-spin ensembles by dynamical decoupling, *Phys. Rev. Lett.* **105**, 093602 (2010).
[5] R. J. Sewell, M. Napolitano, N. Behbood, G. Colangelo, M. W. Mitchell, Certified quantum non-demolition measurement of a macroscopic material system, *Nat. Photon.* **7**, 517 (2013).
[6] F. M. Ciurana, G. Colangelo, R. J. Sewell, M. W. Mitchell, Real-time shot-noise-limited differential photodetection for atomic quantum control, *Opt. Lett.* **41**, 2946 (2016).
[7] O. Hosten, N. J. Engelsen, R. Krishnakumar, M. A. Kasevich, Measurement noise 100 times lower than the quantum-projection limit using entangled atoms, *Nature* **529**, 505 (2016).

* giorgio.colangelo@icfo.es

Hacking Heisenberg's uncertainty principle with quantum clones

Lambert Giner[1,*] , Guillaume S. Thekkadath[1], Rebecca Y. Saaltink[1], Jeff S. Lundeen[1]
[1] Department of Physics, Centre for Research in Photonics, University of Ottawa,
25 Templeton Street, Ottawa, Ontario K1N 6N5, Canada
[*] e-mail: lambert.giner@gmail.com

Summary: Performing simultaneous non-commuting measurements on a single quantum system is impossible because of the disturbances generated by the measurements. However, if one possesses two copies of the system, this problem can be overcome. We perform simultaneous non-commuting measurements and fully determine the state of the system using quantum clones.

1. Introduction

In classical physics, the position and the momentum of a particle can be fully determined. Indeed, one can first measure the position of a particle, then its momentum (or the other way around) to acquire full knowledge of the state of the particle. However, as all quantum physicists know, because of Heisenberg's uncertainty principle, it is not possible to simultaneously measure complementary observables with an arbitrary precision. In this case, if one precisely determines the position of the particle, then its momentum will be random, and thus only one aspect of the full quantum state of the particle will be known.

One possible way to get around this problem is to use weak measurements. In this situation, the state of the particle is weakly coupled to a pointer, which is measured. Since the coupling between the particle and the pointer is weak, the particle's state remains unchanged, thereby allowing subsequent measurements of complementary observables. It has been shown that a quantum system can be entirely determined using a series of two non-commuting weak measurements followed by a strong measurement [1].

A second possible way to solve the problem would be to make two identical copies of the particle. Then, one could measure its position on the first copy and its momentum on the second copy. But, the no-cloning theorem states it is impossible to make two perfect copies of a quantum state. Instead, it is possible to generate optimal (but imperfect) clones. Here, optimal means both clones are identical and as similar to the original state as theoretically possible. We simultaneously measure non-commuting observables on each optimal clone. This joint measurement (which can alternatively be described using weak values [2]) can be used to determine the state of the quantum system [3].

2. Experimental results

The optimal clones are generated by interfering on a 50:50 beam splitter two 808 nm photons produced by a type-II spontaneous parametric downconversion (SPDC) process. If the photons are indistinguishable, they will bunch due to Hong-Ou-Mandel interference. To jointly measure complementary observables on each clone, we need to coherently interfere the cases where the clones bunch and anti-bunch. This is done by implementing a square root swap transformation in a subsequent interferometer.

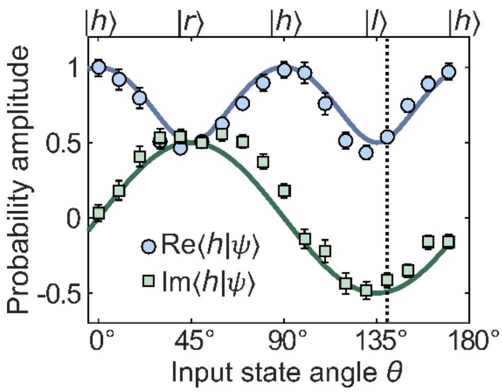

Fig 1. Real and imaginary part of projection of Ψ onto the horizontal polarization as a function of the input state

3. Conclusion

We have shown that using optimal quantum clones, it is possible to perform non-commuting measurements and determine the state of a quantum system.

4. References

[1] G.S. Thekkadath, L. Giner, Y. Chalich, M.J. Horton, J. Banker, and J.S. Lundeen Phys. Rev. Lett. **117**, 120401 (2016)
[2] H.F. Hofmann Phys. Rev. Lett. **109**, 020408 (2012)
[3] G.S. Thekkadath, R.Y. Saaltink, L. Giner, and J.S. Lundeen arXiv:1701.04095v2 [quant-ph] 27 Feb 2017

A tight entropy-power uncertainty relation

Anaelle Hertz,[1,*] Michael G. Jabbour,[1] and Nicolas J. Cerf[1]

[1] *Centre for Quantum Information and Communication, École polytechnique de Bruxelles, CP 165, Université libre de Bruxelles, 1050 Brussels, Belgium*

The uncertainty principle lies at the heart of quantum physics. It exhibits one of the key divergences between a classical and a quantum system. The original uncertainty relation, due to Heisenberg [1] and Kennard [2], relies on the variances of $\hat{x}$ and $\hat{p}$. It is written as

$$\sigma_x^2\,\sigma_p^2 \geq (\hbar/2)^2. \tag{1}$$

Relation (1) is invariant under (x,p)-displacements in phase space and it is saturated by all pure Gaussian states provided that they are squeezed in the x or p direction only. More precisely, the Heisenberg relation is saturated for pure Gaussian states provided the principal axes of the covariance matrix γ are aligned with the x- and p-axes, namely $\sigma_{xp}=0$.

The Heisenberg relation was improved by Schrödinger and Robertson [3, 4] by taking into account the covariance σ_{xp} (through the covariance matrix). For two canonically-conjugate variables $\hat{x}$ and $\hat{p}$, it is written as

$$|\gamma| \geq (\hbar/2)^2. \tag{2}$$

Relation (2) has the advantage that it is now saturated by all pure Gaussian states, regardless of the orientation of the principal axes of the covariance matrix. Thus, this uncertainty relation is invariant under all Gaussian unitary transformations (displacements and symplectic transformations).

A different kind of uncertainty relations, originated by Bialynicki-Birula and Mycielski [5], relies on Shannon differential entropies $h(x)$ and $h(p)$ instead of variances as a measure of uncertainty. It is expressed as

$$h(x)+h(p) \geq \ln(\pi e \hbar). \tag{3}$$

Interestingly, this relation can be written in terms of entropy powers defined as $N_x=(2\pi e)^{-1}\,\exp\{2\,h(x)\} \leq \sigma_x^2$ and $N_p=(2\pi e)^{-1}\,\exp\{2\,h(p)\} \leq \sigma_p^2$ so that eq. (3) becomes

$$N_x\,N_p \geq (\hbar/2)^2\,, \tag{4}$$

which is what we call an *entropy-power uncertainty relation* for a pair of canonically-conjugate variables: it closely resembles the Heisenberg relation (1), but with entropy powers instead of variances. Furthermore, it is now obvious to see that this relation implies the Heisenberg one. However, it is not invariant under all Gaussian unitaries, unlike eq. (2).

In this contribution, we prove by variational calculus (under a reasonable assumption) a tighter form of entropy-power uncertainty relation that is extended to rotated variables by taking correlations into account [6]. It is is written as

$$h(x)+h(p)-\frac{1}{2}\ln\left(\frac{\sigma_x^2\sigma_p^2}{|\gamma|}\right) \geq \ln(\pi e\hbar). \tag{5}$$

in terms of differential entropies or equivalently as

$$N_x\,N_p \geq \frac{\sigma_x^2\,\sigma_p^2}{|\gamma|}\;(\hbar/2)^2 \tag{6}$$

in terms of entropy powers. This relation, like the Schrödinger-Robertson uncertainty relation eq. (2), is saturated by all pure Gaussian states and moreover, we can easily see that it, in fact, implies eq. (2).

We also prove an extended version of the above entropy-power uncertainty relation that is valid for n modes and is saturated for all n-mode Gaussian pure states. It can be expressed as

$$h(\hat{x}_1,...,\hat{x}_n)+h(\hat{p}_1,...,\hat{p}_n)-\frac{1}{2}\ln\left(\frac{|\gamma_x||\gamma_p|}{|\gamma|}\right) \geq n\,\ln(\pi e\hbar) \tag{7}$$

where γ_x (γ_p) is the reduced covariance matrix of the x (p) quadratures.

Finally, we propose, as an extension of the work done by Huang [7], a n-modal version of entropic uncertainty relation expressing the balance between any two n-modal projective Gaussian measurements. Namely, we compute the differential entropies $h(\hat{A}_1,...\hat{A}_n)$ and $h(\hat{B}_1,...\hat{B}_n)$ where $(\hat{A}_1,...\hat{A}_n)$ are the $\hat{x}$-quadratures measured after applying a Gaussian unitary A on the n-mode state $|\psi\rangle$ (and similarly for B). The bound of this uncertainty relation is expressed in terms of $\det(K)$ where $K_{ij}=[A_i,B_j]$ is the commutator between two quadratures.

---

* ahertz@ulb.ac.be

[1] W. Heisenberg, Z. Phys. **43**, 172 (1927).
[2] E. H. Kennard, Z. Phys. **44**, 326 (1927).
[3] E. Schrödinger, Preuss. Akad. Wiss. **14**, 296 (1930).
[4] H.P. Robertson, Phys. Rev. **35** 667A (1930).
[5] I. Bialynicki-Birula and J. Mycielski, Commun. Math. Phys. **44**, 129 (1975).
[6] A. Hertz, M. G. Jabbour and Nicolas J. Cerf, arXiv:1702.07286 (2017).
[7] Y. Huang, Phys. Rev. A **83** 052124 (2011).

Mode engineering for realistic quantum-enhanced interferometry

Konrad Banaszek

We show that appropriate preparation and detection of the modal structure of photons used in quantum-enhanced interferometry can alleviate deleterious effects caused by other, experimentally inaccessible, degrees of freedom. We present an experiment in which spatial mode engineering restores sub-shot noise precision of two-photon interference degraded by residual spectral distinguishability.

Efficient generation and manipulation of photons with single molecules

Stephan Götzinger
MPL Erlangen

I will first discuss our efforts to deterministically generate single photons by using planar dielectric antennas. In the second part I will present experiments where photons and single molecules strongly interact. A single molecule can amplify a weak laser beam and generate nonlinear effects like three-photon amplification and four-wave mixing.

Phonon limit to simultaneous near-unity efficiency and indistinguishability in semiconductor single photon sources

Jake Iles-Smith[a], Dara P S McCutcheon[a,b], Ahsan Nazir[c], and Jesper Mørk[a]

[a] *DTU Fotonik, Department of Photonics Engineering, DTU, Copenhagen, Denmark*
[b] *Department of Electrical and Electonic Engineering, University of Bristol, UK*
[c] *Photon Science Institute, The University of Manchester, UK*

Semiconductor quantum dots have recently emerged as a leading platform to efficiently generate highly indistinguishable photons [1-4], and this work addresses the timely question of how good these solid-state sources can ultimately be. We establish the crucial role of lattice relaxation in these systems [4], which we show gives rise to trade-offs between indistinguishability and efficiency. We analyse the two source architectures most commonly employed: a quantum dot embedded in a waveguide and a quantum dot coupled to an optical cavity. For waveguides, we demonstrate that the broad-band Purcell effect [5] results in a simple inverse relationship, where indistinguishability and efficiency cannot be simultaneously increased. For cavities, the frequency selectivity of the Purcell enhancement results in a more subtle trade-off, where indistinguishability and efficiency can be simultaneously increased, though by the same mechanism not arbitrarily, limiting a source with near-unity indistinguishability ($> 99\%$) to an efficiency of approximately 96%.

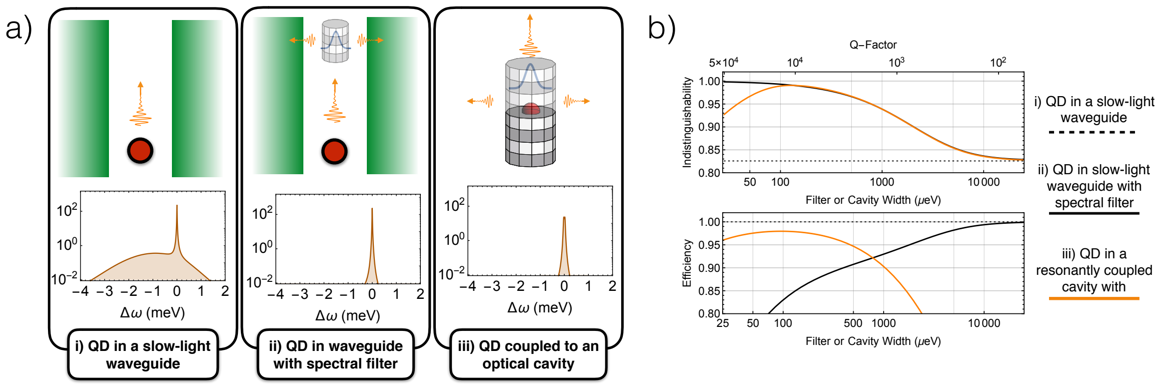

Figure 1: a) (i–iii) show the three single photon source designs we analyse and their associated emission spectra: a QD emitting into a slow-light waveguide with and without a spectral filter, and a QD in a coherently coupled optical cavity. b) Indistinguishability and efficiency of the three source architectures. The indistinguishability plot indicates that the dominant effect of a resonantly coupled cavity is to filter the QD emission, while the efficiency plot demonstrates that Purcell enhancement in a cavity can overcome efficiency losses incurred by filtration of the phonon sideband.

[1] Y.-M. He, Y. He, Y.-J. Wei *et al.*, Nat. Nanotechnol. 8, 213 (2013).
[2] A. Thoma, P. Schnauber, M. Gschrey *et al.*, Phys. Rev. Lett. 116, 033601 (2016).
[3] N. Somaschi, V. Giesz, L. De Santis *et al.*, Nat. Photonics 10, 340 (2016).
[4] J. Iles-Smith, D. P. S. McCutcheon, A. Nazir, and J. Mørk, arXiv:1606.06305 (2016).
[5] P. Lodahl, S. Mahmoodian, and S. Stobbe, Reviews of Modern Physics 87, 347 (2015)

Observation of genuine three-photon interference

Thomas Kauten[1]*, Sascha Agne[2], Jeongwan Jin[2], Evan Meyer-Scott[2,3], Jeff Z. Salvail[2], Deny R. Hamel[4], Kevin J. Resch[2], Gregor Weihs[1], Thomas Jennewein[2]

1. *Institut für Experimentalphysik, Universität Innsbruck, Technikerstraße 25, 6020 Innsbruck, Austria*
2. *Institute for Quantum Computing and Department of Physics and Astronomy, University of Waterloo, Ontario, Canada*
3. *Department of Physics, University of Paderborn, Warburger Straße 100, 33098 Paderborn, Germany*
4. *Département de Physique et d'Astronomie, Université de Moncton, Moncton, New Brunswick E1A 3E9, Canada*

*thomas.kauten@uibk.ac.at

Entangled photons are a key requirement for realizing worldwide quantum communication [1], quantum cryptography and optical quantum computation. The photons can be entangled in various degrees of freedom, usually the photons are polarization entangled, since it is relatively easy to realize. Unfortunately, these photons have limited transmission length through fibers due to polarization mode dispersion. Therefore, the photons have to be entangled in a different, more robust degree of freedom; in this case, we use energy-time entanglement [2]. For some applications it is additionally required to have many photon entanglement, for example multipartite correlations exhibited in the Greenberger-Horne-Zeilinger (GHZ) state [3], where three particles are correlated while no pairwise correlation is found. In this work we present an experiment, which demonstrates three-photon interference that does not originate from two-photon or single photon interference by using energy-time entangled photon triplets produced via cascaded parametric down conversion [4, 5]:

Here we employ a continuous-wave laser at 404 nm to pump a periodically-poled potassium titanyl phosphate crystal cut for type-II down-conversions, which produces pairs of 842/776 nm photons. These photons are separated at a polarizing beam splitter. The 776 nm photons pump a periodically-poled lithium niobate waveguide to generate 1530/1570 nm photon pairs in type-0 down-conversion. Our source creates approximately 2000 entangled photon triplets per hour [5]. After splitting up those photons on a dichroic mirror, all photons are sent into a three-photon Franson-interferometer [2], which is in our case realized as three different spatial modes of an imbalanced single Mach-Zehnder interferometer ($\Delta T = 3.7$ ns). The phases of the photons can be adjusted via motorized glass plates in the long arm of each interferometer. At the output ports of the interferometer, the photons are detected with single photon detectors (avalanche photo diodes and superconducting nanowire detectors), and their arrival time is registered with a time tagger system.

As a result, we observe phase-dependent variation of three-photon coincidences with (92.7 ± 4.6)% visibility (see Fig. 1) while having negligible two-photon and single-photon modulation [6].

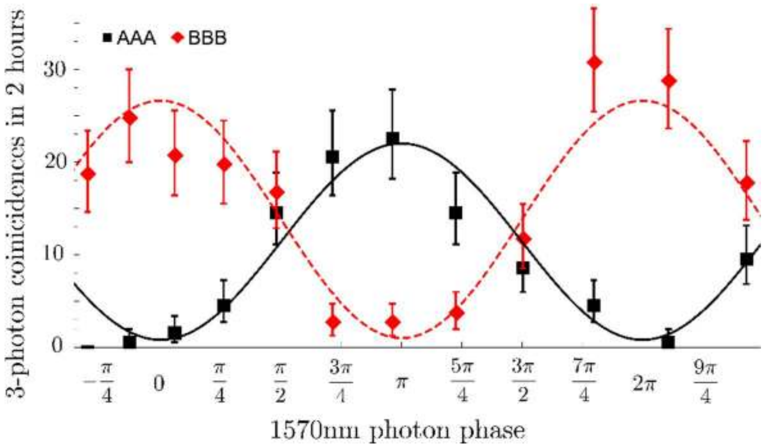

Fig. 1 Measured three-photon coincidences: By changing the phase in one of the interferometers we observe an interference with a visibility of (92.7 ± 4.6)%. The error bars are Poissonian count errors. AAA and BBB denote different output port combinations of the three interferometers.

References

[1] H. J. Kimble, "The quantum internet", Nature 453, 1023-1030 (2008).
[2] J. D. Franson, "Bell inequality for position and time", Phys. Rev. Lett. 62, 2205 (1989).
[3] D. Greenberger, M. Horne, A. Shimony, and A. Zeilinger, "Bell's theorem without inequalities". Am. J. Phys. 58, 1131 (1990).
[4] H. Hübel, et al., "Direct generation of photon triplets using cascaded photon-pair sources", Nature 466, 601-603 (2010).
[5] Shalm, et al., "Three-photon energy-time entanglement", Nat. Phys. 9, 19 (2012).
[6] S. Agne, et al., "Observation of genuine three-photon interference", arXiv:1609.07508 (2016), Phys. Rev. Lett. t.b.p. (2017).

Quantum Optical Magnetometry for Biomedical Applications

Kasper Jensen[1,*], Hans Christian Stærkind[1], Jens Arnbak[1], Bo Hjorth Bentzen[2], Eugene S. Polzik[1]

[1] Niels Bohr Institute, University of Copenhagen, Blegdamsvej 17, 2100 Copenhagen, Denmark.
[2] Department of Biomedical Sciences, University of Copenhagen, Blegdamsvej 3, 2200 Copenhagen N, Denmark.
*kjensen@nbi.dk

Biomagnetometry

Electrical measurements are today widely used in medicine for diagnostics purposes. The advent of highly sensitive magnetometers in the last 50 years has opened the field of bio-magnetometry, where the ionic currents inside living organisms are mapped by measuring the small magnetic fields that they generate. The great advantage of a magnetic probe, compared to an electrical probe, is that it doesn't have to be in direct contact with what it is measuring on. The field has been pioneered by superconducting quantum interference device (SQUID) magnetometers. But these have the major drawback of only working at *cryogenic temperatures*.

Our quantum optical cesium magnetometer

Our optical magnetometer consists of a *room-temperature* cesium vapor cell which is coated on the inside with paraffin. By optical pumping, the cesium atoms are polarized along the direction of an applied static magnetic field. Any bio-magnetic field which is present will drive the atomic polarization away from this direction. The atomic polarization, and thereby the bio-magnetic field, is measured using the Faraday rotation of the light polarization of a probing laser. Our magnetometer has high sensitivity which enables us to detect tiny biological signals. The sensitivity of our optical cesium magnetometer is mainly limited by quantum noise originating from the Heisenberg uncertainty principle of Quantum Mechanics.

Detection of nerve impulses

We have detected animal nerve impulses with our miniature cesium magnetometer [1]. The nerve is stimulated electrically in one end, which triggers an action potential that propagates to the other end. We demonstrate that our magnetometer is capable of detecting the magnetic field from the nerve impulse at several mm distance (Fig. 1), corresponding to the distance between the skin and nerves in medical studies. Possible applications of our magnetometer include diagnostics of multiple sclerosis, myotonia and intoxication in patients.

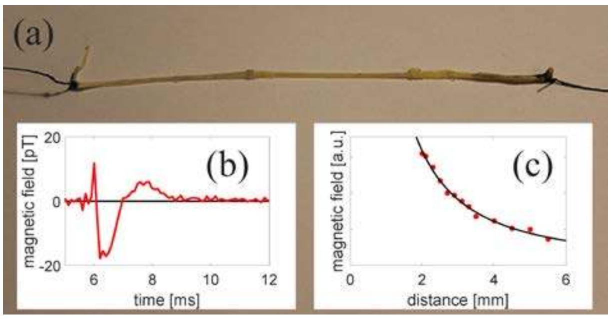

Figure 1: (a) Frog sciatic nerve. (b) Magnetic field from a nerve impulse. (c) Magnetic field as a function of distance from the nerve.

Detection of the heartbeat

We have also measured the magnetocardiogram (MCG) of an isolated guinea-pig heart (Fig. 2). We can resolve the P, QRS and T features consistent with what is seen in a standard electrocardiogram (ECG). Possible applications of our technology include non-invasive detection of the fetal heartbeat (fetal-MCG).

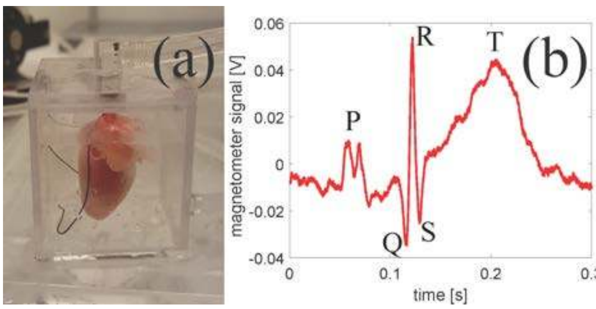

Figure 2: (a) Isolated guinea-pig heart. The heart is perfused with water containing oxygen such that the heart can be kept a live and beating for > 3 hours. (b) Magnetic field from the heart.

[1] K. Jensen et al., *Non-invasive Detection of Animal Nerve Impulses with an Atomic Magnetometer Operating Near Quantum Limited Sensitivity.* Scientific Reports **6**, 29638 (2016).

Quantum sensing with diamond qubits

Fedor Jelezko
Universität Ulm

Novel sensing techniques are at the heart of a wide variety of modern technologies. Nanomedicine, molecular biology, chemistry and material science require the ability to measure properties of matter at the atomic scale. Here we show that diamond spin sensors can provide new tool for sensing at nanoscale. We also show how quantum error correction protocols allows to improve performance of diamond spin magnetometers.

Quantum Communications using Semiconductor Devices

Andrew Shields

Toshiba Research Europe Ltd
208 Science Park, Milton Road, Cambridge CB40GZ. UK
www.quantum.toshiba.co.uk

***andrew.shields@crl.toshiba.co.uk**

Applying quantum theory to information systems brings new functionalities that are not possible in conventional networks and computers. For example, the secrecy of encoded single photons transmitted along optical fibres can be tested directly and used to distribute cryptographic keys and digital signatures on communication networks. I will discuss recent work to realise practical systems for quantum key distribution (QKD) and their application to point-to-point and network-based encryption. In the latter part of the talk I present progress on quantum relays using semiconductor entangled photon sources.

Simple semiconductor devices for the generation and detection of quantum light states are central to the development of practical QKD. Semiconductor avalanche photodiodes operated in gated Geiger mode allow detection of telecom single photons at GHz rates. These room temperature devices enable portable and reliable QKD systems with key rates in excess of 1 Mb/s and individual fibre links over 200km in length.

QKD has been demonstrated using single photons, entangled pairs, attenuated laser pulses and Gaussian modulated coherent pulses. Of these, attenuated laser diodes give the best performance today and, thanks to the decoy pulse protocol and privacy amplification, have identical security to the case of ideal single photon sources. Recently direct phase modulation of laser diodes, based on optical injection locking, has been shown to reduce the complexity of QKD transmitters and allow a very flexible device that can operate several different protocols.

The past few years have seen rapid progress in the technology required to operate QKD in conventional data networks. I will discuss recent progress on introducing QKD to multi-user access networks and to operate QKD on fibres carrying very high bandwidths (up to 10 Terabit/sec) of conventional data simultaneously.

In the future, new quantum sources will be needed for entanglement based networks that can be used for long distance quantum repeater networks, as well as distributed quantum sensing and computing. Entangled photon sources, based on the electroluminescence of a semiconductor quantum dot, offer an attractive solution. I discuss recent work to develop quantum dot sources that emit entangled photons at 1300nm and to apply these to fibre-based quantum relays.

Semiconductor quantum technologies for communications and computing

Dirk Englund
MIT

The Internet is among the most significant inventions of the 20th Century. We are now poised for the development of a quantum internet to exchange quantum information and distribute entanglement among quantum memories (and ultimately quantum computers) that could be great distances apart. This kind of quantum internet would have a range of applications that aren't possible in a classical world, including long-distance unconditionally-secure communication, certain types of precision sensing and navigation, and distributed quantum computing. But we still need to develop or perfect many types of components and protocols to build such a quantum internet. This talk will consider some of these components, focusing on photonic integrated circuits, diamond spin-based quantum memories, and prototype networks. Specifically, the first part of this talk will review our recent progress in adapting one of the leading PIC architectures—silicon photonics—for different types of quantum secure communications protocols. The second part of the talk will consider how photonic integrated circuits technology may extend the reach of quantum communications through all-optical and memory-based quantum repeaters, as well as extensions to modular quantum computers.

Quantum-limited single molecule sensing: probing nanoscale biological machinery in its native state

N. P. Mauranyapin, L. S. Madsen, M. A. Taylor, M. Waleed and W. P. Bowen
Australian Centre for Engineered Quantum Systems, University of Queensland, Australia
E-mail: w.bowen@uq.edu.au

Sensors that are able to detect and track single unlabelled biomolecules are an important tool both to understand biomolecular dynamics and interactions, and for medical diagnostics operating at their ultimate detection limits. Recently, exceptional sensitivity has been achieved using the strongly enhanced evanescent fields provided by optical microcavities and plasmonic resonators [1,2]. However, at high field intensities photodamage to the biological specimen becomes increasingly problematic [3]. Here, we introduce a new approach to evanescent biosensing that combines dark field illumination and heterodyne detection in an optical nanofibre-based platform [4] (see Fig. 1). This allows operation at the fundamental precision limit introduced by quantisation of light. We achieve state-of-the-art sensitivity with a four order-of-magnitude reduction in optical intensity, for the first time reaching beneath known photoinduced biological damage thresholds. We demonstrate quantum noise limited tracking of single biomolecules as small as 3.5 nm, allowing surface-molecule interactions to be monitored over extended periods (inset, Fig. 1).

This research provides a pathway to probe the dynamics of the nanoscale biological machinery of living systems in their native state, without either labels or photoinduced changes in their behavior. By achieving quantum noise limited precision, our approach also presents a step towards quantum-enhanced single-molecule biosensors.

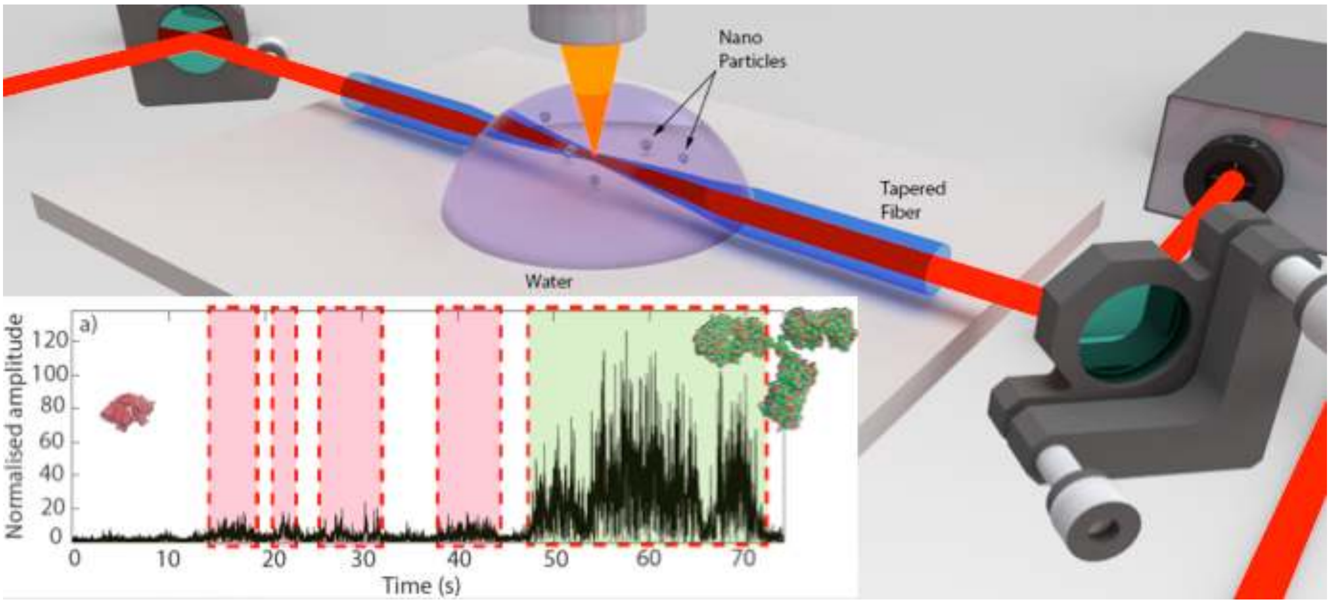

Fig. 1: Diagram of experiment. Inset: Real-time detection of BSA (left) and anti-*e. coli* antibody (right).

[1] M. D. Baaske, M. R. Foreman and F. Vollmer, Nature Nanotechnology **9** 933-939 (2014); [2] Y. Pang and R. Gordon, Nano Letters **12** 402-406 (2012); [3] See e.g. U. Mirsaidov, W. Timp, K. Timp, M. Mir, P. Matsudaira and G. Timp, Phys. Rev. E. **78** 021910 (2008); [4] N.P. Mauranyapin et al. arxiv:1609.05979 (2016).

Quantum communication with coherent states: Realizing communication and information complexity advantages of quantum communication

Norbert Lütkenhaus
IQC Waterloo

We present the basic principle how quantum advantages of communication can be realized using todays technology. The main focus of the presentation will be on optical quantum fingerprinting, but we will also include more recent results.

Gaussian states minimize the output entropy of one-mode quantum Gaussian channels

Giacomo De Palma,[1] Dario Trevisan,[2] and Vittorio Giovannetti[3]

[1] *QMATH, Department of Mathematical Sciences, University of Copenhagen, Denmark*
[2] *Università degli Studi di Pisa, Pisa, Italy*
[3] *NEST, Scuola Normale Superiore and Istituto Nanoscienze-CNR, Pisa, Italy*

We prove the longstanding conjecture stating that Gaussian thermal input states minimize the output von Neumann entropy of one-mode phase-covariant quantum Gaussian channels among all the input states with a given entropy. Phase-covariant quantum Gaussian channels model the attenuation and the noise that affect any electromagnetic signal in the quantum regime. Our result is crucial to prove the converse theorems for both the triple trade-off region and the capacity region for broadcast communication of the Gaussian quantum-limited amplifier. Our result extends to the quantum regime the Entropy Power Inequality that plays a key role in classical information theory. Our proof exploits a completely new technique based on the recent determination of the $p \to q$ norms of the quantum-limited amplifier [De Palma et al., arXiv:1610.09967]. This technique can be applied to any quantum channel.

Based on arXiv:1610.09970.

Signal attenuation and noise unavoidably affect electromagnetic communications through metal wires, optical fibers or free space. Since the energy carried by an electromagnetic pulse is quantized, quantum effects must be taken into account [1]. They become relevant for low-intensity signals, such as for satellite communications, where the receiver can be reached by only few photons for each bit of information [2]. In the quantum regime, signal attenuation and noise are modeled by phase-covariant quantum Gaussian channels [3–7].

The maximum achievable communication rate of a channel depends on the minimum noise achievable at its output, that is quantified by the output von Neumann entropy [5, 8]. We prove in the case of one mode the longstanding constrained minimum output entropy (CMOE) conjecture [9–14] stating that Gaussian thermal input states minimize the output entropy of phase-covariant quantum Gaussian channels among all the input states with a given entropy.

The classical counterpart of the CMOE conjecture states that Gaussian input probability distributions minimize the output Shannon differential entropy of classical Gaussian channels among all the input probability distributions with a given entropy, and it is implied by the Entropy Power Inequality (EPI) [15, 16]. The EPI is fundamental in classical information theory. It is necessary to prove the optimality of Gaussian encodings for the transmission of information through the classical broadcast and wiretap channels [17, 18], and it provides bounds for the information capacities of non-Gaussian classical communication channels [19] and for the convergence rate in the Central Limit Theorem [20]. A quantum generalization of the proof of the EPI permits to prove the quantum EPI (qEPI) [21–25], that provides a lower bound to the output von Neumann entropy of quantum Gaussian channels in terms of the input entropy. However, the qEPI is *not* saturated by quantum Gaussian states, hence it is not sufficient to prove the CMOE conjecture. The MOE conjecture has first been proven in a completely different way in the version stating that pure Gaussian input states minimize the output entropy of any phase covariant and contravariant quantum Gaussian channel among all the possible pure and mixed input states [7, 26–29]. This fundamental result has permitted to determine the classical communication capacity of these channels [30] and to prove that this capacity is additive under tensor product, i.e. it is not increased by entangling the inputs [7]. The CMOE conjecture has then been proven for the one-mode quantum-limited attenuator [31, 32] using Lagrange multipliers. Unfortunately the same proof does not work in the presence of amplification or noise.

We prove the CMOE conjecture for any one-mode phase-covariant quantum Gaussian channel. This result implies the CMOE conjecture also for one-mode phase-contravariant quantum Gaussian channels ([33], Section VI). Our result both extends the EPI to the quantum regime and generalizes the unconstrained minimum output entropy conjecture of [7, 27–30]. Our result is necessary to prove the converse theorems that guarantee the optimality of Gaussian encodings for two communication tasks involving the quantum-limited amplifier [34]. The first is the triple trade-off coding [35], that allows to simultaneously transmit both classical and quantum information and to generate shared entanglement, or to simultaneously transmit both public and private classical information and to generate a shared secret key. The second is broadcast communication [36, 37], i.e. classical communication with two receivers.

Our proof exploits a completely new technique that links the CMOE conjecture to the $p \to q$ norms [7, 38], and is based on the result stating that Gaussian thermal input states saturate the $p \to q$ norms of the one-mode quantum-limited amplifier [39]. This technique can be used to determine the minimum output entropy for fixed input entropy for any quantum channel whose $p \to q$ norms are known.

[1] J. P. Gordon, Proceedings of the IRE **50**, 1898 (1962).
[2] J. Chen, J. L. Habif, Z. Dutton, R. Lazarus, and S. Guha, Nature Photonics **6**, 374 (2012).
[3] V. W. Chan, Lightwave Technology, Journal of **24**, 4750 (2006).
[4] S. L. Braunstein and P. Van Loock, Reviews of Modern Physics **77**, 513 (2005).
[5] A. S. Holevo, *Quantum Systems, Channels, Information: A Mathematical Introduction*, De Gruyter Studies in Mathematical Physics (De Gruyter, 2013).
[6] C. Weedbrook, S. Pirandola, R. Garcia-Patron, N. J. Cerf, T. C. Ralph, J. H. Shapiro, and S. Lloyd, Reviews of Modern Physics **84**, 621 (2012).
[7] A. S. Holevo, Uspekhi Matematicheskikh Nauk **70**, 141 (2015).
[8] M. Wilde, *Quantum Information Theory* (Cambridge University Press, 2013).
[9] S. Guha and J. H. Shapiro, in *Information Theory, 2007. ISIT 2007. IEEE International Symposium on* (IEEE, 2007) pp. 1896–1900.
[10] S. Guha, J. H. Shapiro, and B. I. Erkmen, Physical Review A **76**, 032303 (2007).
[11] S. Guha, B. Erkmen, and J. H. Shapiro, in *Information Theory and Applications Workshop, 2008* (IEEE, 2008) pp. 128–130.
[12] S. Guha, J. H. Shapiro, and B. Erkmen, in *Information Theory, 2008. ISIT 2008. IEEE International Symposium on* (IEEE, 2008) pp. 91–95.
[13] M. M. Wilde, P. Hayden, and S. Guha, Physical Review Letters **108**, 140501 (2012).
[14] M. M. Wilde, P. Hayden, and S. Guha, Physical Review A **86**, 062306 (2012).
[15] T. Cover and J. Thomas, *Elements of Information Theory*, A Wiley-Interscience publication (Wiley, 2006).
[16] N. M. Blachman, Information Theory, IEEE Transactions on **11**, 267 (1965).
[17] P. P. Bergmans, Information Theory, IEEE Transactions on **20**, 279 (1974).
[18] S. K. Leung-Yan-Cheong and M. E. Hellman, Information Theory, IEEE Transactions on **24**, 451 (1978).
[19] C. E. Shannon, ACM SIGMOBILE Mobile Computing and Communications Review **5**, 3 (2001).
[20] A. R. Barron, The Annals of probability , 336 (1986).
[21] R. König and G. Smith, Physical review letters **110**, 040501 (2013).
[22] R. König and G. Smith, Nature Photonics **7**, 142 (2013).
[23] R. Konig and G. Smith, Information Theory, IEEE Transactions on **60**, 1536 (2014).
[24] G. De Palma, A. Mari, and V. Giovannetti, Nature Photonics **8**, 958 (2014).
[25] G. De Palma, A. Mari, S. Lloyd, and V. Giovannetti, Physical Review A **91**, 032320 (2015).
[26] R. Garcia-Patron, C. Navarrete-Benlloch, S. Lloyd, J. H. Shapiro, and N. J. Cerf, Physical Review Letters **108**, 110505 (2012).
[27] A. Mari, V. Giovannetti, and A. S. Holevo, Nature communications **5** (2014).
[28] V. Giovannetti, A. Holevo, and R. García-Patrón, Communications in Mathematical Physics **334**, 1553 (2015).
[29] V. Giovannetti, A. S. Holevo, and A. Mari, Theoretical and Mathematical Physics **182**, 284 (2015).
[30] V. Giovannetti, R. García-Patrón, N. Cerf, and A. Holevo, Nature Photonics **8**, 796 (2014).
[31] G. De Palma, D. Trevisan, and V. Giovannetti, IEEE Transactions on Information Theory **63**, 728 (2017).
[32] G. De Palma, D. Trevisan, and V. Giovannetti, IEEE Transactions on Information Theory **62**, 2895 (2016).
[33] H. Qi, M. M. Wilde, and S. Guha, arXiv preprint arXiv:1607.05262 (2016).
[34] H. Qi and M. M. Wilde, arXiv preprint arXiv:1605.04922 (2016).
[35] M. M. Wilde and M.-H. Hsieh, Quantum Information Processing **11**, 1465 (2012).
[36] J. Yard, P. Hayden, and I. Devetak, Information Theory, IEEE Transactions on **57**, 7147 (2011).
[37] I. Savov and M. M. Wilde, Information Theory, IEEE Transactions on **61**, 7017 (2015).
[38] A. S. Holevo, Russian Mathematical Surveys **61**, 301 (2006).
[39] G. De Palma, D. Trevisan, and V. Giovannetti, arXiv preprint arXiv:1610.09967 (2016).

Composably secure time-frequency quantum key distribution

Nathan Walk[1]* and Jonathan Barrett[1] and Joshua Nunn[2]
[1]*Department of Computer Science, University of Oxford, Wolfson Building, Parks Road, Oxford OX1 3QD, United Kingdom*
[2]*Clarendon Laboratory, University of Oxford, Oxford OX1 3PU, United Kingdom*
(Dated: April 1, 2017)

We present a composable security proof, valid against arbitrary attacks and including finite-size effects, for a high dimensional time-frequency quantum key distribution (TFQKD) protocol based upon spectrally entangled photons. Such schemes combine the impressive loss tolerance of single-photon QKD with the large alphabets of continuous variable (CV) schemes, but finite-size security has previously only been proven under the assumption of collective Gaussian attacks. Here, we derive a composable security proof that predicts key rates on the order of Mbits/s over metropolitan distances (40 km or less) and maximum transmission distances of up to 140 km.

Most photonic QKD implementations fall into one of two regimes. Traditional discrete variable (DV) schemes encode the secret key in a two-dimensional Hilbert space such as the polarisation of a single photon. Such protocols now enjoy general, *composable* security proofs [1] that function with reasonably small finite-size data blocks, and converge to the ideal Devetak-Winter rates [2] in the asymptotic limit. Continuous variable (CV) schemes instead utilise an infinite-dimensional Hilbert space, commonly the quadratures of the optical field. Whilst the finite range and precision of real-life detectors ensures the key is never perfectly continuous, CVQKD nevertheless has the capability to achieve greater than one bit per transmission and hence potentially much higher rates. Furthermore, composable, general, finite-size CVQKD security proofs have also appeared, although the present results either require extremely large block sizes [3], or are very sensitive to losses [4] and fail to converge to the Devetak-Winter rates.

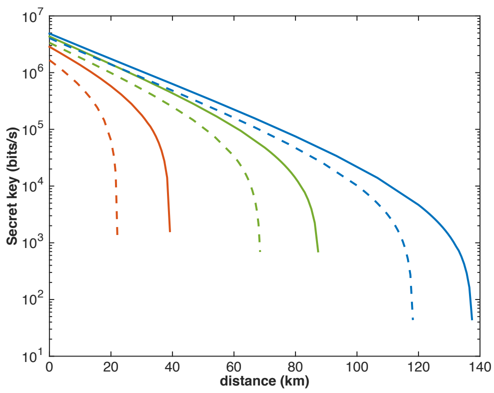

FIG. 1: Secret key rate as a function of transmission distance for protocols where the key is generated from frequency (dashed) or time (solid) variables. Sample sizes are $N = \{10^9, 10^{10}, 10^{11}\}$ in red, green and blue respectively with a security parameter of 10^{-10}.

An alternative approach is to encode the key in the continuous degrees of freedom of single photons, inheriting both the loss tolerance of DVQKD and the larger encoding space of CV protocols [5]. These time-frequency schemes are primarily pursued via the temporal and spectral correlations of single photons emitted during spontaneous parametric down conversion (SPDC) and the security stems from the conjugate nature of frequency and arrival time measurements. Significant progress has been made in security analysis [6], particularly identifying analogies between the time and frequency observables of a single photon and the canonical quadrature observables. However, a general composable security proof is lacking. In this work we present such a proof by combining the entropic uncertainty proofs for CVQKD [4] with efficient, finite-size decoy-state analysis [7] for DVQKD which allows us to rigorously determine the number of single photon events. The resultant proofs allow for high rates key rates over urban and inter-city distances with reasonable block sizes. Detailed proofs, calculations and simulation parameters can be found in [8].

Note added: During the writing up of this work the authors became aware of similar results obtained independently by Niu et al. [9].

References

[1] R. Renner, arXiv:0512258 (2005); M. Tomamichel, C. C. W. Lim, N. Gisin, and R. Renner, Nature Communications **3**, 634 (2012).
[2] I. Devetak and A. Winter, Proceedings of the Royal Society **461**, 207 (2005).
[3] A. Leverrier, Physical Review Letters **114**, 070501 (2015).
[4] F. Furrer et al., Physical Review Letters **109**, 100502 (2012).
[5] B. Qi, Optics Letters **31**, 2795 (2006).
[6] J. Nunn et al., Optics Express **21**, 15959 (2013); Z. Zhang et al., Physical Review Letters **112**, 120506 (2014); C. Lee et al., Quantum Information Processing **14**, 1005 (2015); D. Bunandar et al., Physical Review A **91**, 022336 (2015); H. Bao et al., Journal of Physics A: Mathematical and Theoretical **49**, 205301 (2016).
[7] C. Lim, M. Curty, N. Walenta, F. Xu, and H. Zbinden, Physical Review A **89**, 022307 (2014).
[8] N. Walk, J. Barrett, and J. Nunn, arXiv:1609.09436 (2016).
[9] M. Y. Niu, F. Xu, F. Furrer, and J. H. Shapiro, arXiv:1606.08394, (2016).

An experimental quantum Bernoulli factory

Raj B. Patel[1], Terry Rudolph[2], and Geoff J. Pryde[1]

1. Centre for Quantum Computation and Communication Technology (Australian Research Council), Centre for Quantum Dynamics, Griffith University, Brisbane, QLD 4111, Australia
2. Department of Physics, Imperial College London, Prince Consort Road, London SW7 2AZ, UK.
Author e-mail address: r.patel@griffith.edu.au

In the current absence of full-scale quantum technologies, there has been a concerted effort to prove that a quantum advantage exists across a range information protocols from precision measurement, computation and simulation to secure communications. Recently an area in which a quantum advantage has been revealed is randomness processing which is exemplified in the Bernoulli factory[1].

The Bernoulli factory is an algorithm which takes, as an input, a finite sequence of independent and identically distributed Bernoulli random variables, or coin flips, with an unknown bias *p* and then outputs a new function given by coin with success probability *f(p)*. An early example, attributed to von Neumann[2], is the generation of a fair coin $f(p) = 0.5$ from biased coins for $0 < p < 1$. The coin is flipped twice, if both outcomes are different output the result of the second coin, otherwise repeat. Another example is the case where $f(p) = 2p(1-p)^2$ for which a heads outcome can be simulated when three *p* coins are tossed and either tails/tails/heads or tails/heads/tails are the outcomes, otherwise tails is outputted by the factory. The types of functions simulable by a Bernoulli factory using classical coins of unknown bias *p* was first defined by Keane and O'Brien[1]. A function that cannot be simulated classically with finite resources, but which is of great interest as it may lead to the construction of other Bernoulli factories[3], is $f_\wedge(p) = 2p$.

Recent developments to the theory by Dale *et al.*[4] showed that replacing classical coins with quantum coins or 'quoins' of the form $|p\rangle = \sqrt{p}|0\rangle + \sqrt{1-p}|1\rangle$ not only relaxes the conditions on which functions can be simulated, but also provides a reduction in the number of resources required. Here we report an experimental demonstration of the quantum Bernoulli factory by simulating the function $f_\wedge(p) = 2p$ under two scenarios, one which utilises single qubit measurements in the *X* and *Z* basis[5] and the other which utilises non-classical correlations by performing joint measurements of two qubits in the Bell basis[4]. Qubits given by $|p\rangle = \sqrt{p}|0\rangle + \sqrt{1-p}|1\rangle$ are encoded in the polarisation of single-photons generated from spontaneous parametric downconversion. The exact sequence of measurement outcomes is recorded by time-tagging individual detection events. Sampling from the measurement outcomes, along with classical post-processing, allows $f_\wedge(p)$ to be constructed. For both approaches, we are able to achieve $f_\wedge(0.5) = 0.935$ where we attribute the slight deviation from unity to experimental imperfections. Our experiments reveal that for the single-qubit case, $f_\wedge(p) = 2p$ requires on average 51.6 quoins to construct compared to 11.3 quoins in the two-qubit case, demonstrating that non-classical correlations offer almost a five-fold reduction in resources over single-qubit measurements alone. Fitting the data with a sum of Bernstein polynomials[6] allows us to estimate that ~50000 classical coins would be required to reproduce our data, which shows that the quantum Bernoulli factory, with a resource reduction of three orders of magnitude, shows a clear quantum advantage over the best known classical algorithm.

[1] Keane, M. S. & O'Brien., G. L., "A Bernoulli factory". ACM Trans. Model. Comput. Simul. 4, 213–219 (1994).

[2] Von Neumann, J., "Various techniques used in connection with random digits". Appl. Math Ser. 12, 36–38 (1951).

[3] Nacu, S. & Peres, Y., "Fast simulation of new coins from old". Ann. Appl. Probab. 15, 93–115 (2005).

[4] Dale, H. et al. Provable, "Quantum Advantage in Randomness Processing". Nat. Commun. 6:8203 doi: 10.1038/ncomms9203 (2015).

[5] X. Yuan, "Experimental Quantum Randomness Processing Using Superconducting Qubits". Phys. Rev. Letts. 117, 010502 (2016)

[6] M. Huber, "Nearly Optimal Bernoulli Factories for Linear Functions". Combinatorics, Probability and Computing. 25, 577–591, (2016)

The dawn of quantum networks

Ronald Hanson
TU Delft

This talk will present an overview of our latest progress towards realizing extended quantum networks, including the first loophole-free violation of Bell's inequalities and the first primitive network experiments on a pair of spatially separated two-qubit nodes.

Quantum experiments exploiting the radiation pressure interaction between light and matter

Simon Gröblacher
TU Delft

Mechanical oscillators coupled to light via the radiation pressure force have attracted significant attention over the past years for allowing tests of quantum physics with massive objects and for their potential use in quantum information processing. Recently demonstrated quantum experiments include entanglement and squeezing of both the mechanical and the optical mode. So far these quantum experiments have almost exclusively operated in a regime where the light field oscillates at microwave frequencies. Here we would like to discuss recent experiments where we demonstrate non-classical mechanical states by coupling a mechanical oscillator to single optical photons. These results are a promising route towards using mechanical systems as quantum memories, for quantum communication purposes and as light-matter quantum interfaces.

Measurement-induced quantum state engineering and emulation of strong optical nonlinearities

M. Bellini[1,2], L.S. Costanzo[1,2], N. Biagi[1,2], A.S. Coelho[3], J. Fiurášek[4], A. Zavatta[1,2]

[1]*Istituto Nazionale di Ottica (INO-CNR), Florence, Italy*
[2]*LENS and Department of Physics, University of Firenze, Florence, Italy*
[3]*Departamento de Engenharia Mecânica, Universidade Federal do Piauí, Teresina, PI, Brazil*
[4]*Department of Optics, Palacky University, Olomouc, Czech Republic*

We experimentally perform conditional quantum operations on weak states of light in order to implement highly non-trivial state transformations. Coherently combining sequences of single photon additions and subtractions [1] has recently allowed us to orthogonalize any input light state and to generate coherent superpositions of the input and output states, thus producing arbitrary continuous-variable qubits [2].

Now we show that appropriate combinations of the above elementary quantum operations can faithfully emulate the effect of a strong Kerr nonlinearity on weak states of light. We experimentally demonstrate a nonlinear phase shift at the single-photon level by using weak coherent states as probes and characterizing the output non-Gaussian states with quantum tomography [3]. The strong nonlinearity is clearly witnessed as a change of sign of specific off-diagonal elements of the density matrix expressed in the basis of Fock states.

Both the generation of arbitrary continuous-variable qubits and the emulation of strong Kerr nonlinearities at the single-photon level represent crucial enabling tools for optical quantum technologies and for advanced quantum information processing.

References

[1] M. Bellini and A. Zavatta, Manipulating light states by single-photon addition and subtraction, *Progress in Optics*, **55**, 41-83 (2010)
[2] A.S. Coelho, L.S. Costanzo, A. Zavatta, C. Hughes, M.S. Kim, and M. Bellini, Universal continuous-variable state orthogonalizer and qubit generator, *Phys. Rev. Lett.*, **116**, 110501 (2016)
[3] L.S. Costanzo, A.S. Coelho, N. Biagi, J. Fiurasek, M. Bellini, and A. Zavatta, Measurement-induced strong Kerr nonlinearity for weak quantum states of light, submitted (2017)

Testing fully quantum repeaters on a quantum internet

Stephanie Wehner
TU Delft

A future quantum internet connects small quantum processors by long distance quantum communication. Possibly the most well known application of quantum communication is quantum key distribution, but many other interesting applications already exist. Here, we propose stages towards the development of a full blown quantum internet, where each stage is distinguished by the successively larger type of applications that it supports. We continue by presenting a test to assess the performance of quantum repeaters for transmitting qubits, rather than key bits, which is required by many protocols.

Quantum-Dense Metrology

S. Steinlechner*, J. Zander, M. Ast, and R. Schnabel

Institut für Laserphysik und Zentrum für Optische Quantentechnologien, Universität Hamburg
* email: sebastian.steinlechner@physnet.uni-hamburg.de

Quantum-dense metrology (QDM) constitutes a special case of entanglement-enhanced metrology in which two orthogonal phase space projections of a signal are simultaneously sensed beyond the shot noise limit [1]. In 2013, we showed that the additional sensing channel that is provided by QDM contains information that can be used to identify and to discard corrupted segments from the measurement data. As a potential application, we highlighted the identification of disturbances due to back-scattered light in high-power laser interferometers, such as the GEO600 and AdvLIGO gravitational wave detectors [2] and their future upgrades.
Recently, we proposed and demonstrated a new method in which QDM is used for improving the sensitivity without discarding any measurement segments [3]. Our measurement reached sub-shotnoise performance even though strong classical noise initially polluted the data. Again, applied to the field of gravitational-wave detection, our improved readout could be used to subtract scattering noise shoulders which are known to occur in these detectors, and then go to and beyond the shot-noise limit. The new method has high potential for improving the noise spectral density of gravitational-wave detectors at signal frequencies in the lower audio band, which are of high astrophysical relevance.

References

[1] S. Steinlechner et al., Nat. Phot. **7**, 626-630 (2013)
[2] The LIGO Scientific Collaboration, Class. Quantum Grav. **32**, 074001 (2015)
[3] M. Ast et al., Phys. Rev. Lett. **117**, 180801 (2016)

Correlation Plenoptic Imaging

F.V. Pepe[1,2], F. Di Lena[2,3], A. Mazzilli[3], A. Garuccio[2,3,4], G. Scarcelli[5] and M. D'Angelo[2,3,4]

[1] *Museo Storico della Fisica e Centro Studi e Ricerche "Enrico Fermi", Roma (Italy)*

[2] *INFN Sezione di Bari, Bari (Italy)*

[3] *Dipartimento Interateneo di Fisica, Università degli Studi di Bari, Bari (Italy)*

[4] *Consiglio Nazionale delle Ricerche - Istituto Nazionale di Ottica, Sesto F.no, Italy*

[5] *Fischell Department of Bioengineering, University of Maryland, College Park-MD (USA)*

e-mail: milena.dangelo@uniba.it

Traditional optical imaging faces an unavoidable trade-off between resolution and depth of field (DOF). To increase resolution, high numerical apertures (NA) are needed, but the associated large angular uncertainty results in a limited range of depths that can be put in sharp focus.

Plenoptic imaging was introduced a few years ago to remedy this trade-off. To this end, plenoptic imaging reconstructs the path of light rays from the lens to the sensor [1]. This is practically achieved by inserting a microlens array in the conjugate plane of the object (as created by the main lens), and moving the sensor in the conjugate plane of the main lens (as created by each microlens). The microlens array also enables the single-shot acquisition of multiple-perspective images, thus making plenoptic imaging one of the most promising techniques for 3D imaging. Plenoptic imaging is currently used in commercial digital cameras enhanced by refocusing capabilities. A plethora of innovative applications, from 3D-imaging, to stereoscopy, and microscopy are also being developed (e.g., [2]). However, the improvement offered by standard plenoptic imaging is practical rather than fundamental: the increased DOF leads to a proportional reduction of the resolution well above the diffraction limit imposed by the lens NA [1]. Also, the change of perspective is effectively strongly limited by the small field of view of the microlenses [1].

We demonstrate that this fundamental limitation can be overcome by taking advantage of the position-momentum correlation characterizing both entangled and chaotic sources. In Correlation Plenoptic Imaging (CPI), we exploit the spatio-temporal correlation of such light sources to push plenoptic imaging to its fundamental limits of both resolution and DOF [3-6]. The scheme for the theoretical and experimental demonstration of CPI with a chaotic source is reported in Fig. 1 [5,6]. By measuring intensity correlations between the two sensors, multiple images of the object can be retrieved on S_a, and are focused if the optical distance z_a is equal to the distance z_b. Each image corresponds to a different pixel of S_b, hence to light emitted by a different point of the source. Information encoded in the intensity correlation function can be used to effectively refocus largely out-of-focus images, while keeping diffraction-limited resolution. The intensity correlation function thus possesses plenoptic imaging properties, namely, it encodes both the spatial and the directional information enabling its key refocusing capability. As shown in the right panel of Fig. 1, CPI enables a combination of resolution and DOF that is not accessible to classical imaging systems. In particular, we have demonstrated diffraction limited imaging with a DOF increased by a factor of three with respect to standard imaging (point C in Fig. 1).

Our results represent the theoretical and experimental basis for the effective development of the promising applications of plenoptic imaging. The plenoptic application is the first situation in which the counterintuitive properties of correlated systems are effectively used to beat intrinsic limits of state-of-the-art imaging systems.

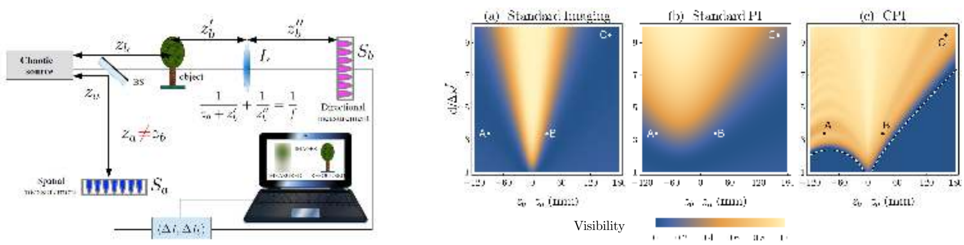

Figure 1: (left panel) CPI setup with chaotic light. (right panel) Visibility of a double-slit mask in the three indicated imaging systems. Points A, B, and C represent experimental measurements of out-of-focus and refocused images.

[1] R. Ng, et al., Tech. Rep. CSTR 2005-02, Stanford Computer Science (2005).
[2] R. Prevedel, et al., Nat. Meth. **11**, 727 (2014).
[3] M. D'Angelo, et al., Phys. Rev. Lett. **116**, 223602 (2016).
[4] F. V. Pepe, et al., Technologies **4**, 17 (2016).
[5] M. D'Angelo, et al., Eur. Pat. App. EP17160543.9
[6] F. V. Pepe, et al., arXiv:1703.03830

Quantum enhanced absorption measurement and wide field microscopy

***Ivano Ruo-Berchera*[1], *Nigam Samantaray*[1], *Alice Meda*[1], *Elena Losero*[1], *Alessio Avella*[1], *Marco Genovese*[1,2]**

1. Istituto Nazionale di Ricerca Metrologica (INRIM), 91Strada delle Cacce, IT-10135 Turin, Italy

2. INFN Sezione di Torino, via P. Giuria 1, 10125, Torino, Italy

Several proof of principle experiments have demonstrated the advantages of quantum metrology and sensing schemes over classical counterparts, although the present challenge is to overcome the gap between the proof of principles and the real applications. For example, probing and imaging delicate systems using small number of photons with true and significant sensitivity improvement (without post selection or a-posteriori loss compensation) is extraordinarily important. Here, we present the latest achievements in quantum enhanced imaging exploiting photon number correlations in twin beams. First we investigate experimentally different estimators of the absorption, and compare the results with the best known strategy (i.e. using Fock states probe) [1], also discussing some practical issues concerning the "hidden" assumptions on the stability of the source and detector response. Then, we describe the realization of a sub-shot-noise (SSN) wide field microscope [2], based on spatially multi-mode non-classical photon number correlations [3]. The microscope produces real-time images of 8000 pixels at full resolution, for $(500\mu m)^2$ field-of-view, with noise reduced at 80% of the shot noise level in each pixel. This is suitable for absorption imaging of complex structures, like biological samples. By simple post-elaboration, specifically applying a "quantum enhanced median filter", the noise is further reduced (less than 30% of the shot noise level) by setting a trade-off with the resolution. It realizes the best sensitivity per incident photon ever achieved in absorption microscopy.

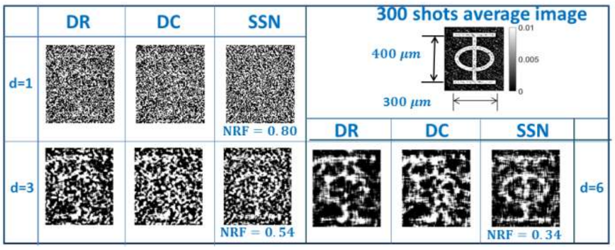

Fig. 1. Experimental imaging of a sample (in this case a ultra-thin metallic deposition on a glass slide with absorption coefficient of 1%). Single shots of direct imaging at the shot noise level (DR), differential classical imaging (DC) and sub-shot-noise imaging (SSN) are compared. The higher spatial resolution is 5 μm (d=1, top left series) while images at lower resolution (L = d*5μm, specifically for d=3 and d=6) are obtained by the application of a median filter to the shots at full resolution. From d = 3 the object start to appear in the SSN image, while it remains almost undefined in the classical images. The number of photon per pixel (which size corresponds to 5 μm in the object plane) is n_{ph}=1000. The top-right panel represents the object reconstructed by 300 shots average.

Fig. 1 shows the wide field imaging of a test sample. The performances achieved in [2] are far beyond the ones reported in previous proofs of principle of lens-less SSN wide field imaging [4], improving the spatial resolution by a factor 10-100 and reaching for the first time a true and significant improvement of the sensitivity with respect to any classical absorption microscopy at the same illumination level without any post-selection.

We believe that this technique has the potentiality for a wide-spread use in absorption microscopy of delicate systems or to investigate the properties of photosensitive structure at few-photons level.

References

[1] G. Adesso, F. Dell'Anno, S. De Siena, F. Illuminati, and L. A. M. Souza," Optimal estimation of losses at the ultimate quantum limit with non-Gaussian states", Phys. Rev. A **79**, 040305 (2009); A. Monras and M. G. A. Paris, "Optimal Quantum Estimation of Loss in Bosonic Channels"Phys. Rev. Lett. **98**, 160401(2007).

[2] N. Samantaray , I. Ruo-Berchera, A. Meda, M. Genovese 2016, "Realisation of the first sub shot noise wide field microscope," Light Sciene & Applications, doi: 10.1038/lsa.2017.5 (to appear); arXiv:1612.06169 [quant-ph].

[3] E. Brambilla, L. Caspani, O. Jedrkiewicz, L. A. Lugiato, and A. Gatti, "High-sensitivity imaging with multimode twin beams", Phys. Rev. A **77**, 053807 (2008).

[4] G. Brida, M. Genovese & I. Ruo Berchera, "Experimental realization of sub-shot-noise quantum imaging," Nature Photonics **4**, 227 (2010); G. Brida, M. Genovese, A. Meda, & I. Ruo Berchera, "Experimental quantum imaging exploiting multimode spatial correlation of twin beams," Phys. Rev. A **83**, 033811 (2011).

Hybrid Quantum Information Processing; A Way for Large-scale Optical Quantum Information Processing

Akira Furusawa
The University of Tokyo, 7-3-1 Hongo, Bunkyo-ku, Tokyo 113-8656, Japan

We are working on hybrid quantum information processing, which combines two methodologies of quantum information processing – qubit and continuous variable (CV) [1]. More precisely, we encode logical qubits by using CV methodology and utilize CV quantum processors for the realization of a fault-tolerant large-scale universal optical quantum computer. The advantage of this methodology is that we can have both high-fidelity nature of qubits and determinisity of CV quantum processors. In other words, we can enjoy both particle- and wave-nature of quantum mechanics. Towards this goal we performed various things, which include quantum error correction with nine-party CV entanglement [2], teleportation of Schrödinger's cat state [3], adaptive homodyne measurement with phase-squeezed states [4], deterministic teleportation of time-bin qubits [5], creation of ultra-large-scale CV cluster states [6], generation and measurement of CV entanglement on a chip [7], and synchronization of photons with cavity-based quantum memories [8].

References

[1] A. Furusawa and P. van Loock, Quantum Teleportation and Entanglement: A Hybrid Approach to Optical Quantum Information Processing, (Wiley-VCH, Weinheim, 2011).
[2] T. Aoki, G. Takahashi, T. Kajiya, J. Yoshikawa, S. L. Braunstein, P. van Loock, and A. Furusawa, Nature Physics 5, 541 (2009).
[3] N. Lee, H. Benichi, Y. Takeno, S. Takeda, J. Webb, E. Huntington, and A. Furusawa, Science 332, 330 (2011).
[4] H. Yonezawa, D. Nakane, T. A. Wheatley, K. Iwasawa, S. Takeda, H. Arao, K. Ohki, K. Tsumura, D. W. Berry, T. C. Ralph, H. M. Wiseman, E. H. Huntington, and A. Furusawa, Science 337, 1514 (2012).
[5] S. Takeda, T. Mizuta, M. Fuwa, P. van Loock, and A. Furusawa, Nature 500, 315 (2013).
[6] S. Yokoyama, R. Ukai, S. C. Armstrong, C. Sornphiphatphong, T. Kaji, S. Suzuki, J. Yoshikawa, H. Yonezawa, N. C. Menicucci, and A. Furusawa, Nature Photonics 7, 982 (2013).
[7] G. Masada, K. Miyata, A. Politi, T. Hashimoto, J. L. O'Brien, and A. Furusawa, Nature Photonics 9, 316 (2015).
[8] K. Makino, Y. Hashimoto, J. Yoshikawa, H. Ohdan, T. Toyama, P. van Loock, and A. Furusawa, Science Advances 2, e1501772 (2016).

CV quantum communication

Gerd Leuchs
MPL Erlangen

Super-resolution from single photon emission: toward biological application

P. Traina, E. Moreva, J. Forneris, F. Picollo, S. Ditalia, I. Ruo-Berchera, P. Olivero, V.Carabelli, I. P. Degiovanni, G. Brida, and M. Genovese

Properties of quantum light represent a tool for overcoming limits of classical optics.
Several experiments have demonstrated this advantage ranging from quantum enhanced imaging to quantum illumination [1].

In this talk, after a general introduction discussing last developments in the field (as sub shot noise quantum microscopy) , I will present a work [2] where we experimentally demonstrate quantum enhanced resolution in confocal fluorescence microscopy. This is achieved by exploiting the non-classical photon statistics of fluorescence emission of single nitrogen-vacancy color centers in diamond. By developing a general model of super-resolution based on the direct sampling of the kth-order autocorrelation function of the photoluminescence signal, we show the possibility to resolve, in principle, arbitrarily close emitting centers.

Finally, ongoing applications in biology will be discussed and presented.

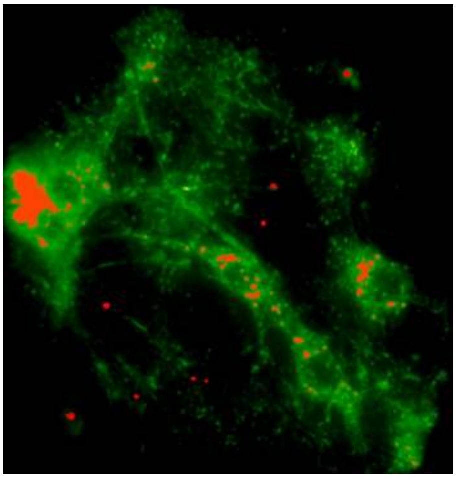

Fluorescence from nanodiamonds in neurons

[1] "Real applications of quantum imaging", M.Genovese, Journal of Optics, 18 (2016) 073002
[2] "Beating the Abbe Diffraction Limit in Confocal Microscopy via Nonclassical Photon Statistics" D. Gatto Monticone, K. Katamadze, P. Traina, E. Moreva, J. Forneris, I. Ruo-Berchera, P. Olivero, I.P. Degiovanni, G. Brida,M. Genovese;
Phys. Rev. Lett. 113, 143602 (2014)

Coupling atomic arrays to nanofibers: generation, storage and reflection of single photons

N.V. Corzo, A. Chandra, J. Raskop, B. Gouraud, D. Kupriyanov, A.S. Sheremet, J. Laurat

Laboratoire Kastler Brossel, UPMC-Sorbonne Universités, CNRS, ENS-PSL Research University, Collège de France, 4 Place Jussieu, 75005 Paris, France

In recent years, the coupling of one-dimensional waveguides and atoms, either real or artificial, has raised a large interest. Beyond the remarkable ability to couple a single emitter to a guided mode, this approach would also enable all-fibered quantum memories and interfaces and the engineering of photon-mediated long-range interactions between multiple qubits. This emerging field of waveguide quantum electrodynamics promises unique applications to quantum networks, quantum nonlinear optics, and quantum simulation.

In this talk, I will present our ongoing efforts based on 1D chains of cold atoms trapped near a subwavelength-diameter optical fiber. I will focus on this implementation and describe our recent observations of collective effects: the demonstration of EIT optical storage in this all-fibered setting [1], the heralding of a single collective excitation and its subsequent conversion in a guided single photon, and the observation of a large Bragg reflection up to 75% for the guided light [2]. While the first two experiments rely on the overall optical depth of the medium, the third one results from long-range order of the atoms. In each experiment, only 2000 atoms were sufficient due to tight transverse confinement. These observations demonstrate key ingredients for the exploration of a variety of emerging and potentially rich protocols based on 1D reservoirs coupled to atoms.

[1] B. Gouraud *et al.*, Demonstration of a memory for tightly guided light in an optical nanofiber, Phys. Rev. Lett. 114, 180503 (2015).

[2] N.V. Corzo *et al.*, Large Bragg reflection from one-dimensional chains of trapped atoms near a nanoscale waveguide, Phys. Rev. Lett. 117, 133603 (2016).

Tunable single photon source from an atomic quantum memory for storage in a highly excited Rydberg state

Pau Farrera[1]***, Emanuele Distante***[1]***, Auxiliadora Padrón-Brito***[1]***, Boris Albrecht***[1]***, David Paredes-Barato***[1]***, Georg Heinze***[1]***, and Hugues de Riedmatten***[1,2]

1. ICFO-Institut de Ciencies Fotoniques, The Barcelona Institute of Science and Technology, 08860 Castelldefels (Barcelona), Spain

2. ICREA-Institució Catalana de Recerca i Estudis Avançats, 08015 Barcelona, Spain

Melvyn Ho[3]***, Matías Chávez***[3]***, Colin Teo***[4,5]***, and Nicolas Sangouard***[3]

3. Department of Physics, University of Basel, Klingelbergstrasse 82, 4056 Basel, Switzerland

4. Institute for Quantum Optics and Quantum Information of the Austrian Academy of Sciences, A-6020 Innsbruck, Austria

5. Institute for Theoretical Physics, University of Innsbruck, A-6020 Innsbruck, Austria

Quantum information science and technology critically rely on generation and processing of single photons, the natural carriers of quantum information in this context. The ability to realize strong interactions between single photons would enable new powerful applications like photonic quantum computing or deterministic Bell state measurements [1]. A promising approach to obtain that capability is based on mediating photon-photon interactions via strong Dipole-Dipole interactions, when one photon is stored via electromagnetically induced transparency (EIT) in a Rydberg atom. This, however, requires single photons, which are spectrally compatible with the conditions set by the atomic energy structure and EIT.

We present a single photon source based on a cold cloud of Rubidium atoms, which is capable of generating single photons with highly tunable wave shape [2]. We follow the DLCZ protocol [3] to generate single read photons, which are emitted on demand after a single collective spin excitation inside the cloud was heralded by an initial write photon. By tuning the shape of the classical read-out pulse, we demonstrate that single read photons with durations varying over three orders of magnitude up to 10 µs can be generated without a significant change of read-out efficiency. We prove the non-classicality of the emitted photons by measuring their antibunching, showing near single photon behavior at low excitation probabilities. We also show that the photons are emitted in a pure state by measuring unconditional autocorrelation functions. Finally, to demonstrate the usability of the source for realistic applications, we create ultra-long single photons with a rising exponential or doubly peaked wave shape which are important for several quantum information tasks.

The tunablility of our source permitted us to generate single photons which are compatible with a Rydberg atomic system. We performed an experiment, in which we first generated single photons of subnatural linewidth and afterwards stored them via EIT as a Rydberg excitation in a different cold Rubidum cloud [4]. We demonstrated that after storage and retrieval of the single photon on a highly excited Rydberg (n=60) the quantum correlations between the initial write photon and the retrieved read photon are preserved. We show that quantum statistics persist up to storage times of around 5 µs in the Rydberg medium and 30 µs in the DLCZ system. Finally, we prove the highly nonlinear response of the Rydberg ensemble by sending weak coherent states.

Our result is an important step towards deterministic photon–photon interactions, and may enable deterministic Bell-state measurements with multimode quantum memories.

References

[1] D. E. Chang, V. Vuletić, and M. D. Lukin, Nat. Photonics **8**, 685-694 (2014).

[2] P. Farrera, G. Heinze, B. Albrecht, M. Ho, M. Chávez, C. Teo, N. Sangouard, and H. de Riedmatten, Nat. Commun. **7**, 13556 (2016).

[3] L. M. Duan, M. D. Lukin, J. I. Cirac, and P. Zoller, Nature **414**, 413 (2001).

[4] E. Distante, P. Farrera, A. Padrón-Brito, D. Paredes-Barato, G. Heinze, and H. de Riedmatten, Nat. Commun. **8**, 14072 (2017).

Experimental demonstration of photonic quantum Fredkin gate and its applications

R. Stárek, M. Mičuda, M. Miková, I. Straka, M. Dušek, P. Marek, M. Ježek, R. Filip, and J. Fiurášek
Department of Optics, Palacký University, 17. listopadu 1192/12, 77146 Olomouc, Czech Republic

Quantum Fredkin gate represents one of the fundamental quantum gates with many potential applications in quantum information processing. Here we report on experimental realization of an optical quantum Fredkin gate for qubits encoded into states of single photons. We utilize this gate for implementation of several important quantum information protocols such as optimal quantum cloning [1, 2], optimal purification of single qubits [3], or direct nondestructive measurements of purity and overlap of quantum states [4, 5].

As shown in Fig. 1, our Fredkin gate is realized as a sequence of a two-qubit quantum CNOT gate, a three-qubit quantum Toffoli gate (a CCNOT gate), and another two-qubit CNOT gate. Combination of several linear optical quantum gates becomes possible due to our specific qubit encoding, where two qubits are encoded into polarization and path degrees of freedom of one photon, while the third qubit is encoded into polarization of a second photon. With this qubit representation, the CNOT gates can be implemented deterministically with linear optics while the quantum Toffoli gate is realized by two-photon interference on an unbalanced beam splitter [6]. The core of our setup is composed of six calcite beam displacers which form an inherently stable multipath optical interferometer. Among other tasks, the beam displacers realize a deterministic SWAP operation between the polarization and path qubits, which enables us to implement all other gates by addressing the polarization degrees of freedom with wave plates and partially polarizing beam splitters.

We have performed full tomographic reconstruction of the implemented quantum Fredkin gate. This tomographic characterization yielded a quantum gate fidelity of $F = 0.901(1)$. By preparing the control qubit of the Fredkin gate in the superposition state $\frac{1}{\sqrt{2}}(|0\rangle + |1\rangle)$ and measuring this qubit at the gate output in the superposition basis $\frac{1}{\sqrt{2}}(|0\rangle \pm |1\rangle)$ we can perform symmetrization or anti-symmetrization of the state of the two target qubits. This is a fundamental quantum operation which has many important applications including optimal quantum cloning [1, 2], purification of single-qubit states [3], implementation of a programmable universal quantum measurement device [7], and measurement of purity and overlap of quantum states [4, 5].

We have successfully tested all these applications with our quantum Fredkin gate and investigated some of their peculiar properties, such as the non-destructive character of the purity measurement. This latter application requires two copies of the quantum state ρ whose purity should be measured. The target qubits are prepared in the state $\rho \otimes \rho$ and the purity is estimated from the measurements on the control qubit. Remarkably, the reduced density matrices of the output target qubits remain unperturbed at the output of the gate. However, the purity measurement introduces correlations between the two copies of the state which prevents subsequent extraction of any further information on the state purity by the same procedure.

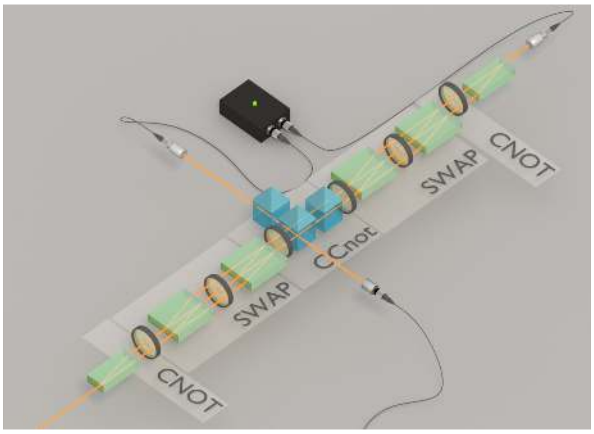

FIG. 1: Schematic experimental setup of the linear optical quantum Fredkin gate. Calcite beam displacers are indicated by light green color and the partially polarizing beam splitters have a blue color.

Our comprehensive characterization of the performance of quantum Fredkin gate clearly confirms its versatility and usefulness in various areas of quantum information processing.

Acknowledgments This work was supported by the Czech Science Foundation (GA16-17314S).

[1] W.T.M. Irvine, A. Lamas Linares, M.J.A. de Dood, and D. Bouwmeester, Phys. Rev. Lett. **92**, 047902 (2004).
[2] M. Ricci, F. Sciarrino, C. Sias, and F. De Martini, Phys. Rev. Lett. **92**, 047901 (2004).
[3] J.I. Cirac, A.K. Ekert, and C. Macchiavello, Phys. Rev. Lett. **82**, 4344 (1999).
[4] R. Filip, Phys. Rev. A **65**, 062320 (2002).
[5] A.K. Ekert *et al.*, Phys. Rev. Lett. **88**, 217901 (2002).
[6] M. Mičuda *et al.*, Phys. Rev. Lett. **111**, 160407 (2013).
[7] J. Fiurášek, M. Dušek, and R. Filip, Phys. Rev. Lett. **89**, 190401 (2002).

Floquet quantum simulation

Oleksandr Kyriienko and Anders S. Sørensen
The Niels Bohr Institute, University of Copenhagen,
Blegdamsvej 17, DK-2100 Copenhagen, Denmark

A quantum simulator is a programmable quantum device, which can mimic the complex quantum system of interest. Given the difficulty for classical treatment of quantum objects, it can potentially allow access to the physics of medium size molecules and frustrated spin lattices, thus solving open problems of quantum chemistry and magnetism.

Typically the quantum simulation can be divided into two separate types: a digital simulation and an analog simulation (emulation). A digital quantum simulation approach relies on discretization of the Hamiltonian evolution using a set of quantum gates. The digital technique has the advantage of being potentially universal and does not depend on the details of the exploited experimental platform. However, typically it requires exploitation of the Trotterization technique, where a fixed product of unitary operators (Trotter step) is repeated many times. Thus it only works in the systems where many quantum gates of very high fidelity are accessible.

An analog quantum simulation approach is based on the engineering of the Hamiltonian of interest in the physical setup, using interactions and controls native to the platform. This allows to largely simplify the simulation and achieve higher fidelities for a restricted operation time, thus being profitable for all modern setups (e.g. atoms in optical lattices, trapped ions, and superconducting qubits). However, the requirement of being able to construct a physical implementation of a tunable Hamiltonian is an obstacle for reconfigurable quantum simulation, and thus makes it very model-specific. Considering the huge interest in quantum simulators, the natural question to ask is: can one join the advantages of an analog and a digital approach?

In the talk we will discuss a Floquet quantum simulation strategy, which bridges the gap between the two simulator types. It relies on the time-dependent modulation of the Hamiltonian $H(t) = H_0 + H_1(t)$, where H_0 is a time-independent part, and $H_1(t) = H_1(t + 2\pi/\omega)$ is periodic, with ω being the frequency of the modulation. When ω is larger than all other frequencies in the Hamiltonian, the dynamics of the system at integer numbers of periods can be described by an effective Floquet Hamiltonian H_F, which can be qualitatively different from the original static Hamiltonian H_0. This allows to engineer various H_F for the system simply by manipulating drive parameters, thus yielding reconfigurable approach to an analog-like quantum simulation. This approach for instance has been applied to shaken optical lattices, and shown to generate effective gauge fields for atoms [1].

We show how Floquet quantum simulation approach can be used for accessing the physics of spin systems using nonlinear superconducting circuits (SC) to represent a chain of qubits (see sketch in Fig. 1). The algorithm relies on fast time modulation of an effective magnetic field for the qubits, such that starting from the isotropic flip-flop interaction, different types of two-qubit couplings can be engineered. The resulting time-averaged Floquet Hamiltonian is of the generic Heisenberg XYZ type, and is controllable by the drive parameters. As examples we show recipes for designing transverse Ising and non-stoquastic XYZ Hamiltonians, and simulate annealing to the ground state of each configuration [2]. Considering the imperfections of SC, corresponding to finite anharmonicity and the associated leakage, we find that the Floquet approach outperforms digital simulation unless ultrahigh fidelity gates are used for the digital approach. For realistic parameters the procedure allows closely following the ideal continuous annealing, yielding a fidelity corresponding to the one achievable by digital evolution with many (>15) Trotter steps. Finally, we show that access to topologically nontrivial generalized cluster and dual cluster Hamiltonians can be attained in the currently existing setups, where the amplitude of the flip-flop interqubit coupling can be modulated in time.

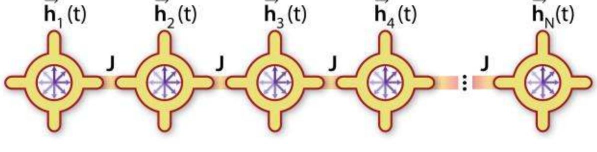

Figure 1. A chain of superconducting qubits coupled through isotropic XY coupling J, each subject to a periodically modulated effective magnetic field $h_j(t)$.

[1] N. Goldman and J. Dalibard, Phys. Rev. X 4, 031027 (2014).
[2] O. Kyriienko and A. S. Sørensen, arXiv:1703.04827 (2017).

Quantum non-Gaussianity of photons and phonons

Radim Filip
Palacký University Olomouc

We will present recent theoretical and experimental achievements in a direct diagnostics of nonclassical and quantum non-Gaussian states of many photons and phonons. We will report on a detection of non-classical light already from many hundreds of single-photon emitters and quantum non-Gaussian light from nine emitters and its application.

A noise-free quantum memory

Joshua Nunn
University of Oxford

We present a new quantum memory protocol for coherent light storage based on off-resonant cascaded absorption (ORCA) in warm atomic vapour. The ORCA memory is broadband and noise free, and we demonstrate the storage of GHz-bandwidth heralded single photons without any degradation in the measured anti-bunching of g(2) = 0.02.

Schrödinger's cats in quantum optics

Alexander E. Ulanov, Demid V. Sychev, Anastasia A. Pushkina, Matthew W. Richards, Ilya A. Fedorov, Philippe Grangier, and A. I. Lvovsky

In famous Schrödinger's thought experiment proposed in 1935 [1], a living or dead cat is entangled with a state of a radioactive atom, thereby forming a macroscopic quantum superposition state. This paradox was originally used to show strangeness of quantum mechanics when applied to macroscopic objects. In modern physics, the Schrödinger's cat state (SCS) is sometimes understood as a coherent superposition of two macroscopically distinct states. Nowadays such states have been obtained in diverse physical systems, for example in ionic ensembles and superconducting circuits. In the optical domain, the SCS is a coherent superposition of two coherent states $\pm\alpha$, which are considered the most classical of all states of light.

SCS are of wide interest both from fundamental and practical points of view. Optical SCS are useful in quantum information science. They can serve as a basis for quantum computation [2], metrology [3] and teleportation[4]. Besides the applied interest, the SCS is expected to help answering a fundamental question [5–7]: at what degree of macroscopicity, if any, does the world stop being quantum?

For the most of the above applications, it is necessary to have SCSs of high amplitude so that states $|\pm\alpha\rangle$ are nearly orthogonal; this is achieved for $\alpha \gtrsim 2$ [2]. But existing methods of optical SCS preparation, such as the photon subtraction from squeezed vacuum [8] or arbitrary Fock-state engineering [9, 10] allow to generate cats only with relatively small amplitudes.

We experimentally implement two protocols of heralded SCS preparation:

1. We develop and test a hybrid protocol of loss-tolerant remote SCS engineering. We experimentally obtain a negative SCS of amplitude 1.84 and fidelity 88% despite 10 dB of total loss between the parties involved in the preparation process [11].

2. We implement a method, proposed by Lund et al. [12], of amplifying optical SCSs by linear optical manipulation and conditional measurements [13]. In the experiment, we convert a pair of negative squeezed SCS of amplitude 1.25 to a single positive SCS of amplitude 2.15 with a success probability of 0.2 and fidelity 86 %. The results are shown in Fig. 1.

[1] Schrödinger, E., *Naturwissenschaften* **23**, 807812 (1935).
[2] Ralph, T. C., Gilchrist, A., Milburn, G. J., Munro, W. J. & Glancy, S., *Phys. Rev. A* **68**, 042319 (2003).
[3] Joo, J., Munro, W. J. & Spiller, T. P., *Phys. Rev. Lett.* **107**, 083601-083601 (2011).
[4] Lee, S.-W. & Jeong, H., *Phys. Rev. Lett.* **87**, 022326 (2012).
[5] Haroche, S., *Rev. Mod. Phys.* **85**, 10831102 (2013).
[6] Wineland, D. J., *Rev.Mod. Phys.* **85**, 11031114 (2013).
[7] Markus, A. & Hornberger, K., *Nature Physics* **10**, 271277 (2014).
[8] Ourjoumtsev, A., Tualle-Brouri, R., Laurat, J. & Grangier, P., ,*Science* **312**, 8386 (2006).
[9] Bimbard, E., Jain, N., MacRae, A. & Lvovsky, A. I., *Nature Photonics* **4**, 243-247 (2010).
[10] Ourjoumtsev, A., Jeong, H., Tualle-Brouri, R. & Grangier, P., , *Nature* **448**, 1784-1786 (2007).
[11] Ulanov, A. E., Fedorov, I. A., Sychev, D., Grangier, P. & Lvovsky, A. I., *Nature Communications* **7**, 11925 (2016).
[12] Lund, A. P., Jeong, H., Ralph, T. C. & Kim, M. S., *Phys. Rev. A* **70**, 020101 (2004).
[13] Sychev, D. V., Ulanov, A. E., Pushkina, A. A., Richards, M. W., Fedorov, I. A., and Lvovsky, A. I., preprint arXiv:1609.08425, accepted to *Nature Photonics.*

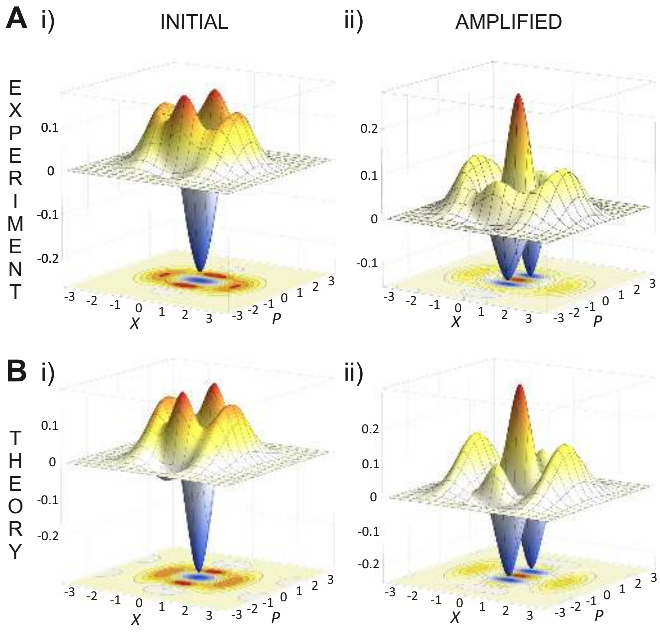

FIG. 1. Wigner functions of the initial and amplified SC states. **A**: Experimental reconstruction via homodyne tomography corrected for the total quantum efficiency of 50%. **B**: Best fit with the ideal, squeezed SC state. Left (i) [right (ii)]: initial [amplified] SC state. The best fit state is $|\mathrm{SC}_-[1.25]\rangle$ [$|\mathrm{SC}_+[2.15]\rangle$] squeezed by 1.73 dB [3.47 dB]. The fidelity between the theoretical and experimental [corrected] states is 93% [86%].

Simulation of complex quantum networks with quantum multimode resources based on optical frequency combs

Valentina Parigi
J. Nokkala, F. Arzani, F. Galve, R. Zambrini , S. Maniscalco, J. Piilo, C. Fabre, N. Treps,

We are currently developing a versatile experimental photonic platform for simulating complex quantum networks. The platform consists of intrinsically multimode systems based on parametric processes pumped by optical frequency combs. The spectrum of these lasers is constituted by hundreds of thousands of frequency components. The parametric process in the non-linear crystal couples all these optical frequencies, and generates non-trivial multimode Gaussian quantum states [1]. These can be equally described as a set of different spectral-temporal modes of light, which can be individually addressed and simultaneously occupied by squeezed vacuum. This resource can be pictured as a network where each node is an electromagnetic-field mode and the connection are entanglement relations involving the quadratures of the field. The structure of the network will be controlled by shaping the pump in the parametric process and by multimode homodyne measurements. The strategy has partly been used for implementing cluster states in a measurement based quantum computing scenario [2,3]. The Bloch-Messiah reduction of the multimode state, which (for pure states), describe the resource as an ensemble of single-mode squeezers and multiport-interferometers is at the core of the method I will present to establish the mapping between our resource and complex networks [4]. We will study the optimization of quantum information protocols in complex structures and we will simulate the dynamics of complex finite quantum environment [5]. Finally, a particular implementation of the parametric process allowing multiplexing in wavelength and time, will simulate networks exhibiting community structures.

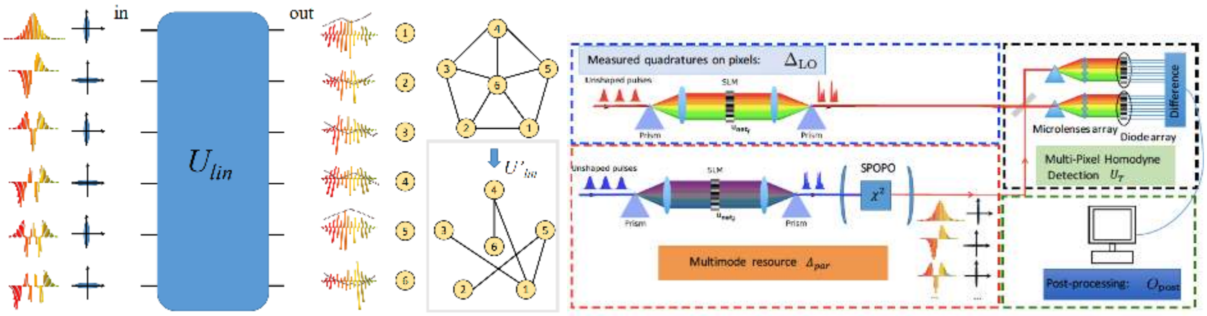

Left: The resource can be described as a collection of squeezed vacua and a basis change like the one given by a multiport-interferometer. The graphical representation of entanglement connections between the output modes shows the network structure. By changing U_{lin}, different kind of networks can be realized. Right: Experimental implementation of the network in the frequency domain.

[1] S. Gerke, J. Sperling, W. Vogel, Y. Cai, J. Roslund, N. Treps, C. Fabre Phys. Rev. Lett. 114,050501 (2015)
[2] R. Medeiros de Araujo et al. Phys. Rev A 89, 053828 (2014)
[3] J. Roslund, R. M. de Araujo, S. Jiang, C. Fabre, and N. Treps, Nat. Photonics 8, 109 (2014)
[4] J. Nokkala, F. Arzani, F. Galve, R. Zambrini , S. Maniscalco, J. Piilo, C. Fabre, N. Treps, V. Parigi, in preparation.
[5] J. Nokkala, F. Galve, R. Zambrini, S. Maniscalco and J. Piilo, Scientific Reports 6, 26861 (2016)

Ultimate precision limit for noisy frequency estimation

A. Smirne[1], J. Kołodyński[2], S. F. Huelga[1], and R. Demkowicz-Dobrzański[3]

[1] *Institute of Theoretical Physics, Universität Ulm, Germany*
[2] *ICFO-Institut de Ciències Fotòniques, Castelldefels (Barcelona), Spain*
[3] *Faculty of Physics, University of Warsaw, Poland*

Quantum metrology protocols allow to surpass the precision limits typical to classical statistics. Given an increasing number N of probes independently prepared to sense a parameter of interest, the central limit theorem constraints the estimation error to decrease at most as $1/N$, while the use of initially entangled probes enables in principle to reach the $1/N^2$ scaling, the so-called Heisenberg limit [1]. The interaction of the probes with the environment is known to limit considerably such an improvement, possibly reducing it to a constant factor over the classical scenario [2,3]. Here [4], we present a novel attainable limit to the precision of the frequency estimation in the presence of noise, which holds for a wide class of qubit open-system dynamics and includes several physical scenarios of practical interest. Exploiting the time inhomogeneous nature of the noisy evolution, we show that the classical limit can be actually overcome by means of initially entangled states, even if the Heisenberg limit is not within reach. The optimal strategy to minimize the estimation error involves measurements on shorter and shorter times, with the increasing of N, and makes use of the deviations from the exponential decay, which are typical of the quantum Zeno regime. We demonstrate that the ultimate attainable precision is fixed by the short-time expansion of the effective noise parameters, irrespective of any possible subsequent memory (non-Markovian) effect. The metrological limit we derive relies on recently introduced powerful techniques [5,6] to evaluate the quantum Fisher information of generic quantum states, and on general properties of the open-system dynamics. As a consequence, our results can be applied to very different real-world settings, without the need for a detailed characterization of the environmental features or the interaction mechanisms.

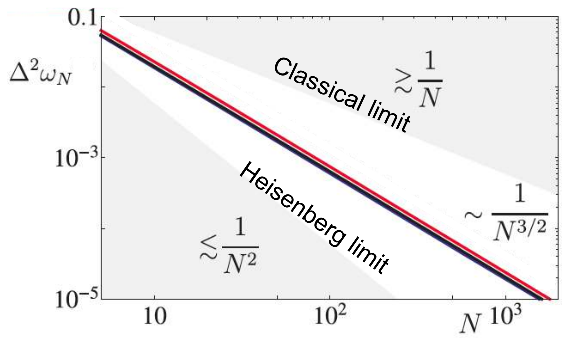

FIG. 1: The interaction with an environment with a finite correlation time allows for noisy metrological limits that surpass the standard quantum limit imposed by the central limit theorem. We demonstrate the existence of a fundamental (Zeno) limit (in black) to the best attainable precision in noisy frequency estimation and its attainability (in red) using quantum probes initially prepared in an entangled state. While the asymptotic Zeno-resolved precision is above the Heisenberg unitary limit, no further improvements are feasible by exploiting non Markovian effects and therefore this bound provides a fundamental limit to the resolution for a broad class of system-environment interactions.

[1] V. Giovannetti, S. Lloyd, and L. Maccone, Science **306**, 1330 (2004)

[2] S. F. Huelga, C. Macchiavello, T. Pellizzari, A. K. Ekert, M. B. Plenio, and J. I. Cirac, Phys. Rev. Lett. **79**, 3865 (1997)

[3] A. W. Chin, S. F. Huelga, and M. B. Plenio, Phys. Rev. Lett. **109**, 233601 (2012)

[4] A. Smirne, J. Kołodyński, S. F. Huelga, and R. Demkowicz-Dobrzański, Phys. Rev. Lett. **116**, 120801 (2016)

[5] B. M. Escher, R. L. de Matos Filho, and L. Davidovich, Nat. Phys. **7**, 406 (2011)

[6] R. Demkowicz-Dobrzańskii, J. Kołodyński, and M. Guţă, Nat. Commun. **3**, 1063 (2012)

Gaussian benchmark for optical communication towards ultimate capacity

Jaehak Lee,[1] Se-Wan Ji,[1] Jiyong Park,[1] and Hyunchul Nha[1,2]

[1] *Department of Physics, Texas A & M University at Qatar, P.O. Box 23874, Doha, Qatar*
[2] *School of Computational Sciences, Korea Institute for Advanced Study, Seoul 130-722, Korea*

We establish the fundamental limit of communication capacity within Gaussian schemes under phase-insensitive Gaussian channels, employing multimode Gaussian states and collective Gaussian operations and measurement. We prove that this Gaussian capacity is additive so that a single-mode communication suffices to achieve the largest capacity under Gaussian schemes.

Sending and receiving signals via optical channels, e.g. optical fiber networks, is a crucial basis of communication. Employing protocols like intensity modulation and phase-shifting in optical communication, there eventually arises a question of fundamental importance—how quantum mechanics sets bound on communication capacity achievable using light beams. A remarkable result was recently established by proving the minimum output entropy conjecture [1], i.e., the ultimate capacity under phase-insensitive Gaussian channels is achieved by using coherent states as information carriers (encoding). However, there still exists an outstanding problem on what quantum receivers (decoding) can practically be used to obtain ultimate capacity. The Holevo-Schumacher-Westmoreland theorem states that the ultimate capacity can be achieved *asymptotically* with a certain joint measurement [2], which however requires highly nonlinear, so very demanding, operations. It is therefore important to identify quantum receivers achieving high communication rates practically.

In this talk, we identify the capacity achievable within *Gaussian communication schemes* [3] employing Gaussian states, operations, and measurements readily available in laboratory. It is unknown to what extent general Gaussian schemes particularly using entangling operations can improve capacity in contrast to separable schemes. So far there are two well-known Gaussian communication schemes, coherent-state scheme with heterodyne detection and squeezed-state scheme with homodyne detection, studied under an ideal situation or channel noises. We recently extended study to general *single*-channel Gaussian communications with arbitrary inputs and measurements and showed that the optimal strategy among them is either coherent-state scheme or squeezed-state scheme [4]. As for multimode scenario, with inputs restricted to coherent states, Takeoka and Guha showed that the optimal Gaussian receiver is a separable one [5]. Since Gaussian receivers with coherent-state inputs do not saturate the ultimate channel capacity although the channel capacity is obtained with coherent-state inputs, their work provides an evidence for the gap between the capacity of Gaussian schemes and the ultimate channel capacity. However, the restriction to coherent-state inputs is not sufficient as other inputs can yield higher capacity under some Gaussian channels [4].

We establish the ultimate limit of Gaussian schemes under phase-insensitive Gaussian channels in a general multimode scenario using arbitrary N-mode Gaussian input states and collective Gaussian measurements. We prove that its upper bound is achieved by separable inputs and separable measurements (additivity of Gaussian communication). The highest capacity of Gaussian schemes is thus obtained by the optimal *single-channel* protocol, i.e., either coherent-state scheme or squeezed-state scheme [4]. As the capacities of those two schemes do not achieve the Holevo bound, we characterize the exact gap between the ultimate channel capacity and the capacity within Gaussian communication. Our results identify an optimal protocol when resources are confined to Gaussian operations and Gaussian receivers. Until now, coherent-state and squeezed-state schemes were used as standard protocols due to simple applicability. We now show that they actually attain the upper limit of capacity within Gaussian resources. This work also establishes a benchmark to rigorously assess enhanced performance of non-Gaussian schemes in terms of mutual information—a central quantity of interest in communication theory. Furthermore, we suggest a non-Gaussian receiver of [6] combined with an appropriate encoding method as a feasible scheme for higher communication rate than Gaussian limit.

[1] V. Giovannetti, R. García-Patrón, N. J. Cerf, and A. S. Holevo, Nat. Photon. **8**, 796 (2014); A. Mari, V. Giovannetti, and A.S. Holevo, Nat. Commun. **5**, 3826 (2014).
[2] A.S. Holevo, IEEE Trans. Inf. Theory **44**, 269 (1998); B. Schumacher and M.D. Westmoreland, Phys. Rev. A **56**, 131 (1997).
[3] J. Lee, S.-W. Ji, J. Park, and H. Nha, Phys. Rev. A **93**, 050302(R) (2016).
[4] J. Lee, S.-W. Ji, J. Park, and H. Nha, Phys. Rev. A **91**, 042336 (2015).
[5] M. Takeoka and S. Guha, Phys. Rev. A **89**, 042309 (2014).
[6] F. E. Becerra, J. Fan, G. Baumgartner, S. V. Polyakov, J. Goldhar, J. T. Kosloski, and A. Migdall, Phys. Rev. A **84**, 062324 (2011); F. E. Becerra, J. Fan, G. Baumgartner, J. Goldhar, J. T. Kosloski, and A. Migdall, Nat. Photon. **7**, 147 (2013).

Measurement of motion in a negative mass reference frame – a new frontier for gravitational wave interferometry

Eugene S. Polzik
University of Copenhagen

A measurement of motion not limited by the standard quantum limit has been recently demonstrated. We report the results of the experiment where motion of a nanomembrane is measured in the reference frame of the atomic spin and outline a proposal for using it for accelerometry and gravitational wave interferometry.

Quantum synchronization and decoherence

Roberta Zambrini
IFISC (UIB-CSIC), UIB Campus, E-07122 Palma de Mallorca, Spain

Synchronization, a universal phenomenon in a broad spectrum of complex systems, has been recently explored in the quantum regime also in relation to quantum correlations. After reviewing the role of dissipative couplings on synchronization, optomechanical devices and an application of synchronization for quantum probing will be presented.

When considering systems composed by many components, the emergence of spontaneous synchronization is a rather robust and universal phenomenon, paradigmatic in physical, biological, chemical and social complex systems [1]. More recently it has been considered also in the quantum regime, where the same definition of this phenomenon is still an open question that has given rise to several approaches (see review [2]).

The phenomenon of spontaneous or mutual synchronization refers to the ability of two or more systems, that would display different dynamics when separate, to evolve coherently when coupled. This corresponds to achieving oscillation at a common frequency in the case of oscillatory dynamics, but generalization are well-known in chaotic systems and in presence of noise. In the quantum regime also non-classical effects, in particular entanglement and quantum correlations, become relevant, beyond the dynamical ones.

Mutual synchronization was predicted for spins interacting with a common bath [3] and for the average positions of quantum optomechanical systems [4]. Quantum synchronization in quantum observables in connection with classical and quantum correlations was reported in harmonic networks [5] where it was established that dissipation can induce the emergence of transient and asymptotic synchronization, even in linear systems. The key condition is that dissipation does not act independently and equivalently on all units, but comes from a common or structured environment. Furthermore, the impossibility of a purely dephasing (common) bath to induce synchronization among decoupled spins was shown in [6] confirming the key role of dissipation. This plays a key role also on super-radiance (when a common light environment is present), a collective phenomenon recently related to quantum synchronization among detuned atoms [7].

Dissipative couplings can be present in different platforms due to the presence of a bulk environment [8] and in particular can arise in optomechanical systems, favoring synchronization and entanglement [9]. The presence of synchronization, a part from being a spontaneous dynamical effect naturally appearing when miniaturizing and increasing the number of components of quantum devices, can also represent a tool in applications [10]. A recent proposal of an application of quantum synchronization deals with probing the features of an out-of-equilibrium qubit not accessible by direct measurement and coupled (en eventually synchronizing) with an external one [11].

Work funded from EU project QuProCS (Grant Agreement No. 641277), MINECO and FEDER (Grant No. FIS2014-60343-P).

Bibliography

[1] A. Pikovsky, M. Rosenblum, J. Kurths, Synchronization: A Universal Concept in Nonlinear Sciences (Cambridge University Press, 2001)

[2] F. Galve, G.L. Giorgi, R. Zambrini, 1610.05060, book chapter to be published by Springer (2017)

[3] P. P. Orth, D. Roosen, W. Hofstetter, and K. Le Hur Phys. Rev. B 82, 144423 (2010).

[4] G. Heinrich, M. Ludwig, J. Qian, B. Kubala and F. Marquardt, Phys. Rev. Lett. 107 043603 (2011); C. A. Holmes, C. P. Meaney, G. J. Milburn, Phys. Rev. E 85, 066203 (2012).

[5] G. Manzano, F. Galve, and R. Zambrini, Phys. Rev. A 87, 032114 (2013); G. Manzano, F. Galve, E. Hernandez-Gracia, G. L. Giorgi, and R. Zambrini, Sci. Rep. 3, 1439 (2013).

[6] G. L. Giorgi, F. Plastina, G. Francica, and R. Zambrini, Phys. Rev. A 88, 042115 (2013).

[7] B. Bellomo, G. L. Giorgi, G. M. Palma, and R. Zambrini, Phys. Rev. A 95, 043807 (2017)

[8]F. Galve, A. Mandarino, M.A. Paris, C. Benedetti, R. Zambrini, Scientific Reports 7, 42050 (2017)

[9] A. Cabot, F.Galve, R.Zambrini, in preparation.

[10] A. Argyris, D. Syvridis, L. Larger, V. Annovazzi-Lodi, P. Colet, I. Fischer, J. Garca-Ojalvo, C. R. Mirasso, L. Pesquera, and A. Shore, Nature 438, 343 (2005)

[11] G.L. Giorgi, F. Galve, Fernando, R. Zambrini, Phys. Rev. A 94, 052121 (2016)

Coherent cancellation of measurement back-action-noise in hybrid atom-optomechancis

Klemens Hammerer
Leibniz Universität Hannover

Continuous position of force measurements of massive systems are subject to measurement back-action resulting in the standard quantum limit of measurement sensitivity. Current experiments with optomechanical systems reached the regime where measurement sensitivity is limited by back-action-noise. I will discuss an approach towards surpassing the standard quantum limit by coherent cancellation of back noise using an auxiliary system exhibiting an effective negative mass. The auxiliary system is a spin polarized atomic ensemble. This method of back action cancellation was recently demonstrated in the lab of Eugene Polzik (Copenhagen).

Practical secure quantum communications

Eleni Diamanti
CNRS - Université Pierre et Marie Curie

We describe recent results in quantum cryptography, focusing on practical photonic implementations, using encodings in discrete or continuous variables of light, of central quantum network protocols, enabling secret key distribution, verification of entangled resources and transactions with quantum money, with maximal security guarantees.

Ultimate precision bounds for the estimation and discrimination of quantum channels [1]

Stefano Pirandola, Cosmo Lupo
York Centre for Quantum Technologies (YCQT), University of York, York YO10 5GH, UK

Quantum metrology deals with the optimal estimation of physical parameters encoded in quantum states or transformations. Its applications are many, from enhancing gravitational wave detectors, to improving frequency standards, clock synchronization and optical resolution. Understanding the ultimate precision limits of quantum metrology is therefore of paramount importance. However, it is also challenging, because the most general strategies for quantum parameter estimation exploit adaptive, i.e., feedback-assisted, quantum operations involving an arbitrary number of ancillas [2, 3].

Our goal is to estimate the ultimate precision in the estimation of θ, as given by the quantum Cramér-Rao bound

$$\sigma_\theta^2 \geq \frac{1}{F_\theta(\rho_{AB}^n)} ,$$

where F_θ is the quantum Fisher information and ρ_{AB}^n is the final state after n iterations, see Fig. 1. To solve this problem we borrow the powerful tool of *teleportation stretching* from the field of quantum communication [4]: if the channel $\mathcal{E}_\theta$ has a suitable symmetry, its action on any input ρ can be simulated by local operations and classical communication (LOCC), see Fig. 2. In this way, the action of the quantum channel on generic inputs is naturally incorporated in the adaptive estimation protocol, allowing us to derive an upper bound on the quantum Fisher information and thus on the ultimate precision for the estimation of the parameter θ. This simulation is possible for channels that are covariant under the action of the unitary transformations involved in the teleportation protocol [5]: examples are the depolarizing and erasure channels, and the Gaussian channels in bosonic systems.

Together with the upper bound we find a matching lower bound obtaining a remarkably simple expression for the ultimate quantum Fisher information:

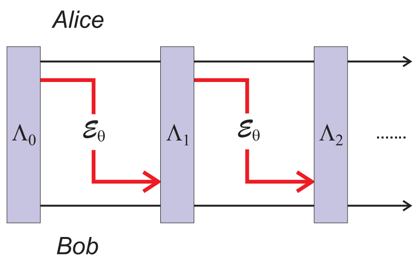

FIG. 1: Schematics for the most general adaptive estimation protocol. First Alice and Bob prepare an initial state by applying a quantum map Λ_0, then Alice uses part of this state to probe the box, while Bob gets the corresponding output. Then they apply a collective quantum operation Λ_1, Alice prepares a new input state, and so on and so forth for n concatenation of this adaptive routine. The state of Alice and Bob obtained in this way, denoted as ρ_{AB}^n, it is finally measured to estimate θ.

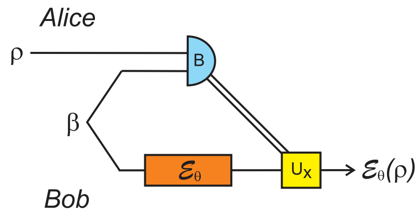

FIG. 2: Teleportation allows us to simulate the quantum channel $\mathcal{E}_\theta$ with an entangled resource (the Choi-Jamiołkowski state of $\mathcal{E}_\theta$) and LOCC, provided it has the required symmetry.

$$F_\theta(\rho_{AB}^n) = nF_\theta(\rho_{\mathcal{E}_\theta}) ,$$

where $\rho_{\mathcal{E}_\theta}$ is the Choi-Jamiołkowski state associated to $\mathcal{E}_\theta$. This finding shows that the adaptive estimation of noise in a teleportation-covariant channel cannot beat the standard quantum limit. Our no-go theorem also establishes that this limit is achievable by using entanglement without adaptiveness.

As an application, we set the ultimate adaptive limit for estimating thermal noise in Gaussian channels, which has implications for continuous-variable quantum key distribution and, more generally, for measurements of temperature in quasi-monochromatic bosonic baths. Because our methodology applies to any functional of quantum states which is monotonic under completely- positive trace-preserving maps, we are able to simplify other types of adaptive protocols, including those for quantum hypothesis testing. Similarly, we find that the ultimate error probability for discriminating two teleportation-covariant channels is reached without adaptiveness and determined by their Choi-Jamiołkowski states.

Our work not only shows that teleportation is a primitive for quantum metrology but also provides remarkably simple and practical results. Setting the ultimate precision limits of noise estimation and discrimination has broad implications, e.g., in quantum tomography, imaging, sensing and even for testing quantum field theories in non-inertial frames.

[1] S. Pirandola, C. Lupo, Phys. Rev. Lett. **118**, 100502 (2017)
[2] R. Demkowicz-Dobrzański, L. Maccone, Phys. Rev. Lett. **113**, 250801 (2014).
[3] M. Hayashi, Commun. Math. Phys. **304**, 689 (2011).
[4] Pirandola et al., arXiv: 1510.08863 (2015).
[5] C. H. Bennett et al., Phys. Rev. Lett. **70**, 1895 (1993).

Semi-device-independent quantum randomness generation

Thomas Van Himbeeck,[1,2] Stefano Pironio,[1,2] and Jonatan Bohr Brask[3]

[1] *Laboratoire d'Information Quantique, Université libre de Bruxelles (ULB), Belgium*
[2] *Centre for Quantum Information and Communication, Université libre de Bruxelles (ULB), Belgium*
[3] *Group of Applied Physics, University of Geneva, 1211 Geneva, Switzerland*

Exploiting quantum systems enables strong security in information processing, e.g. for tasks such as random number generation and cryptography. This can be done under different levels of trust in the devices used. In a completely device dependent scenario, security is analysed based on a full quantum description. Remarkably, security can also be certified in a completely device independent scenario, were the inner workings of the devices are unknown, through the violation of a Bell inequality. The device-dependent approach generally gives high rates, but a full characterisation of the devices may be difficult to obtain or verify, while the device-independent approach is technologically very challenging to implement at present, because it requires Bell inequality violation free of the detection loophole, leading to low rates. It is therefore interesting to explore intermediate regimes, to identify an optimal trade-off between ease of implementation and trust in the devices.

In this talk, we present a new approach [1] to semi device independence for prepare-and-measure protocols, and review two recent experiments realising semi-device-independent quantum random number generation. Previous schemes assumed a bound on the dimension of the Hilbert space characterizing the quantum carriers. Here, we propose instead to constrain the quantum carriers through a bound on the mean value of a well-chosen observable. This modified assumption is physically better motivated than a dimension bound and closer to the description of actual experiments. In particular, we consider quantum optical schemes where the source emits quantum states described in an infinite-dimensional Fock space and model our assumption as an upper bound on the average photon number in the emitted states

In the first part of the talk, we present the new framework in the simplest possible scenario, based on two energy-constrained state preparations and a two-outcome measurement. We find that there exist quantum correlations which cannot be reproduced by any classical model of the devices, and show how this enables generation of certified randomness. This opens the path to more sophisticated energy-constrained semi-device-independent quantum cryptography protocols, such as quantum key distribution.

In the second part of the talk, we review two recent implementations of semi-device-independent randomness generation. The protocols are based respectively on testing a dimension witness [2] (setup illustrated in Fig. 1a), in the spirit of previous approaches, and on unambiguous state discrimination [3] (setup illustrated in Fig. 1b), which is similar in spirit to the new framework introduced in the first part (although different from it). Both implementations allow the user to monitor the entropy in real time. The latter experiment achieved a 16 MHz random bit rate, comparable to commercial quantum random number generators which operate in the device-dependent setting.

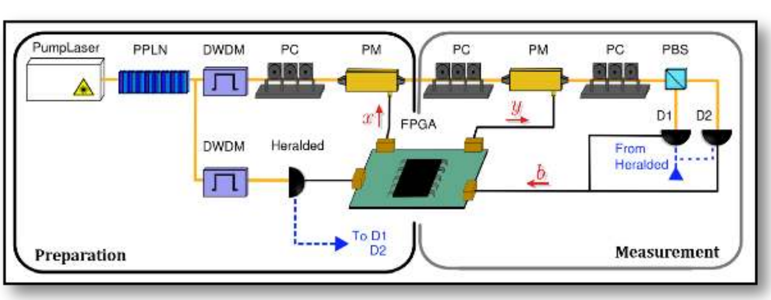

(a) Experimental setup from [2].

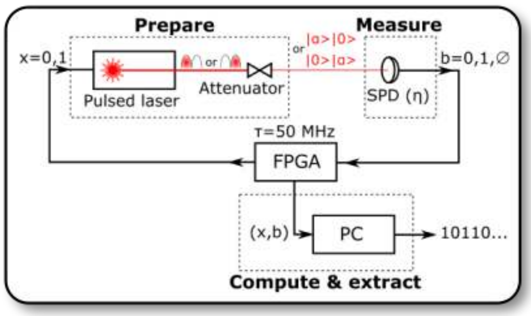

(b) Experimental setup from [3].

[1] T. Van Himbeeck, E. Woodhead, N. J. Cerf, R. García-Patrón, and S. Pironio, arXiv [quant-ph] , 1612.06828 (2016).
[2] T. Lunghi, J. B. Brask, C. C. W. Lim, Q. Lavigne, J. Bowles, A. Martin, H. Zbinden, and N. Brunner, Phys. Rev. Lett. **114**, 150501 (2015).
[3] J. B. Brask, A. Martin, W. Esposito, R. Houlmann, J. Bowles, H. Zbinden, and N. Brunner, Phys. Rev. Applied **7**, 054018 (2017).

Macroscopic superpositions and optical quantum information processing beyond single-photon qubits

Hyunseok Jeong
Seoul National University

In this talk, I will discuss characterizations and quantifications of macroscopic quantum superpositions in various aspects. I will also talk about how such states can be utilized in the context of optical quantum information processing to overcome limitations of the well-known approach based on single-photon qubits.

Quantum Control of Mechanical Oscillators

Ulrich B. Hoff,[1,*] Clemens Schäfermeier,[1] Hugo Kerdoncuff,[1] Hao Fu,[1] Alexander Huck,[1] Jan Bilek,[1] Johann Kollath-Bönig,[1] Glen I. Harris,[2] Warwick P. Bowen,[2] Tobias Gehring,[1] Jonas S. Neergaard-Nielsen,[1] and Ulrik L. Andersen[1]

[1]*Department of Physics, Technical University of Denmark, Fysikvej, 2800 Kgs. Lyngby, Denmark*
[2]*Australian Centre of Excellence for Engineered Quantum Systems, University of Queensland, St Lucia, Queensland 4072, Australia*

We present experimental and theoretical progress within the rapidly advancing field of quantum control of mechanical oscillators. Firstly, we report on recent experimental results [1] demonstrating quantum enhanced feedback cooling of a micro-mechanical oscillator [2, 3]. Using phase squeezed probe light, the mechanical oscillator displacement is transduced in real-time with a sensitivity 1.9 dB below the shot noise limit (Fig. 1), achieving a 50% improvement of the measurement rate and thereby an enhanced cooling rate compared to coherent light probing.

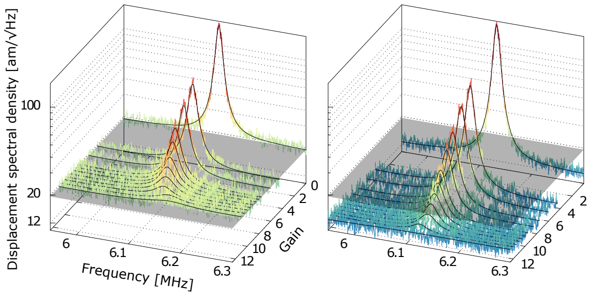

Fig. 1. Experimental feedback cooling of a mechanical oscillator using coherent (left) and phase squeezed light (right).

Secondly, we discuss a proposal for generation of quantum superpositions of macroscopically distinct states of a bulk mechanical oscillator (Fig. 2). Exploiting displaced non-Gaussian quantum states of light in conjuction with an optomechanical quantum non-demolition interaction and measurement-induced feedback, our scheme [4] crucially circumvents the technically challenging need for high single-photon interaction strength [6]. A feasibility study of the scheme reveals that mechanical states with high degree of macroscopicity [5] can be generated under realistic experimental conditions using existing optomechanical and quantum optical resources.

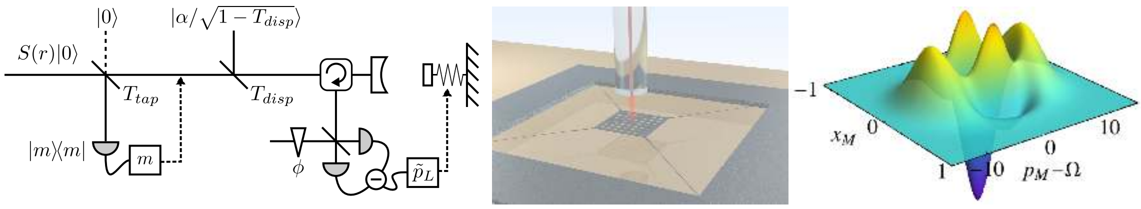

Fig. 2. (left) Proposed scheme for generation of macroscopic superposition states of a mechanical oscillator, (middle) visualisation of envisioned host system, and (right) Wigner function representation of the final mechanical superposition state.

REFERENCES

* ulrich.hoff@fysik.dtu.dk

[1] C. Schäfermeier, H. Kerdoncuff, U. B. Hoff, H. Fu, A. Huck, J. Bilek, G. I. Harris, W. P. Bowen, T. Gehring, and U. L. Andersen, Nat. Commun. **7**, 13628 (2016)
[2] C. Genes, D. Vitali, P. Tombesi, S. Gigan, and M. Aspelmeyer, Phys. Rev. A **77**, 033804 (2008)
[3] K. H. Lee, T. G McRae, G. I. Harris, J. Knittel, and W. P. Bowen, Phys. Rev. Lett. **104**, 123604 (2010)
[4] U. B. Hoff, J. Kollath-Bönig, J. S. Neergaard-Nielsen, and U. L. Andersen, Phys. Rev. Lett. **117**, 143601 (2016)
[5] C. W. Lee and H. Jeong, Phys. Rev. Lett. **106**, 220401 (2011)
[6] S. Bose, K. Jacobs, and P. L. Knight, Phys. Rev. A **56**, 4175–4186 (1997)

Quantum Correlations in Nonlocal BosonSampling

Farid Shahandeh[1], **Austin P. Lund**[1], **and Timothy C. Ralph**[1]

[1]*Centre for Quantum Computation and Communication Technology, School of Mathematics and Physics, University of Queensland, Brisbane, QLD 4072, Australia*

Determining whether the correlations between two systems are quantum or classical is fundamental to our understanding of the physical world and our ability to use such correlations for technological applications. In quantum information theory, quantification of quantum correlations is mainly based on the notion of quantum entropy [1].

In contrast, in quantum optics it is common to study nonclassical features of bosonic systems in a quantum analogue of the classical phase space. While in a classical statistical theory in phase-space the state of the system is represented by a probability distribution, the quantum phase-space distributions can have negative regions, and hence, fail to be legitimate probability distributions [2]. The negativities are thus considered as nonclassicality signatures. Within multipartite quantum states, the phase-space nonclassicality can be associated with quantum correlations, due to the fact that in a classical description of the joint system no such effects are present [3, 4].

Recently, Ferraro and Paris [5] showed that the two definitions of quantum correlations from quantum information and quantum optics are inequivalent. This means that every quantum state which is classically correlated with respect to the quantum information definition of quantum correlations is necessarily quantum correlated with respect to the quantum optical criteria and vice versa. One can also compare the operational differences between the two approaches. On one hand, the quantum correlations of quantum information have been shown to be necessary for specific nonlocal quantum communication and computation tasks to outperform their classical counterparts. On the other hand, however, quantum correlations in quantum optics lack such a nonlocal operational justification, i.e., there is no particular quantum information protocol which exploits phase-space nonclassicality to outperform a classical counterpart protocol.

In this paper, we introduce nonlocal BOSONSAMPLING as an intermediate model of quantum computing which is performed by distant agents (see Fig. 1) and use it to demonstrate the operational interpretation of phase-space nonclassicality in quantum informatics [6]. Specifically, we show that there exists a quantum state, namely a product of fully dephased two-mode squeezed vacuum states,

$$\begin{aligned}\hat{\varrho}_{\mathrm{AB}} &= \hat{\varrho}_i^{\otimes m}\\ &= (1-\epsilon^2)^m \sum_{j_1,\ldots,j_m=0}^{\infty} \epsilon^{2\sum_{k=1}^{m} j_k} \left(\bigotimes_{k=1}^{m} |j_k\rangle_{\mathrm{A}}\langle j_k|\right)\\ &\qquad \otimes \left(\bigotimes_{k=1}^{m} |j_k\rangle_{\mathrm{B}}\langle j_k|\right),\end{aligned} \tag{1}$$

which is strictly classical (CC) with respect to entropic measures of correlations in quantum information allowing for efficient classical simulation of local statistics of two BOSONSAMPLER parties, Alice and Bob, in our protocol, which at the same time, prohibits efficient classical simulation of nonlocal correlations between the two. The only known resource present within the state (1), in contrast to the scatter-shot BOSONSAMPLING [7], is that of phase-space nonclassicality, as shown in [8]. Hence, we see that, nonlocal BOSONSAMPLING takes advantage of phase-space nonclassicality to perform a nonlocal task more efficiently than any classical algorithm.

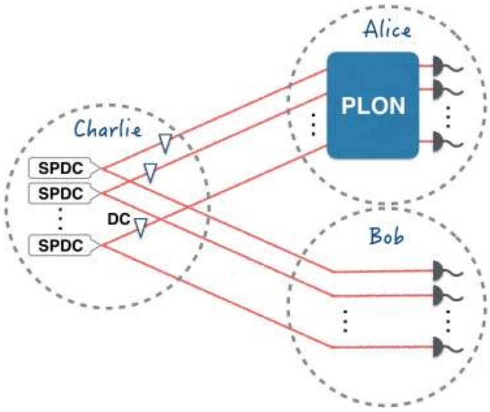

Figure 1: The schematic of a nonlocal BOSONSAMPLING protocol with CC input state. Charlie uses m SPDC sources and a series of dephasing channels (DC) to produce fully dephased two-mode squeezed vacuum states (FDTSV), and shares the final state between two spatially separated agents. Alice performs BOSONSAMPLING using a passive linear-optical network (PLON) and $\{0,1\}$ Fock basis measurements, while Bob only performs $\{0,1\}$ Fock basis measurements. We show that, Alice and Bob can efficiently simulate their local sample statistics classically. However, they cannot efficiently simulate the correlations between their outcomes using classical computers and any amount of classical communication, although there is no entanglement or discord between agents at any time.

References

[1] M. A. Nielsen and I. L. Chunang, *Quantum Computation and Quantum Information* (Cambridge University Press, Cambridge,2000).

[2] U. Leonhardt, *Measuring the Quantum State of Light*, (Cambridge University Press, New York, USA, 1997).

[3] R. J. Glauber, *Quantum Theory of Optical Coherence* (Wiley-VCH, Weinheim, Germany, 2007).

[4] W. Vogel and D.-G. Welsch, *Quantum Optics*, (Wiley-VCH, Weinheim, 2006).

[5] A. Ferraro and M. G. A. Paris, Phys. Rev. Lett. **108**, 260403 (2012).

[6] F. Shahandeh, A. P. Lund, and T. C. Ralph, arXiv:1702.02156 [quant-ph].

[7] A. P. Lund, A. Laing, S. Rahimi-Keshari, T. Rudolph, J. L. OBrien, and T. C. Ralph, Phys. Rev. Lett. **113**, 100502 (2014).

[8] E. Agudelo, J. Sperling, and W. Vogel, Phys. Rev. A **87**, 033811 (2013).

Continuous-Variable Instantaneous Quantum Computing is hard to sample

T. Douce[1,2], D. Markham[2,3], E. Kashefi[2,3], E. Diamanti[2,3],
T. Coudreau[1], P. Milman[1], P. van Loock[4] and G. Ferrini[1,4*]
[1] *Laboratoire Matériaux et Phénomènes Quantiques, Sorbonne Paris Cité, Univ. Paris Diderot, CNRS UMR 7162, 75013, Paris, France*
[2] *Laboratoire d'Informatique de Paris 6, CNRS, UPMC - Sorbonne Universités, 4 place Jussieu, 75005 Paris*
[3] *LTCI, CNRS, Télécom ParisTech, Université Paris-Saclay, 75013 Paris, France and*
[4] *Institute of Physics, Johannes-Gutenberg Universität Mainz, Staudingerweg 7, 55128 Mainz, Germany*
(Dated: February 20, 2017)

Instantaneous Quantum Computing (IQP) is a sub-universal class of computation that has been defined for Discrete Variables (DV) in [1]. In the original formulation, an IQP circuit requires the following ingredients: the input states are Pauli-X eigenstates, each gate in the circuit is diagonal in the Pauli-Z basis and the output corresponds to a Pauli-X measurement. Since all the gates commute they can be performed in any order and possibly simultaneously, hence the name of IQP.

We study the translation of this class of circuits to the Continuous-Variable (CV) formalism. From an experimental point of view, CVs offer the possibility of deterministically preparing resource states, such as squeezed states or cluster states, and typical measurements, such as homodyne detection, have higher detection efficiencies as compared to e.g. photon counting. In order to map the IQP paradigm from DV to CV, we use the correspondence between the universal set of gates described e.g. in [2]. CV IQP circuits have thereby the following structure: the input states are momentum-squeezed states, gates are diagonal with respect to the position quadrature and measurements are homodyne detections in the momentum quadrature. Following the lines of [1], we analyse the computational power of the CV IQP class by exploring the properties of post-selected CV IQP circuits, and we prove that CV IQP circuits are hard to sample [3]. In order to deal with post-selection in CV we consider finite resolution homodyne detectors, which leads to a realistic scheme based on discrete probability distributions of the measurement outcomes. A further peculiar element of CV that necessitate a careful analysis is the finite squeezing of the input squeezed states. We deal with this aspect by adding to the model ancillary GKP states and by relying on a GKP encoding of quantum information, which was shown to enable fault-tolerant CV quantum computation [4]. Finally, we show that, in order to render post-selected computational classes in CVs meaningful, a logarithmic scaling of the squeezing parameter with the circuit size is necessary, translating into a polynomial scaling of the input energy.

* Electronic address: giulia.ferrini@gmail.com

[1] M. J. Bremner, R. Josza, and D. Shepherd, Proc. R. Soc. A **459**, 459 (2010).
[2] M. Gu, C. Weedbrook, N. C. Menicucci, T. C. Ralph, and P. van Loock, Phys. Rev. A **79**, 062318 (2009).
[3] T. Douce, D. Markham, E. Kashefi, E. Diamanti, T. Coudreau, P. Milman, P. van Loock, and G. Ferrini, Phys. Rev. Lett. **118**, 070503 (2017).
[4] N. C. Menicucci, Phys. Rev. Lett. **112**, 120504 (2014).

Quantum key repeaters

Matthias Christandl
University of Copenhagen

QKD is in practice limited to a few hundred kilometres, but can be extended to longer distances by use of a quantum repeater. In this talk, we discuss the possibility of a quantum key repeater, which would work beyond the limits of entanglement distillation and hence conventional quantum repeaters.

Electrically tunable artificial gauge potential for exciton polaritons

Hyang-Tag Lim*,+, Emre Togan*, Martin Kroner, Javier Miguel-Sanchez and Atac Imamoglu

Institute of Quantum Electronics, ETH Zurich, CH-8093 Zurich, Switzerland
+ Presenter: *llim@phys.ethz.ch*

Neutral particles subject to artificial gauge potentials can behave as charged particles in magnetic fields. This fascinating premise has led to implementations of synthetic artificial gauge fields in a number of different optical systems [1-4]. In many cases, however, the design of the optical systems leaves little or no room for fast control of the strength of the artificial gauge field after sample fabrication is completed. On the other hand, it is essential to be able to tune the magnitude of the gauge field during the experiment for many applications [5, 6]. Particularly for the case of nanophotonic structures, fast local control of the gauge field strength may open up new possibilities of investigating many-body physics of light [7].

In this presentation, we report that application of perpendicular electric and magnetic fields can generate a tunable artificial gauge potential for two-dimensional microcavity exciton polaritons [8]. The strength and direction of the artificial gauge potential are controlled electrically. For verification, we perform interferometric measurements of the associated phase accumulated during coherent polariton transport (Figure 1b). Since the gauge potential originates from the magnetoelectric Stark effect, it can be realized for photons strongly coupled to excitations in any polarizable medium. Together with strong polariton-polariton interactions and engineered polariton lattices, we believe that an artificial gauge field could play a key role in investigating non-equilibrium dynamics of strongly correlated photons.

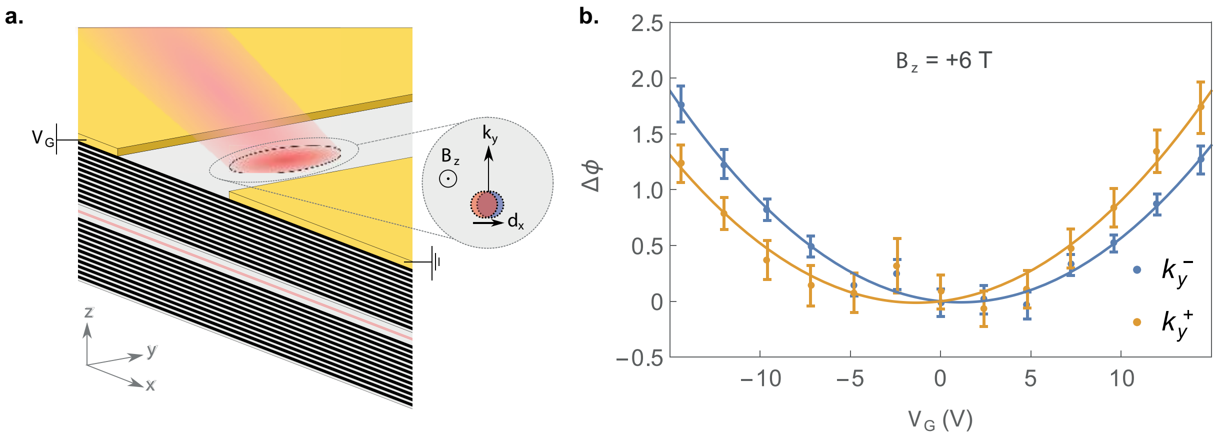

Fig. 1. **a.** The sample, held at 4 K in a helium bath cryostat, contains three $In_{0.04}Ga_{0.96}As$ quantum wells located at an antinode of a cavity formed by two distributed Bragg reflectors (DBRs). An electric potential V_G applied to the metal gates creates an electric field in the x direction. Under a magnetic field along the z direction polaritons excited with in-plane wavevector k_y exhibit a dipole moment d_x. **b.** Change in the extracted phase $\Delta\varphi$ at $B_z = 6$ T between polariton excited with either k_y^+ (yellow) or k_y^- (blue) and the reference beam ($k_y = 0$) as a function of V_G. $\Delta\varphi$ is dependent on both the directions of k_y and B_z.

References

[1] Z. Wang, Y. Chong, J. D. Joannopoulos, and M. Soljacic, Nature **461**, 772 (2009).
[2] M. C. Rechtsman, *et al.*, Nature **496**, 196 (2013).
[3] M. Hafezi, S. Mittal, J. Fan, A. Migdall, and J. M. Taylor, Nature Photon. **7**, 1001 (2013).
[4] N. Schine, A. Ryou, A. Gromov, A. Sommer, and J. Simon, Nature **534**, 671 (2016).
[5] M. Aidelsburger, et al., Phys. Rev. Lett. **111**, 185301 (2013)
[6] G. Jotzu, *et al.*, Nature **515**, 237 (2014).
[7] T. Jacqmin, *et al.*, Phys. Rev. Lett. **112**, 116402 (2014).
[8] H.-T. Lim, E. Togan, M. Kroner, J. Miguel-Sanchez, and A. Imamoglu, Nat. Commun. **8**, 14540 (2017).

Hybrid Quantum Photonic Circuits

Ali W. Elshaari[1, ||], Iman Esmaeil Zadeh[2], Andreas Fognini[2], Michael E. Reimer[3], Dan Dalacu[4], Philip J. Poole[4], Val Zwiller[1], Klaus D. Jöns[1]

[1]Quantum Nano Photonics Group, Department of Applied Physics and Center for Quantum Materials, Royal Institute of Technology (KTH), Stockholm 106 91, Sweden
[2]Kavli Institute of Nanoscience Delft, Delft University of Technology, Delft 2628 CJ, The Netherlands
[3]Institute for Quantum Computing and Department of Electrical & Computer Engineering, University of Waterloo, Waterloo, ON N2L 3G1, Canada
[4]National Research Council of Canada, Ottawa, ON K1A 0R6, Canada
[||]Author e-mail address: elshaari@kth.se

Quantum optical applications require a scalable approach combining bright on-demand quantum emitters and complex integrated photonic circuits. Currently, one of the most promising quantum sources are based on III/V semiconductor quantum dots (QD)[1]. However, demonstrating complex photonic circuitry based on III-V semiconductors faces tremendous technological challenges in circuit fabrication and deterministic integration of single photon sources[2]. On the other hand, silicon and silicon nitride based photonic circuits are CMOS compatible and well-developed for large scale and complex integration. We take the best of both worlds by developing a new hybrid on-chip nanofabrication approach[3, 4]. We demonstrate on-chip generation, spectral filtering, and routing of single-photons from selected single and multiple III/V semiconductor nanowire quantum emitters all deterministically integrated in a CMOS compatible silicon nitride (SiN) photonic circuit. Our new approach eliminates the need for off-chip components, opening up new possibilities for integrated quantum photonic systems with on-chip single- and entangled-photon sources. We performed measurements confirming that the nanowire QDs retain high quality emission properties in terms of linewidth and vanishing probability of multi-photon emission despite going through several fabrication steps.

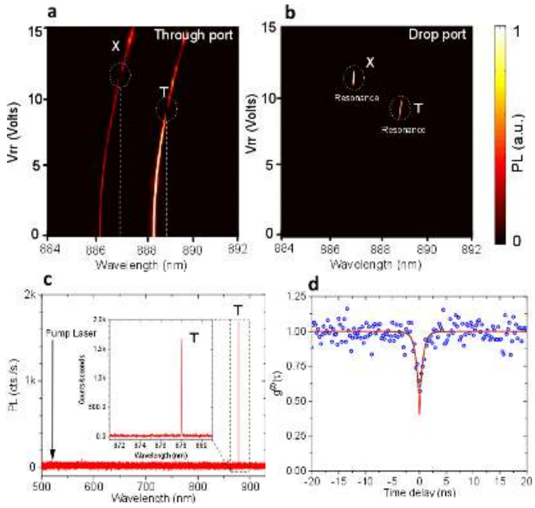

Figure.1 (a) and (b) selective routing of QD excitonic transitions between the drop-port and through-port of the ring resonator. (c) By tuning the resonator, a single QD transition is routed to the drop-port. (d) Second-order correlation measurement ($g^2(0) = 0.41\pm0.05$)

A major problem with integrated quantum photonics is the suppression of excitation lasers and elimination of unwanted emission lines. This proved to be a considerably difficult task, which hindered the demonstration of on-chip single-photons without the use of external bulky filters. Here, we have overcome this hurdle and realized single-photons generation and filtering on-chip. The emission from a nanowire embedded in a SiN waveguide is filtered with the tunable ring resonator filter. Figure.1 (a) and (b) show the collected emission from the ring resonator through-port and drop-port for different tuning voltage V_{rr}. Exciton and Trion lines from the QD are filtered and routed at specific ring-resonator voltage settings. Figure.1 (c) shows filtered Trion line in the drop port with suppression of the excitation pump (at wavelength 532 nm), nanowire bulk emission (at wavelength 830 nm), and all additional emission lines from the QD. To verify the successful filtering, we measured the second-order correlation function ($g^2(0) = 0.41\pm0.05$) directly on the drop-port revealing single-photon emission, as shown in Figure.2(d).

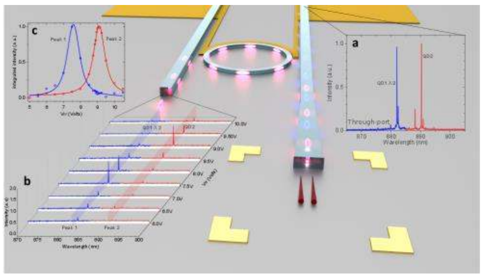

Figure 2: Schematic of the integrated photonic circuit. (a) Collected emission from the through-port waveguide. (b) Drop-port emission as a function of ring resonator voltage Vrr. (c) Integrated intensity of QD1 and QD2 at the drop-port as a function of V_{rr}.

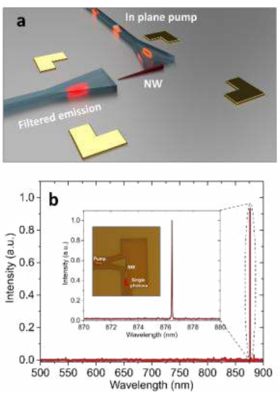

Figure.3 (a) In-plane excitation schematic. (b) emission spectra showing only QD emission

Wavelength and polarization filtering is performed using the electrically-controlled integrated ring resonator filter[5]. Taking advantage of our new on-chip single-photon filtering and routing, we are able to perform wavelength division multiplexing/demultiplexing of on-demand quantum emitters. We realize a multi-frequency quantum channel comprising two independently selected and deterministically integrated nanowire-QDs as shown in Figure.2. The two nanowires launch single photon into the waveguide. The through-port emission of both nanowires is depicted in graph a). By tuning the ring resonator voltage V_{rr}, we can sift single-photons from one or the other nanowire into the drop-port (graph b)). Plot c) shows the integrated intensity of QD1 and QD2 as a function of ring resonator voltage V_{rr}, verifying the filtering and routing of single-photons in an integrated circuit.

Finally, we implemented a scalable in-plane pumping scheme shown in Figure.3 which decouples the excitation laser from the QD emission. The broadband nature of the pump suppression and the absence of resonant photonic structures makes it attractive for performing resonant excitation of QDs on-chip.

References

[1] Somaschi N., et al., Nat Photon, 2016. 10(5): p. 340-345.
[2] Davanco M., et al. ArXiv e-prints, 2016. 1611.
[3] Esmaeilzadeh I., et al., Nano Letters, 2016.
[4] Elshaari A.W., et al. ArXiv e-prints, 2016. 1611.
[5] Elshaari A.W., et al.,. IEEE Photonics Journal, 2016. 8(3): p. 1-9

Hybrid spin-motion system with quantum emitters in hexagonal boron nitride membranes

Mehdi Abdi, Myung-Joong Hwang, Mortaza Aghtar, and Martin B. Plenio
Institut für Theoretische Physik, Albert-Einstein-Allee 11, Universität Ulm, 89069 Ulm, Germany

The recent large flow of reports on the observation of optical single photon emitters in two-dimensional hexagonal boron nitride (hBN) samples in room and cryogenic temperatures [1-3] signals the increasing interest on these objects. The single-photon emitters hosted on hBN flakes have very narrow yet pronounced zero-phonon-lines [2]. Additionally, by sitting in a 2D material, they have the advantage of higher accessibility and sensitivity [4]. Membranes made of few layers of hBN flakes have low mass yet high elasticity modulus, making them high quality mechanical resonators [5]. Their extremely small out-of-plane stiffness also gives them a large zero-point amplitude, i.e. a higher sensitivity to motion. The origin of hBN emitters is not completely understood and despite the *ab initio* computational work by Tran *et al* in [1], which led them to the attribution of the emissions to *anti-site complex* defects, a group theory support is still missing.

In this work, we have employed group theory analyses and *ab initio* computations to study the electronic structure and spin properties of the attributed defect. Based on this knowledge we propose a setup for coupling a spin state of the color centers hosted in a free-standing hBN flake to its vibrational modes. Taking advantage of the exceptional geometry of the proposed setup, a manipulation toolbox for the electronic spin qubit is proposed. This includes initialization, rotations, and readout of the electronic spin qubit via optical excitations and microwave drives. We also propose to control and manipulate the motion of the hBN membrane through the qubit. The possibility of cooling a vibrational mode of the membrane (with frequency ω_m) down to its ground state is demonstrated.

In our setup, the spin-motion coupling rate g_0 can reach and even exceed the fundamental mechanical mode frequency $g_0 \gtrsim \omega_m$, realizing the so-called ultrastrong coupling regime. Such a large coupling rate allows for fast and noise resilient preparation of non-classical states of the membrane within less than a mechanical period. The ability to prepare a mesoscopic hBN membrane in non-classical states can open an avenue for exploring the macroscopic quantum physics.

[1] T. T. Tran, K. Bray, M. J. Ford, M. Toth, and I. Aharonovich, Nat. Nanotech. 11, 37 (2016).
[2] N. R. Jungwirth *et al*, Nano Lett. 16, 6052 (2016).
[3] N. Chejanovsky *et al*, Nano Lett. 16, 7037 (2016).
[4] I. Aharonovich, D. Englund, and M. Toth, Nat. Photon. 10, 631 (2016).
[5] C. Lee, Q. Li, W. Kalb, X.-Z. Liu, H. Berger, R. W. Carpick, and J. Hone, Science 328, 76 (2010).

Nitrogen-Vacancy Ensemble Magnetometry Based on Pump Absorption

Sepehr Ahmadi, Haitham El-Ella, Jørn B. Hansen, Alexander Huck, and Ulrik L. Andersen

Department of Physics, Technical University of Denmark, 2800 Kongens Lyngby, Denmark

Abstract: We demonstrate magnetic field sensing using an ensemble of nitrogen-vacancy centers by recording the variation in the pump light absorption. At a frequency of 10 mHz, we obtain a noise floor of $\sim$30 nT/$\sqrt{\text{Hz}}$.

The nitrogen-vacancy (NV) center is a point defect within the diamond lattice formed by a substitutional nitrogen atom and a nearby vacancy. The long coherence time of the associated electron spin together with optical initialization and readout makes it a promising system for room-temperature highly-sensitive magnetic field detection.

Continuous-wave magnetometry schemes with NV centers are often based on recording the change in the detected fluorescence level upon a frequency shift of the electron spin resonance due to an external magnetic field. The best sensitivity in such a scheme is obtained by probing the electron spin at the steepest point of the optically detected magnetic resonance (ODMR) spectrum. In this contribution, we report for the first time, to the best of our knowledge, the measurement of ODMR based on monitoring the spin-dependent absorption of the pump field.

In our experiment, we use a single-crystal diamond grown by chemical vapor deposition. The diamond was placed at its Brewster angle with respect to the incident pump laser (532 nm). We performed ODMR measurements by recording the pump light transmitted through the diamond while sweeping the microwave (MW) drive frequency across the spin resonance. In order to extract the signal from the low-frequency noisy environment, we use lock-in detection with a 1s time constant by sine-wave modulating the MW drive at 35 kHz modulation rate and 0.7 MHz modulation depth.

For deducing the sensitivity of the magnetometer, we measured three time traces of the lock-in signal. The Fourier transforms of these time traces with a frequency resolution of 0.8 mHz are summarized in Fig. 1(a). The first trace was taken when the MW drive is on resonance with a spin transition (magnetically most-sensitive). The second trace was taken when the MW drive is far from any spin resonance (magnetically insensitive). The third trace was recorded when the detector is blocked, which corresponds to the sum of electronic noise. When the MW drive is off resonance, a noise floor of $\sim$ 30 nT/$\sqrt{\text{Hz}}$ was achieved at a frequency of 10 mHz.

Next, we generated a 10 mHz square-wave magnetic field using a coil and monitored the magnetometer response by recording the lock-in signal which is presented in Fig. 1(b). The standard deviation of 180 data points recorded within 45 seconds duration is 167 nT. This exceeds the magnetically sensitive noise floor in Fig. 1(a) which we think stems mostly from the noise generated by current source fluctuations of the coil.

In conclusion, we report on a low-frequency NV magnetometer based on the variation of the pump power due to absorption. We achieved a noise floor of $\sim$30 nT/$\sqrt{\text{Hz}}$ at a frequency of 10 mHz. Simulations indicate that with an optimized sample and under suitable optical conditions, a shot-noise-limited sensitivity in the $\sim$ sub pT/$\sqrt{Hz}$ range is within reach using our absorption-based approach.

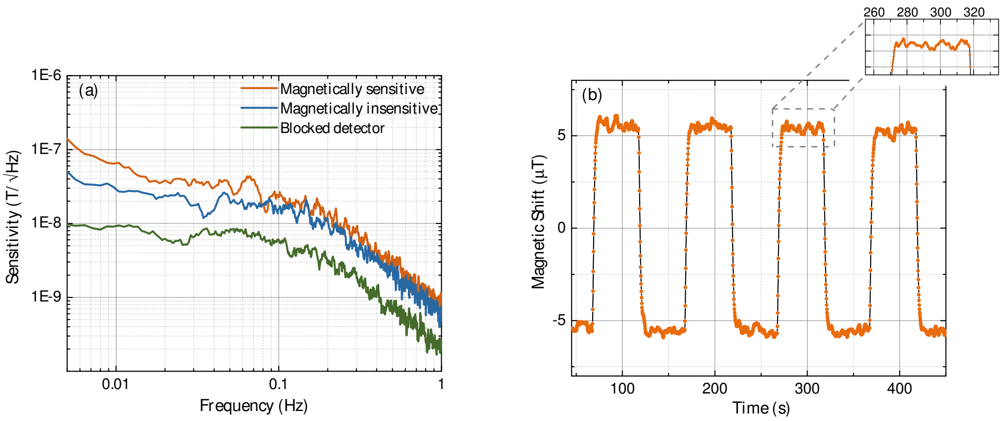

Fig. 1: (a) Plots of the magnetic noise spectral density when the MW drive is set on the maximum slope of the frequency modulated ODMR (magnetically most-sensitive), when the MW drive is far from any spin resonance (magnetically insensitive), and the noise floor of the lock-in and the blocked detector for the same gain setting (adjacent-averaging smoothed). (b) Response of the magnetometer to a 10 mHz applied square-wave magnetic field as a function of time. The zoomed inset shows part of the time trace with a standard deviation of 167 nT for 45 seconds duration.

Towards an on-demand scalable room-temperature heralded single-photon source with long memory time

Michael Zugenmaier,[1] Karsten Dideriksen,[1] Boris Albrecht,[1,*]
Johannes Borregaard,[2] Anders S. Sørensen,[1] and Eugene S. Polzik[1]
[1] *The Niels Bohr Institute, University of Copenhagen, Blegdamsvej 17, Copenhagen Ø DK-2100, Denmark*
[2] *Department of Physics, Harvard University, Cambridge, Massachusetts 02138, USA*

The ability to transmit quantum states over long distances with high efficiency is required to build photonic quantum networks. These will be useful for distributed quantum computing, and for secure communications based on quantum key distribution. Heralded single photon sources are an important building block of modern quantum optics, and are a key element of many of these photonic quantum networks architectures based on quantum repeaters. Quantum repeaters are devices designed to distribute entanglement over large distances, where direct transmission of entangled systems (usually photon pairs) becomes unpractical due to losses through the transmission channel (usually optical fibers). They are made of several independent nodes in which entanglement is generated locally before performing entanglement swapping operations between these nodes, resulting in entanglement distribution over large distances. The synchronization of the different links is crucial due to the probabilistic nature of the entanglement generations. It can be realized with atomic ensembles following the DLCZ protocol, as proposed in [2], using so-called emissive quantum memories. These are heralded single photon sources with in-build memory time allowing for a programmable delay between the two photons of the pair. One of the main limitations of the memory time is atomic motion. It is usually overcome in one of two ways. Ultra-cold atomic ensembles implementations have demonstrated memory times up to 165ms but require complex cooling apparatus. Using ultra-short pulses can lead to high time-bandwidth products but the memory times remain limited to the nano- to micro-second range. Here, we realize an experiment bringing room-temperature atomic ensembles to the long memory times regime, potentially leading to significant improvement in terms of scalability.

We implemented the experimental protocol proposed in [1] to realize such a room-temperature heralded single photon source based on motional averaging in order to alleviate the atomic motion-induced decoherence. The basis of the system is an alkene-coated micro-cell containing a thermal ensemble of cesium atoms. The memory time can then be limited by the T_2 time of the cell itself, given by its dimensions and the type of the coating. We observe long-lived correlations between the heralding and heralded photons, being limited by four-wave mixing noise. The suppression of this noise, either by changing our polarization scheme or the atomic ground-states used to create and store the atomic coherence, would allow us to enter the non-classical regime and violate the Cauchy-Schwarz inequality.

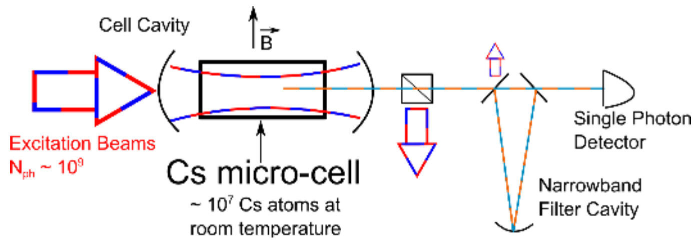

FIG. 1. Simplified experimental setup

In this contribution, I will present the technical implementation of our experimental setup which is depicted in figure 1. The cell containing the atoms is placed inside a low-finesse Fabry-P´rot cavity in order to increase the effective optical depth. At the output, a polarization filtering stage is followed by spectral filtering through a high-finesse triangular cavity. The spectral filtering enables the motional averaging by introducing a random delay to the emitted photons, and also allows to filter out the leakage of the drive pulses.

[1] J. Borregaard *et al.*, "Scalable photonic network architecture based on motional averaging in room temperature gas", Nature communications **7**, 11356 (2016).
[2] L.-M. Duan *et al.*, "Long-distance quantum communication with atomic ensembles and linear optics", Nature **414**, 413-418 (2001).

* boris.albrecht@nbi.ku.dk; http://quantop.nbi.ku.dk/

Hybrid quantum cryptography with high-dimensional multimode coherent states

Romain Alléaume
Télécom ParisTech, LTCI - 46 rue Barrault, 75013 Paris, France

We construct protocols for key distribution, HDH-QKD, where information is encoded on multimode coherent states in high dimension. Within an hybrid security model, we show that HDH-QKD can strongly improve on QKD performances and could break the fundamental rate-loss tradeoff for secure communications with a realistic experimental set-up.

One typical use case for quantum key distribution (QKD) is data link encryption, where QKD-generated keys are used to feed the AES link encryption devices. This solution has the advantage of allowing to use fast AES encryptors, compatible with data rates in the Gbit/s range. On the other hand, the encryption security is only computational and the overall benefit of using QKD, instead of another computational key distribution technique, can be questioned [1, 2]. We propose here to reverse the perspective and to study how computational techniques be combined with quantum cryptographic techniques to enhance the performance of the latter, while keeping a clear advantage, in terms of everlasting security.

We introduce an hybrid security model called *esquimo* (acronym for encryption stronger than quantum noisy memory). In this framework, it is assumed the existence of computational one-way functions that offer perfect security over a short time τ_{comp} but can possibly be inverted at later time possible. It is moreover assumed that quantum memory suffer from technological limitations and decohere in a time shorter than τ_{comp}, the time necessary to break computational one-way functions. This model can be seen as a combination of time-release encryption [4] with the noisy quantum memory model [5]. It allows to build quantum cryptographic protocols based on accessible information analysis , with the objective of guaranteeing everlasting security, i.e. information-theoretic security against computationally unbounded adversary, provided this adversary cannot successfully break computational one-way function at time shorter than τ_{comp} *and* does not possess a memory capable of storing quantum information with good fidelity at larger times.

In this framework, we build a family of key distribution protocol, implementable with current technology, relying on high-dimensional coherent states and mutually unbiased basis encoding. The security analysis requires to upper bound the success probability of state discrimination with post-measurement information [6]. This allows to establish an upper bound on the information that can be obtained by an eavesdropper Eve. Eve is given the states sent at the channel channel, but is not given an ephemeral secret, that can be generated by computational key expansion, ans that is known by Alice and Bob. The bound Eve information scales like $1/d$ and can be obtained without monitoring the channel disturbance, which represents an important advantage in practice. As a consequence, that the input optimal photon number used in HDH-QKD scales like $O(d)$ photons per codeword, as opposed to $O(1)$ in QKD. This allows to boost key rates and may lead to a spectacular increase of the reachable distance for large values fo d. For example if HDH-QKD can be operated with encodings performed in dimension $d = 10^6$ -foreseable based on existing multimode optical communication technologies- then the tolerable loss would be extended by 60 dB ($\sim$ 300 km on fiber). It is perhaps even more interesting to see that HDH-QKD allows to break the fundamental rate-loss trade-off with a number of modes of $d \simeq 30$. We will discuss the options for its experimental realization with spatial modes encoding.

[1] K. Paterson, F. Piper, R. Schack, *Why Quantum Cryptography?* quant-ph/0406147.

[2] R. Alléaume, et. al., *Using quantum key distribution for cryptographic purposes: a survey.* Theoretical Computer Science, 560, 62-81. (2014)

[3] Pirandola, S., Laurenza, R., Ottaviani, C. and Banchi, L. , *Fundamental limits of repeaterless quantum communications.* arXiv preprint arXiv:1510.08863. (2015).

[4] D. Unruh, *Revocable quantum timed-release encryption* (pp. 129-146), Eurocrypt 2014. Springer.

[5] S. Wehner, C. Schaffner, B. M. Terhal, *Cryptography from noisy storage.* Phys. Rev. Lett., 100(22), 220502, (2008).

[6] D. Gopal, S. Wehner, *Using postmeasurement information in state discrimination*, Physical Review A, 82(2), 022326, (2010).

Homodyne-like detection with photon-number-resolving detectors for coherent-state discrimination in the presence of phase noise

Alessia Allevi[1,2], Matteo Bina[3], Stefano Olivares[3], and Maria Bondani[2]

[1]*Department of Science and High Technology, University of Insubria, Via Valleggio 11, 22100 Como, Italy*
[2]*Institute for Photonics and Nanotechnologies, CNR, Via Valleggio 11, 22100 Como, Italy*
[3]*Department of Physics, University of Milan, via Celoria 16, 20133 Milano, Italy*

The generation, manipulation and measurement of quantum states of light is at the base of optical Quantum Information. For such applications, the use of high-repetition-rate pulsed optical states (from kHz up to GHz) containing sizeable numbers of photons is desirable. On the side of measurements, during the last decade a significant effort has been devoted to the development and testing of different detection methods, such as optical homodyne techniques [Lvo09] and direct detection schemes employing photon-number resolving (PNR) detectors [FI14, Har16].
The two methods are complementary since the former gives access to the wave-like properties of light, e.g. the quadrature distributions of the processed state, whereas the latter allows the investigation of particle-like features, i.e. the number of photons the light pulse is endowed with. While in the past the boundary between the two detection strategies was very sharp, nowadays it is progressively vanishing thanks to the several recent advances in merging the two technologies [And15].
Here we present the implementation of a homodyne-like detection scheme, in which a low-energy local oscillator (LO) and two hybrid photodetectors, which are a commercial class of PNR detectors operated at room temperature, are used instead of the traditionally-employed high-energy LO and pin photodiodes [Bina17].
With such a hybrid configuration, we gain direct access to the number of photons measured by each detector separately, but we can also calculate the photon-number difference, which is then processed to retrieve phase-space information about the signal.
At variance with other existing homodyne-like detection schemes [Pue09, Lai10] which can characterize very low-intensity states, the new detection apparatus will operate in a wider dynamic range (up to tens of photons), thus offering the possibility to investigate different regimes of LO intensity.
We apply the scheme to the discrimination between two phase-shifted coherent states affected by either uniform or Gaussian phase noise, performing a proof-of-principle experiment [Bina17]. The performance of the discrimination strategy is quantified in terms of the error probability of discriminating the noisy coherent signals as a function of the characteristic noise parameters.
In particular, we demonstrate that in such conditions the homodyne-like scheme is near-optimal, being it endowed with a discrimination error probability that approaches the Helstrom bound, *i.e.* the minimum error probability allowed by quantum mechanics.

References

[And15] U. L. Andersen et al., Nature Physics 11, 713-719 (2015).
[Bina17] M. Bina et al., to be published in Opt. Express, preprint arXiv:1609.00643.
[FI14] Feature Issue, J. Opt. Soc. Am. B 31, Issue 10 (2014).
[Har16] G. Harder et al., Phys. Rev. Lett. 116, 143601 (2016).
[Lai10] K. Laiho et al., Phys. Rev. Lett. 105, 253603 (2010).
[Lvo09] A. I. Lvovsky et al., Rev. Mod. Phys. 81, 299-332 (2009).
[Pue09] G. Puentes et al., Phys. Rev. Lett. 102, 080404 (2009).

Regimes of Operation of Plasmonic Nanolaser

***Evgeny S. Andrianov*[1,2], *Nikita E. Nefedkin*[1,2,3], *Alexander A. Zyablovsky*[1,2], *Alexander A. Dorofeenko*[1,2,3], *Alexander A. Pukhov*[1,2,3], *Alexey P. Vinogradov*[1,2,3]**

1. Dukhov Research Institute of Automatics (VNIIA), 22 Sushchevskaya, Moscow, 127055, Russia

2. Moscow Institute of Physics and Technology, Moscow, 141700, Russia

3. Institute for Theoretical and Applied Electromagnetics, 13 Izhorskaya, Moscow, 125412, Russia

Recent progress in creation of nanostructures enables to create devices which support electromagnetic field excitation – surface plasmons – in region which size is small compared to wavelength at least in one dimension [1]. Among other things it should be noted plasmonic metallic waveguides, plasmonic grooves, arrays of nanoparticles, perforated metallic films, etc. [2] Amplification and generation of the electromagnetic field in such structures is crucial for creating nanosize sources of coherent electromagnetic field. Notwithstanding experimental progress in the creation of plasmonic nanolasers [3−6] there is the question about coherent properties of such devices [7]. From theoretical point of view difficulties arise from necessity of taking into account large number of both electromagnetic field modes of plasmonic structures and atoms of active medium. Another important point is the high level of dissipation and noise in metal and, as a consequence, the low number of excited plasmons and the crucial role of quantum fluctuations.

In this work we present the investigation of regimes of operation of plasmonic nanolaser consisting from plasmonic groove with gain layer and investigation of coherence function of the first and the second order. For this purpose at the first step we find the eigenmodes of plasmonic structures using numerical simulations, perform the procedure of second quantization and introduce creation and annihilation operators for the modes of electromagnetic field. Second, we obtain in the Born-Markov approximation the master equation which takes into account losses in metal and atoms as well as pumping of active medium. Finally, we develop the theory which is based on cluster expansion method for the open quantum system [8, 9] and self-consistently takes into account quantum correlation between different modes and atoms of active medium.

We show that there are two possible modes of operation of plasmonic laser. The first one is connected to loss compensation of the electromagnetic field which propagates along the nanostructure. The second regime corresponds to generation of definite electromagnetic modes. In the recent experiments on plasmonic lasers only the first regime has been obtained [3-6]. By using quantum regression theorem [10] we obtain the coherence function of the first order and calculate the generation spectrum by using Wiener-Khintchin theorem. We show that at the first regime the spectral line begin to narrow up to the value which is not depend on the pumping and is determined by the losses in metal. This behaviour of the spectral line has been observed in vast majority of the experiments [3-6]. The Schawlow-Townes limit is obtained in the second regime which have higher threshold. We show that above the second threshold the coherence function of second order tends to unity as for usual lasers.

References

[1] D. K. Gramotnev, and S .I. Bozhevolnyi, "Plasmonics beyond the diffraction limit," Nat. Photon. **4**, 83 (2010).

[2] S.A. Maier, *Plasmonics: Fundamentals and Applications*, (Springer, New York, 2007).

[3] F. Beijnum, P.J. Veldhoven, E.J. Geluk, M.J.A. Dood, G.W.t. Hooft, and M.P. van Exter, " Surface Plasmon Lasing Observed in Metal Hole Arrays," Phys. Rev. Lett. **110**, 206802 (2013).

[4] W. Zhou, M. Dridi, J.Y. Suh, C.H. Kim, D.T. Co, M.R. Wasielewski, G.C. Schatz, and T.W. Odom, "Lasing action in strongly coupled plasmonic nanocavity arrays," Nat. Nanotechnol. **8**, 506 (2013).

[5] A.H. Schokker, and A.F. Koenderink, " Lasing at the band edge of plasmonic lattices," Phys. Rev. B. **90**, 155452 (2014).

[6] A. Yang, T.B. Hoang, M. Dridi, C. Deeb, M.H. Mikkelsen, G.C. Schatz, and T.W. Odom, " Real-time tunable lasing from plasmonic nanocavity arrays," Nat Commun. **6**, 6939 (2015).

[6] A. Yang, T.B. Hoang, M. Dridi, C. Deeb, M.H. Mikkelsen, G.C. Schatz, and T.W. Odom, " Real-time tunable lasing from plasmonic nanocavity arrays," Nat Commun. **6**, 6939 (2015).

[7] W.E. Hayenga, H. Garcia-Gracia, H. Hodaei, C. Reimer, R. Morandotti, P. Likamwa, and M. Khajavikhan, "Second-order coherence properties of metallic nanolasers," Optica **3**, 1187 (2016).

[8] H. A. M. Leymann, A. Foerster, and J. Wiersig, "Expectation value based equation-of-motion approach for open quantum systems: A general formalism," Phys. Rev. B. **89**, 085308 (2014).

[9] M. Kira, and S. W. Koch, "Cluster-expansion representation in quantum optics," Phys. Rev. A. **78**, 022102 (2008).

[10] M.O. Scully, and M.S. Zubairy, *Quantum Optics*, (Cambridge University Press, Cambridge, 1997).

Nonclassicality Invariant of General Two-Mode Gaussian States

Ievgen I. Arkhipov,[1,*] Jan Peřina Jr.,[1] Jiří Svozilík,[1] Jan Peřina,[2] and Adam Miranowicz[3]

[1]RCPTM, Joint Laboratory of Optics of Palacký University and Institute of Physics of Academy of Sciences of the Czech Republic, Faculty of Science, Palacký University, 17. listopadu 12, 77146 Olomouc, Czech Republic

[2]Joint Laboratory of Optics of Palacký University and Institute of Physics of Academy of Sciences of the Czech Republic, Faculty of Science, Palacký University, 17. listopadu 12, 77146 Olomouc, Czech Republic

[3]Faculty of Physics, Adam Mickiewicz University, PL-61-614 Poznan, Poland

We introduce a new quantity for describing nonclassicality of an arbitrary two-mode Gaussian state which remains invariant under any global photon-number preserving transformation of the covariance matrix of the state, which we call global nonclassicality invariant (GNI) [1]. The GNI naturally splits into an entanglement invariant (EI) $I_{\rm ent}$ and local-nonclassicality invariant (LNI) $I_{\rm ncl}^{(j)}$ applied to the reduced state $\hat\rho_j$, $j=1,2$.

The LNI $I_{\rm ncl}^{(j)}$ is defined as the determinant of the diagonal block of the normally-ordered covarince matrix taken with a negative sign, which corresponds to the given reduced state $\hat\rho_j$, and is directly related to the Lee nonclassicality depth. The entanglement invariant $I_{\rm ent}$ is defined through symplectic invariants of the symmetrically-ordered covariance matrix, and is shown to be a monotone of the logarithmic negativity.

Given the found relations for LNIs and EI we find the global nonclassicality invariant

$$I_{\rm ncl} = I_{\rm ncl}^{(1)} + I_{\rm ncl}^{(2)} + 2I_{\rm ent},$$

which is resistant to any passive unitary transformations, and which explictly shows the distribution of the global nonclassicality between one-mode squeezing and two-mode entanglement.

Mutual transformations of local nonclassicalities and entanglement induced by a beam splitter (Fig. 1) are analyzed considering incident noisy twin beams, single-mode noisy squeezed vacuum states, and two single-mode squeezed vacuum states, as well as states encompassing both squeezed states and twin beams (Fig. 2). A rich tapestry of interesting nonclassical output states is predicted [2].

A global nonclassicality invariant is also suggested and verified for pure three-mode states.

* ievgen.arkhipov01@upol.cz

[1] I. I. Arkhipov, J. Peřina Jr., J. Svozilík, and A. Miranowicz, Nonclassicality invariant of general two-mode Gaussian states, *Sci. Rep.* **6**, 26523 (2016).

[2] I. I. Arkhipov, J. Peřina Jr., J. Peřina, and A. Miranowicz, Interplay of nonclassicality and entanglement of two-mode Gaussian fields generated in optical parametric processes, *Phys. Rev.* A **94**, 013807 (2016).

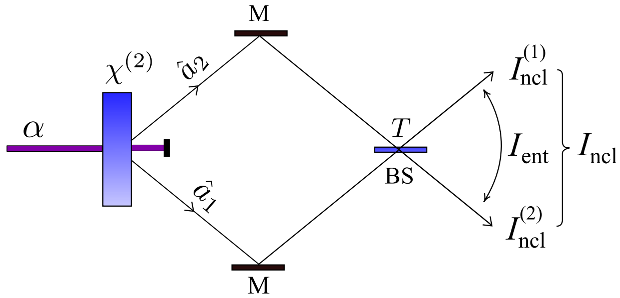

FIG. 1. The local ($I_{\rm ncl}^{(1)}$ and $I_{\rm ncl}^{(2)}$) and global ($I_{\rm ncl}$) nonclassicality invariants are analyzed in relation with the entanglement, described by the invariant $I_{\rm ent}$, for the light generated by the optical parametric process (described by the second-order susceptibility $\chi^{(2)}$) and then combined at a beam splitter BS with varying transmissivity T. Here, α is the amplitude of a classical pump field, $\hat a_1$ and $\hat a_2$ are the annihilation operators of the generated light, and M denotes a mirror.

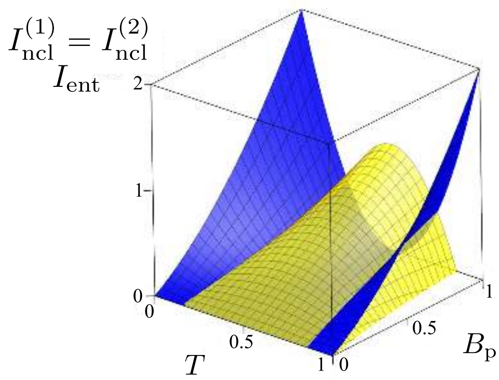

FIG. 2. The local nonclassicality invariants $I_{\rm ncl}^{(1)} = I_{\rm ncl}^{(2)}$ [yellow (light) surface] and entanglement invariant $I_{\rm ent}$ [blue (dark) surface] as functions of mean photon-pair number $B_{\rm p}$ and transmissivity T of the beam splitter for pure twin beams (only positive values are plotted).

Simultaneous measurement of conjugate variables : reaching the Cramèr-Rao bound with coherent states

Matthieu Arnhem[1],* Evgueni Karpov[1], and Nicolas J. Cerf[1]
[1]*QuIC, Ecole Polytechnique, Universite Libre de Bruxelles, Belgium*

In quantum mechanics, the precision on the measurement of two conjugated variables, such as the position and momentum of a particle, is limited by the Heisenberg uncertainty principle. One can consider these conjugated variables as parameters to be estimated. The figure of merit used for the precision on the estimation of a variable can be taken as the variance associated to the estimator of the variable after the measuring process. Since we want to estimate two variables simultaneously, we face a multi-parameter estimation problem where the task is to minimize the variances of the estimators of both conjugated variables. A lower bound on the variance of some variable estimator is given by the Quantum Cramèr-Rao bound (QCRB) in terms of the Quantum Fisher Information (QFI). In our work, we focus on reaching the QCRB simultaneously for parameters encoded in the quadratures of coherent states of light.

In 2001, N. J. Cerf and S. Iblisdir [1] proposed a measurement scheme for coherent states inspired by previous work on global measurement [2, 3] and anti-parallel spins [4]. The measurement scheme introduced by N. J. Cerf and S. Iblisdir provides an enhancement on measuring quadratures x and p of two phase-conjugated coherent states compared to heterodyne or homodyne measurements of two identical states. More precisely, the authors of [1] showed that the variances of the quadratures measured by using phase-conjugated coherent states are lowered by a factor 2 compared to the twin coherent states. Notice that, as well as for the anti-parallel spins, phase-conjugated states are states related by a non-unitary operation. Moreover, they conjectured that using phase conjugated coherent states as input states in the measurement scheme they proposed is optimal for measuring simultaneously both quadratures. Despite much effort to show the superiority of global measurement strategies in such measurement scheme and an experimental confirmation of the results (see [5]) no proof of optimality was found.

We fill the gap by showing that the measurement scheme proposed by N. J. Cerf and S. Iblisdir saturate the associated QCRB for both quadratures and is thus *optimal*. Therefore, it is an optimal and implementable scheme for simultaneous measurement of conjugate variables of coherent states. Moreover, we extend their scheme to any number n of input coherent states where we consider n classical parameters encoded in the quadratures of the n input coherent states. Finally, we analyze the features that make the measurement scheme work optimally and emphasize the role played by the non-unitary operation that relates the two coherent input states of the N. J. Cerf and S. Iblisdir measurement protocol. Future work will focus on optimal measurement scheme for non-classical states of light such as squeezed states.

[1] N.J. Cerf and S. Iblisdir, Phys. Rev. A **64**, 032307 (2001)
[2] A. Peres, and W. K. Wootters, Phys. Rev. Lett. **66**, 9, 1119 (1991).
[3] S. Massar, and S. Popescu, Phys. Rev. Lett. **74**, 8, 1259 (1995).
[4] N. Gisin and S. Popescu, Phys. Rev. Lett. **83**, 432 (1999)
[5] J. Niset *et al.*, Phys. Rev. Lett. **98**, 260404 (2007)

* marnhem@ulb.ac.be

Generation of Highly Pure Schrödinger's Cat States with Exponentially Rising Wave Packet and Real-Time Quadrature Measurement

Warit Asavanant[1], Kota Nakashima[1], Yu Shiozawa[1], Jun-ichi Yoshikawa[1,2], and Akira Furusawa[1]

[1] *Department of Applied Physics, School of Engineering, The University of Tokyo, 7-3-1 Hongo, Bunkyo-ku, Tokyo 113-8656, Japan*

[2] *Quantum-Phase Electronics Center, School of Engineering, The University of Tokyo, 7-3-1 Hongo, Bunkyo-ku, Tokyo 113-8656, Japan*

Photon subtraction [1] is one of the most widely used method for generation of quantum states with high nonclassicality due to its simplicity. By subtracting single photons from squeezed vacua, depending on the squeezing level, one can generate single photon states, Schrödinger's cat states, and squeezed single photon states.

The generation of Schrödinger's cat states using photon subtraction has already been done [2-4]. However, there is one aspect of photon subtraction that has not been addressed yet; From which frequency bandwidth should the single photon be subtracted from a squeezed vacuum?

In our group, we have shown that the frequency bandwidth of the subtracted single photon limits the achievable purity, and to generate highly pure cat states or any states by photon subtraction, the frequency bandwidth of the subtracted photon should be narrower than that of the squeezed vacua as much as possible.

In this experiment, we made a broadband OPO [5] and a narrowband filtering cavity that is used to limit the frequency bandwidth of the subtracted photon. Also, another advantage of narrowband filtering cavity is that the temporal mode of the cat state becomes exponentially rising which allow us to make a real-time quadrature measurement [6] on cat states.

The experiment results is shown in figure 1. Temporal mode of the cat state match with the theoretical prediction and has the shape of exponentially rising, not double-sided exponential. The Wigner function of the states we generated possessed negativity of -0.184 without loss correction, which is, to our knowledge, the largest value ever observed. In case of the real-time quadrature measurement, the negativity of the reconstructed Wigner function is -0.162, which shows high nonclassicality and also is a another solid proof that the states we generated indeed possess exponentially rising temporal mode.

In conclusion, we demonstrated the generation of Schrödinger's cat states using a broadband degenerated OPO and a narrowband filtering cavity. In theory, this method possess no limit in the purity and can be extended to any states that can be generated using a degenerated OPO and photon subtraction.

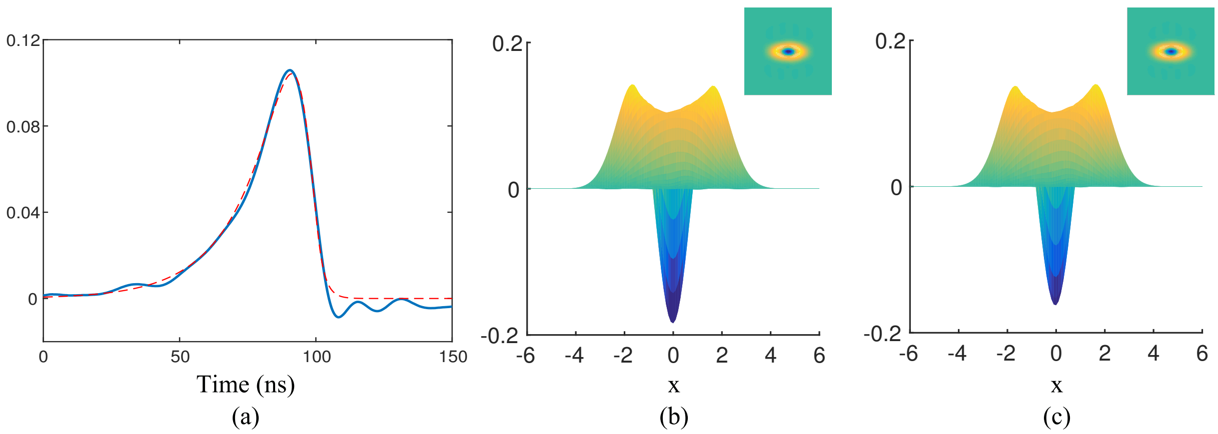

Figure 1: Experiment results. (a) Blue: Temporal mode of cat state estimated from experiment. Red: Theoretical prediction from experiment parameters. (b) Wigner function of cat state estimated by quadrature from post-processing measurement. (c) Wigner function of cat state estimated by quadrature from real-time measurement. Top view of the Wigner function is shown in the top-right of (b) and (c).

Reference [1] M. Dakna *et al.*, Phys. Rev. A **55**, 3184 (1997). [2] A. Ourjoumtsev *et al.*, Science **312**, 83 (2006). [3] J. S. Neergaard-Nielsen *et al.*, Phys. Rev. Lett. **97**, 083604 (2006). [4] K. Wakui *et al.*, Opt. Express **15**, 3568 (2007). [5] T. Serikawa *et al.*, Opt. Express **24**, 28383 (2016). [6] H. Ogawa *et al.*, Phys. Rev. Lett. **116**, 233602 (2016).

Temporal shaping of heralded photons by modulating the pump in cavity-assisted parametric down-conversion

V.A. Averchenko[1], G. Schunk[1,2], U. Vogl[1,2], D. Sych[3], Ch. Marquardt[1,2], and G. Leuchs[1,2]
[1]Max Planck Institute for the Science of Light, Staudtstraße 2, 91058 Erlangen, Germany
[2]University of Erlangen-Nuremberg, Staudtstraße 7/B2, 91058 Erlangen, Germany
[3]Lebedev Physical Institute, Leninsky Prospekt 53, 119991 Moscow, Russia

Heralding a single photon from a photon pair generated in spontaneous parametric down-conversion is the most common way to produce pure, single mode photons up to date [1]. An important next step is to tailor photon properties, such as temporal and spatial profiles and polarization pattern. The motivation is the following: tailored photons are superior in a number of optical tasks, where light intensity is restricted to a single quantum level. Amongst them we recall efficient excitation of a single quantum emitter (single atom, molecule, quantum dot, etc.), quantum information processing with single photons and quantum emitters.

In this work we study theoretically the temporal shaping of heralded photons by tailoring pump pulses which drives the parametric process in the resonator-assisted configuration. Under these conditions the resonator defines a spatio-polarization mode of the generated photons and makes them suitable for various quantum optics applications. In turn, pump modulation provides an additional control over temporal properties of heralded photons.

The adopted theoretical model is a triply-resonant optical parametric oscillator operating far below the oscillation threshold. Such model reproduces the main features of experiments on spontaneous parametric down-conversion in a monolithic nonlinear whispering gallery mode resonator (WGMR). Recently, the generation of narrowband and wavelength tunable heralded photons has been demonstrated with this setup [2]. Here, we calculate the temporal distribution of the generated signal photons excited by different temporally shaped pump pulses and analyze its control via the pump temporal modulation.

The developed model provides a theoretical basis to control the generation of quantum light in the cavity-assisted parametric down-conversion via the temporal modulation of the pump field. In particular, it describes the generation of temporally shaped heralded photons [4], required for an efficient coupling of single photons to single quantum emitters.

[1] M. Förtsch et al., “A versatile source of single photons for quantum information processing”, Nat. Commun. **4**, 1818 (2013);
[2] M. Stobinska, G. Alber, G. Leuchs, “Perfect excitation of a matter qubit by a single photon in free space“, Europhys. Lett. **86**, 14007 (2009);
[3] J.I. Cirac et al., “Quantum State Transfer and Entanglement Distribution among Distant Nodes in a Quantum Network”, PRL 78, 3221 (1997);
[4] D. Sych, V. Averchenko, and G. Leuchs, “Shaping a single photon without interacting with it”, arXiv:1605.00023 (2016).

Frequency-entangled qudits in AlGaAs waveguides

***G. Maltese*[1], *A. Minneci*[1], *C. Autebert*[1], *A. Lemaître*[2], *F. Baboux*[1], *M. Amanti*[1], *T. Coudreau*[1], *P. Milman*[1] and *S. Ducci*[1]**

1. Laboratoire Matériaux et Phénomènes Quantiques, Université Paris Diderot, Sorbonne Paris Cité, CNRS-UMR 7162, 75205 Paris Cedex 13, France

2. Centre de Nanosciences et de Nanotechnologies, CNRS/Université Paris Sud, UMR 9001, 91460 Marcoussis, France

The generation, manipulation and detection of non-classical states of light on a miniaturized chip is a major issue for future quantum information technologies. Among the different material platforms explored in these last years AlGaAs attracts a particular interest due to its compliance with electrical injection [1] and electro-optic effect. Here we demonstrate AlGaAs waveguides with unprecedented signal-to-noise ratio (SNR) of biphoton generation, and the ability to generate frequency-entangled qudits (quantum units of information that may take any of d states) in the telecom band at room temperature.

Our devices, based on a modal phase-matching scheme, include two Bragg mirrors providing both a photonic band gap confinement for a TE Bragg pump mode around 780 nm and total internal reflection claddings for the twin photons TE and TM modes centered at 1560 nm. Recent technological improvements, which we will detail in the talk, have allowed increasing the confinement of the interacting modes and improving the coupling efficiency of the emitted photons, resulting in a generation of photon pairs with a maximum SNR of $5\text{x}10^4$ and a high pair generation rate of 2.7 MHz at SNR of 10^3. This potentially brings us in the condition of achieving a fidelity of 99% for the generation of entangled states.

Furthermore, the dispersion properties of our devices, together with the modal reflectivity on the waveguide facets allow engineering the joint spectrum of the emitted biphoton state to get comb-like spectral correlations, corresponding to frequency-entangled qudits. Indeed the facets create a Fabry-Perot cavity for both output modes, inducing regular time-delays between photons directly transmitted through the waveguide facet and photons having experienced one or more round trips [2]. Taking this into account the expression of the joint spectral density $|\phi(\omega_s,\omega_i)|^2$ of the emitted biphoton state is:

$$|\phi(\omega_s,\omega_i)|^2 = N^{-1}\left|\alpha_p(\omega_s+\omega_i)\right|^2 |A(\omega_s,\omega_i)|^2\, f_{\mathrm{TE}}(\omega_s,\omega_i)\, f_{\mathrm{TM}}(\omega_s,\omega_i)$$

Here $\alpha_p(\omega_s+\omega_i)$ is the spectral amplitude of the pump beam, $A(\omega_s,\omega_i)$ is the three-wave-mixing phasematching function, f_{TE} and f_{TM} describe the effect of the reflection on the waveguide facets for the generated TE and TM polarized photons, respectively and N is a normalization constant.

Figure 1 reports the measurement of a portion of the JSD for the biphoton state emitted by our device under CW pumping, as well as a Hong-Ou-Mandel measurement. The amplitude of the biphoton wavefunction is distributed along $\omega_s+\omega_i=\omega_p$ and oscillates with peaks at $\omega_s-\omega_i$. This suggests that the generated state is an entangled qudit structure $|\Psi\rangle = \sum_i^n a_i|\omega_i\omega_{n-i}\rangle$ as pointed out also in [3]. Contrary to recent experiments that required spectral filters and/or modulators, or external cavities to engineer the target state, our devices represent a miniaturized source, working at room temperature and telecom wavelength. Combined with the high SNR of our devices this ability to generate frequency-entangled qudits could be directly exploited for quantum information processing in optical fibers, in particular to increase channel capacity and security in quantum communications.

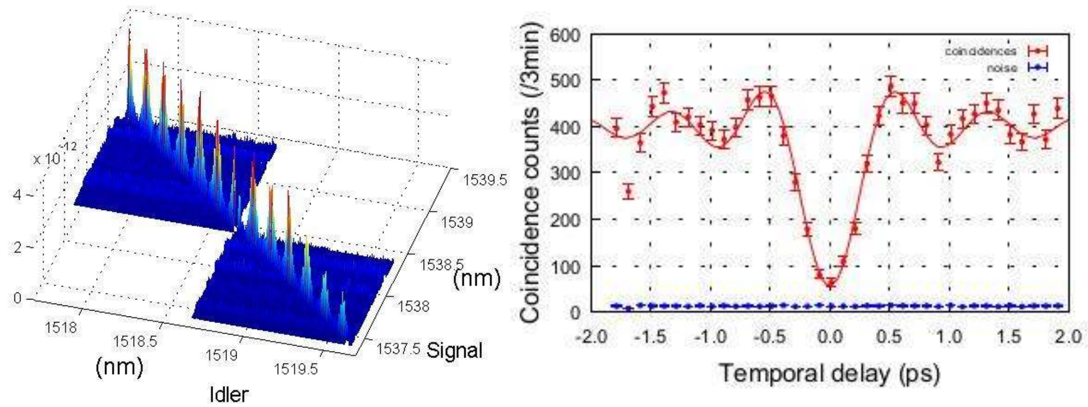

Fig. 1 Left : Measurement of the joint spectral density. Right: HOM dip measured by pumping the sample with a CW Ti:Sa laser; the generated photons are filtered on a 10.8 nm bandwidth.

References

[1] F. Boitier, A. Orieux, C. Autebert, A. Lemaître, E. Galopin, C. Manquest, C. Sirtori, I. Favero, G. Leo, S. Ducci, "Electrically Injected Photon-pair Source at Room Temperature", Phys. Rev. Lett **112**, 183901 (2014).

[2] A. Eckstein, G. Boucher, A. Lemaître, P. Filloux, I. Favero, G. Leo, J. E. Sipe, M. Liscidini, S. Ducci, "High-resolution spectral characterization of two photon states via classical measurements", Laser Photon. Rev., **8**, 76 (2014).

[3] R-B Jin, R. Shimizu, M. Fujiwara, M. Takeoka, R. Wakabayashi, T. Yamashita, S. Miki, H. Terai, T. Gerrits, M. Sasaki, "Simple method of generating and distributing frequency-entangled qudits", Quantum Sci. Technol. **1**, 015004 (2016).

Hamiltonian Engineering under constrained Quantum Marginals

Giuseppe Baio[1,2], Dariusz Chruściński[2] & Antonino Messina[1]

[1]*Università degli Studi di Palermo, Italy*,
[2]*Nicolaus Copernicus University in Toruń, Poland*

Abstract

The preparation of a quantum system in a certain state of interest is considered as a reachable target in several contexts. However, a robust coherent manipulation is still regarded as a far reaching challenge [1]. Among the major research directions in Quantum Control, some address the possibility of shaping the features of a quantum system in such a way to optimize the fidelity of a process of interest. The idea behind this inverse dynamical problem is referred to as *Process or Hamiltonian Engineering* [2]. A *control problem* for any quantum system is typically conceived in terms of a semi-classical controller and the closed system case (*unitary*) is solvable by means of group theoretical techniques [3]. However, the situation is different in the *open* system case. In particular, we address what follows: How to extend the above problem to non-unitary case? (e.g. subdynamics of a multipartite (MP) system)
The present work [4] focuses on a control scheme in which a set of trajectories for a MP system in its space of states is prescribed, either starting from a set of experimental data or a theoretical scheme of interest. In particular, assuming the knowledge, at any time instant, of the single particle states (marginals), we seek the constrained class of compatible joint states. Such constraints can be efficiently described by a set of spectral inequalities answering the so-called *Quantum Marginal Problem* (QMP), of interest in Quantum Chemistry [5] and Information Theory [6]. However, the time-dependent nature of the problem leads us to the introduction of the two following generalizations of the QMP:

1. **Kinematic QMP**: To investigate, for a given simple MP system, whether prefixed reduced trajectories for more subsystems are compatible with a unitary or non-unitary time evolution of the compound system.
2. **Dynamical QMP**: To search the dynamical origin of the kinematic solutions found as a result of the first point, providing the construction of dynamical scenarios (unitary or not) of MP quantum systems evolving under constrained marginals.

In order to address such problems, we start from the bipartite case and propose to exploit the well known algorithm of Cholesky factorization, applied to a suitable parametrization of matrices with fixed partial traces, in order to characterize the necessary and sufficient conditions on the free parameters to ensure positivity. An important value of the proposed method is its portability to higher dimensional cases. Moreover, once we achieve the first, the second problem reduces to the search of a suitable multipartite Hamiltonian when considering a joint state evolving unitarily and, therefore, to a method of parametrization of evolution operators. In the proposed protocol, such an upgrade is guaranteed by the *stereographic parametrization*(SP), namely an elegant and easily applicable method based on the orbit formalism of quantum dynamics and on Lie group decomposition, still valid in arbitrary dimension [7]. Finally, we applied the whole proposed procedure in order to reconstruct the class of generators of a reduced subsystem undergoing non-unitary evolution. This last result can be regarded as an extension of the applicability of the SP method to the case of non-unitary evolution. We hope that such a perspective could represent an interesting applicative platform in order to provide examples and to shed light on some still open problems, such as the necessary and sufficient conditions for the legitimacy of a Non-Markovian time evolution generator [8].

References

[1] J.S. Glaser *et. al*, "Training Schrödinger's cat: quantum optimal control", Eur. Phys. J. D, 69: 279, 2015.

[2] H. M. Wiseman & G.J. Milburn, *Quantum Measurement and Control*, (Cambridge Univ. Press, Cambridge, 2009).

[3] C. Altafini & F. Ticozzi, "Modeling and control of quantum systems: An introduction", IEEE Trans. Automat. Control, 57: 1898–1917, 2012.

[4] G. Baio, *Engineering dynamical scenarios of bipartite quantum systems under constrained Quantum Marginals*, (M.Sc. Thesis, 2016).

[5] A. A. Klyachko, "Quantum marginal problem and N-representability", Journal of Physics: Conference Series, 36: 72-86, 2006.

[6] M. Walter, B. Doran, D. Gross & M. Christandl, "Entanglement Polytopes: Multiparticle Entanglement from Single-Particle Information", Science 340, Issue 6137, pp. 1205-1208, 2013.

[7] J. Bernatska & A. Messina, "Reconstruction of Hamiltonians from a given time evolution", Physica Scripta, 85: 015001, 2012.

[8] D. Chruściński, "On Time-Local Generators of Quantum Evolution", Open Syst. Inf. Dyn., 21: 1440004, 2014.

Measuring and detecting quantum entanglement or nonlocality via Hong-Ou-Mandel interference

Karol Bartkiewicz,[1,2,*] Grzegorz Chimczak,[1] Antonín Černoch,[2] Karel Lemr,[2] and Adam Miranowicz[1]
[1]*Faculty of Physics, Adam Mickiewicz University, 61-614 Poznań, Poland*
[2]*RCPTM, Joint Laboratory of Optics of Palacký University and Institute of Physics of Academy of Sciences of the Czech Republic, 17. listopadu 12, 772 07 Olomouc, Czech Republic*

We present a direct method for measuring the negativity [1, 2] of an arbitrary two-qubit mixed state with 11 measurements performed on up to four copies of the two-qubit system [3]. Our method is based on experimentally accessible Hong-Ou-Mandel interference [4] occurring on up to four paris of pairs of polarization correlated photons [3, 5–7]. In particular, our method permits the application of the Peres-Horodecki [8, 9] separability criterion to an arbitrary two-qubit state [3]. We explicitly show that measuring entanglement in terms of negativity requires three measurements more than detecting two-qubit entanglement [3] and five more than measuring the maximal degree of Bell-CHSH inequality violation [6, 7]. Partial results obtained with this method can be used for directly determining the maximal degree of Bell-CHSH inequality violation and other practical measures of nonclassical correlations, which were directly measured in an entanglement relay [5, 7].

We demonstrate that the set of nine Makhlin's invariants [10–12] needed to express the negativity can be measured by performing 13 multicopy projections (see Fig. 1). Thus, we demonstrate both that these invariants are a useful theoretical concept for designing specialized quantum interferometers and that their direct measurement within the framework of linear optics does not require performing complete quantum state tomography [3]. This minimal set of interferometric measurements provides a complete description of bipartite quantum entanglement in terms of two-photon interference. In all cases, this set is smaller than the set of 15 measurements needed to perform a complete quantum state tomography of an arbitrary two-qubit system. The simplest nonlinear nonuniversal two-copy tests of quantum entanglement require even less measurements [5, 7].

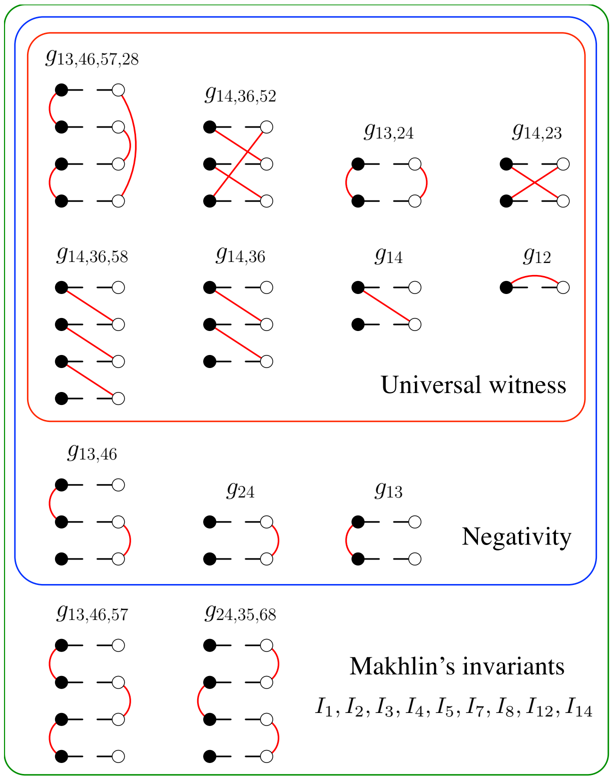

FIG. 1. The minimal set of singlet-projection-based observables needed to measure nine negativity-related Makhlin's invariants [3, 10], negativity, and universal entanglement witness (Peres-Horodecki criterion). Singlet projections are marked as solid curves; dashed lines combine subsystems (black and white discs) of the same copy of an arbitrary two-qubit state.

* bark@amu.edu.pl

[1] K. Życzkowski, P. Horodecki, A. Sanpera, and M. Lewenstein, Phys. Rev. A **58**, 883 (1998).
[2] G. Vidal and R. F. Werner, Phys. Rev. A **65**, 032314 (2002).
[3] K. Bartkiewicz, G. Chimczak,and K. Lemr, Phys. Rev. A **95**, 022331 (2017).
[4] C. K. Hong, Z. Y. Ou, L. Mandel , Phys. Rev. Lett. **59**, 2044 (1987).
[5] K. Lemr, K. Bartkiewicz, A. Černoch, Phys. Rev. A **94**, 052334 (2016).
[6] K. Bartkiewicz, B. Horst, K. Lemr, and A. Miranowicz, Phys. Rev. A **88**, 052105 (2013).
[7] K. Bartkiewicz, K. Lemr, A. Černoch, and A. Miranowicz, Phys. Rev. A **95**, 030102(R) (2017).
[8] A. Peres, Phys. Rev. Lett. **77**, 1413 (1996).
[9] M. Horodecki, P. Horodecki, and R. Horodecki, Phys. Lett. A **223**, 1 (1996).
[10] Y. Makhlin, Quant. Info. Proc. **1**, 243-252 (2002).
[11] K. Bartkiewicz, P. Horodecki, K. Lemr, A. Miranowicz, and K. Życzkowski, Phys. Rev. A **91**, 032315 (2015).
[12] K. Bartkiewicz, J. Beran, K. Lemr, M. Norek, and A. Miranowicz, Phys. Rev. A **91**, 022323 (2015).

Quantising the electromagnetic field near a semi-transparent mirror

Nicholas Furtak-Wells, Lewis A. Clark, Robert Purdy and Almut Beige
The School of Physics and Astronomy, University of Leeds, Leeds LS2 9JT, United Kingdom
(Dated: April 4, 2017)

This paper uses a quantum image detector method to model light scattering on flat surfaces which range from perfect to highly-absorbing mirrors. Instead of restricting the Hilbert space of the electromagnetic field to a subset of modes, we double its size. In this way, the energy of the mirror images and the possible exchange of energy between the electromagnetic field and mirror surface charges can be taken into account. Finally, we derive the spontaneous decay rate of an atom in front of a semi-transparent mirror as a function of its reflection and transmission rates. Our approach reproduces well-known results, like free-space decay and the sub and super-radiance of an atom in front of a perfect mirror, and paves the way for the modelling of more complex systems with a wide range of applications in quantum technology.

The question of how to model the emission of light from atomic systems is older than quantum physics itself. For example, Planck's seminal paper on the spectrum of black body radiation is what eventually lead to the discovery of quantum physics. Nowadays, we routinely use quantum optical master equations or a quantum jump approach to analyse the dynamics of atomic systems with spontaneous emission. For example, the spontaneous decay rate of a two-level atom with ground state $|1\rangle$ and excited state $|2\rangle$ equals

$$\Gamma_{\rm free} = \frac{e^2\omega_0^3\|\mathbf{D}_{12}\|^2}{3\pi\hbar\varepsilon c^3} \tag{1}$$

in a medium with permittivity ε. Here e is the charge of a single electron and c denotes the speed of light in the medium. Moreover, ω_0 denotes the frequency and $\mathbf{D}_{12}$ is the dipole moment of the 1-2 transition.

Other authors studied the spontaneous photon emission of atomic systems in front of a perfect mirror. This is usually done by imposing the boundary condition of a vanishing electric field amplitude along the mirror surface, thereby reducing the available state space of the electromagnetic field in front of the mirror to a subset of photon modes. Compared to modelling an electromagnetic field without boundary conditions, only half of the Hilbert space is taken into account. As a result, the spontaneous decay rate $\Gamma_{\rm mirr}$ of an atom in front of a perfect mirror differs strongly from the free space decay rate $\Gamma_{\rm free}$ in Eq. (1), when the atom-mirror distance x is of the same order of magnitude as the wavelength λ_0 of the emitted light. Although the effect of the mirror is very short range, the sub and super-radiance of atomic systems near perfect mirrors has already been verified experimentally.

In this paper, we quantise the electromagnetic field near a semi-transparent mirror with finite transmission and reflection rates. Depending on the direction of the incoming wave packet, we denote these rates t_a, r_a and t_b, r_b, as illustrated in Fig. 1. One way of quantising the electromagnetic field near a semi-transparent mirror is to proceed as in the case of a perfect mirror and to consider a subset of photon modes . However, the stationary eigenmodes of semi-transparent mirrors are no longer pairwise orthogonal. After treating both sides of the interface separately, solutions have to be matched across the mirror surface. An alternative and purely phenomenological approach to the modelling of the electromagnetic field in front of a semi-transparent mirror is the so-called input-output formalism. Moreover, when modelling the transmission of single photons through a beam splitter, we usually employ transition matrices. The consistency and relation of these qualitatively different approaches remains an open question. Here, we propose an alternative field quantisation scheme.

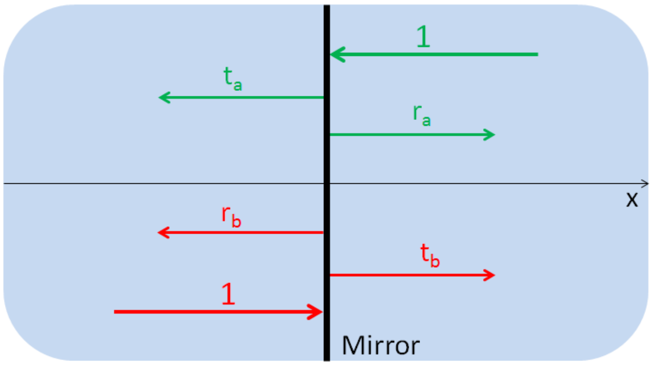

FIG. 1. [Colour online] Schematic view of a semi-transparent mirror with light incident from both sides with finite transmission and reflection rates. Depending on the direction of the incoming light, we denote these rates t_a, r_a and t_b, r_b. For simplicity we assume that the medium on both sides of the mirror is the same. The possible absorption of light in the mirror surface is explicitly taken into account.

The main difference between our approach and the above-described approaches is that the energy of mirror surface charges, i.e. the energy of the mirror images, is explicitly taken into account. For example, as we shall see below, when placing a wave packet in front of a perfect mirror, half of the energy of the system belongs to the original wave packet and the other half belongs to its mirror image.

Quantum-Enhanced Optomechanical Magnetometry

Beibei Li,[2] Jan Bilek,[1*] Clemens Schäfermeier,[1] Ulrich B. Hoff,[1]
Tobias Gehring, Warwick P. Bowen[2] and Ulrik L. Andersen[1]

[1]Department of Physics, Technical University of Denmark, Kgs. Lyngby, Denmark
[2]Australian Centre of Excellence for Engineered Quantum Systems,
University of Queensland, Queensland, Australia

*jbilek@fysik.dtu.dk

Cavity optomechanical field sensors serve as effective magnetometers with high sensitivity under ambient condition, spatial resolution in order of tens of microns and microwatt optical power requirements. Here, for the first time we are interfacing a cavity optomechanical magnetometer with squeezed light to experimentally demonstrate quantum enhanced magnetic field sensing. Specifically, a magnetic field induced expansion of a magnetostrictive material is transduced onto the physical structure of a toroidal whispering gallery mode resonator and sensed as a modulation of on the optical cavity field. Probing the system with squeezed light lowers the noise floor of the magnetometer and therefore enables measurements with a greater bandwidth than would be possible with classical light. With weak probing powers quantum sensing outperforms classically driven systems also on peak sensitivity. Our results are a proof-of-principle demonstration of the performance improvement of quantum enhanced force sensing in cavity optomechanical field sensors.

References

1. U. B. Hoff, G. I. Harris, L. S. Madsen, H. Kerdoncuff, M. Lassen, B. M. Nielsen, W. P. Bowen and U. L. Andersen, Opt. Lett. **38**, 1413 (2013).

2. S. Forstner, J. Knittel, E. Sheridan, J. D. Swaim, H. Rubinsztein-Dunlop and W. P. Bowen, Photonic Sensors **2**, 259 (2012).

3. S. Forstner, E. Sheridan, J. Knittel, C. L. Humphreys, G. A. Brawley, H. Rubinsztein-Dunlop and W. P. Bowen, Advanced Materials **26**, 6348 (2014).

Analysis of multiplexed single-photon sources operated with photon-number-resolving detectors

Ferenc Bodog,[1,*] Peter Adam,[1,2] and Matyas Mechler[3]
[1]*Institute of Physics, University of Pécs, H-7624 Pécs, Ifjúság útja 6, Hungary*
[2]*Institute for Solid State Physics and Optics, Wigner Research Centre for Physics, Hungarian Academy of Sciences, H-1525 Budapest, P.O. Box 49, Hungary*
[3]*MTA-PTE High-Field Terahertz Research Group, H-7624, Pécs, Ifjúsag útja 6, Hungary*

On-demand single-photon sources and single-photon detectors are the key elements of linear optical quantum computing (LOQC) [1]. A promising approach for realizing high efficiency single-photon sources is to multiplex several heralded single-photon sources (HSPS). We consider HSPSs, where correlated photon pairs are generated in nonlinear optical media via spontaneous parametric down-conversion (SPDC). The detection of one member of the pair will herald the presence of its twin partner. The main issue of such a source is the random number of down-converted photon pairs. Multiplexing can overcome this issue by suppressing the probability of multipair events. Multiplexing can be realized in two ways: either with several HSPSs operated in parallel called spatial multiplexing [2–5], or by the repeated use of a single HSPS, called time multiplexing [6–9].

In Ref. [10] we have introduced a theoretical framework that describes all spatial and time multiplexed single-photon sources realized or proposed thus far. This statistical description takes into account all the possible relevant loss mechanisms. It was shown that multiplexed sources can be optimized for maximal single-photon probability. This can be achieved by the appropriate choice of the number of multiplexed units of spatial multiplexers or multiplexed time intervals and the input mean photon number. Furthermore, we have proposad a novel time-multiplexed scheme which can be realized in bulk optics. This system could provide a single-photon probability of 85% with a choice of experimental parameters which are feasible according to the experiments known from the literature.

In Ref. [11] we have extended our theoretical description to sources where time and spatial multiplexing is applied simultaneously. We have shown, that the number of multiplexed time intervals and the number of spatially multiplexed HSPSs can be significantly reduced whithout any drastical change in the single-photon probability of the source. In all of our previous analyses we have only considered HSPSs where heralding was realized with binary detectors.

In this communication we show that multiplexed sources can be further enhanced to approximate better an ideal deterministic source. In order to increase the single-photon probability we consider HSPSs operated with photon-number-resolving detectors (PNRD). The application of such detectors modifies the operating principle of a multiplexed single-photon source in the following way: only those photons are allowed to enter the multiplexing system, for which exactly one photon was detected in the corresponding arm during the heralding process. In the case of ideal PNRDs, this would mean that only single-photons enter the system.

We present a statistical framework which is suitable for describing all kinds of spatially and time multiplexed sources operated with PNRDs. Our description takes into account all possible errors in the photon number state discrimination of the detectors, as well as all possible kinds of losses in the multiplexing system. Using our mathematical description we show that the single-photon probability of multiplexed sources can be further enhanced by PNRDs. Our analysis reveals, furthermore, that the increased efficiency is achieved with a reduced number of multiplexed units when compared to sources operated with binary detectors.

* ferencbodog@gamma.ttk.pte.hu

[1] E. Knill, R. Laflamme, and G. J. Milburn, Nature **409**, 46-52 (2001)
[2] A. L. Migdall, D. Branning, and S. Castelletto, Phys. Rev. A **66**, 053805 (2002).
[3] J. H. Shapiro and F. N. Wong, Opt. Lett. **32** , 2698 (2007).
[4] X.-s. Ma, S. Zotter, J. Kofler, T. Jennewein, and A. Zeilinger, Phys. Rev. A **83**, 043814 (2011).
[5] M. Collins, C. Xiong, I. Rey, T. Vo, J. He, S. Shahnia, C. Reardon, T. Krauss, M. Steel, A. Clark, and B. Eggleton, Nat. Commun. **4**, 2582 (2013).
[6] T. B. Pittman, B. C. Jacobs, and J. D. Franson, Phys. Rev. A **66**, 042303 (2002).
[7] E. Jeffrey, N. A. Peters, and P. G. Kwiat, New J. Phys. **6**, 100 (2004).
[8] J. Mower and D. Englund, Phys. Rev. A **84**, 052326 (2011).
[9] C. T. Schmiegelow and M. A. Larotonda, Appl. Phys. B **116**, 447 (2014).
[10] P. Adam, M. Mechler, I. Santa, and M. Koniorczyk, Phys. Rev. A **90**, 053834 (2014).
[11] F. Bodog, P. Adam, M. Mechler, I. Santa, and M. Koniorczyk, Phys. Rev. A **94**, 033853 (2016).

Nanomagnetometry of paramagnetic centers using single nitrogen-vacancy centers in diamond

Florian Böhm(1), Nikola Sadzak(1), Bernd Sontheimer(1), Niko Nikolay(1), Claudia Widmann(2), Christoph Nebel (2), Oliver Benson(1)
(1) Humboldt-Universität zu Berlin
(2) Fraunhofer-Institut für Angewandte Festkörperphysik, Freiburg

Nuclear magnetic resonance (NMR) spectroscopy allows us to investigate the properties of a broad range of chemical compounds. However, conventional NMR is quite insensitive as it requires relatively large amounts of the sample and strong magnetic fields. Single nitrogen-vacancy (NV) centers in diamond can be used to overcome this limitation, showing nanoscale spatial resolution and high sensitivity even at room temperature. Thus they can be used to detect small ensembles and even individual electron spins inside and outside the diamond crystal.

The ground state of the NV center, which is effectively an electron spin-1 system, can be initialized and read out optically and controlled coherently using microwave radiation. The quantum state of the spin bath (‘dark’ paramagnetic centers surrounding the NV sensor) can be controlled by a resonant radio frequency.

In a first experiment we examined the coupling between a single NV center and the intrinsic electron spin bath in Type 1b diamond due to surrounding nitrogen impurities. We established an experimental setup where we are able to coherently control both the NV centers spin, as well as the surrounding bath spin. We used this tool to perform double electron-electron resonance (DEER) spectroscopy on a small ensemble of electron spins. By combining a spin echo sequence on the NV center and controlling the spin bath we were able to probe the spin dynamics of the bath and its characteristics.

We were able to observe coherently driven Rabi oscillations on the spin bath, demonstrating that we have achieved quantum control of the substitutional P1 impurities. With a spin echo double resonance (SEDOR) scheme, where the spin bath is driven actively during a spin echo sequence on the NV, we could show the faster decay of the NV spin echo. This allows us to measure the coupling strength between different external spins and the NV sensor. By resolving the hyperfine coupling to the nitrogen atoms we were also able to effectively distinguish surface spins from intrinsic spins.

By combining this platform with the capability of 3D laser printing we aim towards an hybrid integrated sensing platform combining optical and microfluidic elements.

Determining the internal quantum efficiency of Nitrogen-Vacancy defects in diamond

I. P. Radko[1], M. Boll[1], N. M. Israelsen[2], N. Raatz[3], J. Mejer[3], F. Jelezko[4], U. L. Andersen[1] and A. Huck[1]

[1]Department of Physics, Technical University of Denmark, 2800 Kgs. Lyngby, Denmark
[2]Department of Photonics Engineering, Technical University of Denmark, 2800 Kgs. Lyngby, Denmark
[3]Institute for Experimental Physics II, University of Leipzig, 04103 Leipzig, Germany
[4]Institute for Quantum Optics, Ulm University, 89073 Ulm, Germany
E-mail: alexander.huck@fysik.dtu.dk

Nitrogen-Vacancy (NV) defects in diamond are highly attractive due to their paramagnetic ground state, which allows for optical spin state initialization and readout. These properties make the NV defect a powerful optical sensor for magnetic and electric fields with nano-meter scale spatial resolution. Many applications depend on the stability and high brightness of the NV defects. The high brightness of the emitters is only guaranteed by a large internal quantum efficiency (IQE), a parameter that has not been determined so far for NV defects in a bulk diamond environment. In this contribution, we present our implementation of Drexhage's scheme [1] to quantify the IQE of ensembles of NV defects in bulk diamond. We measure the total decay rate of the NV ensemble in the vicinity of a metallic mirror. The curvature of the mirror allows for a calibrated modification of the local density of optical states which affects only the radiative decay rate of the emitter, hence allowing to determine the IQE. For NV defects implanted 4.5±1 and 8±2 nm below the diamond surface, we measure the IQE to be 0.70±0.07 and 0.82±0.08, respectively. Furthermore, from these measurements we extrapolate the IQE of NV defects far from the diamond surface to be >0.86 [2].
Our approach is robust and versatile and can be used for investigations of less studied quantum emitters, such as silicon or germanium vacancy defects in diamond or defects found in hexagonal boron nitride, all of which are expected to have a high IQE due to their high brightness. Furthermore, the presented implementation of Drexhage's scheme may be used for improving the signal-to-noise ratio of the NV defects optical spin state readout, resulting in an enhanced external field sensitivity [3].

References

[1] K.H. Drexhage, Journal of Luminescence 1-2, 693-701 (1970)
[2] I. P. Radko et al., Optics Express 24, 27715-27725 (2016)
[3] S. A. Wolf et al., Phys. Rev. B 92, 235410 (2015)

Measurement of photon antibunching in the mesoscopic intensity domain

Alessia Allevi[1,2] and Maria Bondani[2]

[1]*Department of Science and High Technology, University of Insubria*
Via Valleggio 11, 22100 Como, Italy
[2]*Institute for Photonics and Nanotechnologies, CNR*
Via Valleggio 11, 22100 Como, Italy

Antibunching is one of the peculiar traits of quantum systems, evidencing the very definition of “photon” as “light quantum”. Since many years, anti-bunching experiments are routinely exploited to test the quality of single-photon sources. The standard technique is based on the Hanbury Brown-Twiss interferometer, in which the emitted light is divided at a 50/50 beam-splitter (BS) and two single-photon detectors are placed at the two outputs. The presence of anti-coincidences between the two outputs reveals anti-bunching.

At higher intensity regimes, the correlations between the parts of an optical state divided at a beam splitter reflect the statistical nature of the state. In particular, the observation of anti-correlations indicates that the incoming state is sub-Poissonian, that is nonclassical.
Thus, antibunching manifests itself with anti-correlations.

We have realized a compact setup involving a balanced beam splitter and three photon-number-resolving detectors for the observation of photon anti-bunching at a mesoscopic intensity level. The experimental scheme is based on the realization of a parametric-down-conversion process in which multimode twin-beam states containing many photons per pulse are generated. One of the two parties of the twin beam, say the idler, is directly detected, whereas the signal is divided at the beam splitter, at whose outputs other two photon-number-resolving detectors are placed.

The statistics of the signal impinging on the beam splitter can be modified by applying a conditional measurement that exploits the nonclassical correlations between signal and idler and the photon-number resolution of the detectors. If we select the values of the signal according to a rule set on the idler, we can manipulate the signal to obtain a sub-Poissonian state, which, once divided at the beam splitter, generates a pair of beams anti-correlated in the number of photons.

The result is relevant because the nonclassicality of the conditional state is robust against losses, introduced by both the detectors and the beam splitter.

References

[1] R. Hanbury Brown and R. Q. Twiss, *A Test of a New Type of Stellar Interferometer on Sirius,* Nature 178, 1046-1048 (1956).
[2] B. Lounis and M. Orrit, *Single-photon sources*, Rep. Prog. Phys. 68(5) 1129-1179 (2005).
[3] M. Förtsch, J. U. Fürst, C. Wittmann, D. Strekalov, A. Aiello, M. V. Chekhova, Ch. Silberhorn, G. Leuchs, and Ch. Marquardt, *A versatile source of single photons for quantum information processing*, Nature Commun. 4, 1818 (2013).
[4] A. Allevi and M. Bondani, *Photon antibunching in the mesoscopic intensity domain*. Submitted.

Constructing higher order Hamiltonians out of quadratic collective spin operator ${J_z}^2$

Šimon Bräuer
Optics Department, Faculty of Science, Palacký University
17. Listopadu 12, 77146 Olomouc, Czech Republic

To connstruct quantum simulators or quantum computers on quasi-continuous variables, one needs ideally all powers of operators $J_k, {J_k}^2, {J_k}^3, ..., {J_k}^n, k = x, y, z$, where J_k are the components of the collective spin operator. Having the quadratic operator ${J_z}^2$ and linear operators, one can use the Suzuki–Trotter expansion and commutation rules, as, e.g. $e^{-iAt}e^{-iBT}e^{iAt}e^{iBT} \approx e^{[A,B]t^2}$.

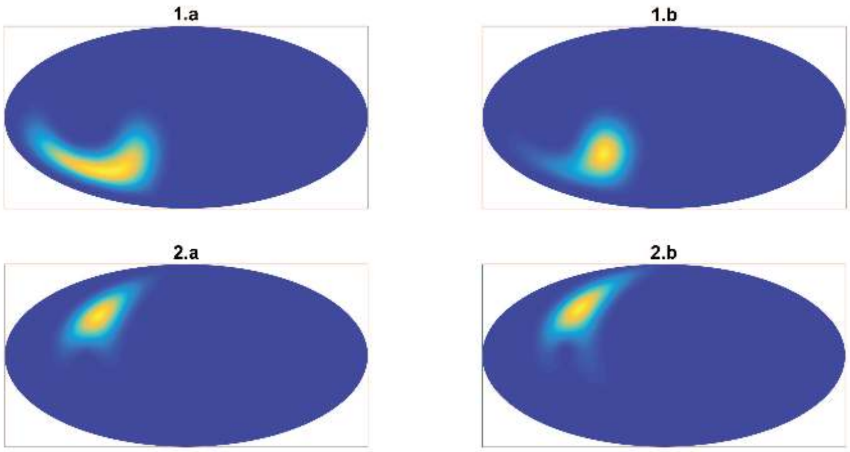

Fig. 1: Bloch sphere in Mollweide projection. Left panels: original operators acting on a spin coherent state, right panels: operators expanded as commutators acting on the same state.

- **1.a**
  $e^{(-2i(J_y^2 J_x + 2J_y J_x J_y + J_x J_y^2) + i(J_z^2 J_x + 2J_z J_x J_z + J_x J_z^2))\Delta T^2} \mid \Psi_0\rangle;$
  $\mid \Psi_0\rangle =$ coherent state
- **1.b**
  $\left(e^{i(J_x^2 - J_y^2)\frac{\Delta T}{\sqrt{N}}} e^{i(J_y J_z + J_z J_y)\frac{\Delta T}{\sqrt{N}}} e^{-i(J_x^2 - J_y^2)\frac{\Delta T}{\sqrt{N}}} e^{-i(J_y J_z + J_z J_y)\frac{\Delta T}{\sqrt{N}}}\right)^N \mid \Psi_0\rangle;$
  $N = 5$
- **2.a**
  $e^{(-4i(J_x^3 - J_y * J_x * J_y - J_z * J_x * J_z) + 3ix)\Delta T^2} \mid \Psi_0\rangle$
- **2.b**
  $\left(e^{i(J_x J_z + J_z J_x)\frac{\Delta T}{\sqrt{N}}} e^{i(J_x J_y + J_y J_x)\frac{\Delta T}{\sqrt{N}}} e^{-i(J_x J_z + J_z J_x)\frac{\Delta T}{\sqrt{N}}} e^{-i(J_x J_y + J_y J_x)\Delta T}\right)^N \mid \Psi_0\rangle;$
  $N = 5$

STIRAP-like process in Quantum Plasmonics

A. Castellini[1,2,3*], **H. R. Jauslin**[1], **G. Colas des Francs**[1], **A. Messina**[2,3] **and S. Guérin**[1,†]
[1]*Laboratoire Interdisciplinaire Carnot de Bourgogne, CNRS UMR 6303, Université Bourgogne Franche-Comté, BP 47870, 21078 Dijon, France*
[2]*Dipartimento di Fisica dell'Università di Palermo, Via Archirafi 36, I-90123 Palermo, Italy*
[3]*INFN Sezione di Catania, Catania, Italy*

Plasmonics is a new branch of Physics with future applications in the integration of plasmonic circuits into electronic devices [1]. This has increased the interest for metallic nanowires and nanostructures supporting propagating and localised surface plasmon polaritons (P-SPPs and L-SPPs, respectively) [2][3][4]. Plasmonic Quantum Electrodynamics (PQED) is the natural generalization, to this context, of the principles of Quantum Optics already used for Cavity Quantum Electrodynamics (cQED). The general purpose of our research is to theoretically implement quantum information processes between quantum emitters (QEs), coherently controlling them and exploiting their strong coupling with plasmonic platforms. We analyse how we can use the highly confined LSPP electromagnetic field, supported by a spherical MNP, as mediator of the exchange of the internal states of two 3-level QEs [5]. This process is numerically implemented as a population transfer between two metastable states of the global hybrid system. A Stimulated Raman Adiabatic Passage (STIRAP)-like set-up (see fig.1(a)) is simulated in order to avoid plasmonic losses [5]. We show that, for a strong coupling satisfied for emitters very close to the MNP, a free-decoherence quantum channel $|g, f\rangle \leftrightarrow |f, g\rangle$ can be found between the two QEs, for angular distances between them smaller than $\pi/2$ and for specific area of the pulses (see fig.1(b)).

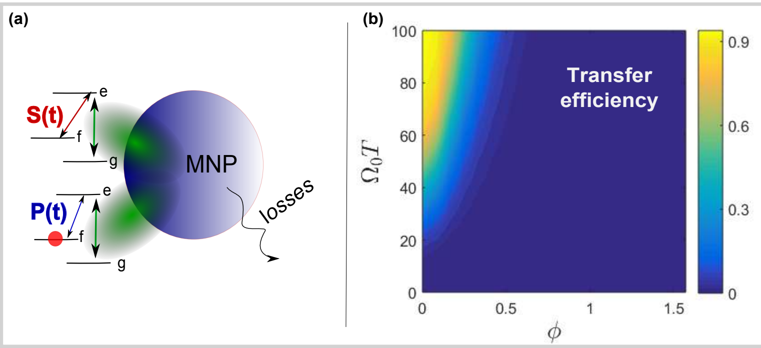

Figure 1: (a) Hybrid emitter / metallic nano-sphere system. (b) Contour plot of the excitation transfer efficiency in function of the pulse area and of the angle between the QEs ($\phi \in [0, \pi/2]$).

**alessia.castellini@unipa.it* †*sguerin@u-bourgogne.fr*

References

[1] S. A. Maier, "Plasmonics, Fundamentals and Applications", Springer (2007).

[2] A. Delga, J Feist, J Bravo-Abad, and F. J. Garcia-Vidal, "Theory of strong coupling between quantum emitters and localized surface plasmons", J. Opt. 16, 114018 (2014).

[3] D. Dzsotjan, B. Rousseaux, H. R. Jauslin, G. Colas des Francs, C. Couteau, S. Gurin, " Mode-selective quantization and multimodal effective models for spherically layered system", Phys. Rev. A 94, 023818 (2016).

[4] H. Varguet, B. Rousseaux, D. Dzsotjan, H. R. Jauslin, S. Guérin, and G. Colas des Francs, "Dressed states of a quantum emitter strongly coupled to a metal nanoparticle", Opt. Lett. 41, 4480-4483 (2016).

[5] B. Rousseaux, D. Dzsotjan, G. Colas des Francs, H. R. Jauslin, C. Couteau, and S. Guérin, "Adiabatic passage mediated by plasmons: A route towards a decoherence-free quantum plasmonic platform", Phys. Rev. B 93, 045422 (2016).

Experimental tests of coherence and entanglement conservation

Antonín Černoch[1], Karol Bartkiewicz[1,2], Karel Lemr[1], Jan Soubusta[3]

[1]RCPTM, Joint Laboratory of Optics of Palacký University and Institute of Physics of Academy of Sciences of the Czech Republic, 17. listopadu 12, 771 46 Olomouc, Czech Republic
[2]Faculty of Physics, Adam Mickiewicz University, PL-61-614 Poznań, Poland
[3]Institute of Physics of the Czech Academy of Sciences, Joint Laboratory of Optics UP and PI AS CR, 17.listopadu 50A, 772 07 Olomouc, Czech Republic

Classical coherence of a given system can be transformed by unitary operations into quantum correlations (entanglement) and vice versa [1]. One can show that the sum of suitable coherence and entanglement measures is conserved and equals the overall purity of the system.

We test the relationship between coherence and entanglement for three different unitary operations:

1) Single photon interference using a Mach-Zehnder interferometer with general beam splitters [2] – beam splitter generates path entanglement.

2) Two qubit interaction in linear optical controlled phase gate [3] – c-phase gate entangles separable input states, the degree of entanglement depends on the phase shift introduced by the gate.

3) Nonlinear process of spontaneous parametric down-conversion – the coherence of pump beam is transformed into the degree of entanglement of photon pairs produced in a crystal cascade.

In all mentioned processes, we experimentally validate the coherence-entanglement conservation. This research is supported by the Czech Science Foundation under the project No. 17-10003S.

REFERENCES

[1] Jiří Svozilík, Adam Vallés, Jan Peřina, Jr., and Juan P. Torres, "Revealing Hidden Coherence in Partially Coherent Light", *Phys. Rev. Lett.* **115**, 220501 (2015).
[2] Adam Miranowicz, Karol Bartkiewicz, Neill Lambert, Yueh-Nan Chen, and Franco Nori, "Increasing relative nonclassicality quantified by standard entanglement potentials by dissipation and unbalanced beam splitting", *Phys. Rev. A* **92**, 062314 (2015).
[3] Karel Lemr, Antonín Černoch, Jan Soubusta, Konrad Kieling, Jens Eisert, and Miloslav Dušek, "Experimental Implementation of the Optimal Linear-Optical Controlled Phase Gate", *Phys. Rev. Lett.* **106**, 013602 (2011).

Entanglement-Enhanced Message Recovery Over an Amplitude Damping Channel

Robert J. Chapman [1,2], *Akib Karim* [1,2], *Steven T. Flammia* [3,4],
Marco Tomamichel [3,5], *and Alberto Peruzzo* [1,2]

1. Quantum Photonics Laboratory and Centre for Quantum Computation and Communication Technology, School of Electrical and Computer Engineering, RMIT University, Melbourne, Victoria 3000, Australia

2. School of Physics, The University of Sydney, Sydney, New South Wales 2006, Australia

3. Centre for Engineered Quantum Systems, School of Physics, The University of Sydney, Sydney, New South Wales 2006, Australia

4. Center for Theoretical Physics, Massachusetts Institute of Technology, Cambridge, USA

5. Centre for Quantum Software and Information, School of Software, University of Technology Sydney, New South Wales 2007, Australia

Amplitude damping describes spontaneous emission in atomic systems [1] as well as the degrading effect of spontaneous decay in trapped ion quantum computing [2] and general energy dissipation [3]. While it is well known for many noisy channels that quantum states can increase the channel capacity in the limit of infinitely many channel uses [4], this is not well known in the regime of limited resources, which is applicable for today's quantum technologies [5]. In this regime it is no longer possible to achieve arbitrarily small errors and therefore, the challenge is to maximise the probability that a transmitted message is correctly received.

Here, we propose and experimentally demonstrate a methodology for transmission over an amplitude damping channel where each bit is encoded in the state of a few qubits and, by entangling the qubits after the channel, the probability of successful message recovery is significantly enhanced over an equivalent number of classical uses of the channel. We present numerical simulations with up to eight uses of the channel and predict that an entangling decoder gives an enhancement in all cases compared to the best classical strategies and coherent (separable) schemes. Using polarisation photonic qubits, we experimentally implement an amplitude damping channel and demonstrate that, by using the channel twice and entangling the states at the decoder, we can enhance the one-bit message recovery by >20% over the corresponding classical approach. The circuit we implement is shown in Fig. 1a and the polarisation photonic realisation shown in Fig. 1b. We use a spontaneous parametric down-conversion photon pair source and implement an interferometric circuit for the amplitude damping channel and entangling decoder.

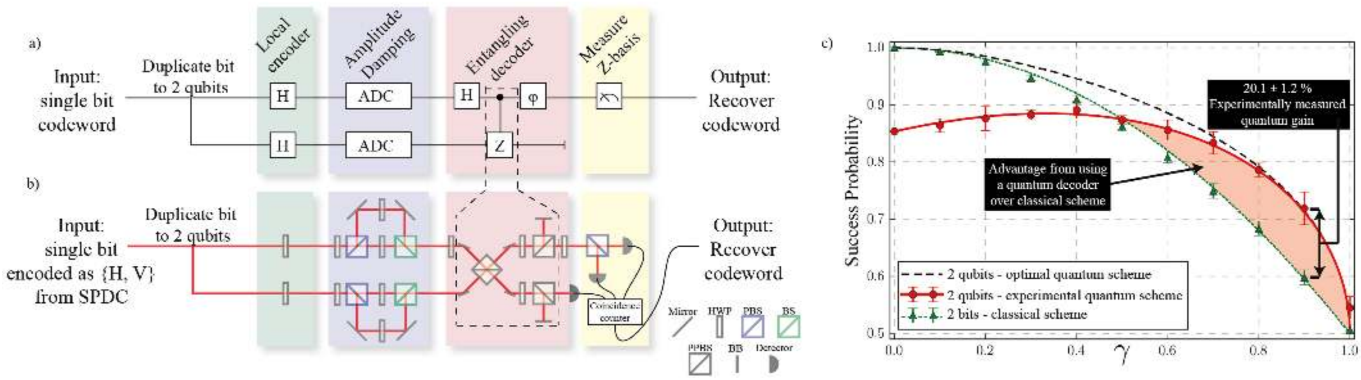

Fig 1 (a) The circuit for transmitting a one-bit message as two qubits over an amplitude damping channel with an entangling decoder to enhance message recovery. (b) The polarisation photonic implementation of the circuit, components are half-wave plate (HWP), polarising beamsplitter (PBS), 50:50 beamsplitter (BS), partially polarising beamsplitter (PPBS) and beam-block (BB). (c) The experimental success probability for two classical channel uses (green triangles), our quantum decoder scheme (red circles) and the analytic maximum (black dashed line).

The probability of successfully recovering the one-bit message after two uses of the noisy channel is plotted in Fig. 1c, where γ is the damping parameter. We plot the analytic maximum success probability (black dashed line) which takes into account all possible decoders, the experimental classical success probability (green triangles) and the success probability with the experimentally implement entangling decoder (red circles). The red shaded region indicates the area where there is an advantage for encoding in quantum states and using our entangling decoder. Given the modest additional resources for the quantum scheme of only five gates, we measure an up to 20.1±0.2% gain in success probability. Our decoder is numerically optimised for large-γ, where it reaches the analytic maximum. Finally, we demonstrate how our methodology extends to larger codewords. We propose a scheme for transmitting a two-bit message with three uses of the channel and show that an entangling decoder can enhance the message recovery by >50% over three classical uses of the channel.

The methodology we present here is a new direction for enhancing resilience to an amplitude damping channel with only small numbers of qubits, and we show how this technique can be extended to larger codeword messages and greater numbers of qubits. The protocol does not require the sharing of entangled states and entangling operations are only necessary after the channel. The full generalisation of our scheme to longer messages, larger quantum states and other noise channels is an important avenue for future work.

[1] Santori *et al.*, "Indistinguishable photons from a single-photon device", *Nature* 419, 594 (2002)
[2] Schindler, *et al.*, "A quantum information processor with trapped ions", *New J. Phys.* **15** 123012 (2013)
[3] Nielsen and Chuang, "Quantum Computation and Quantum Information", *Cambridge University Press* (2000)
[4] Holevo, "Bounds for the Quantity of Information Transmitted by a Quantum Communication Channel", *Probl. Inform. Transm.* **9**, 177 (1973)
[5] Tomamichel *et al.*, "Quantum coding with finite resources", *Nat. Commun.* **7**, 11419 (2016)

Equilibration of observables for initial coherent states in a simple atom-field model.

S. Lerma-Hernández[1,2], J.Chávez-Carlos[1], B. López-del-Carpio[2], M. Bastarraceha-Magnani[3] and J.G. Hirsch[1].

[1] Instituto de Ciencias Nucleares, Universidad Nacional Autónoma de México.

[2] Facultad de Física, Universidad Veracruzana, Mexico

[3] Physikalisches Institut, Albert-Ludwigs-Universitat Freiburg, Germany

We present a study on the dynamics of initial coherent states for the Dicke model with a number of atoms N$\sim$ 200. This number of atoms allows interpreting the quantum results in the light of the corresponding semi-classical limit. We explore the long time behavior of different observables, like the survival probability. Emphasis is placed on identifying quantum signatures of regularity and chaos in the temporal evolution of observables. In particular, the long-time temporal average of the survival probability (the Inverse Participation Ratio or IPR) is shown to decay as $1/N^C$ with C >0. The value of C depends on the regular or chaotic nature of the region where the initial coherent state is located. For coherent states in the regular region of the underlying semi-classical phase space C is smaller than one and close to 1/2, whereas for chaotic ones the decay is faster and C>1.

Multimode Quantum Optomechanics with Ultra-coherent Nanomechanical Resonators

***Junxin Chen*[1], *Yeghishe Tsaturyan*[1], *Yannick Seis*[1], *Massimiliano Rossi*[1], *Albert Schliesser*[1]**

1. Niels Bohr Institute, Copenhagen University, Blegdamsvej 17, 2100 Copenhagen, Denmark

We demonstrate an optomechanical system that features quantum cooperativity $C_q = 4g^2/\kappa\gamma \gg 1$ already at moderate cryogenic temperature [1], implemented as a membrane-in-the-middle system [2] with a high-stress silicon nitride membrane. Here, $\gamma = k_B T/\hbar Q$ is the quantum decoherence rate of the mechanical system due to the thermal bath at temperature T~4 K, whereas Q~10^7 the mechanical quality factor. In this regime, the quantum measurement backaction creates quantum correlations between the optical and mechanical degrees of freedom, which are measured as sub-vacuum noise (-2.4 dB) of the light emerging form the cavity—ponderomotive squeezing [3]. We investigate this effect in a multimode setting and observe (Fig 1a) the generation of squeezed light by optically hybridised mechanical modes [1].

We also report on the development of a novel type of membrane (Fig 1b-d) and string resonators with dramatically reduced decoherence [4]. By patterning a phononic crystal directly into the stressed membrane we realise a "soft clamp" for a localised defect mode. Its engineered mode shape has dramatically reduced curvature and therefore dissipation, reaching room-temperature Qf-products in excess of 100 THz—the highest reported to date—as well as Q~10^9 at T~4 K. The corresponding room temperature coherence time γ^{-1} approaches those of optically trapped dielectric particles, and for cryogenic (4 K) operation approaches 1 ms. Extensive characterisation through laser-based imaging of mode shapes [5] and stress distribution [6] confirms a model that quantitatively predicts the quality factors over a wide parameter range [4]. We also present measurements of frequency noise, relevant for some sensing protocols.

Together, these developments open new avenues for the generation of nonclassical mechanical states—such as entangled mechanical states—and the implementation of quantum-enabled optomechanical sensors and transducers, including those linking microwaves to light.

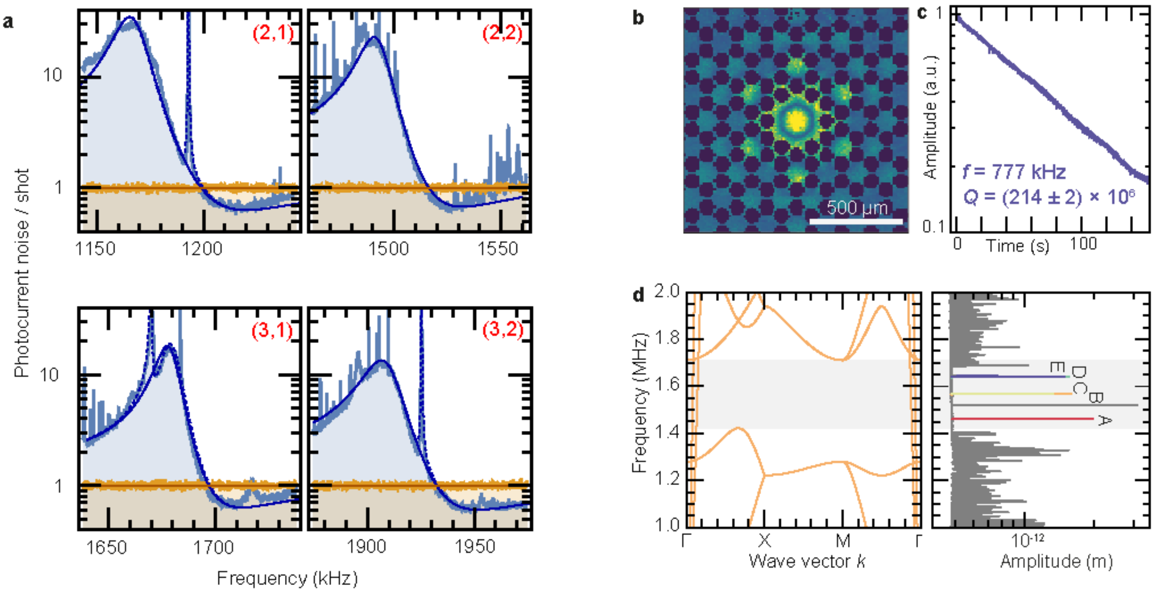

Fig. 1 a) Multimode ponderomotive squeezing [1] of optical amplitude noise (blue) below the vacuum noise level (yellow) near mechanical modes with indices (i, j) as indicated in each panel. Near-degenerate mode pairs (i, j)-(j, i) are optically hybridised, enhancing squeezing. Dark blue lines are models. b) Displacement pattern of soft-clamped, ultra-coherent modes in a stressed SiN membrane with phononic patterning [4], as measured with a scanning laser interferometer [5]. c) Room-temperature ringdown of a similar localised mode d) Left, simulated band diagram of the phononic pattern, with a quasi-bandgap in the MHz region. Right, thermal displacement noise spectrum, which confirms the presence of the bandgap, as well as the five defect modes A-E (grey peak is for calibration).

References

[1] W. H. P. Nielsen, Y. Tsaturyan, C. B. Møller, E. S. Polzik, and A. Schliesser, PNAS **114**, 62 (2017).
[2] J. D. Thompson, B. M. Zwickl, A. M. Jayich, F. Marquardt, S. M. Girvin, and J. G. E. Harris, Nature **452**, 72–75 (2008).
[3] C. Fabre, M. Pinard, S. Bourzeix, A. Heidmann, E. Giacobino, and S. Reynaud, Physical Review A **49**, 1337–1343 (1994).
[4] Y. Tsaturyan, A. Barg, E. S. Polzik, and A. Schliesser, arXiv:1608.00937 (2016).
[5] A. Barg, Y. Tsaturyan, E. Belhage, H. P. W. Nielsen, C. B. Møller, and A. Schliesser, Applied Physics B **123**, 8 (2017).
[6] T. Capelle, Y. Tsaturyan, A. Barg, and A. Schliesser, arxiv.org:1702.01732 (2017)

Conditions for a legitimate memory-kernel master equation

Dariusz Chruściński
Institute of Physics, Faculty of Physics, Astronomy and Informatics
Nicolaus Copernicus University
Grudziądzka 5/7, 87–100 Toruń, Poland

Abstract

We derive conditions for the memory-kernel governing nonlocal master equation which guarantee a legitimate (completely positive and trace-preserving) dynamical map. It turns out that these conditions provide natural parameterizations of the dynamical map being a generalization of the Markovian semigroup. This parametrization is defined by a pair of maps: monotonic quantum operation and completely positive map. It is shown that such class of maps covers almost all known examples from the Markovian semigroup, the semi-Markov evolution, up to collision models and their generalization.

Microwave sideband cooling of nanofiber-trapped atoms

C. Clausen, B. Albrecht, Y. Meng, A. Dareau, P. Schneeweiss, and A. Rauschenbeutel

Vienna Center for Quantum Science and Technology, TU Wien–Atominstitut, Stadionallee 2, 1020 Vienna, Austria

Optical microtraps provide a strong spatial confinement for laser-cooled atoms. They can, e.g., be realized with strongly focused trapping light beams or the optical near fields of nano-scale waveguides and photonic nanostructures. Atoms in such traps often experience strongly spatially varying AC Stark shifts which are proportional to the magnetic quantum number of the respective energy level. These inhomogeneous fictitious magnetic fields can cause a displacement of the trapping potential that depends on the Zeeman state.

Hitherto, this effect was mainly perceived as detrimental. However, it also provides a means to probe and to manipulate the motional state of the atoms in the trap by driving transitions between Zeeman states. Furthermore, by applying additional real or fictitious magnetic fields, the state-dependence of the trapping potential can be controlled. Here, using laser-cooled atoms that are confined in a nanofiber-based optical dipole trap [1], we employ this control in order to tune the microwave coupling of motional quantum states. We record corresponding microwave spectra which allow us to infer the trap parameters as well as the temperature of the atoms. Finally, we reduce the mean number of motional quanta in one spatial dimension to $\langle n\rangle=0.3\pm0.1$, close to the motional ground state, by using microwave sideband cooling. Our work shows that the inherent fictitious magnetic fields in optical microtraps expand the experimental toolbox for interrogating and manipulating cold atoms.

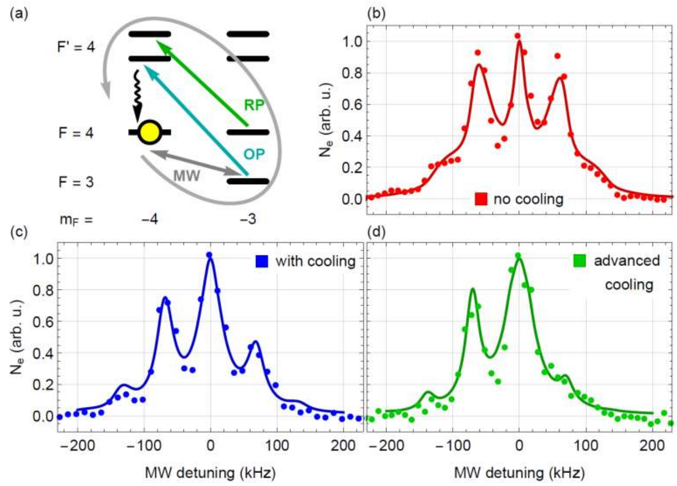

Fig. 1 (a) Principle of the cooling cycle: Atoms are initially prepared in the hyperfine-Zeeman state F=4, m_F=-4 and then transferred to F=3, m_F=-3 via microwave coupling (MW) upon removal of a motional quantum. Two light fields (OP and RP) optically pump the atoms back to the initial hyperfine-Zeeman state. (b-d) Measured microwave spectra (b) without cooling, (c) with 200 cooling cycles and (d) with 200 cooling cycles plus 30 additional cycles without RP. Solid lines are fits using an optical Bloch equation model; the microwave detuning is specified with respect to the carrier transition.

References

[1] E. Vetsch et al., Phys. Rev. Lett. 104, 203603 (2010).
[2] B. Albrecht et al., Phys. Rev. A 94, 061401(R) (2016).

Implementation of Continuous-Variable QKD Using Pilot Assisted Synchronization

L. C. Comandar, H. H. Brunner, F. Karinou, S. Bettelli, F. Fung, S. Mikroulis, D. Hillerkuss, Q. Yi, D. Wang, M. Kuschnerov, C. Xie, M. Peev and A. Poppe

Huawei Technologies Duesseldorf GmbH, Germany Research Center, Riesstrasse 25, D-80992 Munich, Germany.
e-mail: lucian.comandar@huawei.com

Quantum key distribution (QKD) has been subject to constant development and research since its original proposal, particularly using discrete variable implementations [1]. This was enabled by advances in terms of detection techniques, protocols and security analyses resulting in breakthroughs in terms of both key rates and distance. Continuous variable (CV) QKD, even though less researched, is considered more resilient to noise caused by classical communication multiplexing [2]. Furthermore, experimental implementations of CV-QKD systems are realized using mature technologies developed for classical communication.

Traditionally, CV-QKD systems use a co-propagating laser signal that serves as local oscillator (LO) in Bob's receiver [3], which may open security loopholes as it allows the eavesdropper Eve to manipulate the LO intensity. Furthermore, the channel losses have to be compensated for the co-propagating LO, requiring large optical power on the transmitter side. Recently, more practical implementations using a separate laser as local LO in Bob's receiver synchronized using a pilot tone were proposed [4-6]. This removes the possibility for LO attacks and enables high local oscillator powers on the coherent detector.

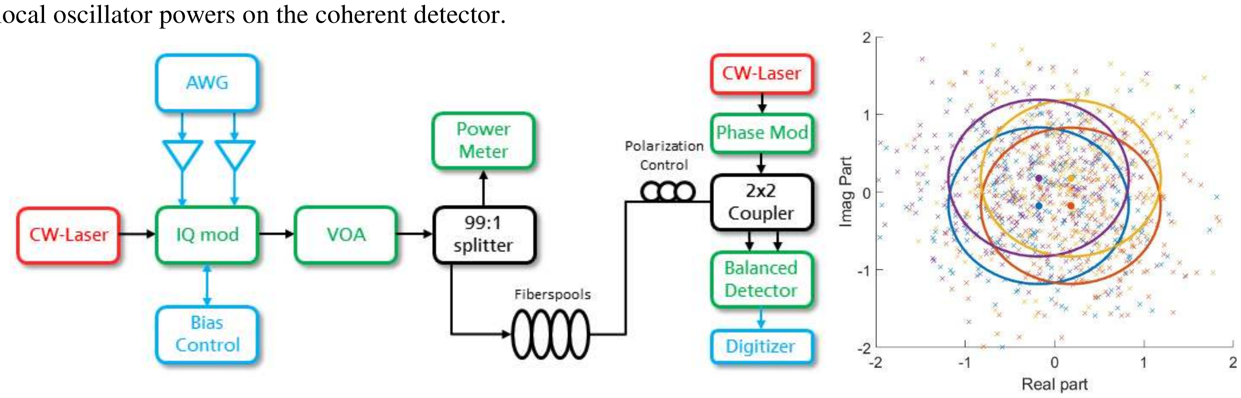

Fig. 1. Experimental setup and results. Left: CV-QKD implementation using pilot assisted synchronization. Right: Constellation diagram of measured values (crosses) for a QPSK signal with 0.1 photons/symbol at the receiver. The larger dots and the circles represent the mean and the variance, respectively, fitted to the measurement points.

Here, we present the development of a CV-QKD system using the pilot tone assisted scheme. Alice prepares weak coherent pulses that are modulated using QPSK at a repetition rate of 10 MHz. A pilot tone serves as frequency reference for Bob. The pilot tone has a power of 30 dB larger than the quantum signal and a frequency offset of 25 MHz with respect to the quantum signal. On Bob's side, signal and pilot are mixed with a strong LO (>6 dBm) before reaching a balanced detector with a shot noise to excess noise ratio exceeding 20 dB. The electrical signal is measured with a digitizer at a sampling rate of 200 MSa/s and 14 bit resolution. The frequency information obtained from the pilot tone is used to compensate for frequency drifts and laser phase noise. Subsequently, we demodulate the QPSK signal and apply the security analysis [7]. We further study the effect of Raman scattering and four wave mixing in a multiplexing configuration with 20 classical channels, each with a launch power of -1 dBm, confirming the feasibility of distilling a usable secure key rate for co-propagation of classical signals with our CV-QKD signal over distances of several km.

[1] E. Diamanti, H.-K. Lo, B. Qi and Z. Yuan, "Practical challenges in quantum key distribution", Npj Quantum Information **2** 16025 (2016);
[2] R. Kumar et al. "Coexistence of continuous variable QKD with intense DWDM classical channels", New J. Phys. **17** 043027, (2015);
[3] P. Jouguet et al. "Experimental demonstration of long-distance continuous-variable quantum key distribution", Nat. Photonics **7**, 378 (2013);
[4] B. Qi, P. Lougovski, R. Pooser, W. Grice and M. Bobrek, "Generating the Local Oscillator "Locally" in Continuous-Variable Quantum Key Distribution Based on Coherent Detection", Phys. Rev. X **5**, 041009 (2015);
[5] D. Huang et al. "High-speed continuous-variable quantum key distribution without sending a local Oscillator", Opt. Lett. **40**, 3695 (2015);
[6] D. Soh, et al. "Self-Referenced Continuous-Variable Quantum Key Distribution Protocol," Phys. Rev. X **5**, 041010 (2015);
[7] A. Leverrier et al. "Continuous-variable quantum-key-distribution protocols with a non-Gaussian modulation" Phys. Rev. A83, 042312 (2011).

Teleportation simulation of non-Pauli channels

Thomas Cope,[1] Leon Hetzel,[2] Leonardo Banchi,[3] and Stefano Pirandola[1]
[1]*Computer Science and York Centre for Quantum Technologies, University of York, York YO10 5GH, United Kingdom*
[2]*Department of Physics, University of Bremem, Germany*
[3]*Department of Physics and Astronomy, University College London, Gower Street, London WC1E 6BT, United Kingdom*
(Dated: March 27, 2017)

Teleportation [1] is one of the most captivating ideas of quantum information. It exploits the resource of quantum entanglement to allow us to perfectly transfer a state from one system to another, with the help of **L**ocal **O**perations and **C**lassical **C**ommunication (LOCC). We can interpret this protocol as the simulation of a noiseless quantum channel or transfer operator, and ask if we can alter the protocol to simulate other, noisy channels.

To begin with, we review the motivation behind simulating quantum channels using resource states and (arbitrary) LOCCs. In fact, this simulation allows one to upper bound the ultimate, two-way capacities for quantum communication, entanglement distribution, and secret key generation by just computing the **R**elative **E**ntropy of **E**ntanglement (REE) of the resource states. This work was done by Stefano Pirandola, Riccardo Laurenza, Carlo Ottaviani and Leonardo Banchi in Ref. [2].

Then, we look at the simplest generalization of the teleportation simulation argument of Ref. [3], which was based on the perfect use of Pauli corrections, and therefore limited to the simulation of Pauli channels, as proven in Ref. [4]. In fact, we show how we may generalize this idea much further by replacing the hitherto assumed perfect classical communication of Alice by a noisy classical channel, so that the Pauli corrections are stochastically implemented. In this stochastic version of teleportation, we may simulate a much more general class of quantum channels, and for qubits we also provide an explicit formula for the channel simulated, given a resource state and noisy classical channel.

Finally, we characterise all possible channels simulatable by using the Choi Matrix of an amplitude damping channel and a noisy classical channel. In particular, this approach allows us to define a new class of quantum channels that we call "Pauli-damping" channels, because of their peculiar decomposition into a Pauli and a damping part. For this class, we compute their minimum trace-norm and diamond-norm distance from the set of Pauli channels. Most importantly, we show a single-letter REE-based upper bound for their two-way quantum and secret-key capacities.

Finally, we conclude with an explanation of the logical next steps which this work will take, along with some intuitive ideas about what we may find.

[1] Bennett, C. H., Brassard, G., Crepeau, C., Jozsa, R., Peres, A. & Wootters, W. K. Teleporting an unknown quantum state via dual classical and Einstein-Podolsky-Rosen channels. *Phys. Rev. Lett.* **70**, 1895–1899 (1993).

[2] S. Pirandola, R. Laurenza, C. Ottaviani, and L. Banchi, "Fundamental Limits of Repeaterless Quantum Communications," *Preprint arXiv*:1510.08863 (2015). In press on Nature Communications.

[3] Bennett, C. H., DiVincenzo, D. P., Smolin, J. A. & Wootters, W. K. Mixed-state entanglement and quantum error correction. *Phys. Rev. A* **54**, 3824–3851 (1996).

[4] Bowen, G. & Bose, S. Teleportation as a Depolarizing Quantum Channel, Relative Entropy and Classical Capacity. *Phys. Rev. Lett.* **87**, 267901 (2001)

Discrete model of quantum filtering for environment prepared in single photon state

Anita Dąbrowska, Gniewomir Sarbicki
Nicolaus Copernicus University, Toruń, Poland

(Dated:)

PACS numbers:

We propose a discrete model of stochastic evolution of a quantum system interacting with the environment consisting of q-bits prepared initially in non factorisable state. We consider a quantum system $\mathcal{S}$ of the Hilbert space $\mathcal{H}_{\mathcal{S}}$ interacting with the environment consisting of a sequence of two-level systems which interact in turn one by one with the system $\mathcal{S}$ each during the time interval of the length τ. The Hilbert space of environment is $\mathcal{H}_{\mathcal{E}} = \bigotimes_{k=1}^{+\infty} \mathcal{H}_{\mathcal{E},k}$, where $\mathcal{H}_{\mathcal{E},k} = \mathbb{C}^2$ is the Hilbert space of the k-th q-bit interacting with $\mathcal{S}$ in the time interval $[(k-1)\tau, k\tau)$. The ground and excited states of the k-th two-level system we indicate respectively by $|0\rangle_k$ and $|1\rangle_k$. We assume that the environment is prepared initially in the state

$$|1_\xi\rangle = \sum_{k=1}^{+\infty} \xi_k \sqrt{\tau} \sigma_k^+ |vac\rangle,$$

where $|vac\rangle = |0\rangle_1 \otimes |0\rangle_2 \otimes |0\rangle_3 \otimes |0\rangle_4 \ldots$ is the vacuum vector in $\mathcal{H}_{\mathcal{E}}$, the operators $\sigma_k^- = |0\rangle_k\langle 1|$, $\sigma_k^+ = |1\rangle_k\langle 0|$ act non-trivially only in the space $\mathcal{H}_{\mathcal{E},k}$, and $\sum_{k=1}^{+\infty} |\xi_k|^2\tau = 1$. Thus $|\xi_k|^2\tau$ is the probability that k-th q-bit is prepared in the upper state and all the others q-bits are in their ground states. The unitary operator defining the evolution of the total system consisting of $\mathcal{S}$ and the environment up to the time $j\tau$ is given by

$$U_{j\tau} = V_{j-1}V_{j-2}\ldots V_1, \qquad U_0 = \mathbb{1},$$

where V_k acts non-trivially only in the space $\mathcal{H}_{E,k} \otimes \mathcal{H}_S$,

$$V_k = \exp(-i\tau H_k)$$

and

$$H_k = H_{\mathcal{S}} + \frac{i}{\sqrt{\tau}} \left(\sigma_k^+ \otimes L - \sigma_k^- \otimes L^\dagger \right).$$

The operator $H_{\mathcal{S}}$ is the free Hamiltonian of $\mathcal{S}$, and L is a bounded operator acting in $\mathcal{H}_{\mathcal{S}}$. We put, for simplicity, the Hamiltonian of the environment $H_{\mathcal{E}} = 0$. We make the assumption that the total system is initially in the state

$$|1_\xi\rangle \otimes |\psi\rangle.$$

Thus the environment q-bits do not interact with each other and they are initially in the entangled state.

We describe the evolution of $\mathcal{S}$ conditional on the results of the measurement performed subsequently on the environment q-bits at the time instances $\tau, 2\tau, 3\tau, \ldots$.

We prove that the conditional state of $\mathcal{S}$ and the part of the environment which has not interacted with $\mathcal{S}$ up to $j\tau$ is at the moment $j\tau$ given by

$$|\tilde{\Psi}_j\rangle = \frac{|\Psi_j\rangle}{\sqrt{\langle \Psi_j|\Psi_j\rangle}},$$

where

$$|\Psi_j\rangle = \sum_{k=j+1}^{+\infty} \xi_k \sqrt{\tau} \sigma_k^+ |vac\rangle_{[j+1} \otimes |\alpha_j\rangle + |vac\rangle_{[j+1} \otimes |\beta_j\rangle$$

is the conditional vector from the Hilbert space $\bigotimes_{k=j+1}^{+\infty} \mathcal{H}_{E,k} \otimes \mathcal{H}_S$, $|vac\rangle_{[j+1} = |0\rangle_{j+1} \otimes |0\rangle_{j+2} \otimes \ldots$, and $|\alpha_j\rangle$, $|\beta_j\rangle$ are vectors from the Hilbert space $\mathcal{H}_{\mathcal{S}}$ which satisfy the recurrence equations

$$\begin{aligned} |\alpha_{j+1}\rangle &= M_{j+1}|\alpha_j\rangle, \\ |\beta_{j+1}\rangle &= N_{j+1}|\beta_j\rangle + R_{j+1}|\alpha_j\rangle. \end{aligned}$$

Initially we have $|\alpha_0\rangle = |\psi\rangle$, $|\beta_0\rangle = 0$. The exact forms of the operators M_{j+1}, N_{j+1}, R_{j+1} depend on the type of performed measurement and the $(j+1)$-st output. Thus $|\alpha_j\rangle$, $|\beta_j\rangle$ are the conditional vectors depending on all results of the measurements up to the time $j\tau$. To obtain the state of $\mathcal{S}$ depending on all results of the measurements up to the time $j\tau$, we have to take the trace from $|\tilde{\Psi}_j\rangle\langle\tilde{\Psi}_j|$ over the environment degrees of freedom.

The form of $|\tilde{\Psi}_j\rangle$ indicates that at each moment (except $t = 0$) the system $\mathcal{S}$ is entangled with this part of the environment which has not interacted with $\mathcal{S}$ yet. It is the main difference between the considered situation and the standard cases when the environment is in the factorisable state. The physical interpretation of $|\tilde{\Psi}_j\rangle$ is very intuitive. The first term means the following scenario - all q-bits of the environment up to time $j\tau$ were prepared in the ground state and the q-bit prepared in the excited state will happen in the future. The second term represents the scenario that $\mathcal{S}$ has already interacted with the q-bit prepared in the excited state and in the future it will interact with the environment being in the vacuum. The evolution of $\mathcal{S}$ is not Markovian and the conditional evolution of $\mathcal{S}$ is given by the set of four coupled equations. We prove that our approach is equivalent to the procedure of derivation of quantum filtering with making use of ancila system being a source of non-classical state [1].

[1] A. Dąbrowska, arXiv:1611.06359

Photon Scattering from a system of multiple emitters in a dielectric medium: General formalism and application to emitters coupled to 1D waveguide

Sumanta Das[1], Vincent E. Elfving[1], Florentin Reiter[2] and Anders S. Sørensen[1]
1. Niels Bohr Institute, University of Copenhagen, Blegdamsvej 17, 2100 Copenhagen, Denmark
2. Department of Physics, Harvard University, Cambridge, MA 02138, US.

Acquiring efficient light-matter interface at the single photon level is key to future quantum technologies. The required coupling to achieve this can be realized in regime of cavity QED with atoms in optical cavities [1]. However these systems are not readily scalable and may be hard to integrate in quantum circuits. A viable alternative that has emerged in recent years is 1D waveguides coupled to quantum emitters [2]. This in turn has motivated theoretical study of photon scattering dynamics in such waveguide systems [2,3]. However evaluating the reflection and transmission amplitudes of the scattered photon pulse from a multi-emitter system in a waveguide QED setup is a nontrivial problem.

We here provide a solution to this problem. We introduce a general formalism of photon scattering from a system of multilevel emitters in a dielectric medium in the single photon/weak field limit. We derive a scattering relation between the input $\vec{E}_{in}(\vec{r},t)$ and the scattered photon $\vec{E}(\vec{r},t)$ of the form

$$\vec{E}(\vec{r},t) = \vec{E}_{in}(\vec{r},t) + \left(\frac{i\omega}{2\hbar\epsilon}\right)\sum_{jj'}\sum_{gg'}\hat{\rho}_{g'g}\mathbb{G}(\vec{r},\vec{r_j},\omega)\sum_{ee'}\left(\overrightarrow{d^{j}_{ge}}[H_{nh}]^{-1}\overrightarrow{d^{j'}_{e'g'}}\right)\vec{E}_{in}(\vec{r_{j'}},t)\,. \quad (1)$$

Here $\vec{r_j},\vec{r_{j'}}$ stands for the spatial position of the emitters, $\hat{\rho}_{g'g}$ gives the dynamical evolution of the emitters ground state, $\mathbb{G}(\vec{r},\vec{r_j},\omega)$ is a Green function corresponding to the dynamics of the field in the medium at frequency ω while $\sum_{ee'}\left(\overrightarrow{d^{j}_{ge}}[H_{nh}]^{-1}\overrightarrow{d^{j'}_{e'g'}}\right)$ represent the response of the emitters on the field in terms of a non-hermitian Hamiltonian $H_{nh} = H_e - \frac{i}{2}\sum_k L_k^\dagger L_k$. Here H_e is the excited state Hamiltonian while L_k is the Lindbald operator for decay from the excited manifold M_e, shown in the figure.

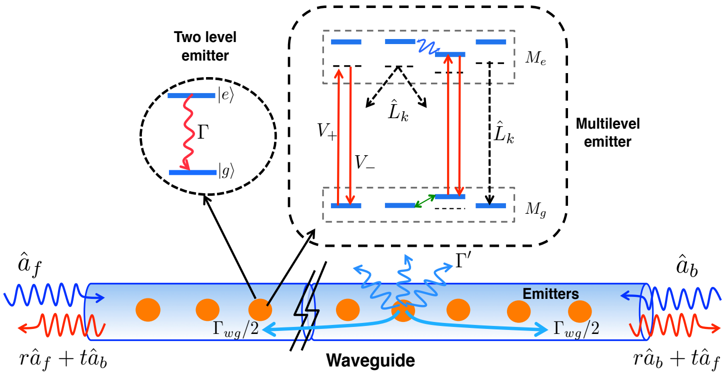

For an array of multilevel emitters in a 1D waveguide shown schematically in the figure, Eq. (1) reduces to $\boldsymbol{a_{l,o}(z,t) = a_{l,in}} + \boldsymbol{i}\sum_{l'}\sum_{jj'}\sum_{gg'}\rho_{g'g}\sum_{ee'}\left(\sqrt{\Gamma^{l,j}_{1D,ge}}[H_{nh}]^{-1}\sqrt{\Gamma^{l',j}_{1D,e'g'}}\right)\boldsymbol{a_{l,in}}. \quad (2)$

Here l,l' stands for the directionality of propagation of the photon, $\Gamma^{l,j}_{1D,ge}$ is the decay into the 1D waveguide for the jth emitter corresponding to the dipole transition between the states $(|e\rangle,|g\rangle)$. It can be seen from Eq. (2) that solution of the ground state dynamics and knowledge of the system non-hermitian Hamiltonian gives the complete solution of the photon scattering problem. The amplitude of reflection and transmission for an input photon can be found by simply evaluating the second term of the above equation. Eq. (2) in waveguide QED setup is thus, analogous to the input-output relation of quantum optics with the following salient features **(a)** it provides exact solution of the scattering problem for Markovian dynamics, **(b)** it considers multiple emitters with no assumption about the level structure of emitters, and **(c)** the dynamics of the complicated multi emitter system reduced to that concerning only the ground states.

[1] A. Reiserer and G. Rempe, Rev. Mod. Phys. **87**, 1379 (2015).
[2] P. Lodahl, S. Mahmoodian, and S. Stobbe, Rev. Mod. Phys. **87**, 347 (2015).
[3] J.-T. Shen and S. Fan Phys. Rev. Lett. **95**, 213001 (2005).

Phonon number QND measurement in electro-mechanics

Luca Dellantonio[1], Oleksandr Kyriienko[1], Florian Marquardt[2], Anders Søndberg Sørensen[1]
[1] The Niels Bohr Institute, University of Copenhagen, Blegdamsvej 17, DK-2100 Copenhagen Ø, Denmark.
[2]Institute for theoretical Physics, University of Erlangen-Nürnberg, Staudtstraße 7, 91058 Erlangen, Germany.

In the past few years opto- and electro-mechanics has shown tremendous progress. Best known for the recent successes in sensing technologies that lead to the detection of gravitational waves, it can be used for cooling a mechanical resonator to its ground state and ultimately proving non-classical behaviours in macroscopic objects. Most experiments in this field fall into the category of Gaussian operations which severely restricts the accessible quantum features. To overcome this, we consider a method to achieve non-Gaussian operations and focus on the Quantum Non-Demolition (QND) measurement of the phonon number operator in mechanical membranes. Previously studied in a two-mode optical cavity [1], it has been shown that the influence of the environment forbids the detection of the mechanical mode occupation, unless large single photon optomechanical coupling is achieved [2]. Differently from the optical case, we show that in an electro-mechanical setup the deleterious effects of the environment can be diminished, which facilitates the QND measurement of the mechanical occupation number $\hat{n}_b$.

Our setup consists of the circuit presented in Fig. 1a, in which the two capacitors share a single moving plate. Following the standard procedure, we expand the electrical frequency ω_e with respect to the position $\hat{x}$ of the membrane – but keeping both the linear g_1 and the quadratic g_2 terms. In the interaction Hamiltonian, this last term gives rise to a coupling between the electrical mode and $\hat{n}_b$, allowing us to measure the phonon number operator without disturbing its time evolution. However, the linear term proportional to g_1 does not commute with $\hat{n}_b$, and is responsible for heating the membrane and eventually ruin the experiment. We identify a parameter λ that describes how well we can distinguish between two measurements with different phonon numbers, taking into account the membrane's heating that can spoil the experimental outcome. For the circuit in Fig. 1a, λ takes the form:

$$\lambda = 2\frac{g_2^2}{g_1^2}\frac{Z_{out}\,L_0^2\,\omega_e^2}{R\,(R_0+Z_{out})^2},$$

where R, R_0 and L_0 are the resistances and inductance of the circuit and Z_{out} the impedance of the transmission line. For values of $\lambda > 1$ it is then possible to discriminate whether the membrane is in its ground or excited state, as it is suggested by our numerical simulations presented in Fig. 1b. The histogram, that collects the outcomes $\langle \hat{V}_M \rangle$ of the experiment, is clearly made by two distinct peaks, relative to $\langle \hat{n}_b \rangle = 0$ and 1. Importantly, compared to a standard RLC circuit λ is increased by a factor of $[(R_0+Z_{out})\omega_e^2]/[2\,R\,\omega_m^2]$, which can be much larger than unity. This opens the doors to a feasible QND measurement of the phonon number operators in (possibly) macroscopic membranes, which is one of the main objectives in the field.

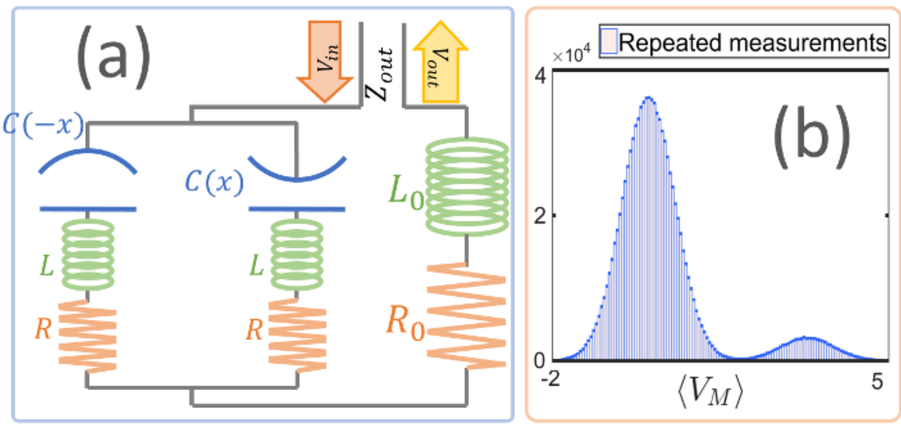

(a): Circuit diagram of the electrical circuit coupled to a mechanical resonator. (b): Simulated outcome for $\lambda = 10$. Two peaks, corresponding to $\hat{n}_b = 0$ and $\hat{n}_b = 1$ are clearly visible.

[1]: J. D. Thompson, B. M. Zwickl, A. M. Jayich, F. Marquardt, S. M. Girvin & J. G. E. Harris, *Nature* ***452****, 72* (2008).

[2]: H. Miao, S. Danilishin, T. Corbitt, & Y. Chen, *Phys. Rev. Lett.* ***103****, 100402* (2009).

Role of nuclear spin fluctuations in spin-photon and multi-photon entanglement protocols based on charged quantum dots

E. V. Denning[1], J. Iles-Smith[1], Dara P.S. McCutcheon[2] and J. Mørk[1]

[1] *DTU Fotonik, Department of Photonics Engineering, Technical University of Denmark, Copenhagen, Denmark*
[2] *Department of Electrical and Electronic Engineering, University of Bristol, Bristol, UK*

Spin-photon and multi-photon entanglement are crucial for the realisation of optical quantum computers and quantum communication devices. Charged quantum dots constitute a promising platform due to its internal spin degree of freedom that can act as a quantum register. In the recent years, several experiments have demonstrated entanglement between a single photon and the spin of a charged quantum dot [1–3]. The main limitation to the fidelities in these experiments is posed by the nuclear spins in the semiconductor host material of the quantum dot. The nuclear spins act as an effective magnetic Overhauser field that fluctuates on a μs time scale, deteriorating the entanglement coherence. Despite these recent experimental advances in the field, the theory describing the detrimental effects presented by the nuclear spin environment is less developed. We study these effects in detail and show how they can be divided into two parts.

The first part is related to the dynamics while the photon and quantum dot are in contact (c.f. Fig 1a). Here, the effect of the Overhauser field is a modification of the optical selection rules, which can be overcome by applying an external magnetic field. We perform in-depth calculations that show how reduction of the nuclear spin fluctuations change the fidelity in different parameter regimes of cavity quantum electrodynamics.

The second part describes the free propagation after a projective measurement has been made on one of the qubits in the entangled state. Even in the presence of an external magnetic field, this second part is still strongly influenced by the environmental spin fluctuations, leading to a decay of the coherence on a ns time scale (c.f. Fig 1b). Hence, to increase the fidelity further, the nuclear fluctuations must be mitigated, for example by polarising the spins. This result is general to any spin-photon entanglement device based on a charged quantum dot.

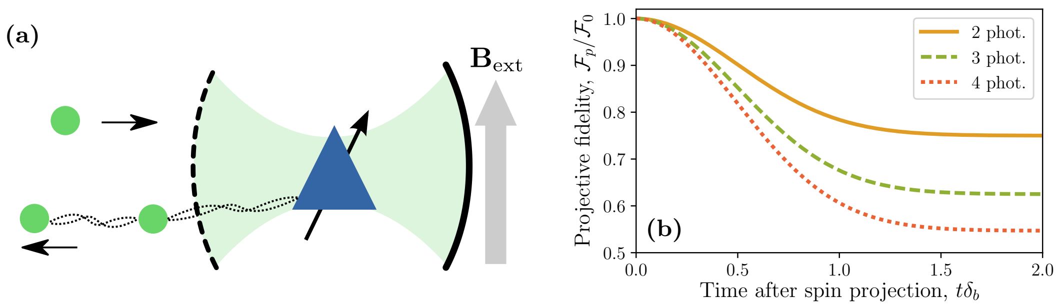

FIG. 1. **(a)** Spin-photon entanglement scheme based on scattering of single photons off a charged quantum dot in an external magnetic field. Upon interaction, spin-flip Raman scattering and coherent scattering take place in superposition, entangling the scattered photon with the spin of the quantum dot. Repeating this process leads to a multipartite entangled cluster state between the photons and the spin, and subsequently performing a projective spin measurement results in an all-photonic cluster state. **(b)** Decoherence of multi-photon entangled state fidelity after spin projection due to ensemble dephasing induced by slow nuclear spin fluctuations. The parameter δ_b is the dispersion of the nuclear Overhauser field distribution. The generation fidelity, $\mathcal{F}_0$, quantifies the success with which the composite spin-multiphoton state in (a) has been generated before the projective spin measurement.

[1] W. Gao, P. Fallahi, E. Togan, J. Miguel-Sánchez, and A. Imamoğlu, Nature **491**, 426 (2012).
[2] J. Schaibley et al., Physical Review Letters **110**, 167401 (2013).
[3] K. De Greve et al., Nature **491**, 421 (2012).

Quantum noise generated by local random Hamiltonians

Marcin Markiewicz,[1] Zbigniew Puchała,[2,1] Anna de Rosier,[3]
Wiesław Laskowski,[3] and Karol Życzkowski[1,4]

[1]*Institute of Physics, Jagiellonian University, Łojasiewicza 11, 30-348 Kraków, Poland*
[2]*Institute of Theoretical and Applied Informatics,*
Polish Academy of Sciences, Bałtycka 5, 44-100 Gliwice, Poland
[3]*Institute of Theoretical Physics and Astrophysics,*
Faculty of Mathematics, Physics and Informatics,
University of Gdańsk, 80-952 Gdańsk, Poland
[4]*Center for Theoretical Physics, Polish Academy of Sciences, Warsaw, Poland*

We investigate the impact of a local random unitary noise on multipartite quantum states of an arbitrary dimension. We follow the dynamical approach, in which the single-particle unitaries are generated by local random Hamiltonians. Assuming short evolution time we derive a lower bound on the fidelity between an initial and the final state transformed by this type of noise. This result is based on averaging the Tamm-Mandelstam bound and is expressed in terms of mean quantum Fisher information (QFI). We showed that in the case of pure states the mean QFI is determined by lower-order correlations (single particle and bipartite only). This fact leads us to the conclusion that, among states that are genuinely entangled, the more correlations are stored in the higher-order correlation sector, the more the state is insensitive to the local random noise. Furthermore, when comparing collective and noncollective noise, it appears that states often used in the theory of quantum information can be considered strongly nontypical. These states are more fragile with respect to the collective random noise, in contrast to generic random pure states, which suffer more under the action of noncollective noise. From the point of view of the problems of random dynamics, our research demonstrates the difference between static (uniform average over a symmetry group) and dynamical approaches, in which we average over generators of evolution for a given evolution time treated as a parameter. Moreover, we showed that, within the dynamical approach, the impact of the noisy random channel is actually identical for any distribution of the random Hamiltonians which fulfill very general symmetry conditions.

Vacuum Squeezing from Kerrlike Cavities under Two-Tone Driving

Rafael Garcés and Germán J. de Valcárcel
Universitat de València, Spain (german.valcarcel@uv.es)

We show in a unified way that optomechanical, nonlinear superconducting, and semiconductor-polariton cavities yield strong vacuum squeezing under two-tone driving. The advantages of this bichromatic pump over the usual monochromatic one are that maximum squeezing is unrelated to optical bistability and that no mean field affects the squeezed field (vacuum squeezing).

Optical Kerr cavities (driven by monochromatic fields) are sources of squeezed light, getting strongest at their optical bistability regime [1]. This is the case of optomechanical [2,3], nonlinear superconducting [4], and semiconductor-polariton cavities [5], as demonstrated by recent experiments [6-10]. Two main features characterize this type of light squeezing: (i) it's maximized at the turning points of the optical bistability, and (ii) there's a bias coherent mean field. Both features are detrimental, in general, for applications, either because of stability issues or because of a macroscopic background.

On the other hand, Kerr cavities pumped by a two-tone (bichromatic) field [11] have been recently addressed, showing that the usual bistable response of the monochromatic scenario is substituted by a four-wave-mixing bifurcation, in a sense similar to the threshold of a degenerate optical parametric oscillator. Inspired by this result we have recently reported that optomechanical and superconducting circuit cavities driven by two frequencies close to the same cavity mode yield very strong vacuum squeezing [12].

Here we give a unified description of the phenomenon including semiconductor-polariton microcavities in the appropriate limits where such systems behave Kerr-like. In particular, we show that the optical bistability typical of the usual monochromatic driving is replaced by a degenerate four-wave mixing bifurcation in all cases, at which ideally perfect squeezing is got, only slightly degraded by mechanical noise in the optomechanics case and by excitonic noise in the polariton case. As the phenomenon no more depends on bistable scenarios, it is insensitive to noise-induced jumps between coexisting solutions and, moreover, the strong coherent background present in the monochromatic driving case is absent in this case.

Apart from this unified description we analyze in some detail the effects brought about by the specific physical interaction underlying each of the systems: the effect of the mechanical resonance in optomechanical cavities and that of the photon-exciton interaction (which leads to two polaritonic modes) in polaritonic cavities.

[1] M. J. Collet and D. F. Walls, "*Squeezing spectra for nonlinear optical systems*," PRA **32**, 2887 (1985).
[2] C. Fabre et al., "*Quantum-noise reduction using a cavity with a movable mirror*," PRA **49**, 1337 (1994).
[3] S. Mancini and P. Tombesi, "*Quantum noise reduction by radiation pressure*," PRA **49**, 4055 (1994).
[4] J. Bourassa, F. Beaudoin, J. M. Gambetta, and A. Blais, "*Josephson-junction-embedded transmission-line resonators: from Kerr medium to in-line transmon*," PRA **86**, 013814 (2012).
[5] A. Baas, J. P. Karr, H. Eleuch, and E. Giacobino, "*Optical bistability in semiconductor microcavities*," PRA **69**, 023809 (2004).
[6] D. W. C. Brooks et al., "*Non-classical light generated by quantum-noise-driven cavity optomechanics*," Nature **488**, 476 (2012).
[7] A. H. Safavi-Naeini et al., "*Squeezed light from a silicon michromecanical resonator*," Nature **500**, 185 (2013).
[8] T. P. Purdy et al., "*Strong optomechanical squeezing of light*," PRX **3**, 031012 (2013).
[9] M. A. Castellanos-Beltrán et al. "*Amplification and squeezing of quantum noise with a tunable Josephson metamaterial*," Nature Phys. **4**, 929 (2008).
[10] T. Boulier et al., "*Polariton-generated intensity squeezing in semiconductor micropillars*," Nature Comm. 5, 3260 (2014).
[11] G. J. de Valcárcel and K. Staliunas, "*Phase-bistable Kerr cavity solitons and patterns,*" PRA **87**, 043802 (2013).
[12] R. Garcés and G. J. de Valcárcel, "*Strong vacuum squeezing from bichromatically driven Kerrlike cavities: from optomechanics to superconducting circuits*," Sci. Rep. **6**, 21964 (2016).

Squeezing Frequency Combs by Optomechanical Cavities

Rafael Garcés and Germán J. de Valcárcel
Universitat de València, Spain (german.valcarcel@uv.es)

We prove analytically that optical frequency combs get squeezed by optomechanical cavities, where the maximally squeezed supermode coincides with the pumping comb. This simplifies radically the choice of the local oscillator for squeezing detection, which is a bottleneck in multimode quantum optics. The effect should be observable with actual experiments.

Almost twenty years after the first theoretical predictions [1,2], recent experiments have demonstrated the ability of optomechanical cavities to squeeze light [3–5]. The origin of such quantum noise reduction lies on the effective Kerr nonlinearity underlying the actual optomechanical interaction [1,2]. However, in the optomechanical case the mechanical inertia plays a role, which manifests, at least, as a source of mechanical noise. Such difference is of relatively little importance in dc regimes, like the ones considered in [1–5], but can be significant in multimode regimes, where the beating between different optical modes can affect the mechanical response.

Here we study synchronously pumped optomechanical (SPOM) cavities, so that adjacent "teeth" excite adjacent cavity modes. We assume that all cavity modes interact with a common mechanical mode [6] –a sensible approximation if the mechanical frequency is much less than the cavity free spectral range (Ω_{FSR}), as in usual experiments. This way the radiation pressure harmonics at multiples of Ω_{FSR} the so that now the mechanical inertia can play a clear role. In the usual case, which we consider, when do not play a significant role and the mechanical resonator just responds to the averaged radiation pressure. In other words, we assume that the mechanical element is not able to scatter photons between different cavity modes.

Under the above conditions the SPOM cavity can be modelled following the lines as in [1,2,5]: each cavity mode (labelled by "m", with boson operators $a_m^\dagger$ and a_m) is affected by a dynamical detuning proportional to the mechanical displacement, and such displacement responds to the averaged radiation pressure $\sum_m \hbar g_m a_m^\dagger a_m$ (g_m are the vacuum optomechanical couplings).

We have studied the case where all modes have the same g_m (quite a reasonable assumption under realistic conditions), and have proven analytically that: (I) a bistable response emerges at the red detuning side, (II) maximum (and strong) light quantum noise reduction is observed at the turning points of the bistable cycle, and (III) the object maximally squeezed is a so-called supermode (i.e. a linear combination of cavity modes) [7,8] having the very same shape as the pumping frequency comb, whichever it be. We have checked that these results are almost unaffected by differences among the g_m's under realistic conditions.

Finally, inspired by recent work on bichromatically driven optomechanical cavities [9] we propose the use of frequency combs in which each tooth is split into two equal ones (e.g. using an electro-optic modulator). When that splitting is much smaller than Ω_{FSR} we obtain similar results in the previous case, with the following advantages: now we get vacuum squeezing, and the phenomenon is unrelated to bistability, which is good for stability issues.

[1] C. Fabre et al., "*Quantum-noise reduction using a cavity with a movable mirror*," Phys. Rev. A **49,** 1337 (1994).
[2] S. Mancini and P. Tombesi, "*Quantum noise reduction by radiation pressure*," Phys. Rev. A **49,** 4055 (1994).
[3] D. W. C. Brooks et al., "*Non-classical light generated by quantum-noise-driven cavity optomechanics*," Nature **488,** 476 (2012).
[4] A. H. Safavi-Naeini et al., "*Squeezed light from a silicon michromecanical resonator*," Nature **500,** 185 (2013).
[5] T. P. Purdy et al., "*Strong optomechanical squeezing of light*," Phys. Rev. X **3,** 031012 (2013).
[6] D. Lee et al., "*Multimode optomechanical dynamics in a cavity with avoided crossings*," Nat. Comm. **6**, 6232 (2015).
[7] G. J. de Valcárcel et al., "*Multimode squeezing of frequency combs*," Phys. Rev. A **74**, 061801(R) (2006).
[8] J. Roslund et al., "*Wavelength-multiplexed quantum networks with ultrafast frequency combs*," Nat. Photon. **8**, 109 (2014).
[9] R. Garcés and G. J. de Valcárcel, "*Strong vacuum squeezing from bichromatically driven Kerrlike cavities: from optomechanics to superconducting circuits*," Sci. Rep. **6,** 21964 (2016).

Quantum mechanics and the efficiency of simulating classical complex systems

Carlo Di Franco[1,2] and Mile Gu[1,2,3]

[1]*School of Physical and Mathematical Sciences, Nanyang Technological University, 639673, Singapore*
[2]*Complexity Institute, Nanyang Technological University, 639673, Singapore*
[3]*Centre for Quantum Technologies, National University of Singapore, 117543, Singapore*

The development of tools allowing us to infer models from observed data, and thus to simulate possible future outputs, has a central role in several fields. Many fundamental questions in nature and society can be addressed only by isolating indicators of future behavior in highly complex systems. However, even the most efficient constructions often require information about the past that is uncorrelated with future predictions. In terms of energetic costs, this brings a waste of resources in the computer simulations based on such models. Even if the systems to simulate are completely classical, it has been proved that quantum information can reduce this waste beyond classical limits [1].

During the talk I will sketch this scenario, and present some of the aforementioned results. In particular, I will describe a possible implementation of a quantum model that breaks this classical bound. Such experiment can be realized by exploiting tools and schemes already used for the implementation of quantum walks in linear-optics setups [2].

[1] M. Gu, K. Wiesner, E. Rieper, and V. Vedral, *Nat. Commun.* **3**, 762 (2012).
[2] C. Di Franco and M. Gu, in preparation.

Quantum key distribution using space division multiplexing.

Yunhong Ding†, Davide Bacco*, Kjeld Dalgaard, Karsten Rottwitt, and Leif Katsuo Oxenløwe

Department of Photonics Engineering, Technical University of Denmark, 2800 Kgs. Lyngby, Denmark.
*† yudin@fotonik.dtu.dk, * dabac@fotonik.dtu.dk*

Quantum key distribution (QKD), a technique based on quantum physics laws, provides unconditional secure quantum keys shared between two or more clients (Alice and Bob) [1]. Most of QKD systems are implemented in a point-to-point link using bulky and expensive devices. Consequently, a large scale deployment of this technology has not been achieved. A solution may be represented by integrated photonic circuits, which provide excellent performances (compacts, good optical phase stability, access to new degrees of freedom), and are particularly suitable for the manipulation of quantum states. Some recent experiments have already demonstrated conventional binary QKD systems, using polarization and phase reference degrees of freedom [2, 3]. Moreover, by using integrated solution new high-dimensional quantum states can be generated and propagated. High-dimensional quantum states are suitable for longer transmission distance and higher secret key rate transmission, being more robust to noise level and allowing an higher channel capacity [4]. In this paper, we show the first silicon chip-to-chip high dimensional decoy-state quantum key distribution protocol based on spatial degrees of freedom (the cores of a multi-core fiber -MCF-). By tuning cascaded Mach-Zehnder interferometers (MZIs), it is possible to prepare high dimensional quantum states in different mutually unbiased basis (MUBs) (Fig. 1 (b)). In particular a train of weak coherent pulses are injected into the transmitter chip (Alice), where multiple variable optical attenuators (VOAs) are used to decrease the number of photons per pulse ($\mu < 1$) [5]. Furthermore, through a combination of MZIs and VOAs, a decoy state-technique is implemented in order to avoid some particular eavesdropping intrusion, like photon-number-splitting (PNS) attack. During the key generation process, Alice, by using an FPGA board (Fig. 1(a)), randomly chooses one of the bases and one of the four states to transmit to Bob. The ququart are matched to four cores of a multi-core fiber, through a highly efficient MCF grating coupler. After the transmission link, the quantum states are coupled into Bob's chip (Fig. 1(a)) through the MCF coupler, and randomly measured in one of the bases. In the subsequent distillation process, counts measured in the wrong bases are discarded. Acquired experimental data show stable and good results for more than 11 minutes of measurement with a quantum bit error rate below the threshold level of individual and coherent attacks.

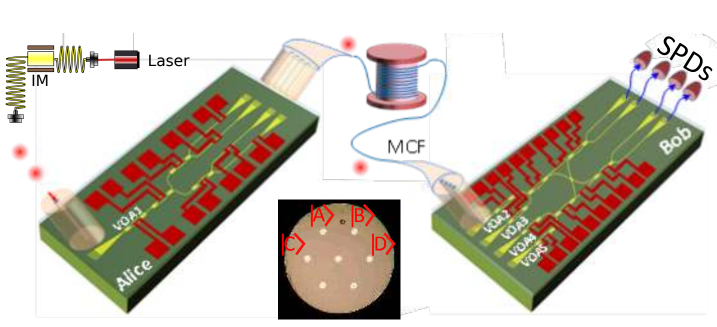

(a) Experimental setup

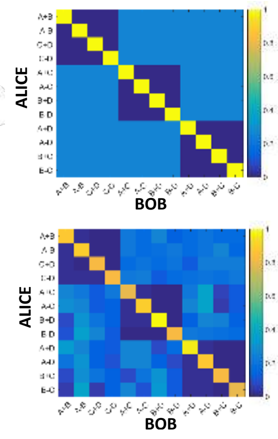

(b) MUBs

Fig. 1 The setup used in the HD-QKD proof of concept experiment in (a). In (b) are reported MUBs tomographies (theoretical and experimental). By using the (classical) definition of fidelity ($F(x, y) = \sum_i \sqrt{p_i q_i}$, we obtain 0.977 ± 0.01

References

[1] C. H. Bennett, G. Brassard, "Quantum Cryptography: public key distribution and coin tossing," in Proceeding of IEEE International Conference on Computer, Systems & Signal Processing 175–179 (1984).
[2] P. Sibson, et al., "Chip-based Quantum Key Distribution," *Nat. Commun.* **8**:13984 (2017)
[3] C. Ma, et al., "Silicon photonic transmitter for polarization-encoded quantum key distribution," *Optica* **3** (2016)
[4] N. J. Cerf , et al. Security of Quantum Key Distribution Using d-level system. *Phys. Rev. Lett.* **88** (2002)
[5] Y. Ding, et al., "High-Dimensional Quantum Key Distribution based on Multicore Fiber using Silicon Photonic Integrated Circuits," arXiv:1610.01812 (2016)

Laser written integrated programmable multiport interferometer

I.V. Dyakonov[1], A.A. Kalinkin[1], M.Yu. Saygin[1], I.V. Radchenko[1], I.B. Bobrov[1], I.A. Pogorelov[1], S.A. Evlashin[2], P.V. Dyakonov[2], S.M. Zyryanov[1,2], S.S. Straupe[1] and S.P. Kulik[1]

[1] Faculty of Physics, Lomonosov Moscow State University, Russia
[2] Skobeltsyn Institute of Nuclear Physics, Lomonosov Moscow State University, Russia

Current challenges in experimental quantum optics become utterly demanding to optical hardware performance. Traditional bulk optical setups no longer fulfil the photonic processing requirements for tasks like linear optical quantum computing [1], boson sampling [2], quantum walks [3], etc., which should be implemented on an essentially scalable, flexible and low loss optical platform. Semiconductor industry disposes cutting-edge technology for programmable integrated photonic device fabrication and packaging providing all the necessary tools for boosting experimental research in the areas listed above. However, this technology is hardly available for average quantum optical laboratory.

In our work we demonstrate the power of femtosecond laser micromachining for active integrated photonic device prototyping. Femtosecond laser writing is an established tool for rapid prototyping of sophisticated optical waveguide structures [4]. Laser writing of thermooptically controlled devices has recently been demonstrated on individual tunable element scale [5]. We further develop the technique and fabricate 4×4 integrated interferometer thermooptically adjustable applying voltage to 12 chrome heaters patterned using femtosecond laser writing facility on a metallic film deposited on the chip surface. We demonstrate 5 ms switching time and design adaptive algorithms for precise calibration of the device to perform desired unitary transformation. We believe our results may boost research in integrated quantum photonics field endowing researchers with an affordable programmable integrated device fabrication approach.

References

[1] Jacques Carolan et al. Universal linear optics. *Science*, 349(6249):711–716, 2015.

[2] Scott Aaronson and Alex Arkhipov. The computational complexity of linear optics. *arXiv:1011.3245v1*, 2010.

[3] Hagai B. Perets et al. Realization of quantum walks with negligible decoherence in waveguide lattices. *Phys. Rev. Lett.*, 100:170506, 2008.

[4] Andrea Crespi et al. Integrated multimode interferometers with arbitrary designs for photonic boson sampling. *Nature Photonics*, 7:545–549, 2013.

[5] Fulvio Flamini et al. Thermally reconfigurable quantum photonic circuits at telecom wavelength by femtosecond laser micromachining. *Light: Science and Applications*, 4:e354, 2015.

Continuous-Phase Frequency Modulated Drive of a Nitrogen-Vacancy Spin Ensemble

Haitham A.R. El-Ella, Sepehr Ahmadi, Alexander Huck, Ulrik L. Andersen
Department of Physics, Technical University of Denmark, 2800 Kongens Lyngby, Denmark

The coherent control and readout of a spin ensemble is of great interest to quantum-information-based protocols and sensing, for which both implementations are limited by the ensembles coherence time. Amongst the many studied spin ensemble systems, nitrogen-vacancy centres (NVs) in diamond stand out as having the longest measured coherence time under ambient conditions, and are therefore amongst the most promising candidates for the development of quantum memory units and as ultra-sensitive magnetometers [1,2].

The main hinder towards their successful implementation is in circumventing decoherence which is intrinsic to diamond as well as that instilled by external control fields. These issues are usually addressed through the application of dynamically-decoupling pulse sequences which have been shown to extend the coherence times of NV ensembles up to half of the longitudinal spin relaxation time [3]. However, when attempting to apply the same scheme to denser ensembles spanning larger volumes (e.g. >1 ppm spanning >0.01 mm^3), extending decoherence times are stalled by difficulties in ensuring sufficient uniform spin polarisation and equal spin rotation throughout the macroscopic volume the ensemble occupies, which is further compounded by inherent inhomogeneous broadening.

Here we explore an alternative continuous-wave strategy which is based on continuous-phase frequency modulation (CPSFK) of the microwave field. This scheme is implemented using a vector signal generator and phase-sensitive detection locked to the CPFSK modulation rate, as shown in Fig.1. By optically measuring the phase sensitive magnetic resonance from a nitrogen-vacancy ensemble while modulating both the phase are frequency of the spin driving field using CPFSK, we demonstrate hyperfine linewidth narrowing down to 20% of the resolved natural linewidth using continuous-wave amplitude modulation under continuous laser excitation, as shown in Fig. 2.

[1] Grezes *et al.* "Multimode storage and retrieval of microwave fields in a spin ensemble", Phys. Rev. X. **4** 021049 (2014).

[2] Rondin *et al.* "Magnetometry with nitrogen-vacancy defects in diamond", Rep. Prog. Phys. **77** 56503 (2014).

[3] Bar-Gill *et al.* "Solid-state electronic spin coherence time approaching one second", Nature Comm. **4** 1743 (2013).

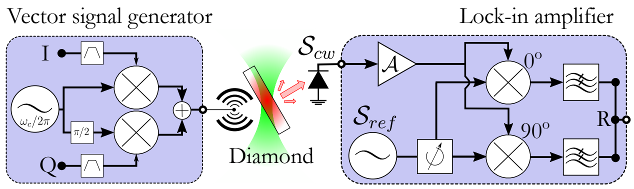

FIG. 1. Schematic of the experimental setup, where the in-phase (I) and quadrature (Q) waveforms are filtered and mixed with the carrier frequency $\omega_c/2\pi$ to create a CPFSK microwave field which is delivered to the diamond via a microwave resonator antenna. The detected signal $\mathcal{S}_{cs}$ is passed to a lock-in amplifier which uses the modulation rate of the CPFSK waveform ($\mathcal{S}_{ref}$) as its reference.

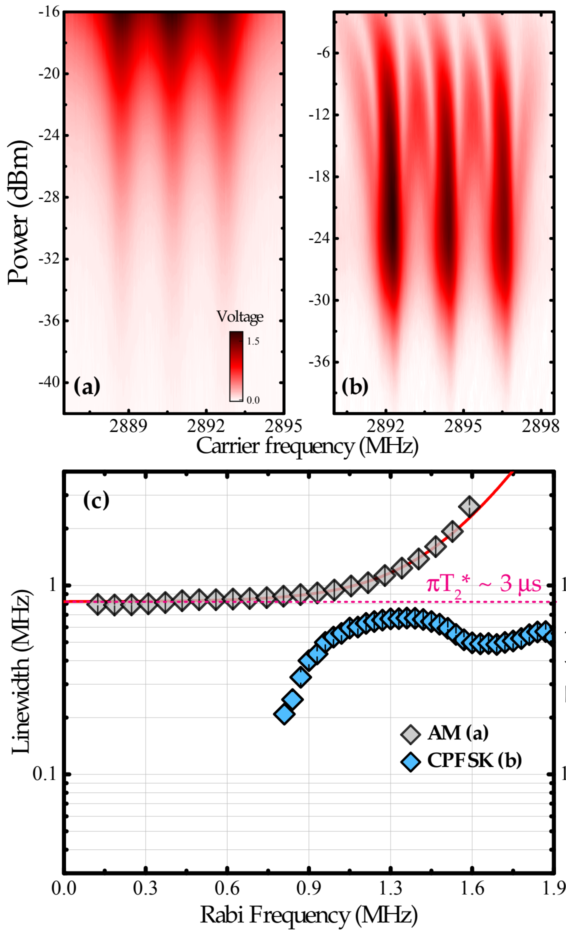

FIG. 2. (a) Amplitude modulated and (b) continuous phase modulated lock-in spectra as a function of carrier frequency power before amplification (40 dB amplifier), showing the three hyperfine resonances of a single crystallographic subgroup. (c) Extracted hyperfine resonance linewidth as a function of the power equivalent Rabi frequency.

Coupling a superconducting qubit to light using hybrid qubit-quantum dot nanostructures

°V. E. Elfving*, S. Das*, A. S. Sørensen*, (*Niels Bohr Institute, University of Copenhagen)
E-mail: vincent.elfving@nbi.ku.dk

Several advances in quantum computation have been achieved with superconducting qubits in recent years. In parallel to this, methods of quantum communication and quantum key distribution have been developed using optical photons as flying qubits. In order for quantum computers to effectively communicate with each other, and for quantum networks to extend their range by quantum repeaters, an interface between these two physical systems is highly desirable.

Strenuous efforts have been made to coherently couple superconductors and light. However, such an interface is complicated by the large energy mismatch between superconducting qubits (micro eV's) and optical photons (eV's). As a consequence of this mismatch even the absorption of a single or few optical photons can significantly disturb a superconducting qubit, making it necessary to screen them from light.

To tackle this issue, we theoretically propose a hybrid system incorporating a semiconductor quantum dot (QD) embedded in a photonic nanostructure as an interface between a superconducting qubit and an optical photon.

The oscillating Cooper pair occupying a single superconducting island introduces an electric field in its immediate surroundings depending on the state of the superconducting qubit. Due to the strong dipole moment and the associated Stark shift in quantum dots, combined with the recently achieved narrow linewidth, a significant shift in the QD transition energy can be achieved by the oscillation of a single cooper pair.

We theoretically describe a Raman scheme mediated by the QD, which flips the state of the superconducting qubit state by emitting a red detuned optical photon. A QD embedded in a photonic nanostructure, e.g., a cavity, can have light-matter coupling on the same order of magnitude as the superconducting qubit transition frequency, while the QD can simultaneously be strongly coupled to the qubit through the Stark shift. As a consequence the effective Raman process can be made highly efficient. The Raman scheme can be extended to generate entanglement between distant superconducting qubits through entanglement swapping with an interferometry setup, and can thus connect different superconducting quantum computers through teleportation.

Strong light-matter coupling can be achieved for quantum dots, with efficient coupling to single photons. As a consequence, the light matter interface we envision can be achieved at very low light levels, possibly involving incident photons fields containing merely few or a single photon(s). This alleviates the challenge of the large energy mismatch between superconductors and optical fields since it will lead to minimal absorption in the superconducting qubits. The resulting hybrid system can then form the basis of a large scale "quantum internet" based on super conducting systems.

Correction of atmospheric turbulent effects with a double fast steering mirror system for fast free-space quantum communications

Jorge Gómez-García, Miguel Ángel Báez-Chorro, Natalia Denisenko, Verónica Fernández-Mármol,
Spanish National Research Council (CSIC), Institute of Physical and Information Technologies (ITEFI), Serrano 144, 28006 Madrid, Spain.

Atmospheric beam wander causes random fluctuations of the beam's angle of arrival originating loss of signal and increased quantum bit error rates that can severely limit the performance of free-space quantum communication systems. Stabilization techniques maintain the quantum signal aligned within the receiver field of view in the presence of fast turbulence (up to 100 Hz) by using fast steering mirrors (FSMs) and position sensitive detectors (PSDs). A correcting system with two FSMs (see Figure 1), each in feedback loop with a quadrant detector (QD), enables stabilization of the beam throughout the whole optical axis of the receiver. The correcting system was tested under a free-space 30 m link for several weather conditions. A reduction of the long-term beam diameter — taking into account all turbulent effects over an statistically-meaningful period of time at the end of the propagation path — by a factor of 3 (see Figure 2) was measured after correction. This corresponds to one order of magnitude a lower long-term beam area (an thus, potential background coupled into the quantum receiver). The performance of the system up to 600m distances than 30m was estimated from experimental data confirming the reduction in background of one order of magnitude is still present.

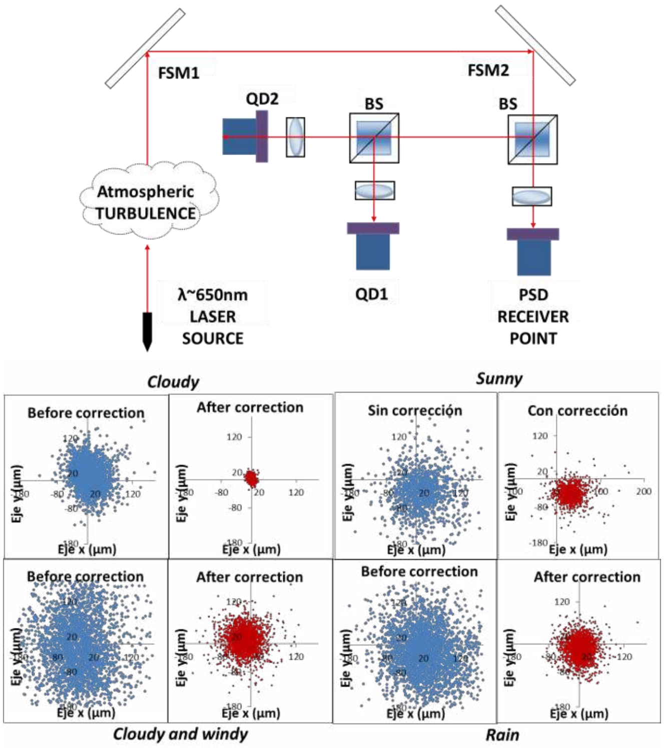

Figure 1.Double FSM correcting system (top) and beam centroid position at the receiver's PSD before and after correction at different atmospheric conditions (bottom).

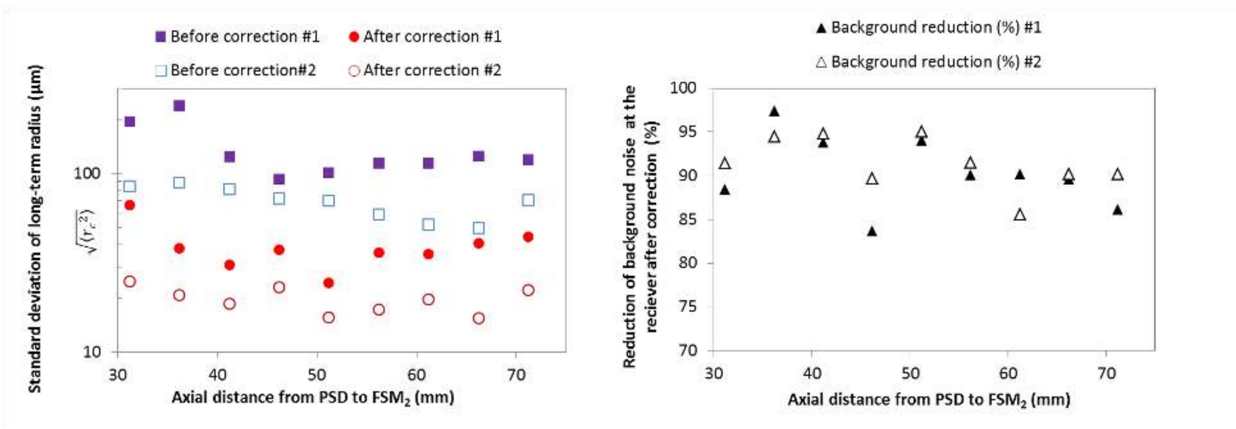

Figure 2. Standard deviation of the long-term beam diameter at the reciever before and after correction measured at different days (left) and the corresponding reduction in the background after correction (right).

Ultimate completely positive divisibility and eternal indivisibility of dynamical maps in collisional models

Sergey N. Filippov
Moscow Institute of Physics and Technology, Dolgoprudny, Moscow Region, Russia and Institute of Physics and Technology, Russian Academy of Sciences, Moscow, Russia

The open system dynamics in the Schrödinger picture is $\varrho_S(t) = \Phi_t \varrho_S(0)$, where $\Phi_t(\varrho_S) = \mathrm{tr}_E \left\{ U_t \varrho_S \otimes \varrho_E U_t^\dagger \right\}$, U_t is the unitary evolution of the system and the environment, ϱ_E is the fixed state of environment.

Unital qubit processes Φ_t are characterized by three real parameters $\lambda_1(t), \lambda_2(t), \lambda_3(t)$ as follows:

$$\Phi_t[\varrho_S] = \frac{1}{2} \left(\mathrm{tr}[\varrho_S] I + \sum_{j=1}^{3} \lambda_j(t) \mathrm{tr}[\sigma_j \varrho_S] \sigma_j \right), \quad (1)$$

where $\lambda_0 = 1$ and $(\sigma_1, \sigma_2, \sigma_3)$ is a conventional set of Pauli operators. The map Φ_t is known to be completely positive if $1 \pm \lambda_3(t) \geqslant |\lambda_1(t) \pm \lambda_2(t)|$.

Process Φ_t is called CP-divisible if $\Phi_{t+s} = \Theta_{t,t+s} \cdot \Phi_t$, where $\Theta_{t,t+s}$ is a completely positive map for all t and s. Analogously, the process Φ_t is called P-divisible if $\Theta_{t,t+s}$ is a positive map for all t and s. The relation between P- and CP-divisible dynamics is reviewed in [1].

Consider a semigroup dynamics $\Phi_t = e^{\mathcal{L}t}$, where $\mathcal{L} : \mathcal{B}(\mathcal{H}_2) \mapsto \mathcal{B}(\mathcal{H}_2)$ is time-independent generating map. Evolution of the density operator is given by equation $\frac{\partial \varrho}{\partial t} = \mathcal{L}[\varrho]$. Semigroup dynamics is CP-divisible since $\Theta_{t,t+s} = \Phi_s = e^{\mathcal{L}s}$.

Let us consider time-dependent perturbation

$$\frac{\partial \varrho}{\partial t} = \big(\mathcal{L} + \delta\mathcal{L}(t)\big)[\varrho], \quad (2)$$

where $\delta\mathcal{L}(0) = 0$. The term $\delta\mathcal{L}(t)$ describes infinitesimal deviations from dynamics (2), which can be caused by fluctuations of the system-environment Hamiltonian.

In most cases the perturbed dynamical map $\widetilde{\Phi}_t$ remains CP-divisible since $\delta\mathcal{L}(t)$ makes minor changes in the map $\Theta_{t,t+s}$. However, for exceptional semigroups there exists an infinitesimal fluctuation $\delta\mathcal{L}(t)$ which makes the dynamical map $\widetilde{\Phi}_t$ not CP-divisible at some time. We will call such processes Φ_t *ultimate* CP-divisible.

We obtain that Φ_t is ultimate CP-divisible if

$$\frac{\dot{\lambda}_i}{\lambda_i} + \frac{\dot{\lambda}_j}{\lambda_j} = \frac{\dot{\lambda}_k}{\lambda_k}, \quad (3)$$

where indices i, j, k are permutations of $1, 2, 3$.

Physical examples of ultimate CP divisible processes:

- pure phase damping process, when $\lambda_i(t) = 1$ and $\lambda_j(t) = \lambda_k(t) = e^{-\Gamma t}$;
- generalized amplitude damping process with high-temperature environment, i.e. a spontaneous decay with equal probabilities of energy absorption and emission, when $\lambda_i(t) = \lambda_j(t) = e^{-\Gamma t}$ and $\lambda_k(t) = e^{-2\Gamma t}$ in Markov approximation. If this is the case, then $\mathcal{L}[\varrho] = \Gamma\left(\sigma_+ \varrho \sigma_- + \sigma_- \varrho \sigma_+ - \varrho\right)$, where $\sigma_\pm = \frac{1}{2}\left(\sigma_i \pm i\sigma_j\right)$ are excitation creation and annihilation operators.

The dissipator $\mathcal{L}$ of a *general* ultimate CP-divisible process contains at most two terms:

$$\mathcal{L}[\varrho] = \frac{\gamma_i}{2}\left(\sigma_i \varrho \sigma_i - \varrho\right) + \frac{\gamma_j}{2}\left(\sigma_j \varrho \sigma_j - \varrho\right), \quad (4)$$

and the trajectory in the parameter space is $\lambda_i = e^{-\gamma_j t}$, $\lambda_j = e^{-\gamma_i t}$, $\lambda_k = e^{-(\gamma_i + \gamma_j)t}$.

Physically, the evolution $\frac{\partial}{\partial t}\varrho = \mathcal{L}[\varrho]$ with dissipator (4) is achievable as a result of sequential interactions of the system qubit with environment qubits. Such a type of interaction is called *collisional* model and has been intensively studied recently [2]. Let all the environment qubits be in the same state $\xi = \frac{1}{2}I$. The system qubit and the n-th environment qubit interact pairwise during the time period Δt, with the interaction Hamiltonian being

$$H_{\mathrm{int}} = \frac{1}{2}\left(\alpha \sigma_x \otimes \sigma_x + \beta \sigma_y \otimes \sigma_y\right). \quad (5)$$

The system qubit and the n-th environment qubit experience the unitary transformation $U_{\Delta t} = \exp(-i H_{\mathrm{int}} \Delta t)$. As a result of such an interaction, $\varrho \longrightarrow \Phi_{\Delta t}[\varrho] = \mathrm{tr}_2 \left\{ U_{\Delta t}\, \varrho \otimes \frac{1}{2} I\, U_{\Delta t}^\dagger \right\}$ and $\Phi_{\Delta t}[\varrho] = \frac{1}{2}\Big(\mathrm{tr}[\varrho] I + \cos(\beta\Delta t)\mathrm{tr}[\sigma_x \varrho]\sigma_x + \cos(\alpha\Delta t)\mathrm{tr}[\sigma_y \varrho]\sigma_y + \cos(\alpha\Delta t)\cos(\beta\Delta t)\mathrm{tr}[\sigma_z \varrho]\sigma_z\Big)$.

Since the system qubit always interacts with a fresh environmental particle, after $\frac{t}{\Delta t}$ interactions we get $\Phi_t = (\Phi_{\Delta t})^{t/\Delta t}$ with parameters $\lambda_1(t) = [\cos(\beta\Delta t)]^{t/\Delta t}$, $\lambda_2(t) = [\cos(\alpha\Delta t)]^{t/\Delta t}$, and $\lambda_3(t) = \lambda_1(t)\lambda_2(t)$. In the stroboscopic limit [3] $\Delta t \to 0$, $\alpha^2 \Delta t \to 2\gamma_1$, $\beta^2 \Delta t \to 2\gamma_2$ we get the continuous dynamics $\lambda_1(t) = e^{-\gamma_2 t}$, $\lambda_2(t) = e^{-\gamma_1 t}$, and $\lambda_3(t) = e^{-(\gamma_1 + \gamma_2)t}$. Thus, parameters $\lambda_1(t)$, $\lambda_2(t)$, and $\lambda_3(t)$ satisfy condition (3) and the induced dynamics is *ultimate* CP-divisible.

We find a general form of *eternal* CP-indivisible processes and their realization via collisional models.

[1] F. Benatti, D. Chruscinski, S. Filippov. Tensor power of dynamical maps and positive versus completely positive divisibility. Phys. Rev. A **95**, 012112 (2017).

[2] T. Rybar, S. N. Filippov, M. Ziman, V. Buzek. Simulation of indivisible qubit channels in collision models. J. Phys. B: At. Mol. Opt. Phys. **45**, 154006 (2012).

[3] I. A. Luchnikov, S. N. Filippov. Quantum evolution in the stroboscopic limit of repeated measurements. Phys. Rev. A **95**, 022113 (2017).

On bounding the quantum limits of phase estimation through a thermal loss channel: application to covert sensing

Christos N. Gagatsos,[1] Boulat A. Bash,[2] Saikat Guha,[2] and Animesh Datta[1]

[1]Department of Physics, University of Warwick, Coventry CV4 7AL, United Kingdom
[2]Quantum Information Processing Group, Raytheon BBN Technologies, Cambridge, Massachusetts, USA 02138

The performance of any sensing task can be captured by the variance of an unbiased estimator $\hat{\mu}$ and is limited by the quantum Cramér-Rao bound,

$$\langle(\mu-\hat{\mu})^2\rangle \geq F_Q^{-1}, \tag{1}$$

where F_Q is the quantum Fisher information (QFI). When it is hard to calculate the QFI, it is possible to draw some conclusions about the precision of the estimates by finding analytical or numerical upper bounds, denoted as C_Q, on the QFI [1–4], i.e., by lower bounding the lower bound on the variance $\langle(\mu-\hat{\mu})^2\rangle$ described by the Cramér-Rao bound of Eq. (1). Indeed, the upper bound C_Q gives some information for the variance of the estimator $\hat{\mu}$ through the relation $F_Q \leq C_Q \Rightarrow F_Q^{-1} \geq C_Q^{-1}$ and Eq. (1). We follow the formalism developed in Ref. [1], which provides a technique to derive an upper bound for estimating a parameter encoded in a state by some unitary or non-unitary process. Let the final state be $\hat{\rho}(\mu)$, where μ is the parameter to be estimated, also let F_Q be the associated QFI for the parameter μ corresponding to the state $\hat{\rho}(\mu)$. The physical interpretation of the method is that the QFI C_Q for the parameter μ that corresponds to any purification $|\Psi(\mu)\rangle$ of the state $\hat{\rho}(\mu)$ gives an upper bound for F_Q, i.e., $F_Q \leq C_Q$. This is because one can extract more information if the system and the environment are monitored together rather than monitoring the system alone. The purification of a quantum state is not unique. Therefore, if one is interested in finding the tightest bound, one should optimise over all possible purifications or at least selectively optimise over some possible purifications. The non-uniqueness of the purification is linked to unitary ambiguity of Kraus operators, since both of these ambiguities are rooted in the freedom of choosing the environments' basis up to some unitary. Specifically, the unitary ambiguity of Kraus operators means the following: two Kraus representations $\{\mathbf{K}_n\}$ and $\{\mathbf{K'}_n\}$ represent the same quantum channel if and only if $\mathbf{K}_n = \sum_{n,m} U_{mn}\mathbf{K'}_m$, where U_{mn} are the elements of the matrix representation of a unitary operator that acts on the environment's Hilbert space. Therefore, in order to find the tightest bound we need to optimise over all possible equivalent representations of the given quantum channel. While this is an impossible task in most cases, even a limited optimisation over a subset of equivalent Kraus representations should yield better results than not optimizing at all.

In this work, we consider the phase estimation problem for the case where an n-mode probe state, with total mean photon number $\langle N_S\rangle$ and total photon number variance $\langle\Delta N_S^2\rangle$, pick up a phase on each mode and is evolved under n independent and identical thermal loss channels with $\bar{n}_B$ mean thermal photon number per mode and transmittance η. We optimise the bound C_Q on F_Q by applying local phases to the environment and thus deleting information on the estimating parameter acquired by the environment's degrees of freedom. We get the bound [5],

$$C_Q = \frac{1}{D}[4n\eta\langle\Delta N_S^2\rangle\langle N_S\rangle(1+\bar{n}_B(1-\eta)) \\ +4\eta^2\langle\Delta N_S^2\rangle\langle N_S\rangle^2]. \tag{2}$$

where $D = \eta^2\langle N_S\rangle^2 + \eta n\langle N_S\rangle(1+(1-\eta)\bar{n}_B) + (1-\eta)\eta\langle\Delta N_S^2\rangle\langle N_S\rangle(1+2\bar{n}_B) - (1-\eta)\eta\langle\Delta N_S^2\rangle n\bar{n}_B(1+\bar{n}_B) + (1-\eta)n\langle\Delta N_S^2\rangle(1+\bar{n}_B)^2$. The bound behaves reasonably with thermal photons, i.e., it decreases with $\bar{n}_B$, and therefore is useful for certain interesting quantum sensing tasks as for example *active covert sensing* [6]. Specifically, we consider [6] that a target to be sensed is interrogated using an n-mode probe with a total of $\langle N_S\rangle = n\bar{n}_S$ photons, and total photon number variance of the probe is $\langle\Delta N_S^2\rangle = \mathcal{O}(n)$. Then, the sensing attempt is either detected by the adversary with arbitrarily low detection error probability, or the estimator has mean squared error $\langle(\theta-\hat{\theta}_n)^2\rangle = \Omega(1/\sqrt{n})$. The proof relies on the fact that he sensor must use an n-mode probe with $\langle N_{\mathrm{S}}\rangle = \mathcal{O}(\sqrt{n})$ photons to avoid detection, which implies, by (1) and (2), that the mean square error for any estimator of θ is $\langle(\theta-\hat{\theta}_n)^2\rangle = \Omega(1/\sqrt{n})$. Therefore covert sensing is governed by a square root law in the number of the channel uses similarly to covert communications [7].

[1] R. M. Escher, R. L. M. Filho, and L. Davidovich, Nature Physics **7**, 406 (2011).
[2] B. M. Escher, L. Davidovich, N. Zagury, and R. L. de Matos Filho, Phys. Rev. Lett. **109**, 190404 (2012).
[3] R. Demkowicz-Dobrzański, J. Kołodyński, and M. Guţă, Nature Communications **3**, 1063 (2012).
[4] J. Kołodyński and R. Demkowicz-Dobrzański, New Journal of Physics **15**, 073043 (2013).
[5] C. N. Gagatsos, B. A. Bash, S. Guha, and A. Datta, arXiv preprint arXiv:1701.05518 (2017).
[6] B. A. Bash, C. N. Gagatsos, A. Datta, and S. Guha, arXiv preprint arXiv:1701.06206 (2017).
[7] B. A. Bash, A. H. Gheorghe, M. Patel, J. L. Habif, D. Goeckel, D. Towsley, and S. Guha, Nature Communications **6**, 8626.

Molecular state transitions controlled with nanoantennas

A. Gajewski[1], M. Kosik[1], M. Kubek[1], J. Straubel[2], E. Rusak[2], F. Weigend [3], C. Rockstuhl[2], K. Słowik[1*]

[1] Institute of Physics, Nicolaus Copernicus University, Torun, Poland
[2] Institute for Theoretical Solid State Physics, Karlsruhe Institute of Technology, Germany
[3] Institute for Physical Chemistry, Karlsruhe Institute of Technology, Germany

Plasmonic nanoantennas sustain extraordinary ability to concentrate light in subwavelength spatial domains. A molecule positioned in such hot-spots is subject to the electromagnetic field of extreme strength. However, a nanoantenna can do much more than just enhance the coupling of light to molecules. It allows overcoming paradigms prevalent for a long time when considering the light-matter interactions in free-space or traditional cavities. There, the electric field can be considered as constant across the molecule. This allows using the dipole-approximation where quantum state transitions are considered as purely electric dipolar. With nanoantennas this assumption is lifted. They provide not just huge electric fields but also huge electric field modulations, allowing to drive state transitions that are usually considered as hardly accessible in free space: those of higher multipolar moments [1].

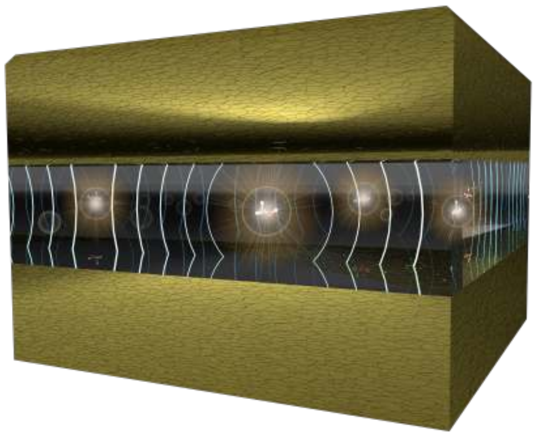

Fig. 1: Artistic vision of a patch nanoantenna coupled to adjacent molecules.

In our work, we explore the possibility of superimposing and coherently controlling different molecular pathways linked to different multipolar contributions of the same transition [2]. This is possible by exploiting their quantum interference. Combining methods of quantum chemistry, molecular physics and nanophotonics, we identify scenarios where the local density of states is largely enhanced or fully suppressed. Such suppression means orders of magnitude longer lifetime of the emitter: the key for many applications for quantum computing, storage, and communication. In a similar scenario, nanoantennas can be exploited to enhance the typically weak magnetic interaction pathway and in this way induce circular dichroism in molecules that normally hardly show this property.

References

[1] Robert Filter, Stephan Mühlig, Toni Eichelkraut, Carsten Rockstuhl, Falk Lederer, Phys. Rev. B 86, 035404.
[2] Evgenia Rusak et al., in preparation.

Microscopic origins of collective dissipation in extended systems

Fernando Galve[1] , Roberta Zambrini[1]
Antonio Mandarino[2], Matteo G. A. Paris[2] , Claudia Benedetti[2]
J. Alonso[3]

[1]Institute for Interdisciplinary Physics and Complex Systems, Mallorca, Spain
[2]Quantum Technology Lab, Dipartimento di Fisica, Uni. degli Studi di Milano, I-20133 Milan, Italy
[3]Eidgenössische Technische Hochschule Zürich (ETH), Zurich, Switzerland

Practical implementations of quantum technology are limited by unavoidable effects of decoherence and dissipation. With achieved experimental control for individual atoms and photons, more complex platforms composed by several units can be assembled enabling distinctive forms of dissipation and decoherence, in independent (separate) heat baths (SB) or collectively into a common bath (CB), with dramatic consequences for the preservation of quantum coherence. The cross-over between these two regimes has been widely attributed in the literature to the system units being farther apart than the bath's correlation length.

Starting from a microscopic model of a structured environment (a crystal) sensed by two bosonic probes [1], here we show the failure of such conceptual relation, and identify the exact physical mechanism underlying this cross-over, showing that it is not only a matter of system size. Peculiar scenarios in 1D environments or beyond isotropic dispersion relations are predicted, with collective dissipation possible for very large distances between probes, opening new avenues to deal with dissipation in phononic baths.

Further, we investigate the scenario of anomalous heating in ion traps [2], a major promising platform for quantum information processing, where this limiting factor in the rush for miniaturization is believed to be caused by a yet unknown source of dipole fluctuations in the electrodes' surfaces. A geometric crossover between CB and SB, and back to anti-CB (a common bath which dissipate the relative motion instead of the center of mass) is predicted which strongly depends on spatial correlations between dipoles, and also on their orientation. We propose a protocol to measure this peculiar effect in recent state of the art segmented Paul traps, allowing for a better insight into the microscopic origin of this elusive phenomenon.

[1] F. Galve, A. Mandarino, M. G. A. Paris, C. Benedetti & R. Zambrini, *Scientific Reports* **7**, 42050 (2017).

[2] F. Galve, J. Alonso & R. Zambrini, *manuscript in preparation.*

Enhancement of Polarization through deGaussification

Iulia Ghiu[1], Paulina Marian[1,2], and Tudor A. Marian[1]
[1] *Centre for Advanced Quantum Physics, Department of Physics, University of Bucharest, R-077125 Bucharest-Măgurele, Romania and*
[2] *Department of Physical Chemistry, University of Bucharest, Boulevard Regina Elisabeta 4-12, R-030018 Bucharest, Romania*

Polarization of light is a property that can easily and accurately be manipulated. Accordingly, it is widely used for encoding quantum information in various experiments. In any discussion on the polarization of the quantum radiation field, a quasi-monochromatic light beam is decomposed into two orthogonal transverse oscillating modes which are described by a definite two-mode state $\hat{\rho}$. The quantum treatment of polarization starts from the Stokes operators built with the amplitude operators of the conventional horizontally (H) and vertically (V) oscillating modes [1]:

$$\hat{S}_1 := \hat{a}_H^\dagger \hat{a}_V + \hat{a}_H \hat{a}_V^\dagger, \qquad \hat{S}_2 := \frac{1}{i}\left(\hat{a}_H^\dagger \hat{a}_V - \hat{a}_H \hat{a}_V^\dagger\right),$$

$$\hat{S}_3 := \hat{a}_H^\dagger \hat{a}_H - \hat{a}_V^\dagger \hat{a}_V; \; \hat{S}_0 := \hat{a}_H^\dagger \hat{a}_H + \hat{a}_V^\dagger \hat{a}_V.$$

Their expectation values correspond to the classical Stokes parameters:

$$\langle \hat{S}_0 \rangle = \mathrm{Tr}(\hat{\rho}\hat{S}_0), \qquad \langle \hat{S}_j \rangle = \mathrm{Tr}(\hat{\rho}\hat{S}_j), \quad (j = 1, 2, 3).$$

In classical optics, a definition of the degree of polarization was given by using the Stokes parameters. Originally, in the quantum domain, the standard degree of polarization was defined by replacing the Stokes variables by the expectation values of the Stokes operators. However, this definition based on first-order moments cannot give a complete description for all quantum fields, since assigns the zero value in some cases of pure polarized states. Therefore, the necessity of construction of the polarization measures by using second-order moments of the Stokes operators occured [2]. Moreover, taking inspiration from quantum information tool-box, the degree of polarization was quantified as the distance between the given quantum field state and the set of all unpolarized states. A state $\hat{\tau}$ is unpolarized if its polarization sector $\hat{\tau}_{\rm pol}$ remains invariant under any polarization transformation. It has the spectral decomposition

$$\hat{\tau} = \sum_{N=0}^{\infty} \pi_N \, \frac{1}{N+1} \, \hat{P}_N,$$

where $\hat{P}_N := \sum_{n=0}^{N} |n, N-n\rangle\langle n, N-n|$ is an N-photon manifold and $\pi_N = \mathrm{Tr}(\hat{\tau}\hat{P}_N)$ is the photon-number distribution of the state $\hat{\tau}$. Distance-type degrees of polarization have considered several metrics such as Bures and Chernoff ones [3]. As an example, the Bures degree of polarization is defined as

$$\mathbb{P}_{\rm B}(\hat{\rho}) := 1 - \max_{\hat{\tau}\in\mathcal{U}} \sqrt{\mathcal{F}(\hat{\rho},\, \hat{\tau})}\,,$$

where $\mathcal{F}$ is Uhlmann's fidelity between two states,

$$\mathcal{F}(\hat{\rho}_1,\, \hat{\rho}_2) := \left[\mathrm{Tr}\sqrt{\hat{\rho}_1^{1/2}\hat{\rho}_2\,\hat{\rho}_1^{1/2}}\right]^2.$$

and $\mathcal{U}$ is the set of all the unpolarized states.

Our work here deals with the behavior of different degrees of polarization under a deGaussification process. Specifically, we consider addition of photons to a two-mode thermal state to get mixed nonGaussian and nonclassical states which are still Fock-diagonal. We investigate both the Stokes-operators-based degrees of polarization and two distance-type measures defined with Bures and Hilbert-Schmidt metrics. We compare the evaluated degrees for photon-added states with the corresponding ones for two-mode thermal states for which we derive for the first time analytically simple expressions. Note that the thermal states are the only Fock-diagonal Gaussian states. We present interesting findings which tell us that the results obtained with different degrees are not fully consistent. However they indicate an enhancement of polarization by deGaussification.

[1] G. Björk, J. Söderholm, L. L. Sánchez-Soto, A. B. Klimov, I. Ghiu, P. Marian, and T. A. Marian, Opt. Commun. **283**, 4440-4447 (2010).
[2] A. B. Klimov *et al.*, Phys. Rev. Lett. **105**, 153602 (2010).
[3] I. Ghiu, G. Björk, P. Marian, and T. A. Marian, Phys. Rev. A **82**, 023803 (2010).

Conditioned electron spin and population dynamics of a quantum dot

(Abstract submission for CEWQO 2017)

Eliska Greplova[1], Edward Laird[2], Andrew Briggs[2] and Klaus Mølmer[1]
[1]Aarhus University, [2]University of Oxford

We describe the modeling of spin and charge dynamics of a single electron quantum dot as a three-level system subjected to incoherent and coherent transitions. We use a stochastic master equation both to simulate the system dynamics and to model the state of the system, as inferred by an observer with access to only part of the dynamics (using a quantum point contact (QPC) for instance). As in classical hidden Markov models, measurements obtained after a given time t contribute to our knowledge about the system at time t, and we show that a quantum version of such reasoning, the past quantum state [1, 2] (PQS) analysis, contributes quantitatively to the analysis of the evolving system. As a novel extension of the PQS formalism, we use parameter estimation [3, 4] to determine the the parameters for the spin dynamics of the quantum dot. Furthermore, the past quantum state analysis reproduces the well known situations of the ABL rule [5] and weak value amplification associated with post-selection in quantum experiments. In our system of study, we thus find an effect related to the so-called 3-box paradox.

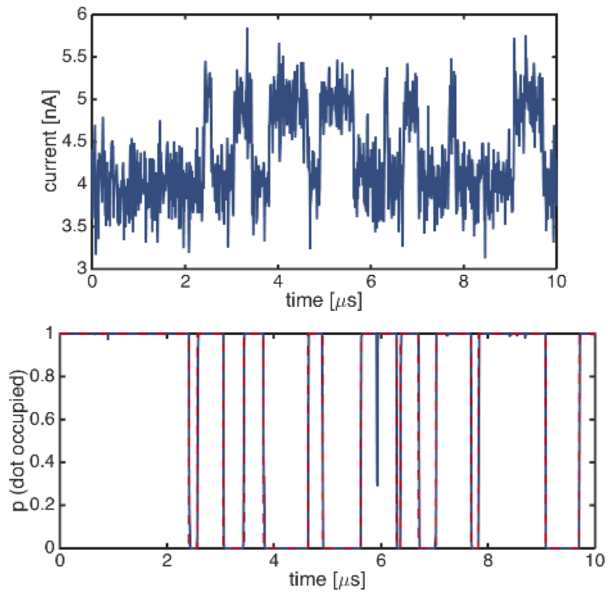

Figure 1: An example of the use of PQS method for the purpose of determining the dot dynamics: in the upper panel the blue line is the record of the experimental current of the observer using QPC, in the lower panel, this record is smoothed using PQS and red line corresponds to the 'real' state of the dot (i.e. the dot occupation based on the record of the observer with the direct access to the tunneling events).

[1] Søren Gammelmark, Brian Julsgaard, and Klaus Mølmer. Past quantum states of a monitored system. *Phys. Rev. Lett.*, 111:160401, Oct 2013.

[2] Qing Xu, Eliska Greplova, Brian Julsgaard, and Klaus Mølmer. Correlation functions and conditioned quantum dynamics in photodetection theory. *Physica Scripta*, 90(12):128004, 2015.

[3] Søren Gammelmark and Klaus Mølmer. Bayesian parameter inference from continuously monitored quantum systems. *Phys. Rev. A*, 87:032115, Mar 2013.

[4] S. Gammelmark, K. Mølmer, W. Alt, T. Kampschulte, and D. Meschede. Hidden markov model of atomic quantum jump dynamics in an optically probed cavity. *Phys. Rev. A*, 89:043839, Apr 2014.

[5] Yakir Aharonov, Peter G. Bergmann, and Joel L. Lebowitz. Time symmetry in the quantum process of measurement. *Phys. Rev.*, 134:B1410–B1416, Jun 1964.

Quantum dynamics of two coupled spins under controllable and fluctuating magnetic fields

R. Grimaudo,[1,2] Yu. Belousov,[3] H. Nakazato,[4] and A. Messina[1,2]

[1] *Dipartimento di Fisica e Chimica dell'Università di Palermo, Via Archirafi, 36, I-90123 Palermo, Italy.*
[2] *I.N.F.N., Sezione di Catania, Catania, Italy.*
[3] *Moscow Institute of Physics and Technology, 141700, Dolgoprudny, Institutsky lane 9, Russia.*
[4] *Department of Physics, Waseda University, Tokyo 169-8555, Japan.*

SUMMARY

In this work we investigate the quantum dynamics of two spins $\hat{\mathbf{j}}_1$ and $\hat{\mathbf{j}}_2$ (with values $j_1 \geq j_2$), subjected to external and controllable time-dependent magnetic fields and under a $\hat{\mathbf{J}}^2 = (\hat{\mathbf{j}}_1 + \hat{\mathbf{j}}_2)^2$-conserving bilinear coupling. Each eigenspace of $\hat{\mathbf{J}}^2$ is dynamically invariant and the Hamiltonian of the total system restricted to any one of such $(2j_2+1)$ eigenspaces, possesses the SU(2) structure of the Hamiltonian of a single fictitious spin acted upon by the given controllable magnetic field. We show that such a reducibility holds regardless of the time-dependence of the externally applied field as well as of the statistical properties of the Overhauser noise, we considered as a classical fluctuating magnetic field. Exploiting such a remarkable result, we examine the time evolution of the joint transition probabilities of the two spins $\hat{\mathbf{j}}_1$ and $\hat{\mathbf{j}}_2$ between two prefixed factorized states, bringing to light peculiar dynamical properties of the system under scrutiny. In particular, when the noise-induced non unitary dynamics of the two coupled spins is properly taken into account, we get explicit analytical expressions for the joint Landau-Zener transition probabilities.

The experimental physical scenarios of interest where our approach and results may be useful are several. An isolated dimeric unit of ions, each one exhibiting an effective spin $\hat{\mathbf{J}}$, may be regarded, for example, as a system of two interacting spins. For some compounds of dimeric units it has been experimentally proven that neglecting the couplings between spins in neighbouring units is legitimate, implying that the quantum dynamics of the same compound may be derived from that of a single dimer [1].

Experimental investigations on biradical compounds provide a further example of a physical system describable in terms of two interacting spins. A radical pair, containing two close molecular fragments, each one possessing a spin degree of freedom, may be indeed described by a two coupled spin Hamiltonian. When the two fragments are identical the radical pair is called biradical. In a liquid solution a compound of biradicals, neglecting hyperfine interaction with magnetic nuclei present in the molecular fragments, can be described by a symmetric spin Hamiltonian model [2].

In the area of quantum computing, finally, spin Hamiltonian models describing the quantum dynamics of two electron spins in a double quantum dot [3] or in a double quantum well [4], furnish the indispensable theoretical basis to investigate the possibility of manipulating two-electron based qubits.

To achieve realistic descriptions of these spin systems, exploitable for both applicative and fundamental purposes, one cannot however ignore environmental disturbs [5]. The magnetic field acting upon such a spin system, therefore, results from a controllable, generally time-dependent, contribution and a random one originated by unavoidable hyperfine interactions with the environmental nuclear spin bath around the system under scrutiny. Such uncontrollable contributions to the quantum dynamics of the system may be taken into account as classical fluctuating magnetic fields, known as the Overhauser, or, better, as sources of noise, characterized by quantum degrees of freedom [6, 7]. To control the origin of decoherence in a given spin system is an indispensable issue to be pursued for a full understanding of its dynamical behaviour and for tailoring on demand applicative performances of the same system [8]. Postulating that the Overhauser field acting upon the spins stems from mechanisms independent of the applied controllable field, we show that the results achieved in this paper allow to propose an experimental scheme for checking the classical versus quantum description of the Overhauser random field. To this end we exploit our approach in the case of a Landau-Zener scenario involving the two coupled spins.

---

[1] R. Calvo, J. E. Abud, R. P. Sartoris, and R. C. Santana, Phys. Rev. B 84, 104433 (2011).
[2] Weil J A and Bolton J R Electron Paramagnetic ResonanceElementary Theory and Practical Applications 2nd edn, John Wiley & Sons, Inc., Hoboken, New Jersey.
[3] J. R. Petta, *et al.*, (2005) Science, **309** (5744), 2180-2184.
[4] M. Anderlini, P. J. Lee, B. L. Brown, J. Sebby-Strabley, W. D. Phillips, and J. V. Porto, (2007) Nature, **448**(7152), 452-456.
[5] 46H. Bluhm, S. Foletti, I. Neder, M. Rudner, D. Mahalu, V. Umansky, and A. Yacoby, Nat. Phys. 7, 109 (2011).
[6] V. L. Pokrovsky and N. A. Sinitsyn, Phys Rev. B **69**, 104414 (2004).
[7] M. B. Kenmoe, H. N. Phien, M. N. Kiselev, and L. C. Fai, Phys. Rev. B, **87**, 224301 (2013).
[8] A. C. Johnson, *et al.*, (2005) Nature, **435** (7044), 925-928.

Ambiguity–Losses Trade-Off for State Discrimination

Frédéric Grosshans[1]

[1] Laboratoire Aimé Cotton, CNRS, Univ. Paris-Sud, ENS Cachan, Univ. Paris-Saclay, 91405 Orsay Cedex, France

NON-ORTHOGONALITY of quantum states is a key feature of quantum mechanics, which prevents to perfectly distinguish the elements of a set $\{|\psi_z\rangle\}_z$ of non-orthogonal states. Such e set is then often studied with one of the following two approaches:

- either one characterizes the ambiguity by an application-dependent figure of merit, usually a conditionnal (Rényi) entropy;
- or one looks at the optimal unambiguous measurement, *i.e.* a post-selected measurement which is never wrong, with a post-selection probability $\eta_0 < 1$.

For example, the conditional von Neumann entropy like $H(B|Z)$ is relevant for asymptotic communications; the Rényi conditional entropy $\tilde{H}^{\downarrow}_{\min}$ gives the probability of guessing Z by the optimal measurement.

I study here trade-off between ambiguity and losses in the intermediate regime, where $\eta_0 < \eta < 1$. For a set of pure states $\{|\psi_z\rangle\}_{0\leq z<d}$, symmetric under z-shifts[2], I find the minimal value of all the conditional α, z entropies $H^{\updownarrow}_{\alpha,z}(Z|B)$ for any efficiency η.

[2] Formally, there exists a function s *s.t.*

$$s(\tilde{z} - z \mod d) \stackrel{\text{def}}{=} \langle\psi_z|\psi_{\tilde{z}}\rangle\,.$$

The classical conditional α-Rényi entropies has different quantum analogues $H^{\updownarrow}_{\alpha,z}$, defined through the α, z-relative Rényi entropy introduced by Audenaert and Datta in 2013 $D_{\alpha,z}(\rho\|\sigma)$, and with ($H^{\downarrow}$) or without ($H^{\uparrow}$) minimization over σ. The interesting values of z are $z = 1$ (H) and $z = \alpha$ ($\widetilde{H}$), so this gives us four possible conditional entropies for each α.

Let $|\Psi\rangle_{ABC}$ be the purification of Alice-Bob CQ state, then there exists four duality relations for $H^{\updownarrow}_{\alpha,z}(A|B) + H^{\updownarrow'}_{\beta,z'}(A|C) = 0$, for β given in Table 1.

Table 1: Values of β where $H_\beta(A|C)$ is dual of a relevant $H^{\updownarrow}_{\alpha,z}(Z|B)$.

β	$H^{\downarrow}_{\alpha}$ $\alpha+\beta=2$	$H^{\uparrow}_{\alpha}$ $\alpha\cdot\beta=1$	$\widetilde{H}^{\downarrow}_{\alpha}$ $\alpha\cdot\beta=1$	$\widetilde{H}^{\uparrow}_{\alpha}$ $\frac{1}{\alpha}+\frac{1}{\beta}=2$
∞	—	0	—	$\frac{1}{2}$
2	0	$\frac{1}{2}$	$\frac{1}{2}$	$\frac{2}{3}$
1	1	1	1	1
$\frac{1}{2}$	$\frac{3}{2}$	2	2	∞
0	2	—	∞	—

The symmetry condition allows to express the state in a "Fourier basis", where the different $|\psi_z\rangle$ only differ by a dephasing [3]. One can show that an optimal measurement of efficiency η is then described by a filter diagonal in the Fourier basis, changing S to a new function S^η.

[3] $|\psi_z\rangle = \sum_x \mathrm{e}^{-\mathrm{i}xz\frac{2\pi}{d}}\sqrt{\frac{S(x)}{d}}\,|x\rangle$, where S is the discrete Fourier transform (DFT) of s: $S(x) \stackrel{\text{def}}{=} \sum_{\zeta=0}^{d-1} \mathrm{e}^{-\mathrm{i}x\zeta\frac{2\pi}{d}}\, s(\zeta)$.

$|\psi\rangle_{ABC}$ is then easily expressed [4], and the conditional Rényi entropies $H^{\updownarrow}_{\beta,z}(A|C)$ is shown to only depend on β. This gives

[4] $|\Psi\rangle_{ABC} = \frac{\sum_{x'}\sqrt{S(x')}|x'\rangle_B|\Phi^{x'}\rangle_{AC}}{d}$, with $|\Phi^{x'}\rangle_{AC}$ being maximally entangled states.

$$H^{\updownarrow}_{\alpha}(Z|B) = \log d - \frac{1}{1-\beta}\log\sum_{x=0}^{d-1}\left(\frac{S^\eta(x)}{d}\right)^{\beta},$$

Which can then be optimized over possible S^η. The filtered distribution S^η with minimal conditional entropy is the same for all β, the "flat-top" distribution, where a fraction $1-\eta$ is clipped out of the top of $\frac{S(\cdot)}{d}$, in order to give it the flattest possible top.

This allows to compute $H^{\updownarrow,\eta}_{\alpha,z}(Z|B)$ for any efficiency η. For example, Figure 1 plots this distribution for a constellation of 8 coherent states $|\sqrt{\mu}\mathrm{e}^{iz\frac{2\pi}{8}}\rangle$, with mean photon number $\mu \in \{0.5, 1, 2, 4\}$ (top to bottom).

Figure 1: $H^{\updownarrow,\eta}_{\alpha,z}(Z|B)$. Each beam of curve corresponds to same set of states, with β describing $\{\frac{1}{2}, 1, 2, \infty\}$ upwards.

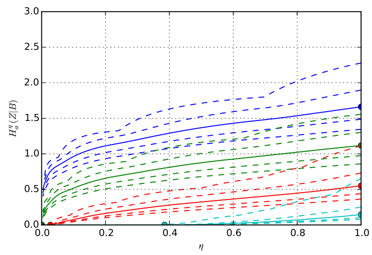

Towards experimental realization of High-Fidelity Teleportation of Continuous-Variable Quantum States in the telecom band

Xueshi Guo[1,*], Casper R. Breum[1], Jonas S. Neergaard-Nielsen[1], and Ulrik L. Andersen[1]

[1]Department of Physics, Technical University of Denmark, Fysikvej, 2800 Kongens Lyngby, Denmark.
[*]xguo@fysik.dtu.dk

ABSTRACT

We experimentally study a high-fidelity teleportation scheme for continuous-variable quantum states with delocalized single photons at telecommunication wavelength. An all-fiber laser at the wavelength of 1550 nm is frequency doubled and down converted by PPKTP crystals in cavities to generate high purity single photons as entanglement sources.

Quantum teleportation provides an efficient way to transfer quantum bits not by actually sending the quantum state, but by sharing entanglement sources and sending the measurement result through classical channels. It is theoretically important in quantum information science and useful in the applications such as quantum computing and quantum key distribution[1].

Up to now, two types of teleportation schemes are frequently demonstrated – the discrete variable (DV)[1,2] and the continuous-variable (CV)[3] teleportation. The latter uses two-mode squeezed state as an entanglement source and can teleport both CV and DV quantum states deterministically, but the fidelity is confined by the squeezing degree of the two-mode squeezing. As a comparison in the former scheme, the entanglement source is entangled photons, and it can, in principle, have perfect fidelity for the DV quantum state. However, the fidelity decreases dramatically as the average photon number of the state to teleport increases, making it hard to teleport CV quantum state. However, it is possible to increase the teleportation fidelity of the CV quantum state by using the follow CV and DV hybrid teleportation schemes[4,5]: firstly, coherently separate the CV quantum state to sub-states with fewer photon number; secondly, teleport the sub-states with delocalized photons; finally recombine the quantum state coherently. Further more, even with two stages splitting, the fidelity could be better than that of CV teleportation with 10 dB two-mode squeezing.

Here we experimentally study the approach of realizing this high-fidelity teleportation scheme for CV quantum state with delocalized single photons at the telecommunication wavelength. An all-fiber laser at the wavelength of 1550 nm is frequency doubled to 775 nm by a second harmonic generator (SHG) with a type-0 PPKTP crystal in the cavity. The 775 nm light serves as the pump of two optical parametric oscillators (OPOs) with type-II PPKTP crystals in the cavities to generate polarization entangled photon pairs. Therefore, single photons in high purity could be generated by first separating the photon pairs with polarization beam splitter and then detecting with proper filtering at the heralding channel. The photons are further sent to a 50/50 beam splitter to create a path entangled state as the source for teleportation[2].

To maximize the mode matching and minimize the intra cavity loss, the SHG cavity and the OPOs are in bow-tie setup with identical dimensions[6]. The SHG cavity has an overall conversion efficiency of 83.5% at the pump power of 1W and a higher conversion is possible as the pump power increase, and the intra-cavity loss is as low as 0.012%. The homodyne detector is built with diodes of $> 99\%$ quantum efficiency at 1550nm wavelength to better characterize the quantum state. To increase the successful rate of the teleportation, high efficiency superconducting nanowire single photon detector is adapted[7], and the down converted light is coupled into single mode fiber with aspheric lenses. The phase control of the cavities and quantum states in our experiment is achieved with low cost discrete FPGA-based data acquisition boards, which makes it easy to extend the setup to more splitting stages. Though still under construction, the existing result indicates the experimental system is suitable to realize the high-fidelity teleportation scheme in telecom band for it's high purity spatial mode, high detection efficiency and adequate parametric gain.

References

1. Bennett, C. H. *et al.* Teleporting an unknown quantum state via dual classical and einstein-podolsky-rosen channels. *Phys. Rev. Lett.* **70**, 1895–1899 (1993).

2. Babichev, S. A., Ries, J. & Lvovsky, A. I. Quantum scissors: Teleportation of single-mode optical states by means of a nonlocal single photon. *Europhys. Lett.* **64**, 1 (2003).

3. Braunstein, S. L. & Kimble, H. J. Teleportation of Continuous Quantum Variables. *Phys. Rev. Lett.* **80**, 869–872 (1998).

4. Andersen, U. L. & Ralph, T. C. High-fidelity teleportation of continuous-variable quantum states using delocalized single photons. *Phys. Rev. Lett.* **111**, 1–5 (2013).

5. Kogias, I., Ragy, S. & Adesso, G. Continuous-variable versus hybrid schemes for quantum teleportation of gaussian states. *Phys. Rev. A* **89**, 052324 (2014).

6. Neergaard-Nielsen, J. S., Nielsen, B. M., Takahashi, H., Vistnes, a. I. & Polzik, E. S. High purity bright single photon source. *Opt. express* **15**, 7940–7949 (2007).

7. Liu, D. *et al.* Multimode fiber-coupled superconducting nanowire single-photon detector with 70% system efficiency at visible wavelength. *Opt. express* **22**, 21167–74 (2014).

CEWQO 2017

Title:

Quantum Correlations without Discord and a Hong-Ou-Mandel-Dip without Photons

Authors:
Kai Barnscheidt, Karsten Boelts, Tom Ettrich, Boris Hage, Semjon Köhnke, Melanie Mraz, Oskar Schlettwein
All authors affiliated to:
Experimental Quantum Optics Group, Institute of Physics, University of Rostock, 18051 Rostock, Germany

We report on the experimental characterization of a phase randomized two mode squeezed state by means of a full two mode quantum state tomography yielding a nonclassical Glauber-Sudarshan P-representation as proposed by Agudelo et al. [1]. Remarkably, this state in theory shows neither entanglement nor quantum discord, which is in good agreement with our experimental data. Also, the individual modes are in thermal states. These results indicate that the discussion of the various notions of nonclassicality needs to be kept up.

We use the same setup without the phase randomization to perform a full two mode quantum state homodyne tomography on a continuous two mode squeezed state. Exploiting the entanglement between the two modes we show that in the ensemble average we can produce individual Fock states, qubit-like superpositions of Fock-states in one of mode induces by measurements of the other mode. We show that this can also be used to produce two indistinguishable photons exhibiting the Hong-Ou-Mandel two photon interference effect. This is done via the idea of statistically weighting the individual measurements in one detector conditionally on the measurement value of the other detector and the pattern functions relating the Fock density matrix to quadrature measurements. We extend the concept from two modes and the diagonal elements of the Fock density matrix[2–4] to off-diagonal elements in order to form superpositions and four modes for the Hong-Ou-Mandel effect. We would like to initiate a discussion about the extent to which this concept is equivalent to any or all single photons – click detectors – linear network protocols.

1. Agudelo, E., Sperling, J. & Vogel, W. Quasiprobabilities for multipartite quantum correlations of light. *Phys. Rev. A* **87,** 33811 (2013).
2. Hage, B. *et al.* Demonstrating various quantum effects with two entangled laser beams. *Eur. Phys. J. D* **63,** 457–461 (2011).
3. Chrzanowski, H. M. *et al.* Reconstruction of photon number conditioned states using phase randomized homodyne measurements. *J. Phys. B At. Mol. Opt. Phys.* **46,** 104009 (2013).
4. Chrzanowski, H. *et al.* Photon-number discrimination without a photon counter and its application to reconstructing non-Gaussian states. *Phys. Rev. A* **84,** 050302(R) (2011).

A new type of EIT in combined Tripod and Lambda- atom-light coupling schemes

Hamidreza Hamedi[1], Julius Ruseckas[1], Gediminas Juzeliūnas[1]

[1]Institute of Theoretical Physics and Astronomy, Vilnius University, Saulėtekio 3, Vilnius LT-10222, Lithuania

Electromagnetically induced transparency (EIT) [1] plays an important role in controlling the propagation of light pulses in resonant media. Due to the EIT a weak probe beam of light tuned to an atomic resonance can propagate slowly and is almost lossless when the medium is driven by one or several control beams of light with a higher intensity [2]. The EIT is formed because the control and probe beams drive the atoms to their dark states representing a special superposition of the atomic ground states immune to the atom-light coupling. There has been a considerable amount of activities on slow light in atomic media induced by the EIT [3, 4]. In this work, we propose and analyze a novel five-level closed-loop scheme [5] supporting the EIT. The scheme involves three atomic ground states coupled to two excited states by five light fields. It is demonstrated that dark states can be formed for such an atom-light coupling. This is essential for formation of the EIT and slow light. In the limiting cases the scheme reduces to conventional Lambda- or N- type atom-light couplings providing the EIT or absorption, respectively. Thus the atomic system can experience a transition from the EIT to the absorption by changing the amplitudes or phases of control lasers [6].

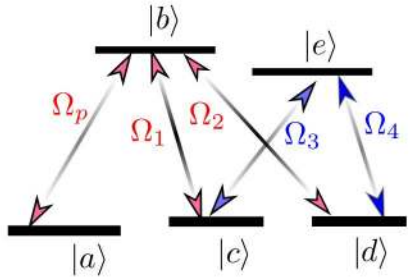

Fig. 1. Schematic diagram of the five-level Lambda-tripod quantum system.

References

[1] S. E. Harris, *Phys. Today* 50 (1997), pp. 36.

[2] Michael Fleischhauer, and Atac Imamoglu, and Jonathan P. Marangos, *Rev. Mod. Phys.* 77 (2005) 633--673.

[3] Julius Ruseckas, Gediminas Juzeliūnas, Patrik Öhberg, and Stephen M. Barnett, *Phys. Rev. A* 76 (2007), pp. 053822.

[4] M.-J. Lee, J. Ruseckas, Ch.-Y. Lee, V. Kudriašov, K.-F. Chang, H.-W. Cho, G. Juzeliūnas and I. A. Yu, Nat. Commun. **5**, 5542 (2014);

[5] H. R. Hamedi and G. Juzeliūnas, G., *Phys. Rev. A* 91 (2015), pp. 053823.

[6] Hamid Reza Hamedi, Julius Ruseckas, Gediminas Juzeliūnas. To be submitted in Phys. Rev. A

Local versus global strategies in multiparameter estimation

A.J. Hayes*,[1] P.A. Knott,[1] T.J. Proctor,[2,3] J.F. Ralph,[4] P. Kok,[5] and J.A. Dunningham[1]

[1]*Department of Physics and Astronomy, University of Sussex, Brighton BN1 9QH, UK*
[2]*School of Physics and Astronomy, University of Leeds, Leeds LS2 9JT, UK*
[3]*Berkeley Quantum Information and Computation Centre, Department of Chemistry, University of California, Berkeley,California 94720, USA*
[4]*Department of Electrical Engineering and Electronics, University of Liverpool, Brownlow Hill, Liverpool L69 3GJ, UK*
[5]*Department of Physics and Astronomy, University of Sheffield, Sheffield S3 7RH, UK*

We consider the problem of estimating multiple phases using a multimode interferometer. In this setting we show that while global strategies that estimate all the phases simultaneously can lead to high precision gains, the same enhancements can be obtained with local strategies in which each phase is estimated individually. A key resource for the enhancement is shown to be a large particle-number variance in the probe state, and for states where the total particle number is not fixed, this can be obtained for mode separable states, and the phases can be read out with local measurements. This has important practical implications because local strategies are generally preferred to global ones for robustness to local estimation failure, flexibility in the distribution of resources, and comparatively easier state preparation. We obtain our results by analysing two different schemes: the first uses a set of interferometers, which can be used as a model for a network of quantum sensors, and the second looks at measuring a number of phases relative to a reference, which is concerned primarily with quantum imaging.

DOI: 10.1103/PhysRevA.94.062312

I. BACKGROUND

This work has applications in quantum enhanced metrology and in particular, the potential enhancements that can be provided when estimating multiple parameters in practice e.g in gravitational wave detection and quantum imaging. It has been shown that for multimode interferometers, mode entanglement in probe states and simultaneous measurements can provide precision enhancement. However, in other applications of quantum metrology, entanglement has been shown to be detrimental. Furthermore, multimode entangled states are notoriously difficult to experimentally produce and are very susceptible to imperfection and loss. This work compares local and global strategies for multiparameter estimation in optical interferometry where a strategy is defined as local if (i) the probe state is mode separable and (ii) the state measurement can be implemented with local operations only. A global strategy is defined to be one that is not local i.e simultaneous parameter estimation. This work considers fixed-number and indefinite-number probe states, which is a more general setting than previous work demonstrating precision gains with global strategies. Note that this work has been extended and generalized by authors, P.A. Knott, T.J. Proctor and J.A. Dunningham [arXiv:1702.04271].

II. RESULTS

The results of this work are obtained by analysing two different multiparameter estimation protocol and contrasting global and local schemes for each. The quantum Fisher information is used in combination with the Cramér Rao bound to determine the phase estimation-precision bounds. The first scheme considered is a collection of parallel interferometers, this network of quantum sensors has applications in gravitational wave detection. Considering each interferometer individually, the standard quantum-enhanced precision for each parameter, in terms of the total photon number $\bar{N}$ over d modes, is the well known Heisenberg scaling $\phi_i \geq d/\bar{N}$. A global scheme using a generalised entangled coherent state gives an order d improvement. Considering a mode separable unbalanced cat state $|\psi_{\mathrm{UCS}}\rangle = \mathcal{N}_C(|\alpha\rangle + \nu|0\rangle)^{\otimes d}$, using the same amount of resources as in the global analogue, the estimation precision bound is found to match or beat that of the global scheme's for $\nu = 1$ or $\nu^2 \geq 2d$ respectively. The optimal local measurements consist of simple beam splitter and photon number counting readouts. Similar analysis is performed for a second scheme where d phase shifts are measured relative to a reference mode. This has application to quantum imaging. Here a global scheme using a generalised "NOON" state is compared to local scheme using an unbalanced "NO" state $|\psi_{\mathrm{NO}}\rangle = \mathcal{N}(|N\rangle + \nu|0\rangle)^{\otimes d+1}$. For $\nu = 1$ or $\nu \propto \sqrt{d}$ the local scheme matches or beats the global analogue respectively. From this it's clear the desired property of the pure probe state is large correlations within individual modes. A general prescription for finding the superior local probe state, for a given a global scheme, is presented.

*Corresponding author: Anthony.Hayes@sussex.ac.uk

Quasi-number-resolving detection and heralded single photon sources

Lukas G. Helt and Michael J. Steel

Centre for Ultrahigh bandwidth Devices for Optical Systems (CUDOS), MQ Photonics Research Centre, Department of Physics and Astronomy, Macquarie University, NSW 2109, Australia

Heralded photon sources, in which a photon pair is generated and one member of the pair detected to herald the presence of the other, are traditionally operated in the regime of a low probability of pair production per pump pulse. This allows on-off detectors, only able to distinguish between zero and nonzero incident photons, to herald single photons with reasonable accuracy. Yet as quantum optical circuits become more complex, it is becoming desirable to operate heralded sources at higher pair generation probabilities, ideally up to 25%, and thus methods are needed to reliably distinguish one photon from more than one photon.

Number-resolving detectors such as transition edge sensors present one method, but are complex, expensive, and must be operated at low temperatures. Thus, quasi-number-resolving (QNR) detection schemes that make use of the more convenient on-off detectors have been explored [1-5]. They operate by first splitting the incoming light up many times, in either time or space, before detection via an on-off detector, such that each individual detection need only distinguish between zero or nonzero photons for accurate number resolution. However, previous theoretical treatments of these schemes have largely ignored the application of single photon heralding as well as, with the exception of [4], the impact of detector dark counts.

In this work, we develop a simple, closed-form expression for the fidelity of the heralded state to a single photon state, and quantify the trade-offs that come with increasing dark noise as more detectors are added. We begin with a downconverted state, and split the photons in heralding mode A equally across M (temporal or spatial) modes, $|\psi\rangle = \sum_n c_n \sqrt{n!/M^n} \sum_{k_i|k_1+k_2+\cdots+k_M=n} (k_1!\,k_2!\cdots k_M!)^{-1/2}\, |k_1\rangle_{A_1} |k_2\rangle_{A_2} \cdots |k_M\rangle_{A_M} |n\rangle_B$, where $|c_n|^2 = \mu^n/(1+\mu)^{1+n}$ with μ the average number of photon pairs per pump pulse. For imperfect on-off detection in mode X, with detection efficiency parameter η_X, and low dark count probability δ_X, represented with POVM elements $\hat{\pi}_{0;X} = (1-\delta_X)\sum_n (1-\eta_X)^n\, |n\rangle_X\langle n|_X$, and $\hat{\pi}_{\text{click};X} = \mathbb{I}_X - \hat{\pi}_{0;X}$, we write an operator for m-photon detection across M modes as $\hat{\pi}^M_{m;X} = \binom{M}{m} \prod_{i=1}^{m} \hat{\pi}_{\text{click};X_i} \prod_{j=m+1}^{M} \hat{\pi}_{0;X_j}$, where the binomial coefficient appears because we do not care which modes the detection is in. We can then write the m-photon QNR detection probability as $P^M_A(m) = \mathrm{Tr}\left(\hat{\pi}^M_{m;A}|\psi\rangle\langle\psi|\right)$ and thus the fidelity of the resulting heralded state to $|o\rangle_B$ as $F^M(o|m) = \langle\psi|\hat{\pi}^M_{m;A}|o\rangle_B\langle o|_B|\psi\rangle / P^M_A(m)$. In particular, setting $\delta_{A_i} = \delta$ and $\eta_{A_i} = \eta$ for all i, we find

$$F^M(1|1) = \frac{\mu\left[\frac{\eta}{M} + \delta(1-\eta)\right](1+\eta\mu)[M+\eta\mu(M-1)]}{(1+\mu)^2\{\eta\mu + \delta[M+\eta\mu(M-1)]\}}. \tag{1}$$

We note that for $M = 1$ the QNR scheme is just a single threshold detector, whereas as $M \to \infty$ it only approaches a number-resolving detector for the unrealistic $\delta = 0$. In fact, for $\delta > 0$, it can be shown that there is always a point beyond which increasing the number of modes M will have a detrimental effect on the fidelity. Setting $\mu = 1$ to maximise the single pair generation probability in $|\psi\rangle$, we plot this maximum M for a variety of detector efficiencies and dark count probabilities in Fig. 1. For the representative detector parameters $\eta = 0.8$, $\delta = 5\times10^{-4}$, it is seen that it is not worth utilising more than 22 QNR modes.

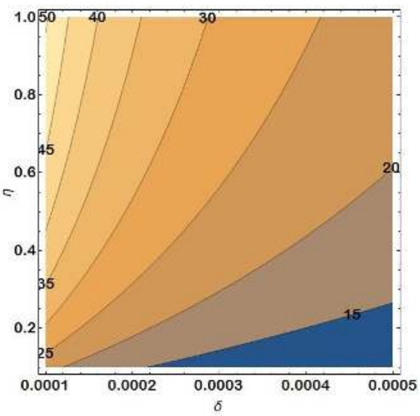

Fig. 1 Contours representing the maximum number of QNR detection modes M, in the heralding arm of a heralded photon source with $\mu = 1$, beyond which the fidelity of the heralded state to a single photon state only decreases.

References

[1] H. Paul, P. Törmä, T. Kiss, and I. Jex, Phys. Rev. Lett. **76**, 2464 (1996).
[2] M. J. Fitch, B. C. Jacobs, T. B. Pittman, and J. D. Franson, Phys. Rev. A **68**, 043814 (2003).
[3] D. Achilles *et al.*, J. Mod. Opt. **51**, 1499 (2004).
[4] J. Sperling, W. Vogel, and G. S. Agarwal, Phys. Rev. A **85**, 023820 (2012).
[5] J. C. F. Matthews *et al.*, npj Quantum Inf. **2**, 16023 (2016).

Random numbers generated using photons without post-processing

Aldo C. Martínez, Aldo Solis, Alí M. Angulo Martínez, Hector Cruz Ramírez, Alfred B. U'Ren, Jorge G. Hirsch
Instituto de Ciencias Nucleares, Universidad Nacional Autónoma de México,
Apdo. Postal 70-543, Cd. Mx., México, C.P. 04510

Is the randomness of quantum phenomena a physical assumption that is testable? Many attempts have been made to answer this question. Single-photon polarization measurement outcomes pass the NIST suit of tests as well as computer-based random number generators[1].

Has quantum randomness been experimentally proved? There are deep differences between quantum-generated random sequences and computer-generated ones. Quantum randomness can be proven incomputable; that is, it is not exactly reproducible by any algorithm [2], while software-generated random numbers, known as pseudo-random, can be reproduced if the computer code and the seed are known. Is it possible to distinguish between them? Algorithmic randomness provides a quantitative method to assess the Borel normality of a given sequence of numbers, a necessary condition for it to be considered random. Performing finite tests of randomness on large pseudo-random strings (finite sequences) generated with software (Mathematica, Maple), which are cyclic (so, strongly computable), the bits of pi, which are computable, but not cyclic, and strings produced by quantum measurements (with the commercial device Quantis and by the Vienna IQOQI group), failures of quantum sources in randomness probes were reported [3].

In our previous work, we have used ten sequences of 10^6 bits generated from the differences between detection times of photon pairs generated by spontaneous parametric downconversion (SPDC). These sequences fulfill the Borel normality randomness criteria without difficulties [4]. To understand these diverging observations, we extended our study, analyzing longer (4×10^9) photon-derived random sequences, obtained both with an attenuated laser and SPDC light, and with a beamsplitter introduced both in one arm of an SPDC source and on the path of an attenuated laser. The random sequences were generated both employing the beam splitter outputs, assigning detections in each channel the symbols 0 or 1 or, alternatively, employing the distribution of arrival times at the detectors divided in two blocks. The sequences built using the difference in arrival time are shown to be validated as random employing the Borel normality criteria, and also the stronger Bayesian inference procedure, which can characterize not only the bit strings but the source itself [5].

In this contribution we report the challenges found in generating chains which pass the Borel normality test without post-processing. Many different sources of correlations are analyzed: time modulations, differences in detector efficiencies, which composed with the dead time and afterpulsing give rise to not obvious correlations in a

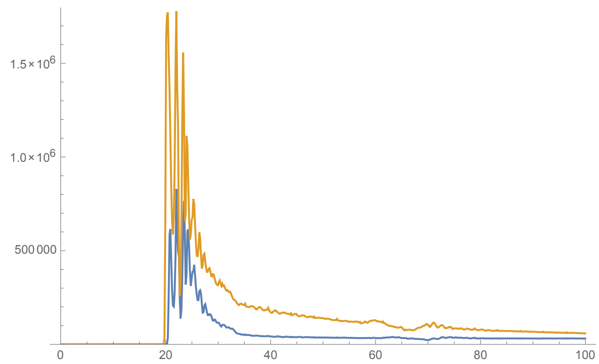

FIG. 1. Histogram of the number of photons detected in two similar detectors at the output of a delicately balanced beam splitter, as a function of the difference in arrival time, in nsec

delicately balanced bean splitter. The presence of some of these effects can be clearly observed in Fig. 1. Afterpulsing in the photodiodes can be modeled efficiently [6], but the generation of high quality random series is strongly affected. Obtaining good random chains without post-processing employing a beam splitter exhibits many technical difficulties, while employing the detection time seems to be more robust.

[1] D. Branning, M. Bermudez, J. Opt. Soc. Am. B 27 (2010) 1594.
[2] Aldo Solis and Jorge G. Hirsch, Journal of Physics: Conference Series 624 (2015) 012001 and references therein.
[3] C. S. Calude, M. J. Dinneen, M. Dumitrescu, K. Svozil, Phys. Rev. A 82 (2010) 022102.
[4] A. Solis, A. M. Angulo Martinez, R. Ramirez Alarcon, H. Cruz Ramirez, A. B. U'Ren, J. G. Hirsch, Phys. Scr. 90 (2015) 074034. Invited Comment.
[5] R. Diaz-H.R., A. Solis, A. M. Angulo Martinez, A. B. U'Ren, J. G. Hirsch, M. Marsili, I. Perez Castillo, https://arxiv.org/abs/1608.05119.
[6] C. Wiechers, R. Ramirez-Alarcon, O. R. Muñiz-Sanchez, P. Daniel Yepiz, A. Arredondo-Santos, J. G. Hirsch and A. B U'Ren, Applied Optics 55 (2016) 7252-7264.

Constructing two dimensional spin lattices with state transfer

Antonín Hoskovec*[1] and Igor Jex[1]

[1] *Department of Physics, Faculty of Nuclear Sciences and Physical Engineering, Czech Technical University in Prague, Czech Republic*

L. Vinet and A. Zhedanov have described a method of constructing one dimensional spin chains for quantum state transfer [1]. It deals with Hamiltonians of the form

$$H = \frac{1}{2}\sum_{i=0}^{N-1}\left[I_{i+1}\left(\sigma_i^x\sigma_{i+1}^x + \sigma_i^y\sigma_{i+1}^y\right) + B_i\left(\sigma_i^z + 1\right)\right], \tag{1}$$

defined on the Hilbert space $(\mathbb{C}^2)^{\otimes(N+1)}$ of $(N+1)$ qubits. It relies on finding $V_i(s)$ that solve recurrence relations induced by H

$$I_{i+1}V_{i+1}(s) + B_iV_i(s) + I_iV_{i-1}(s) = x_sV_i(s),\ s \in \{0\dots N\}, \tag{2}$$

where x_s is an eigenvalue of H, using orthogonal polynomials. We show that the method can also be used to construct $(M+1)$ by $(N+1)$ 2D spin lattices, where the Hamiltonian takes the form of

$$H = \frac{1}{2}\sum_{i,j=0}^{N-1,M-1}\left[I_{i+1,j}\left(\sigma_{ij}^x\sigma_{i+1,j}^x + \sigma_{ij}^y\sigma_{i+1,j}^y\right) + J_{i,j+1}\left(\sigma_{i,j}^x\sigma_{i,j+1}^x + \sigma_{i,j}^y\sigma_{i,j+1}^y\right) + B_{ij}\left(\sigma_{ij}^z + 1\right)\right], \tag{3}$$

and induces similar recurrence relations

$$\begin{aligned} x_{st}W_{i,j}(s,t) &= I_{i+1,j}W_{i+1,j}(s,t) + J_{i,j+1}W_{i,j+1}(s,t) \\ &\quad + B_{ij}W_{i,j}(s,t) + I_{ij}W_{i-1,j}(s,t) + J_{ij}W_{i,j-1}(s,t). \end{aligned} \tag{4}$$

The solutions to this recurrence can be found in a factorized form

$$W_{i,j}(s,t) = V_i(s)W_j(t), \tag{5}$$

where $V_i(s)$ and $W_j(t)$ both solve a recurrence relation in the form of (2). This gives a mean of directly constructing networks in the shape of a lattice from 1D spin chains.

References

[1] L. Vinet and A. Zhedanov. How to construct spin chains with perfect state transfer. *Phys. Rev. A*, 85:012323, Jan 2012.

*antonin.hoskovec@fjfi.cvut.cz

Application of adiabatic following to three specific three-sate quantum system

Wei Huang[1]**, Bruce W Shore**[2]**, Andon Rangelov**[3]**, Elica Kyoseva**[4]

[1]*Singapore University of Technology and Design, 8 Somapah Road, 487372 Singapore*

[2]*618 Escondido Cir., Livermore, CA, USA*

[3]*Sofia University, James Bourchier 5 blvd., 1164 Sofia, Bulgaria*

[4]*Institute of Solid State Physics, Bulgarian Academy of Sciences, 1784 Sofia, Bulgari*

Adiabatic time-evolution found in various forms of adiabatic following and adiabatic passage is often advantageous for controlled manipulation of quantum systems due to its insensitivity to deviations in the pulse shapes and timings. In this paper we discuss controlled adiabatic evolution of a three-state quantum system, a natural advance to the widespread use of two-state systems in numerous contemporary applications. We discuss, and illustrate, not only possibilities for population transfer but also for creating, with prescribed relative phase, 50:50 superpositions of two Zeeman sublevels in a letter-vee coupling linkage.

Adiabatic evolution is a widely used quantum control technique that has found numerous applications in different atomic systems, including two-level, three-level, and multi-level quantum systems. One of the main advantages of adiabatic following is its robustness to varying Rabi frequencies and/or detunings. Previous work in three-level configurations showed only specific transfer patterns such as starting from the excited state. In this work, we overcome this constriction and show how to implement adiabatic following in a general three-state quantum system. The evolution of a three-state systems is described by the Schrödinger equation (in RWA),

$$i\frac{d}{dz}C(t) = \begin{bmatrix} -\Delta(t) & \frac{1}{2}\widetilde{\Omega}(t) & 0 \\ \frac{1}{2}\widetilde{\Omega}^*(t) & 0 & \frac{1}{2}\widetilde{\Omega}(t) \\ 0 & \frac{1}{2}\widetilde{\Omega}^*(t) & \Delta(t) \end{bmatrix} C(t), \tag{1}$$

where $C(t)$ is the amplitude vector of states 1, 2 and 3, and $\widetilde{\Omega}(t) = \Omega(t)e^{i\phi}$ is the Rabi frequency with ϕ is a phase that can be externally controlled by a laser pulse.

When the initially populated state is state 1 or 3, and we have a large detuning, then the state of the system coincides with an adiabatic state $|a_-\rangle$ or $|a_+\rangle$. Then, by increasing adiabatically the Rabi frequency, the systems evolves into state $|a_\pm\rangle$. This translated to 50% population in state 2 and 25% in both states 1 and 3. We present this scenario in Fig. 2 (a) where the coupling parameters are $\Omega(t) = \Omega_0 \exp[-(t-\tau)^2/T^2]$ and $\Delta(t) = \Delta_0 \exp[-(t+\tau)^2/T^2]$.

For the same initial state, but linear with time detuning the evolution of the system is different and we show it in Fig. 2 (b). The coupling parameters are $\Omega(t) = \Omega_0 \exp(-t^2/T^2)$ and $\Delta(t) = \delta_0 + \Delta_0 t$. For this evolution, at $t \to 0+$, we have a crossing of the adiabatic states. Finally, due to that complete population transfer is obtained.

Finally, starting at state 2, we start in state $|a_0\rangle$ and then adiabatically transfer to lager Rabi frequency. We show the final state superposition in Fig 2 (c). with coupling strength and detuning the same for Fig 2 (a). More details of this work can be found in ref.[1].

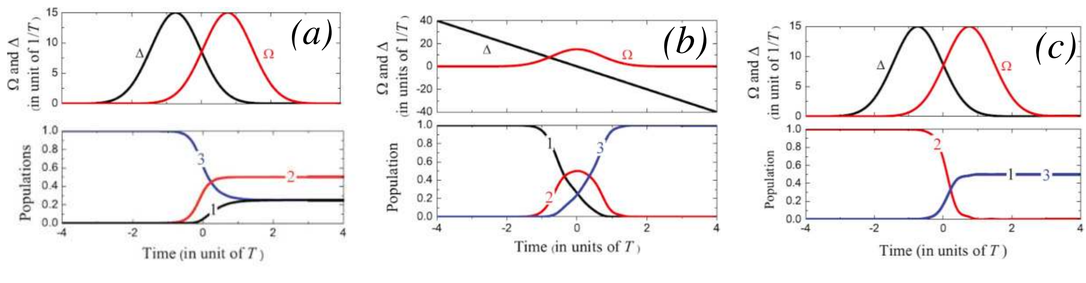

Figure 1: The coupling strength $\Omega(t)$ and detuning $\Delta(t)$, and the corresponding population evolution.

References [1] W. Huang, B. W. Shore, A. Rangelov and E. Kyoseva, Optics Communications **382**, 196-200 (2017).

Cryptographic quantum metrology

Zixin Huang,[1] Chiara Macchiavello,[2] and Lorenzo Maccone[2]
[1]School of Physics, University of Sydney, NSW 2006, Australia
[2]Dip. Fisica and INFN Sez. Pavia, University of Pavia, via Bassi 6, I-27100 Pavia, Italy

We develop a general framework for the secure measurement and transmission of unitary parameters, whilst retaining the highest precision allowed by quantum mechanics. We design protocols where the estimation is performed optimally, and measurement outcomes are cheat-sensitive. These protocols are realizable with currently available technology.

Information privacy has gained increasing attention in the past two decades. Classical protocols for sharing measurement results, e.g. secret location sharing, use classical encryption schemes that rely on assumptions such as a bounded computational capacity of the adversaries. Quantum cryptography [1–3] instead promises unconditional security. Here we introduce a general framework for quantum cryptographic protocols specifically suited to the task of making parameter estimation cheat-sensitive [4] while retaining the highest available precision allowed by quantum mechanics.

Clearly, one can estimate the parameter then use conventional quantum cryptography to transmit the result. Now, thanks to the quantum nature of the states employed in quantum metrology, this two-step procedure is unnecessary and simple modifications of conventional quantum metrology protocols allow secure transmission of the estimated parameter. This is particularly relevant in multi-party scenarios where the measurement outcomes must be shared.

Our goal is to securely and optimally estimate an arbitrary parameter φ, encoded by a unitary operator $U_\varphi = e^{-i\varphi H}$, where H is a known Hermitian operator, in an ideal noiseless scenario. A known optimal state and observable are:

$$|\Psi^{\pm}_{\text{probe}}\rangle = (|\lambda_m\rangle^{\otimes N} \pm |\lambda_M\rangle^{\otimes N})/\sqrt{2}, \qquad (1)$$

$$\hat{O}^{\pm}_N = \pm(|+\rangle\langle+| - |-\rangle\langle-|)^{\otimes N} \qquad (2)$$

where $|\lambda_{m/M}\rangle$ are the eigenvectors of H corresponding to the minimum/maximum eigenvalues [5], and $|\pm\rangle = (|\lambda_m\rangle \pm |\lambda_M\rangle)/\sqrt{2}$.

We illustrate the protocol with a two-party scenario as followed. Alice is in charge of state preparation and Bob is responsible for the measurements (see Fig. 1). They both wish to recover the parameter in a cheat-sensitive way. We also require that any classical information they exchange must be useless to a third party. Here we assign Eve, an eavesdropper the possibility of performing arbitrary operations on Alice's probes allowed by quantum mechanics, and she can access the quantum channel where the states travel.

Alice randomly sends either $|\Psi^{\pm}_{\text{probe}}\rangle$ or $|\Psi_{\text{eig}}\rangle$ to Bob, where $|\Psi_{\text{eig}}\rangle$ is an element randomly chosen from $\{|\lambda_m\rangle^{\otimes N}, |\lambda_M\rangle^{\otimes N}\}$. The phase sensitive states evolve to be $(e^{iN\varphi\lambda_m}|\lambda_m\rangle^{\otimes N} \pm e^{iN\varphi\lambda_M}|\lambda_M\rangle^{\otimes N})/\sqrt{2}$. Upon receiving a state, Bob independently chooses to measure either $\hat{O}^{\pm}_N$ or $\hat{\Pi}_{\text{eig}}$, where $\hat{\Pi}_{\text{eig}} = (|\lambda_m\rangle\langle\lambda_m|)^{\otimes N}$. They reconcile immediately their choice of basis, and discard all the result if they do not agree. Bob checks his outcome on $\hat{\Pi}_{\text{eig}}$, since measuring $\hat{\Pi}_{\text{eig}}$ on $|\Psi_{\text{eig}}\rangle$ is deterministic, his result should correlate perfectly with Alice's preparation. If this is not the case, they know their probes have been tampered with and they terminate.

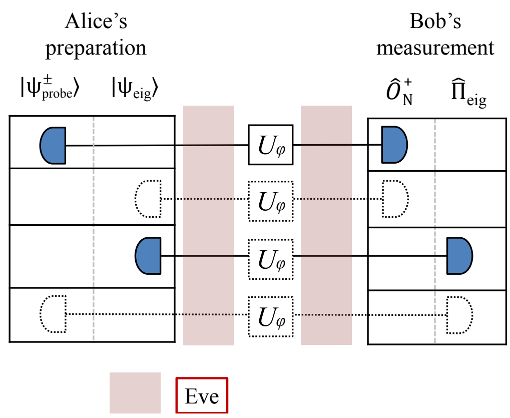

FIG. 1. Alice sends either $|\Psi^{\pm}_{\text{probe}}\rangle$ or $|\Psi_{\text{eig}}\rangle$ into the quantum channel which encodes the parameter φ onto the probes. Bob randomly measures either $\hat{O}^{\pm}_N$ or $\hat{\Pi}_{\text{eig}}$. They retain only the copies for which their choice of basis agree, denoted by the solid blue markers. The probes are also subjected to possible manipulation by an eavesdropper, Eve, given by the pink shaded regions.

Once they confirm that their communication is secure, Alice announces whether she has prepared $|\Psi^{+}_{\text{probe}}\rangle$ or $|\Psi^{-}_{\text{probe}}\rangle$ on half the probe states, and Bob reveals his measurement outcomes on the other half. They compute $\hat{O}^{\pm}_N$ correspondingly, where the sum of the expectation values is $\cos[N\varphi(\lambda_M - \lambda_m)]$, from which φ can be recovered.

Now, if their probes are not tampered with, then the information they exchange is meaningless to a third party. In addition, if Eve has access to only one end of the channel, then she cannot gain any information at all, even if she steals all the probes and overhears their communication.

The two-party protocol can be naturally extended to a multiple party scenario. If there are k parties involved, the state $|\Psi^{\pm}_{\text{probe}}\rangle$ with $N + k - 1$ probes are used.

[1] C. H. Bennett and G. Brassard, Proceedings of the IEEE , 175 (1984).
[2] N. Gisin, G. Ribordy, W. Tittel, and H. Zbinden, Rev. Mod. Phys. **74**, 145 (2002).
[3] C. H. Bennett, Phy. Rev. Lett. **68**, 3121 (1992).
[4] L. Hardy and A. Kent, Phys. Rev. Lett. **92**, 157901 (2004).
[5] V. Giovannetti, S. Lloyd, and L. Maccone, Phys. Rev. Lett. **96**, 010401 (2006).

Adaptive phase estimation with two-mode squeezed-vacuum and parity measurement

Zixin Huang,[1] Keith R. Motes,[2] Jonathan P. Dowling,[3] and Dominic W. Berry[2]
[1]School of Physics, University of Sydney, NSW 2006, Australia
[2]Department of Physics and Astronomy, Macquarie University, Sydney NSW 2113, Australia
[3]Hearne Institute for Theoretical Physics and Department of Physics & Astronomy, Louisiana State University, Baton Rouge, LA 70803

A proposed phase-estimation protocol based on measuring the parity of a two-mode squeezed-vacuum state at the output of a Mach-Zehnder interferometer shows that the Cramér-Rao sensitivity is sub-Heisenberg. However, it is unclear if this sensitivity can be obtained with a finite number of measurements. This sensitivity is only for phase near zero, and in this region, the sign of the phase is ambiguous. Here we show that an adaptive technique gives a highly accurate estimate regardless of the phase. We show that the Heisenberg limit is reachable with a finite number of measurements, and the estimation is unambiguous in the interval $(-\pi/2, \pi/2)$.

Phase estimation and optical interferometry are the basis for many precision measurement applications. Quantum states of light has received much attention, since they can achieve a finer precision than the shot-noise limit, $\Delta\varphi^2 \geq \bar{n}^{-1}$, where φ is the unknown phase, and $\bar{n}$ is the mean photon number.

We consider a scheme based on measuring the parity of the state of light at the output of a Mach-Zehnder interferometer, with a two-mode squeezed-vacuum (TMSV) input. A parity measurement focuses on whether the output photon number is odd or even, rather than the the actual number itself. It turns out that this particular scheme [1] has sub-Heisenberg sensitivity, due to the fact that the photon number uncertainty for the state of light inside of the MZI is greater than the average photon number used for the measurement [2].

The expected value of the parity signal $\langle\hat{\Pi}\rangle$ for the estimation scheme being considered is [1]

$$\langle\hat{\Pi}\rangle = \frac{1}{\sqrt{1 + \bar{n}(\bar{n}+2)\sin^2(\theta - \varphi)}},$$

where φ is the phase on one arm of the interferometer, and θ is the controllable phase on the other arm; the Cramer-Rao bound sensitivity at $\theta - \varphi = 0$ is $\varphi^2 \geq 1/M\bar{n}(\bar{n}+2)$, M being the number of repeated measurements. It was previously unclear whether this is achievable.

However, simply measuring the number of even/odd events cannot distinguish the sign of the phase. For example, for $\bar{n} = 3$ and $\theta = 0$, if 512 parity measurements are performed and 466 turn out to be even, the estimate of φ has two solutions: $\varphi = 0.18$ and $\varphi = -0.18$ (see Fig. 1). This ambiguity comes about because the term containing φ is squared. In addition, the most sensitive region is confined to a small interval around $\theta - \varphi = 0$, where the ambiguity of the sign is most problematic. Moving away from this region, the phase sensitivity decays quickly.

We apply an adaptive technique [3, 4], where the controlled phase θ is adjusted based upon previous detection results and controlled phases. This resolves the ambiguity, and also gives highly accurate estimates regardless of φ. In Fig. 2 we plot the ratio of the simulated phase mean-square errors to the Heisenberg limit for different mean photon number $\bar{n}$. Evidently, for $\bar{n} = 1$, the Heisenberg limit is reachable, where the number of trials needed for mean photon number $\bar{n} = 1$ is approximately one hundred [4].

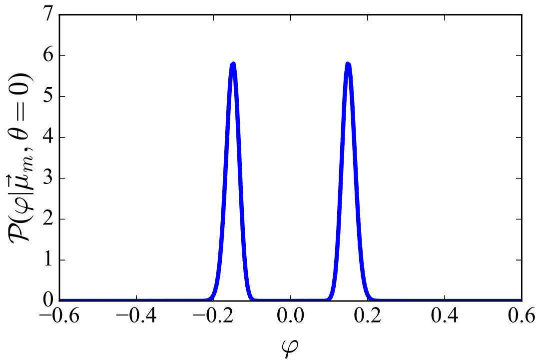

FIG. 1. The probability distribution for the phase φ for an example measurement record, generated for an actual phase of $\varphi = 0.15$ and the control phase $\theta = 0$. The record consists of $M = 512$ parity detections for $\bar{n} = 3$, of which 466 are even. The distribution has two maxima distributed symmetrically around 0.

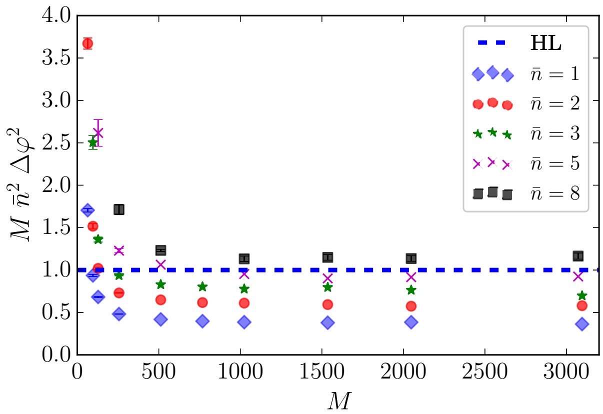

FIG. 2. The ratio of the phase mean-square error to the Heisenberg limit versus the measurement record length M, for TMSV states with a range of mean photon numbers. The Heisenberg limit (blue dashed line) is plotted for comparison(it is 1 on this plot).

[1] P. M. Anisimov, G. M. Raterman, A. Chiruvelli, W. N. Plick, S. D. Huver, H. Lee, and J. P. Dowling, Phys. Rev. Lett. **104**, 103602 (2010).
[2] H. F. Hofmann, Phys. Rev. A **79**, 033822 (2009).
[3] D. W. Berry and H. M. Wiseman, Phys. Rev. Lett. **85**, 5098 (2000).
[4] Z. Huang, K. R. Motes, P. M. Anisimov, J. P. Dowling, and D. W. Berry, arXiv preprint arXiv:1609.04689 (2016).

Non-Markovianity and nonequilibrium physics in atom-surface interactions

Francesco Intravaia
Max-Born-Institut and Humboldt-Universität zu Berlin, 12489 Berlin, Germany
Email: francesco.intravaia@mbi-berlin.de

Progress in manipulating atomic and condensed matter systems has stimulated the investigation of atom-surface dispersion forces. In recent years these phenomena have attracted a constantly growing attention due to their relevance for fundamental physics as well as for modern nanotechnology. These forces, whose origin is deeply rooted in quantum theory, have been studied both in equilibrium (van der Waals/Casimir-Polder forces) and out of equilibrium (quantum friction) configurations. Common approaches for their quantitative description often rely on techniques based on the Markov and the local thermal equilibrium approximations. The latter treats interacting subsystems in a general nonequilibrium system as being locally in equilibrium with their immediate surrounding environment.

We show that in some cases these approximations can lead to erroneous predictions on atom-surface interactions with regard to both strength and functional dependencies on system's parameters [1-3]. In particular, we show that the long-time power-law tails of temporal correlations, and the corresponding low-frequency behavior, of two-time correlations, neglected in the Markovian limit, affect the prediction of the equilibrium and the nonequilibrium force [1,3]. In addition, the local thermal equilibrium approximation fails for quantum friction and underestimates by approximately 80% the magnitude of the drag force [2]. Our results highlight the importance of non-Markovian effects in dispersion forces and also call for a critical reexamination of the use of the local thermal equilibrium approximation for describing the physics of nonequilibrium systems.

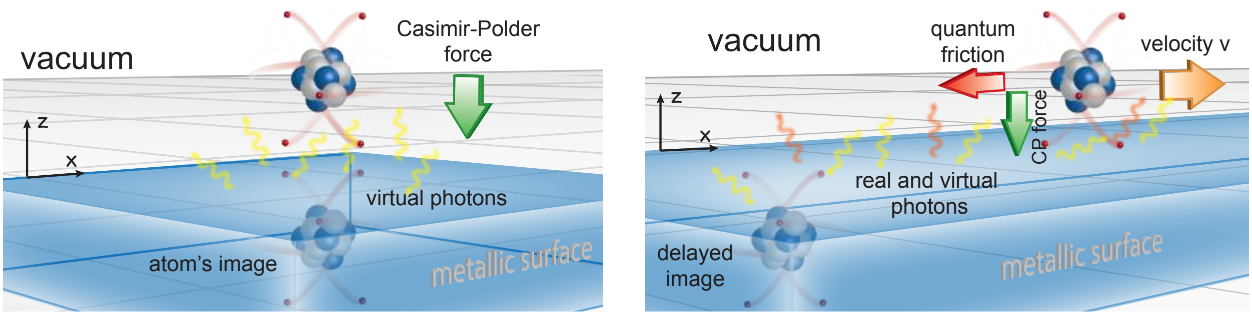

Figure 1: (Left) Schematic of an atom above a surface experiencing the Casimir-Polder force. The force can be qualitatively understood as stemming from the interaction of the atom with its image within the material. (Right) Schematic of quantum friction on an atom moving at constant velocity parallel to a surface. As in the static case, the appearance of a frictional force can be qualitatively related to the interaction of the atom with its *delayed* image within the material.

References

[1] F. Intravaia, R. O. Behunin, C. Henkel, K. Busch, and D. A. R. Dalvit, *Non-Markovianity in atom-surface dispersion forces*, Phys. Rev. A **94**, 042114 (2016).
[2] F. Intravaia, R. O. Behunin, C. Henkel, K. Busch, and D. A. R. Dalvit, *Failure of local thermal equilibrium in quantum friction*, Phys. Rev. Lett. **117**, 100402 (2016).
[3] F. Intravaia, R. O. Behunin, and D. A. R. Dalvit, *Quantum friction and fluctuation theorems*, Phys. Rev. A **89**, 050101(R) (2014).

Generation of quantum correlations in two-mode Gaussian open systems

Aurelian Isar

National Institute of Physics and Nuclear Engineering, Bucharest-Magurele, Romania

e-mail: isar@theory.nipne.ro

We analyze the possibility to generate quantum correlations (quantum entanglement and Gaussian quantum discord) in a system consisting of two coupled non-resonant bosonic modes immersed in a common thermal reservoir, in the framework of the theory of open systems, based on completely positive quantum dynamical semigroups. The dynamics of quantum correlations is described in terms of the covariance matrix for Gaussian initial states and the evolution under the quantum dynamical semigroup assures the preservation in time of the Gaussian form of the states. We calculate the logarithmic negativity and show that for separable initial squeezed thermal states entanglement generation may take place, for definite values of the squeezing parameter, average photon numbers, temperature of the thermal bath, dissipation constant and the strength of interaction between the two modes. After its generation one can observe temporary suppressions and revivals of the entanglement [1]. For entangled initial squeezed thermal states, entanglement suppression takes place, for all temperatures of the reservoir, and temporary revivals and suppressions of entanglement can be observed too. In the limit of large times the system evolves asymptotically to an equilibrium state which may be entangled or separable. Likewise, for initial uni-modal squeezed states, the generation of Gaussian quantum discord takes place during the interaction with the thermal bath, for all nonzero values of the strength of interaction between the bosonic modes. The asymptotic discord depends on the values of the parameters characterizing the thermal bath (temperature and dissipation coefficient), as well as on the strength of interaction between modes, which determines the generation and preservation in time of the quantum discord. For initial squeezed vacuum states, the initial non-zero Gaussian discord non-monotonically decreases in time and tends asymptotically for large times to some definite non-zero value [2].

[1] A. Isar, Open Sys. Information Dynamics **23**, 1650007 (2016)

[2] T. Mihaescu, A. Isar, submitted (2017)

Continuous-Variable Quantum Computing on Encrypted Data

Kevin Marshall,[1,*] Christian S. Jacobsen,[2,*] Clemens Schäfermeier,[2]
Tobias Gehring,[2,†] Christian Weedbrook,[3,‡] and Ulrik L. Andersen[2]

[1]*Department of Physics, University of Toronto, 60 St. George St., Toronto, M5S 1A7, Canada*
[2]*Department of Physics, Technical University of Denmark, Fysikvej, 2800 Kgs. Lyngby, Denmark*
[3]*CipherQ, 10 Dundas St. E, Toronto, M5B 2G9, Canada*

(Dated: April 5, 2017)

Cloud computing services are becoming increasingly prevalent in the information technology industry, and with this comes an increase in the transmission and storage of sensitive information where the client who is using the service is forced to trust the provider of the service. For simple data storage this problem is largely solvable by standard encryption methods, but when server-side computation is required this solution is no longer sufficient. Classically this is resolved by the introduction of homomorphic encryption, which allows meaningful function evaluations on the encrypted data [1].

In the quantum regime homomorphic encryption is in general not feasible without a substantial commitment of resources [2]. The idea of delegated quantum computing was introduced by Childs [3], in which a client delegates a quantum computation to a server with quantum computational capabilities. Progress towards this direction was demonstrated recently by IBM who made available a small (5 qubit) quantum computer for access in the cloud [4]. In the context of security, one might then wish to hide the input and the output of this computation from the server. Such a protocol is termed quantum computing on encrypted data [5]. Our proposal is just such a protocol, but rather than using discrete variables the encryption and quantum computing is implemented in the continuous variable regime.

As seen in Figure 1 our protocol takes place in three steps: the encryption stage, the program stage, and the decryption stage. In the first step the client encrypts her input state by displacing it to a random, but bounded, location in phase space. She transmits this encrypted state to the server, which executes the second stage by putting the received state through the previously agreed upon quantum gate. The output is returned to the client who executes the third stage of the protocol by performing a decryption operations that depends on the quantum gate implemented by the server. Once the decryption has been succesfully performed the client obtains an output corresponding to the quantum gate output of the unencrypted input state.

We test the protocol using linear phase space displacements and squeezing as our quantum gates, i.e., we implement a server performing firstly Z and X gates and secondly a squeezing gate, related to the U_2 gate [6]. In realizing the squeezing gate our setup was constructed such that the input state was squeezed by insertion into the squeezed-source source. To our knowledge this is the first demonstration of in-line squeezing applied as a transformation of quantum information.

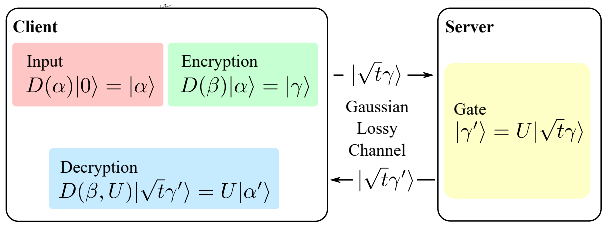

FIG. 1: **Protocol for quantum computing on encrypted data.** The three stages of our protocol: encryption, gates, and decryption are illustrated for a coherent state input where we include a transmission step in both directions between the client and server.

We have developed a continuous-variable protocol for quantum computing on encrypted variables. The feasibility of the scheme was experimentally demonstrated by performing displacements and online squeezing operations on an alphabet of coherent states, with an evaluation of the resulting protocol fidelity. To the best of our knowledge, this is the first time quantum computing on encrypted data has been generalized to continuous variables. We expect these results to pave the way for a deeper investigation into using continuous-variable states to securely carry quantum information on future quantum computing networks.

* These two authors contributed equally to this work
† Electronic address: tobias.gehring@fysik.dtu.dk
‡ Electronic address: christian.weedbrook@gmail.com

[1] Ronald Rivest, Len Adleman, and Michael Dertouzos. On data banks and privacy homomorphisms. In *Foundations of secure computation*, volume 4, pages 169–180. 1978.
[2] A. Broadbent, J. Fitzsimons, and E. Kashefi. Universal blind quantum computation. In *Foundations of Computer Science, 2009. FOCS '09. 50th Annual IEEE Symposium on*, pages 517–526, Oct 2009.
[3] Andrew M. Childs. Secure assisted quantum computation. *Quantum Info. Comput.*, 5(6):456–466, September 2005.
[4] IBM. The IBM quantum experience, Cited July 2016.
[5] KAG Fisher, A Broadbent, LK Shalm, Z Yan, J Lavoie, R Prevedel, T Jennewein, and KJ Resch. Quantum computing on encrypted data. *Nat. Commun.*, 5:3074, 2014.
[6] Kazunori Miyata, Hisashi Ogawa, Petr Marek, Radim Filip, Hidehiro Yonezawa, Jun Ichi Yoshikawa, and Akira Furusawa. Experimental realization of a dynamic squeezing gate. *Physical Review A*, 90(6):060302(R), 2014.

Positive-negative frequency conversion at a refractive index front

Maxime Jacquet[1,*] and Friedrich Koenig[1,†]
[1]School of Physics and Astronomy, SUPA, University of St. Andrews, North Haugh, St. Andrews, KY16 9SS, UK

In our Universe, there exist various conditions under which waves of positive and negative frequency can be made to convert into each other. For example, upon propagating on a curved background, incoming waves of positive and negative frequency mix to generate outgoing waves. As a result of this scattering process, field quanta are spontaneously emitted from the vacuum — the most famous instance of this effect undoubtedly is the mixing of positive and negative frequency waves at the horizon of black holes, which results in a steady thermal flux to be emitted from the hole, Hawking radiation [1].

The event horizon of the black hole is the point at which the curvature of spacetime is such that the escape velocity out to infinity becomes superluminal, thus restricting wave propagation to one direction only: toward the central singularity. Wave propagation on a curved background is not restricted to astrophysics: it is possible to realise such conditions with moving wave media in the laboratory, and, in particular, the kinematics of waves at the horizon [2].

An artificial event horizon can be created by moving a refractive index front (RIF) in a dispersive optical medium at the speed of light [3]. The RIF could be created by a pulse of light that modifies the index by the optical Kerr effect. Light under the pulse will be slowed and thus the front of the pulse exhibits — for some frequencies — a black-hole type horizon capturing light. The back of the pulse acts as an impenetrable barrier, a white-hole horizon. Both event horizons separate two discrete regions: under the pulse, where light is slow and the pulse moves superluminally and outside the pulse, where the pulse speed is subluminal.

We reveal the properties of spontaneous emission from the vacuum at a moving refractive index step in a dispersive dielectric by expanding on an analytical model for light-matter interaction [4]. We establish the conditions for event horizons as a function of the speed and height of the step in the medium, and study the various configurations of modes of the field in the vicinity of the step with and without analogue horizons. We then analytically calculate the emission spectra from all modes of positive and negative frequency in the laboratory frame [5]. We find that, as a result of the various mode configurations, the spectrum is highly structured into intervals with black hole-, white hole-, and no horizon.

The emission spectrum in the laboratory frame, Fig.1, is found to be a combination of emissions corresponding to different frequencies in the frame moving with the pulse, leading to a characteristic shape. In particular, the existence of a peak in the ultraviolet, associated with emission into a mode with negative frequency, is an interesting feature of our spectrum. We show how emission in this peak may be stimulated by scattering a coherent wave at the horizon and investigate this effect experimentally.

We observe the transfer of energy from a positive-frequency wave to outgoing waves of positive and negative frequency at the horizon, Fig.2. The effect of mode conversion is clearly shown to be a feature of horizon physics. This is a stimulated version of the spontaneous quantum effect at the heart of Hawking radiation.

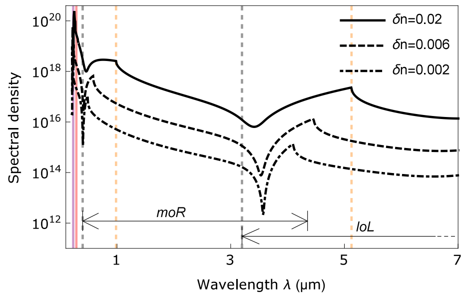

FIG. 1. Spectral density of spontaneous emission from the vacuum at a refractive index front.

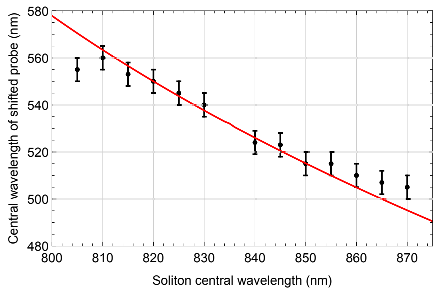

FIG. 2. Location of positive-frequency output light for different soliton-horizon wavelength.

* mj35@st-andrews.ac.uk
† fewk@st-andrews.ac.uk

[1] S. Hawking, Nature **248**, 30 (1974).
[2] W.G. Unruh, Phys. Rev. Let. **46** (1981).
[3] T.G. Philbin *et al* Science **319**, 1367 (2008).
[4] S. Finazzi and I. Carusotto, Phys. Rev. A **87**, 023803 (2013).
[5] M. Jacquet and F. Koenig, Phys. Rev. A **92**, 023851 (2015).

Insecurity of practical quantum key distribution against long-wavelength Trojan-horse attacks

Shihan Sajeed,[1,2] Carter Minshull,[1,3] **Nitin Jain**,[4] and Vadim Makarov[3,1,2]
[1)] *Institute for Quantum Computing, University of Waterloo, Waterloo, ON, N2L 3G1 Canada*
[2)] *Department of Electrical and Computer Engineering, University of Waterloo, Waterloo, ON, N2L 3G1 Canada*
[3)] *Department of Physics and Astronomy, University of Waterloo, Waterloo, ON, N2L 3G1 Canada*
[4)] *Department of Physics, Technical University of Denmark, Fysikvej, Kongens Lyngby 2800, Denmark*

Trojan-horse attacks on practical quantum key distribution (QKD) implementations have received considerable attention in the last 5 years[1–4]. In these attacks, the eavesdropper Eve directs a strong optical pulse from the quantum channel into the targeted QKD subsystem — Alice or Bob — and performs appropriate measurements on the back-reflections. These measurements can yield Eve information about the state of the modulator if it is in the attack path taken by the bright pulse and/or a back-reflection. If the attack can be carried out without alerting Alice or Bob, then the security of the QKD implementation is broken since knowing the state of the modulator is equivalent to knowing the secret bit.

While the basic ideas behind such attacks have been known for more than a decade[5,6], the first actual demonstration on 'Clavis2-Bob', the QKD receiver from ID Quantique (`www.idquantique.com`), was reported recently[1]. It was shown that information about the modulator's state can indeed be gleaned successfully even with back-reflected pulses containing just a few photons. Nonetheless, the overall attack failed, owing to the side effect of increased afterpulsing in the single photon detectors (SPDs) of Bob. This afterpulsing dramatically elevates the noise response of the SPDs, thereby alerting Alice and Bob.

Here we report that a Trojan-horse attack is likely to stay inconspicuous if the attacker uses bright Trojan-horse pulses at a wavelength > 1900 nm. This is primarily because the afterpulsing probability due to such bright pulses is significantly lower than that observed in the previous study[1], where bright pulses at the normal communication wavelengths (around 1550 nm) were used. Figure 1 shows the two afterpulsing profiles, experimentally measured by synchronizing a single Trojan-horse pulse to the first in a sequence of detection gates of Bob, and recording the times at which clicks occurred in the onward gates.

The benefit of reduced afterpulsing at λ_l unfortunately comes at the expense of a much higher attenuation of the Trojan-horse pulse inside Bob. Additionally, the degree of modulation received at λ_l differs from that at λ_s substantially. We quantify the increased optical attenuation and the sub-optimal modulator response by means of further experimental measurements. Taking all these factors into account as well as devising a new attack path through Bob, we evaluate the attack performances in the two wavelength regimes. By means of a numerical simulation, we conclude that a Trojan-horse attack at λ_l is likely to breach the security of the QKD system. We note that a full-fledged apparatus, though hard to build, should be mostly implementable with commercial off-the-shelf components. The attack can be mitigated by using a wavelength filter at the input of the QKD device.

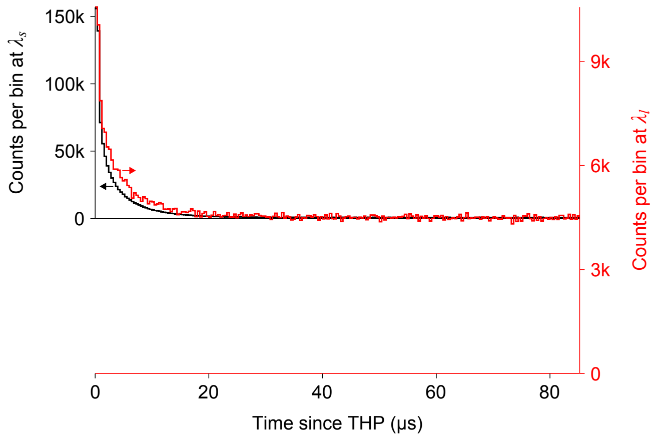

FIG. 1. Afterpulse profiles measured at $\lambda_s = 1536$ nm and $\lambda_l = 1924$ nm. For easier visual comparison, the histograms are rescaled so that their peak counts and dark count rates match in the plot.

[1] N. Jain, E. Anisimova, I. Khan, V. Makarov, C. Marquardt, and G. Leuchs, "Trojan-horse attacks threaten the security of practical quantum cryptography," New J. Phys. **16**, 123030 (2014).
[2] M. Lucamarini, I. Choi, M. B. Ward, J. F. Dynes, Z. L. Yuan, and A. J. Shields, "Practical security bounds against the Trojan-horse attack in quantum key distribution," Phys. Rev. X **5**, 031030 (2015).
[3] N. Jain, B. Stiller, I. Khan, V. Makarov, C. Marquardt, and G. Leuchs, "Risk analysis of Trojan-horse attacks on practical quantum key distribution systems," IEEE J. Sel. Top. Quantum Electron. **21**, 6600710 (2015).
[4] H.-X. Ma, W.-S. Bao, H.-W. Li, and C. Chou, "Quantum hacking of two-way continuous-variable quantum key distribution using trojan-horse attack," Chinese Physics B **25**, 080309 (2016).
[5] A. Vakhitov, V. Makarov, and D. R. Hjelme, "Large pulse attack as a method of conventional optical eavesdropping in quantum cryptography," J. Mod. Opt. **48**, 2023–2038 (2001).
[6] N. Gisin, S. Fasel, B. Kraus, H. Zbinden, and G. Ribordy, "Trojan-horse attacks on quantum-key-distribution systems," Phys. Rev. A **73**, 022320 (2006).

Classical capacity per unit cost for quantum channels

Marcin Jarzyna*
Center of New Technologies, University of Warsaw, ul. Banacha 2c, 02-097 Warsaw, Poland

In theory of communication it is common to consider how much information can be transmitted from sender to receiver per single channel use. In this picture many fundamental results were obtained, both concerning specific transmission protocols and general optimal bounds. Application of laws of quantum mechanics allowed for a deeper analysis of communication and showing such effects as output and input superadditivity or finite optimal rates even for noiseless channels, emerging from nonclassical phenomena like entanglement or uncertainty principle. In most communication schemes there are usually present some constraints on input symbols or features of information carriers that can be used during the information transmission task. These are usually quantified by the cost of using a particular state which encodes transmitted symbol. Instead of capacity, which quantifies how many bits can be transmitted per channel use, the quantity of interest is thus rather a maximum number of bits $C(\beta)$ that can be transmitted per channel use with an average cost not exceeding some given value β.

There are, however, also alternative figures of merit. In the context of fixed resources a particularly important quantity is the minimum cost required for transmission of a single bit of information through a channel, or its reciprocal, the capacity per unit cost $\mathbf{C}$. This quantity is interesting in many instances in which it is the cost of sending a symbol a crucial limitation rather than the number of channel uses. A basic example of such situation is a long distance or deep space communication, important for space missions designs. Since it is the energy budget that is the most sensitive resource in such settings it is crucial to increase the amount of information transmitted with a single unit of energy.

I show how the concept of capacity per unit cost [1] can be generalized to the underlying quantum description of information carriers and measurement devices. In particular I give a simple formula for the capacity per unit cost for any quantum channel assuming existence of a free-cost symbol denoted by 0 in the form $\mathbf{C} = \sup_{x\neq 0} \frac{D(\Lambda[\rho_x]||\Lambda[\rho_0])}{b[x]}$ and show that it can be saturated using simple binary encoding. Here ρ_x, ρ_0 are states encoding symbols x and 0 respectively, $\Lambda[.]$ is quantum channel through which information transfer occurs, $D(.||.)$ is quantum relative entropy, $b[x]$ denotes the cost of using symbol x and the supremum is taken over all symbols in the encoding.

I show that if the output state corresponding to the free symbol $\Lambda[\rho_0]$ does not have the same support as output states corresponding to other symbols (e.g. it is pure), then the channel capacity per unit cost $\mathbf{C}$ is always infinite. On the other hand, if $\Lambda[\rho_0]$ has the same support as output states corresponding to other symbols then capacity per unit cost has to be finite. This has important consequences in realistic communication protocols, where the cost $b[x]$ is usually the average number of photons $\bar{n}$ in the state ρ_x used for communication, and one can always use empty vacuum pulse for free $\rho_0 = |0\rangle\langle 0|$. In this context a quantity closely related to capacity per unit cost is photon information efficiency (PIE) $\Pi(\bar{n}) = C(\bar{n})/\bar{n}$ quantifying how much information can be carried by a single photon. If the channel Λ does not add any energy to the signal (e.g. it is a lossy channel or dephasing channel) then it does not corrupt the vacuum state which remains pure after the evolution $\Lambda[\rho_0] = |0\rangle\langle 0|$. In such cases capacity per unit cost is infinite which means also that PIE is unbounded. This indicates that in a regime of small $\bar{n}$ capacity per single channel use $C(\bar{n})$ has a better than linear scaling with $\bar{n}$, possibly log-linear scaling $\sim \bar{n}\log\frac{1}{\bar{n}}$ [2]. On the other hand, if the channel corrupts the vacuum state so that $\Lambda[|0\rangle\langle 0|]$ has the same support as other output states (e.g. Λ is a thermal channel), the relative entropy, and consequently also the capacity per unit cost and PIE, is finite. In such case, capacity per channel use cannot scale better than linearly for small average numbers of photons $C(\bar{n}) \sim \bar{n}$.

I show also that in the case in which the cost is quadratic the capacity per unit cost is equal to Relative Entropy Quantum Fisher Information [3] and can be bounded by an ordinary Quantum Fisher Information [4], a quantity well known in quantum estimation theory. This situation is typical for actual communication protocols employing coherent states of light in which the quadratic cost function appears naturally since the energy of a light pulse is given by the square amplitude of the state. Finally I give also a detailed analysis of capacity per unit cost for Gaussian quantum channels.

* m.jarzyna@cent.uw.edu.pl

[1] S. Verdu, IEEE Transactions on Information Theory **36**, 1019 (1990).
[2] M. Jarzyna, P. Kuszaj, K. Banaszek, Opt. Express **23**, 3170 (2015).
[3] J. Czajkowski, M. Jarzyna, R. Demkowicz-Dobrzański, arXiv:1603.00472 [quant-ph] (2016).
[4] S. L. Braunstein, C. M. Caves, Phys. Rev. Lett. **72**, 3439 (1994).

Sensitivity, quantum limits, and quantum enhancement of noise spectroscopies

Vito Giovanni Lucivero [1], Aleksandra Dimic [2], Jia Kong [1], Ricardo Jiménez-Martínez[1], and Morgan W. Mitchell [1,3]
[1] ICFO-Institut de Ciencies Fotoniques, The Barcelona Institute of Science and Technology, 08860 Castelldefels (Barcelona), Spain
[2] Faculty of Physics, University of Belgrade, Studentski Trg 12-16, 11000 Belgrade, Serbia
[3] ICREA – Institució Catalana de Recerca i Estudis Avançats, 08015 Barcelona, Spain

We study the fundamental limits of noise spectroscopy using estimation theory, Faraday rotation probing of an atomic spin system, and squeezed light. We find a simple and general expression for the Fisher information, which quantifies the sensitivity to spectral parameters such as resonance frequency and linewidth. For optically-detected spin noise spectroscopy, we find that shot noise imposes "local" standard quantum limits for any given probe power and atom number, and also "global" standard quantum limits when probe power and atom number are taken as free parameters. We confirm these estimation theory results using non-destructive Faraday rotation probing of hot Rb vapor, observing the predicted optima and finding good quantitative agreement with a first-principles calculation of the spin noise spectra. Finally, we show sensitivity beyond the atom- and photon-number-optimized global standard quantum limit using squeezed light.

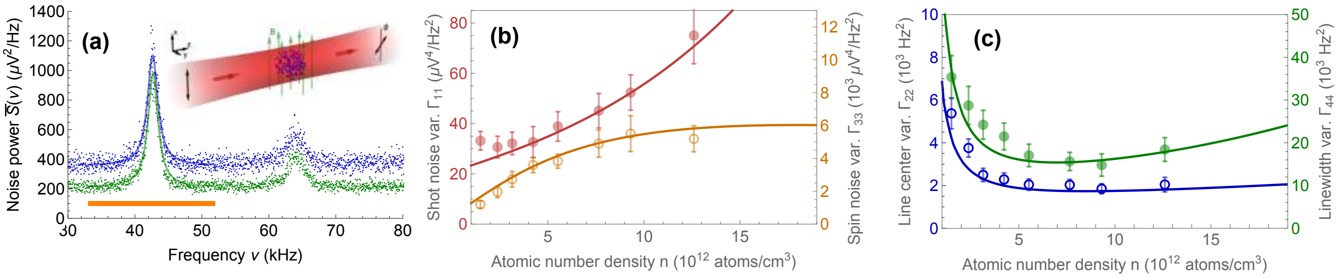

FIG. 1: (a) Spin noise spectra. Representative noise spectra showing spin noise resonances of Rb vapor, upper spectrum (blue) with coherent-state probing, lower spectrum (green) with polarization-squeezed probe light. Orange bar below spectra shows fit region for ^{85}Rb spectra, blue and green curves show fits to the data based on a model consisting of a Lorentzian ,with resonance at the Larmor frequency, and a background due to light shot noise [1, 2] for both coherent and squeezed spectra, respectively. Inset: principle of spin noise measurement. Polarized light experiences Faraday rotation by an angle ϕ proportional to the on-axis magnetization of the atomic ensemble, and is detected with a polarimeter (not shown). (b) - (c) Spin noise sensitivity. Sensitivity of spin noise spectroscopy versus atomic density in theory and experiment. Optical power is $P = 2$ mW throughout. (b) Lower, blue curve shows Γ_{22}, the variance of the Larmor frequency estimate, computed by theory [2] and from experiment (blue hollow circles), on left (blue) axis. Upper, green curve shows Γ_{44}, the variance of the resonance linewidth estimate, and observed variance (green filled circles), on right (green) axis. (c) Upper, red curve shows Γ_{11}, the variance of the shot noise estimate, from theory and from experiment (red filled circles), on left (red) axis. Lower, orange curve shows Γ_{33}, the variance of the resonance amplitude, due spin noise, estimate, and observed variance (orange hollow circles), on right (orange) axis. Error bars show plus/minus one standard error.

[1] V. G. Lucivero, et al., "Squeezed-light spin noise spectroscopy", Phys. Rev. A **93**, 053802 (2016).
[2] V. G. Lucivero, et al., "Sensitivity, quantum limits, and quantum enhancement of noise spectroscopies", arXiv preprint: 1610.02356

Few-photon scattering in arbitrary waveguide geometries

Kristoffer Joanesarson,[1] Jake Iles-Smith,[1] Jesper Mørk[1]

[1]*DTU Fotonik, Department of Photonics Engineering, DTU, Copenhagen, Denmark*

Photonic crystal waveguides offer a potential architecture for scalable on-chip quantum information processing, operating at a single-photon level. One example of a possible application is as an all-optical few-photon switch [1] as illustrated in Figure 1.

Recent demonstrations have shown that a waveguide geometry consisting of a side-coupled cavity and a partially transmitting element (PTE) exhibits ultrafast switching properties owing to its characteristic Fano lineshape transmission spectrum [2,3]. Here, we take the quantum analogy of such a geometry by replacing the PTE with an effective two level emitter (TLE) such as an atom or a quantum dot (Figure 1a) and investigate its few-photon switching properties. We compare it to well-known geometries, namely a side-coupled cavity (Figure 1b) and a TLE (Figure 1c) [4,5].

We model the waveguide as a linear dispersive medium and construct the one- and two-photon scattering matrices from an input-output formalism [6]. We take the one- and two-photon input state to be Gaussian wavepackets and calculate the probability that a measurement would detect the transmission of any photons. As a figure of merit for the switching properties we use the difference in transmission probability between the two-photon and one-photon input state. This is plotted for the three aforementioned geometries in Figure 2 as a function of the spectral width of the Gaussian input wavepacket.

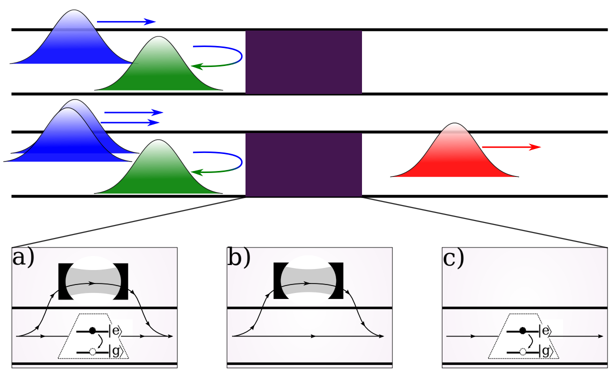

Figure 1: Illustration of the few-photon switch principle. Ideally, a single photon input will be reflected whereas a two photon input is partially transmitted. For the box in the waveguide path we here use either a) a mutually uncoupled TLE and side-coupled cavity, b) a side-coupled cavity, c) or a TLE.

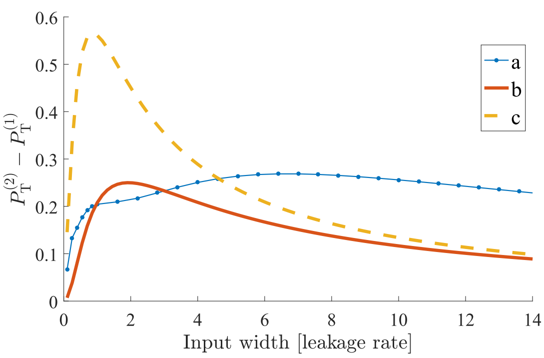

Figure 2: Difference in one- and two-photon transmission probability as a function of the wavepacket input width for the waveguide geometries in Figure 1a, 1b, and 1c.

[1] D. E. Chang, V. Vuletić, and M. D. Lukin, Nature Photonics **8**, 685 (2014).
[2] M. Heuck, P. T. Kristensen, Y. Elesin, and J. Mørk, Optics letters **38**, 2466 (2013).
[3] Y. Yu et al., Applied Physics Letters **105**, 061117 (2014).
[4] A. Nysteen, P. T. Kristensen, D. P. McCutcheon, P. Kaer, and J. Mørk, New Journal of Physics **17**, 023030 (2015).
[5] A. Nysteen, D. P. McCutcheon, and J. Mørk, Physical Review A **91**, 063823 (2015).
[6] S. Fan, Ş. E. Kocabaş, and J.-T. Shen, Physical Review A **82**, 063821 (2010).

Strain-tuning the properties of scalable, site-controlled sources based on pyramidal quantum dots for entangled photon emission

G. Juska*[1], S. T. Moroni[1], T. H. Chung[1], J. Martín-Sánchez[2], R. Trotta[2], A. Rastelli[2], A. Gocalinska[1], and E. Pelucchi[1]

[1]*Tyndall National Institute, University College Cork, Lee Maltings, Dyke Parade, Cork, Ireland*
[2] *Institute of Semiconductor and Solid State Physics, Johannes Kepler Universität, Altenberger Straße 69, 4040 Linz, Austria*

Quantum dots (QD), as sources of quantum bits, are among the promising technologies being studied for the implementation of quantum computation. Despite tremendous progress in the field, technologically challenging application requires progressive improvement of QDs. Reducing/cancelling QD asymmetry, which highly degrades polarization entanglement, is one of the challenges. Some of us previously have shown that QD asymmetry-related issues can be substantially reduced by (111)B oriented QDs grown in pyramidal recesses – a QD system allowing QD position control with a precision of a few nanometres, and with a high density of symmetric QDs emitting polarization-entangled photon pairs either under optical [1] or electrical excitation [2].

In this work, we present preliminary results as a proof of concept demonstrating the possibility to apply a tuning strategy – a stress field – to suppress the remaining, though statistically small, fine-structure splitting (FSS) values reflecting QD asymmetry. The pyramidal structures were bonded onto a monolithic piezoelectric PMN-PT actuator. By applying a voltage across the piezoelectric actuator, the resulting biaxial strain was used to tune QD optical properties: emission energy (Fig. a) and the fine-structure splitting (Fig. b). In a representative case shown in Fig. b, FSS was suppressed to the value <1 μeV allowing clear observation of polarization entanglement. This result is the first one to be observed within the site-controlled QD family, and opens possibilities for the application of more advanced, multiaxial stress field tuning technique [3].

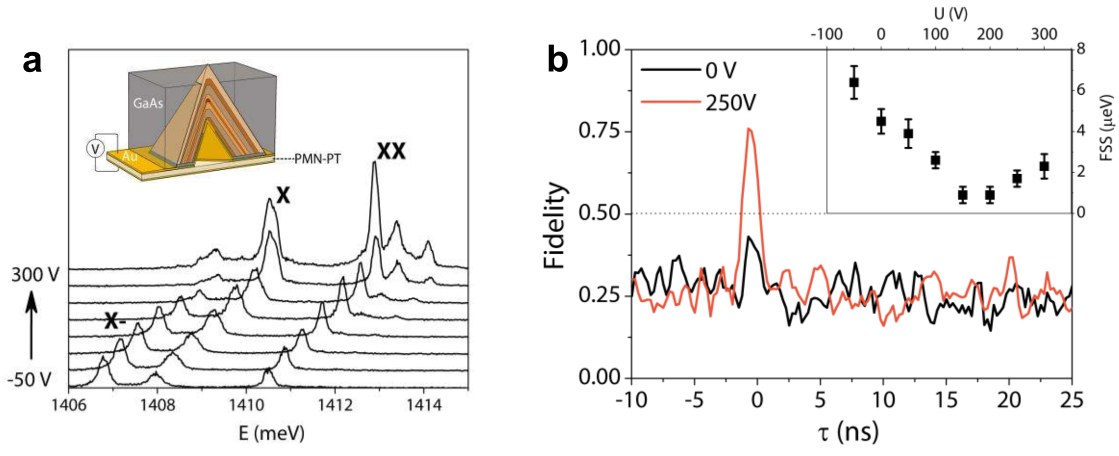

a. QD emission energy tuning by strain. (Inset) The sketch of a device: a pyramidal, epitaxially grown structure with an embedded QD at the center is integrated on a PMN-PT piezoelectric actuator. **b.**. Fidelity with the expected maximally entangled state $\frac{1}{\sqrt{2}}(|LR\rangle + |RL\rangle)$ measured at 0 and 250 V, where 0.5 is the limit for classical light. (Inset) Fine-structure splitting as a function of voltage applied across the monolithic piezoelectric actuator.

References
[1] G. Juska et al., Nat. Photon., 7, 527-531,(2013)
[2] T. H. Chung et al., Nat. Photon., 10, 782-787, (2016)
[3] R. Trotta et al., Nat. Comm., 7, 10375, (2016)

EPR steering and degree of mixedness for a family of three-qubit states

Joanna K. Kalaga,[1,*] Wiesław Leoński,[1] and J. Peřina Jr.[2]

[1]*Quantum Optics and Engineering Division, Institute of Physics, University of Zielona Góra, Z. Szafrana 4a, 65-516 Zielona Góra, Poland*

[2]*RCPTM, Joint Laboratory of Optics of Palacký University and Institute of Physics of the Czech Academy of Sciences, Faculty of Science, Palacký University, 17. listopadu 12, 771 46 Olomouc, Czech Republic*

We consider a family of states describing three-qubit systems, in a context of finding quantum steering effects. In particular, we concentrate on two cases. The first of them corresponds to the situation when one excitation is present in the system (total mean number of photons/phonons is equal to 1, *i.e.* $\langle\hat{n}\rangle = \langle\hat{n}_1\rangle + \langle\hat{n}_2\rangle + \langle\hat{n}_3\rangle = 1$, where the indices 1, 2 and 3 label the qubits). For such a case the wave-function describing considered here three-qubit system can be expressed as

$$|\psi^{(I)}\rangle = C_{001}|001\rangle + C_{010}|010\rangle + C_{100}|100\rangle, \qquad (1)$$

where C_{ijk} are the complex probability amplitudes corresponding to the states $|ijk\rangle = |i\rangle_1 \otimes |j\rangle_2 \otimes |k\rangle_3$.

The second case concerns the situation when the system is double excited ($\langle\hat{n}\rangle = 2$), and the wave-function takes the following form

$$|\psi^{(II)}\rangle = C_{011}|011\rangle + C_{101}|101\rangle + C_{110}|110\rangle\,. \qquad (2)$$

In our study we concentrate on finding of the situations for which steerable states for different pairs of qubits can be generated. As a measure of steering for such qubit-qubit subsystems we apply the steering parameters S_{ij} defined with use of Cavalcanti inequality [1]

$$S_{ij} = \langle\hat{a}_i\hat{a}_j^\dagger\rangle\langle\hat{a}_i^\dagger\hat{a}_j\rangle - \langle\hat{a}_i^\dagger\hat{a}_i(\hat{a}_j^\dagger\hat{a}_j + \frac{1}{2})\rangle, \qquad (3)$$

where indices i and j label the qubits, and $\hat{a}^\dagger$, $\hat{a}$ are boson creation and annihilation operators. When the parameter S_{ij} is positive the qubit j steers that labeled by i.

In this communication we analyze how the mixedness of the states is related to the steering effect. The degree of mixedness we characterize by the linear entropy which is defined with application of the purity [2] as:

$$E(\rho) \equiv \frac{D}{D-1}\left[1 - Tr\left(\rho_{ij}^2\right)\right]. \qquad (4)$$

For the cases considered here, we assume $D = 4$ as it denotes dimension of two-qubits density matrix ρ_{ij}. The linear entropy takes values from 0 for pure states to 1 when the states are maximally mixed. In our considerations we focus on the relations between the linear entropy and two measures of the entanglement appearing in two-qubit subsystem – the concurrence [3, 4] and the negativity [5, 6]. Moreover, we derived here the formulas determining the boundary values of the linear entropy which define borders between the regions corresponding to the steerable and unsteerable states.

* J.Kalaga@if.uz.zgora.pl

[1] E. G. Cavalcanti, Q. Y. He, M. D. Reid, H. M. Wiseman, *Phys. Rev. A* , 84, 032115 (2011)
[2] T. C. Wei, K. Nemoto, P. M. Goldbart, P. G. Kwiat, W. J. Munro, F. Verstraete, *Phys. Rev. A*, 67, 022110 (2003)
[3] S. Hill, W. Wootters, *Phys. Rev. Lett.*, 78, 5022 (1997)
[4] W. K. Wooters, *Phys. Rev. Lett.*, 80, 2245 (1998)
[5] A. Peres, *Phys. Rev. Lett.*, 77, 1413 (1996)
[6] M. Horodecki, P. Horodecki, M. Horodecki, R. Horodecki, *Phys. Lett. A*, 223, 1 (1996)

An Effective Criterion for the existence of Decoherence-Free Subspaces in Open Quantum Systems

Takeo Kamizawa
Faculty of Physics, Astronomy and Informatics, Nicolaus Copernicus University,
87-100 Toruń, Poland

ABSTRACT

The study of open quantum systems revealed that in some cases such systems can possess a "protected" subspace which is free from the environmental noise, so-called a decoherence-free subspace (DFS). It has been an interesting problem to recognise if a given open quantum system has a DFS or not, and there have been several approaches in the literature. Our proposal in this presentation is to establish a criterion for the existence of a DFS for open quantum systems with time-dependent generators and whose evolution is completely positive and trace-preserving (CPTP). An important point is that our method is constructive, so the existence of a DFS can be checked step-by-step and the process finishes in a finite time.

In order to express general situations, let the master equation on the set of states $\mathcal{S}(\mathcal{H}_S)$ be

$$\frac{d}{dt}\rho_t = L(t)\,\rho_t, \tag{1}$$

where $L(t) : \mathcal{L}(\mathcal{H}_S) \to \mathcal{L}(\mathcal{H}_S)$ is the time-dependent generator. We represent the linear evolution operator of (1) by $\Lambda(t)$, which is defined by $\rho_t = \Lambda(t)\,\rho_0$ for a given initial state ρ_0. A non-zero subspace $\mathcal{H}_{DFS}\,(\subset \mathcal{H}_S)$ is called a decoherence-free subspace (DFS) if $\mathcal{S}(\mathcal{H}_{DFS})$ is an invariant subset for $\Lambda(t)$ and it is unitary on $\mathcal{S}(\mathcal{H}_{DFS})$. The main result in this presentation is the existence criterion of a DFS, which is based on the methods in [2, 3], as the following theorem shows:

Theorem. *Suppose the linear evolution operator $\Lambda(t)$ of (1) is represented as*

$$\Lambda(t)\,\rho = \sum_{j=1}^{s} K_j(t)\rho K_j^*(t), \qquad K_j(t) = \sum_{\ell=1}^{p_j} \alpha_j^{(\ell)}(t) K_j^{(\ell)}$$

where $\Lambda(t)$ is CPTP, $\alpha_j^{(\ell)}(t) \in \mathbb{C}$ is a time-dependent scalar function and $K_j^{(\ell)} \in \mathcal{L}(\mathcal{H}_S)$ is a constant operator. Let

$$\Omega(X_1, \ldots, X_\kappa) = \bigcap_{p_j, q_j \geq 0}^{n-1} \ker\left[X_1^{p_1} \cdots X_\kappa^{q_\kappa}, X_1^{q_1} \cdots X_\kappa^{q_\kappa}\right], \tag{2}$$

where $[A, B] = AB - BA$ is the commutator and the intersection is taken so that $\sum_j p_j \neq 0$ and $\sum_j q_j \neq 0$. Then, there is a DFS if and only if

$$\Omega\left(K_1^{(1)}, \ldots, K_1^{(p_1)}, \ldots, K_s^{(1)}, \ldots, K_s^{(p_s)}, K_1^{(1)*}, \ldots, K_1^{(p_1)*}, \ldots, K_s^{(1)*}, \ldots, K_s^{(p_s)*}\right) \neq \{\mathbf{0}\}.$$

One of the most important point of the theorem above is that the condition $\Omega \neq \{\mathbf{0}\}$ can be checked in a finite number of steps because it can be shown that

$$\Omega(X_1, \ldots, X_\kappa) = \sum_{p_j, q_j = 0}^{n-1} \ker\left[X_1^{p_1} \cdots X_\kappa^{q_\kappa}, X_1^{q_1} \cdots X_\kappa^{q_\kappa}\right]^* \left[X_1^{p_1} \cdots X_\kappa^{q_\kappa}, X_1^{q_1} \cdots X_\kappa^{q_\kappa}\right],$$

where the summation is taken so that $\sum_j p_j \neq 0$ and $\sum_j q_j \neq 0$. In this presentation we will apply this criterion to some models of open quantum systems.

[1] A. Jamiołkowski, T. Kamizawa, G. Pastuszak. Int. J. Theor. Phys 54 (2015) 2662-2674.
[2] T. Kamizawa. Algebraic Method in the Analysis of Decoherence-Free Subspaces in Open Quantum Systems (in preparation).
[3] G. Pastuszak, A. Jamiołkowski. Elect. J. Lin. Alg. 30 (2015) 257-270.

Dynamics of single-photon emission from electrically pumped NV centers in diamond

I. A. Khramtsov,[1] M. Agio,[2,3] and D. Yu. Fedyanin[1]

1. Laboratory of Nanooptics and Plasmonics, Moscow Institute of Physics and Technology, 141700 Dolgoprudny, Russian Federation

2 Laboratory of Nano-Optics, University of Siegen, 57072 Siegen, Germany

3. National Institute of Optics and Center for Quantum Science and Technology in Arcetri, 50125 Florence, Italy

Abstract - We introduce a physical model and establish a theoretical approach to address single-photon emission from electrically pumped NV centers in diamond. Using the developed model, we perform rigorous numerical simulations of the single-photon emitting diode and quantitatively reproduce experimentally measured autocorrelation functions. Simulated curves demonstrate remarkable agreement with experiment.

Devices that can produce single photons on demand play a key role in quantum photonic applications. To date, color centers in diamond, such as nitrogen-vacancy (NV) centers, have been unveiled as the most promising candidates for single-photon sources (SPSs) operating at standard conditions. For their immediate application in quantum information processing, color centers should be integrated into electrically driven systems. At the same time, there is a lack of understanding of color center electroluminescence in both steady-state and transient regimes. In spite of significant research efforts, the physics behind this process is still a puzzle.

In this work, we introduce a physical model to address single-photon emission dynamics of electrically pumped NV centers in diamond. Using the developed theoretical framework [1,2], we perform finite difference optoelectronic simulations of the single-photon emitting diode (Fig. 1a) and reproduce recently measured [3] second-order autocorrelation functions $g^{(2)}(\tau)$. Our theoretical findings are in remarkable agreement with the experimental results (Fig. 1b,c), which illustrates the accuracy of the proposed model, which can be readily extended to various color centers in diamond and related materials. We also demonstrate that the dynamics of single-photon emission is governed by the electron and hole capture processes, which are typically significantly slower than the transitions among excited, ground and shelving states of the NV center. Remarkable is that the emission dynamics is determined by the fastest process between the hole capture and electron capture processes. This allows one to observe fast dynamics even at relatively low photon emission rates. To conclude, our findings provide new insights into the photophysics of color centers in electrically driven systems, which can be used in the design of practical single-photon sources.

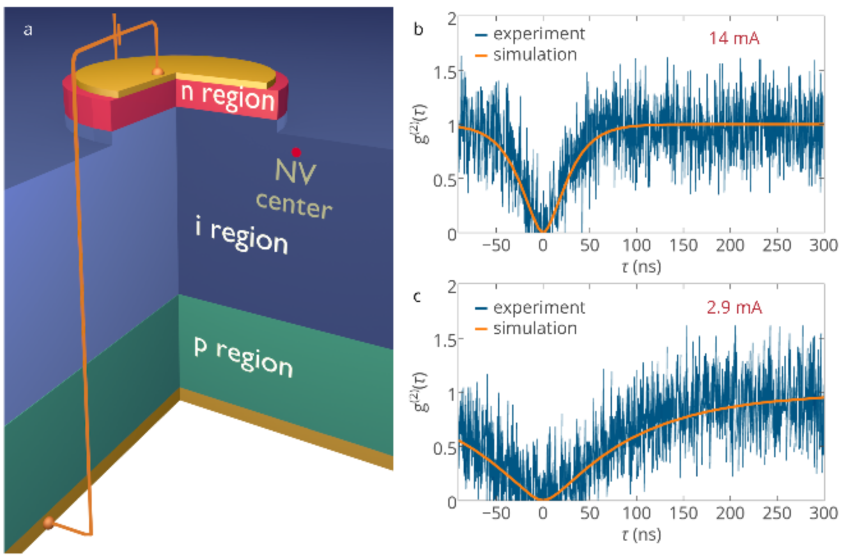

Fig. 1. (a) Schematic view of the single-photon emitting p-i-n diode with an embedded NV center. (b-c) Background corrected $g^{(2)}$ traces retrieved from the experiment [3] and predicted from the simulations at two different pump currents.

[1] D. Y. Fedyanin and M. Agio, New J. Phys. **18**, 073012 (2016).
[2] I. A. Khramtsov, M. Agio, D. Yu. Fedyanin, (submitted) (2017).
[3] N. Mizuochi et al., Nat. Photonics **6**, 299 (2012).

Symmetric blind information reconciliation protocol

E.O. Kiktenko[1,2], **A.S. Trushechkin**[1,3,4], **C.C.W. Lim**[5], **Y. Kurochkin**[6] **and A. Fedorov**[1,7]
[1] *Steklov Mathematical Institute of Russian Academy of Sciences, Moscow 119991, Russia*
[2] *Bauman Moscow State Technical University, Moscow 105005, Russia*
[3] *National Research Nuclear University MEPhI, Moscow 115409, Russia*
[4] *Department of Mathematics and Russian Quantum Center, National University of Science and Technology MISiS, Moscow 119049, Russia*
[5] *Quantum Information Science Group, Computational Sciences and Engineering Division, Oak Ridge National Laboratory, Oak Ridge, Tennessee 37831-6418, USA*
[5] *Russian Quantum Center, 100 Novaya St., Skolkovo, Moscow 143025, Russia*
[6] *LPTMS, CNRS, Univ. Paris-Sud, Universite Paris-Saclay, Orsay 91405, France*
e-mail: *e.kiktenko@rqc.ru*

Quantum key distribution (QKD) is a quantum-proof key exchange scheme which is fast approaching the communication industry. An essential component in QKD classical post-processing [1] is the information reconciliation step, which is used for correcting the quantum channel noise errors.

We have proposed an approach which significantly improves the blind information reconciliation technique [2]—the most progressive low-density parity-check (LDPC) codes [3, 4]-based method for information reconciliation in the QKD systems. The gain comes from employing information from unsuccessful decodings and making the whole information reconciliation process in a symmetric form [5].

Specifically, we have proposed to disclose a number of bits with the positions corresponding to maximal uncertainty of the values upon finishing of decoding procedure rather than certain bits in the punctured positions.

The proposed method guarantees syndrome decoding and ensures a lower level of information leakage. Using practical QKD parameters and short length LDPC codes [6], we show that our method gives an average of 10% improvement in the efficiency and an average of 30% improvement in the information requests number.

The ability of symmetric blind reconciliation to obtain rather low values of efficiency with short-length codes is expected to realize an efficient throughput with hardware implemented syndrome decoding.

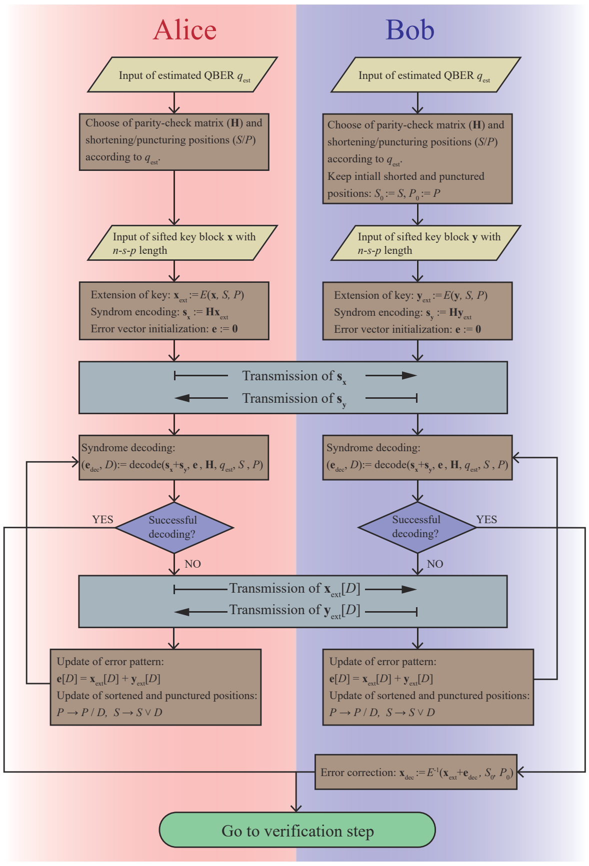

Figure 1: Block scheme of the symmetric blind reconciliation procedure workflow.

[1] E.O. Kiktenko, A.S. Trushechkin, Y.V. Kurochkin, A.K. Fedorov, J. Phys. Conf. Ser. **741**, 012081 (2016).

[2] J. Martínez-Mateo, D. Elkouss, and V. Martin, Quant. Inf. Comp. **12**, 791-812 (2012)

[3] R. Gallager, IRE Trans. Inf. Theory **8**, 21 (1962).

[4] D.J.C. MacKay, IEEE Trans. Inf. Theory **45**, 399 (1999).

[5] E.O. Kiktenko, A.S. Trushechkin, C.C.W. Lim, Y.V. Kurochkin, A.K. Fedorov, arXiv:1612.03673 [quant-ph].

[6] IEEE Standard for Information Technology, 802.11n-2009.

High Precision Metrology from the Fisher Information of a Hong-Ou-Mandel Interferometer

Ashley Lyons[1], ***George C. Knee***[2], *Eliot Bolduc*[1], *Thomas Roger*[1], *Jonathan Leach*[1], *Erik M. Gauger*[1], *and Daniele Faccio*[1]

1. *Institute of Photonics and Quantum Sciences, Heriot-Watt University, Edinburgh, UK, EH14 4AS*
2. *Department of Physics, University of Warwick, Coventry, UK, CV4 7AL*

Sensing devices that exploit the quantum nature of light hold the promise of enjoying greater precision than is possibly classically – but there often remains a significant gap between theory and experiment, which delays the advent of quantum technologies. Further, while much work theoretical work underpins the importance of entanglement and squeezing, multi-particle interference is a phenomenon altogether less well understood insofar as it applies to metrology. We investigated the use of a Hong-Ou-Mandel (HOM) interferometer (where two photons incident on separate inputs of a beam splitter will bunch at a rate which depends on their distinguishability [1]) for the purposes of estimating path length increases or optical delays. Such delays might be induced by birefringent or non-birefringent samples of some unknown thickness or refractive index, or by an optical element mounted on a sample at an unknown displacement.

Theoretical analysis employing the (quantum) Fisher information metric reveals that the optimum sensitivity of a HOM interferometer is not where one might expect: instead of being at the very bottom of the characteristic HOM 'dip' (where the two photons are most indistinguishable) it is displaced by a predictable amount. We confirmed this feature experimentally, successfully predicting the precision of the interferometer for a range of visibilities and sample displacements introduced by a piezo actuator.

Furthermore, tuning the interferometer to operate near the optimal point (with a coarse-grained stage) allowed maximum likelihood estimation to extract estimates of the displacement to less than 5 nm uncertainty, at least an order of magnitude improvement over previous efforts (which used repeated scanning of the dip to construct estimates [1,2,3,4]). The precision we achieved was possible by using detectors with a time resolution far worse than that needed to resolve the optical delay caused by the sample, since the HOM effect implies that only the relative number of bunching events at the output of the beam splitter is sufficiently sensitive to the delay. Moreover, the interferometer is (to first order) phase insensitive, negating the need for stabilisation that a traditional single photon (Mach-Zehnder) interferometer would demand. We believe our results suggest that the HOM interferometer holds great promise for a stable, accurate, precise and reliable tool for measuring optical delays that could find a great many applications in materials analysis, medical science and other sectors.

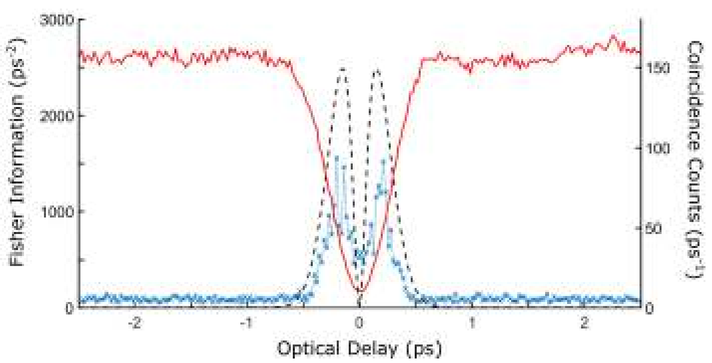

Fig. 1 (Red) Measured Hong-Ou-Mandel dip. (Blue) The inverse variance of a large sample of estimates for the optical delay. (Black) Fisher information theoretically predicted from the extracted parameters of the HOM dip.

References

[1] C. K. Hong, Z. Y. Ou, and L. Mandel, "Measurement of subpicosecond time intervals between two photons by interference," Phys. Rev. Lett. **59**, 2044 (1987)

[2] D. Giovanni, J. Romero, V. Potoček, G. Ferenczi, F. Speirits, S. M. Barnett, D. Faccio, and M. J. Padgett, " Spatially structured photons that travel in free space slower than the speed of light," Science, **347**, 857 (2015)

[3] E. Dauler, G. Jaeger, A. Muller, and A. Midgall, " Tests of a Two-Photon Technique for Measuring Polarization Mode Dispersion With Subfemtosecond Precision," J. Res. Natl. Inst. Stand. Technol. **104**, 1 (2000)

[4] D. Branning, A. L. Midgall, and A. V. Sergienko, " Simultaneous measurement of group and phase delay between two photons," Phys. Rev. A. **62**, 63808 (2000)

Entropy source evaluation of a vacuum fluctuation based quantum random number generator

Arne Kordts[1*], Dino S. Nikolic[1], Tobias Gehring[1], Ulrik L. Andersen[1]

1. Technical University of Denmark(DTU), 2800 Kgs-Lyngby, Denmark

[*] *arnek@fysik.dtu.dk*

Quantum random number generators [1] (QRNGs) offer genuine randomness for cryptographic solutions with unconditional security based on our current understanding of nature alone. The security of each QRNG implementation is based on the strength of assumptions, which have to be made about the used measurement protocol. The most rigorous and secure approach hereby are so called device-independent protocols [2], based on Bell-test like measurements, but these are still limited to low generation rates. By including assumptions about device performance higher generation rates can be achieved. So far, the performance of such devices was most commonly verified by running a battery of statistical tests, like those used for the evaluation of deterministic software-based pseudo random number generators (PRNG), on the generated output. The security of these device-dependent implementations depend on an accurate discrimination between the classical and quantum contribution of a recorded signal [3], as it was done for phase-diffusion QRNG [4].

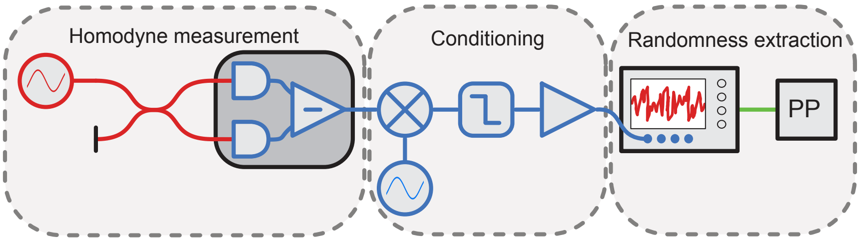

Fig. 1. Vacuum fluctuation QRNG scheme. A shot-noise limited homodyne detection of the vacuum is performed. Part of the detector output is selected by down-mixing and conditioning the signal onto the analog to-digital converter range. Random extraction is performed by post-processing (PP) the raw-data using Toeplitz-hashing.

Here we present such an accurate assessment for an entropy source of a vacuum fluctuation based QRNG setup [5], see Figure 1. The strength of this approach lies in the fact that the vacuum is intrinsically pure. By characterizing all device components we perform an effective quantitative measurement of the vacuum fluctuation power spectral density equal to $\hbar\omega$. Further, in previous implementations the classical noise contribution, introduced by the device components, were assumed to be uncorrelated, here we characterize and consider these in the conservative estimation of the minimal extractable entropy. Random number extraction was implemented on a FPGA board using Toeplitz-hashing. The current work contributes towards a security evaluation standard of high generation-rate device-dependent QRNG implementations.

References

1. Herrero-Collantes, M., Garcia-Escartin, J. C. (2017). Quantum random number generators. Reviews of Modern Physics, 89(1), 15004.
2. Acin, A., Masanes, L. (2016). Certified randomness in quantum physics. Nature, 540(7632), 213219.
3. Hart, J. D., Terashima, Y., Uchida, A., Murphy, T. E., Roy, R. (2016). Commentary: Evaluating photonic random number generators. http://arxiv.org/abs/1612.04415
4. Mitchell, M. W., Abellan, C., Amaya, W. (2015). Strong experimental guarantees in ultrafast quantum random number generation. Physical Review A - Atomic, Molecular, and Optical Physics, 91(1), 110.
5. Gabriel, C., Wittmann, C., Sych, D., Dong, R., Mauerer, W., Andersen, U. L., Marquardt, C., Leuchs, Gerd Leuchs, G. (2010). A generator for unique quantum random numbers based on vacuum states. Nature Photonics, 4(10), 711715.

Quantum-statistical properties of the quantized cavity field interacting with pair of three-level atoms

V I Koroli, S Palistrant and A Nistreanu
Institute of Applied Physics, Academy of Sciences of Moldova, MD-2028, Moldova
E-mail: vl.koroli@gmail.com

We study interaction between the single-mode cavity field and atomic pair, consisting from λ - type three-level atoms. In present model three-level atoms are supposed to be indistinguishable and localized in optical cavity in the ground vibrational state, in which vibrational quantum number $\langle n_v \rangle = 0$ [1].

It is noticed that three-level atoms are localized in given position of the standing wave of cavity. Based on modern optical achievements it is possible to localize a small number of emitters (atoms, ions, molecules) in various geometrical systems like optical cavities, quantum dots, optical lattices and dielectric or disordered media.

In proposed model at initial moment $t = 0$ quantized cavity field is supposed to be in Holstein-Primakoff coherent state $|\xi\rangle$. By using exact analytical solution for state-vector of the coupled atom-field system found with the help of Schrodinger equation quantum-statistical properties of the quantized cavity field are examined as a function of the parameter $|\xi|$. Atomic population inversion, mean photon number and their fluctuations are investigated for different values of $|\xi|$ parameter and initial atomic excitations. Much attention is devoted to the squeezing properties of the quantized cavity field [3]. In this situation higher-order squeezing of cavity field has the tendency towards oscillations, but exact periodicity of these oscillations is violated by the analogy with the micromaser model [2] and squeezing in JCM of a pair of two-level atoms [3].

References

[1] F. Diedrich, J. C. Bergquist, W. M. Itano and D. J. Wineland *Phys. Rev. Lett.* **62** 403 (1989)

[2] V. I. Koroli, *Cooperative interaction of photons and phonons with radiation centers*, *Quantum Optics*, 128 pages (Saarbrucken: LAP, LAMBERT Academic Publishing, 2013)

[3] N. A. Enaki, V. I. Koroli, S. Bazgan, A. Nistreanu and C. H. Raymond Ooi Indian J. Phys. **89** 883 (2015)

Noisy evolution of coherent states in a lossy Kerr medium

Ludwig Kunz,[1, 2, *] Matteo G. A. Paris,[3] and Konrad Banaszek[1, 2]
[1] *Centre of New Technologies, University of Warsaw, Banacha 2c, 02-097 Warszawa, Poland*
[2] *Faculty of Physics, University of Warsaw, Pasteura 5, 02-093 Warszawa, Poland*
[3] *Dipartimento di Fisica, Università degli Studi di Milano, via Celoria 16, I-20133 Milano, Italy*

Squeezing [1] and Schrödinger cat states [2] are striking manifestations of the quantum theory of light. These features can be generated using optical nonlinearities such as Kerr self phase modulation, but attention needs to be paid to suppress noise and decoherence that may mask nonclassical phenomena. The purpose of this work is to discuss the evolution of an initially coherent state in a Kerr medium with distributed loss. We provide a simple picture describing the excess noise generated by the two concurrent processes and analyse its effect on squeezing and information transfer.

The system is described by the Master equation of a damped nonlinear oscillator

$$\frac{d\hat{\varrho}}{dt} = -i\mu[\hat{n}^2, \hat{\varrho}(t)] + \frac{\gamma}{2}\left(2\hat{a}\hat{\varrho}(t)\hat{a}^\dagger - \hat{n}\hat{\varrho}(t) - \hat{\varrho}(t)\hat{n}\right), \quad (1)$$

with the creation (annihilation) operator $\hat{a}^\dagger$ $(\hat{a})$, $\hat{n} = \hat{a}^\dagger\hat{a}$, the nonlinearity strength μ and the linear loss parameter γ. For the following, it will be convenient to use the transmission $\eta = e^{-\gamma t}$ and the ratio $\varkappa = \mu/\gamma$ to characterise the evolution. In order to separate the phenomena that can be attributed solely to either optical nonlinearity or amplitude damping from the excess noise, the interaction picture with the nonlinear Hamiltonian $\mu\hat{n}^2$ is used. Assuming that the system is initially in a coherent state $|\alpha\rangle$ the solution for the density operator $\hat{\varrho}(t) = \exp(-i\mu t\hat{n}^2)\hat{\varrho}'(t)\exp(-i\mu t\hat{n}^2)$ can be determined to take the form [3]

$$\varrho'_{mn}(t) = \langle m|\sqrt{\eta}\alpha\rangle\langle\sqrt{\eta}\alpha|n\rangle e^{-|\alpha|^2\zeta(\eta,(m-n)\varkappa)}. \quad (2)$$

The excess noise is given by the exponential factor which involves the complex-valued function

$$\zeta(\eta,\varkappa) = 1 - \eta + \frac{\eta^{2i\varkappa+1} - 1}{2i\varkappa + 1}. \quad (3)$$

An intuitive picture of this evolution can be derived by approximating ζ with a power series in $\varkappa$ up the second order. This approximation for the density matrix elements is valid for a broad range of parameters of the system with a fidelity of over 99%, e.g. for any $|\alpha|^2 \geq 30$ and $\varkappa \leq 1$. It is straightforward to verify that the result of the approximation is equivalent to a phase diffused state with a Gaussian profile, which width can be identified as $\sigma = 2\varkappa|\alpha|\sqrt{2 - \eta - \eta(1 - \log\eta)^2}$. The overall evolution in the interaction picture can be described by

$$|\alpha\rangle\langle\alpha| \to \int_{-\infty}^{\infty} \mathrm{d}\varphi \exp\left[-\frac{(\varphi-\varphi_0)^2}{2\sigma^2}\right] |e^{i\varphi}\sqrt{\eta}\alpha\rangle\langle e^{i\varphi}\sqrt{\eta}\alpha| \quad (4)$$

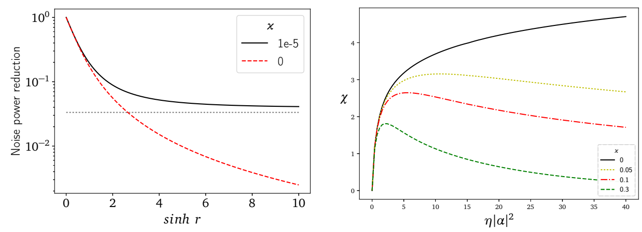

FIG. 1. Left panel: Noise power reduction for a Kerr medium with 90% transmission dependend on the squeezing parameter $\sinh r = 2\mu t\eta|\alpha|^2$. Right panel: Holevo quantity χ for an optical channel with 50% transmission as a function of the output power $\eta|\alpha|^2$ and increasing nonlinearity.

with a phase shift of $\varphi_0 = -2\varkappa|\alpha|^2(1 - \eta + \eta\log\eta)$. This demonstrates that the excess noise can be described with a high accuracy as plain phase noise, characterized by a Gaussian profile, combined with an additional phase shift. The excess noise limits the amount of squeezing that is attainable when generated in a Kerr medium. The left panel of Fig. 1 shows that the power noise reduction in a Kerr medium is severely limited for higher degrees of squeezing by the excess phase noise. Its minimum value can be estimated using the phase diffusion model to be equal to $(1-\eta)/3$. In classsical communication, the excess noise also affects the amount of information that can be transmitted over an optical channel with Kerr nonlinearity. We found that when classical information is encoded in a continuous ensemble of coherent states with a fixed mean photon number, the channel nonlinearity effectively limits the accessible information. The right panel of Fig. 1 shows the Holevo quantity χ for this communication scenario, which is seen to decrease for high powers in contrast to the linear scenario.

We have shown that excess noise in a Kerr medium with distributed losses can simply be described as a phase shift and phase noise with a Gaussian profile acting on an initially coherent state. The additional decoherence introduced by the excess noise limits the degree of attainable squeezing and the amount of information that can be transmitted in an optical communication channel.

* l.kunz@cent.uw.edu.pl

[1] U. L. Andersen, T. Gehring, C. Marquardt, G. Leuchs, Physica Scripta **91**, 5 (2016).
[2] V. Bužek and P. L. Knight, Prog. Opt. **34**, 1 (1995).
[3] M. G. A. Paris, J. Opt. B **1**, 662 (1999).

Active beam-splitting attack for coherent QKD protocols

D.A. Kronberg[1,2], E.O. Kiktenko[3], A.K. Fedorov[4,5] and Y.V. Kurochkin[4]

[1]*Steklov Mathematical Institute of Russian Academy of Sciences, Moscow 119991, Russia*
[2]*Faculty of Computational Mathematics and Cybernetics, Moscow State University, Moscow 119899, Russia*
[3]*Bauman Moscow State Technical University, Moscow 105005, Russia*
[4]*Russian Quantum Center, Skolkovo, Moscow 143025, Russia*
[5]*LPTMS, CNRS, Univ. Paris-Sud, Universite Paris-Saclay, Orsay 91405, France*

We consider a new type of attack on a class of coherent quantum key distribution (QKD) protocols: coherent one-way (COW) protocol [1] and other coherent protocols. We calculate the optimum values of the attack parameters for an arbitrary length of a channel length, compare the results with the standard beam-splitting attack, and provide a new distance limit and detector noise criteria for the COW protocol.

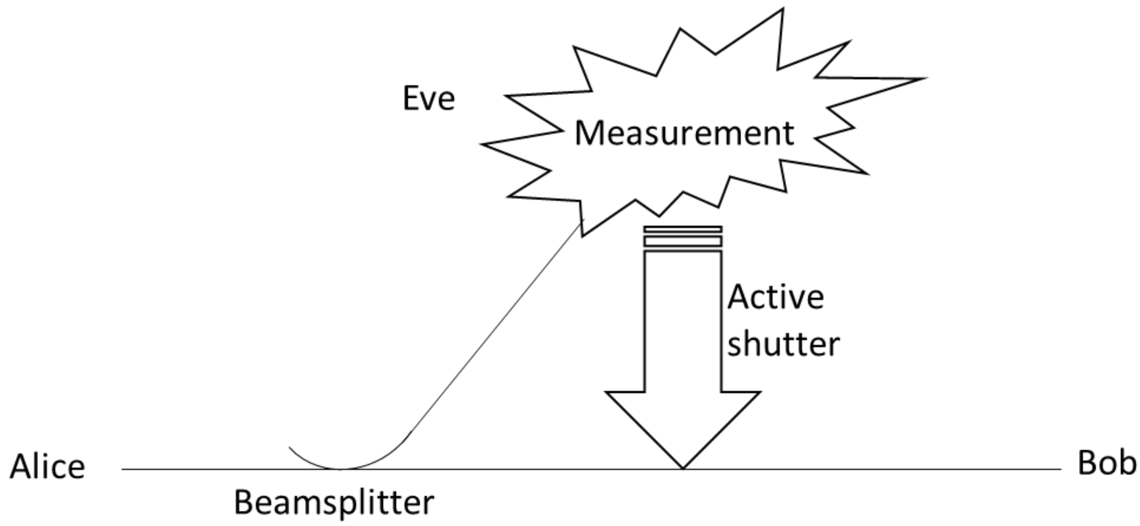

Figure 1. Scheme of the proposed attack.

The key idea of the proposed attack is using of individual measurements of intercepted states on one side of the beamsplitter and transfer of the other part in an unmodified form. In the case of the conclusive result, Eve has a copy of the state. In the case of the inconclusive results of measurements (i.e., no single photon detector clicks received), Eve is able to block state on the way to Bob using active shutter [2]. The suggested attack belongs to the first class (attacks on the protocol). One of its advantages is the fact that realization of this attack does not require using of the quantum memory or sophisticated elements, but it is limited to a common assumption that an eavesdropper has a channel without losses. Finally, the suggested attack has rather simple optical scheme for its realization, allowing one to gain an advantage in comparison with the known beam-splitting attack under certain restrictions on the parameters of a key distribution system.

We acknowledge financial support from Ministry of Education and Science of the Russian Federation (Agreement 14.582.21.0009, ID RFMEFI58215X0009).

[1] D. Stucki, N. Brunner, N. Gisin, V. Scarani, and H. Zbinden, Appl. Phys. Lett. 87, 194108 (2005).

[2] D.A. Kronberg, E.O. Kiktenko, A.K. Fedorov, and Y.V. Kurochkin, Quantum Electron. 47, 163 (2017).

Ultrafast electron switching device based on graphene electron waveguide coupler

Wei Huang,[1] Shi-Jun Liang,[1] Elica Kyoseva,[2] and Lay Kee Ang[1]

[1]SUTD-MIT International Design Centre, Singapore University of Technology and Design, 8 Somapah Road, 487372 Singapore
[2]Institute of Solid State Physics, Bulgarian Academy of Sciences, 72 Tsarigradsko Chaussee, 1784 Sofia, Bulgaria

Abstract: We propose an ultrafast electronic switching device based on dual-graphene electron waveguides, which utilizes the principle of coherent quantum tunneling. Based on a modified coupled mode theory, we analyze the device characteristics, and predict that the switching speed is faster than 1 ps and the on-off ratio exceeds 10^6.

1. Design of a graphene electron switch

We design an ultrafast quantum field-effect transistor-like electron switching device consisting of two parallel graphene electron waveguides as shown in Fig. 1. The gate voltages (V_1 and V_2) applied on each waveguide are used to modulate the Schottky barrier height (V_0) and thickness layer (D) between the waveguides. Depending on the Schottky barrier height and the effective gap spacing between the two graphene waveguides, the evanescent wave of the injected electrons in the source waveguide either can tunnel into the drain waveguide (on-state) or either can not (off-state). The phase of the electrons is maintained during the tunneling process, and quantum mechanically, the injected electrons in the source waveguide can be detected at the drain waveguide with a probability equal to 1 at a certain transfer length L.

2. Coupled mode theory for graphene electron waveguides

CMT is revised to describe the coupling between two parallel graphene electron waveguides as shown in Fig. 1. The electrons inside the graphene waveguide channels are described by Dirac equation and Schrödinger equation is used to describe electrons dynamics in the potential barrier (GaAs). When the graphene electron waveguides are closely positioned, electrons can be efficiently coupled. In the y direction, the motion of the electrons in the graphene electron waveguides is described by the 1D free electron Dirac equation, which produce (after manipulations) a Schrödinger-like set of equations,

$$i\frac{d}{dy}\begin{bmatrix} a_{1m} \\ a_{2n} \end{bmatrix} = \begin{bmatrix} 0 & C_{12}e^{iy\Delta} \\ C_{21}e^{-iy\Delta} & 0 \end{bmatrix}\begin{bmatrix} a_{1m} \\ a_{2n} \end{bmatrix} \qquad \text{Eq. (1)}$$

3. Numerical results for the electron propagation

We numerically evolve Eq. 1 with the Schottky barrier height between the graphene and the GaAs set at 500 meV, which is consistent with recent experiments. In general, higher barrier height allows for a lower coupling strength Ω, which leads to a longer coupling length. We assume that the symmetrical wave mode is the initially populated mode in the source graphene waveguide, which can be coherently excited by the high-quality contact between metal electrode and graphene.

Figure 2 shows a demonstration of Rabi oscillations of the electrons probability amplitudes between the two graphene waveguides, in analogy to the dynamics of a two-level quantum mechanical system. The population of the different modes of the graphene waveguides depends on the gate-controlled guiding of the electrons into the source waveguide. If the electron injected into the source graphene waveguide has a wave packet perfectly matched at a certain waveguide eigenstate, only that specific mode will be excited. The figure also demonstrates the electron coupling transfer length L is up to 1000 nm. For the coupling between the first modes in quantum optical waveguides, the coupling length is L = 654 nm with a transfer frequency of $f_T = 1.53 \times 10^{12}\ \mathrm{s}^{-1}$ or 0.65 ps).

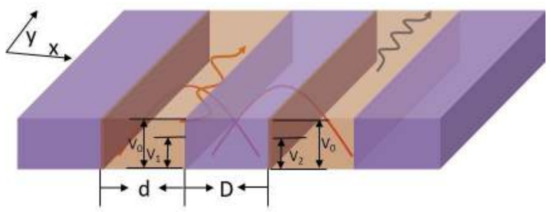

Fig. (1) The scheme of ultra-fast electron switch based on dual graphene electron waveguides and the corresponding energy band structure.

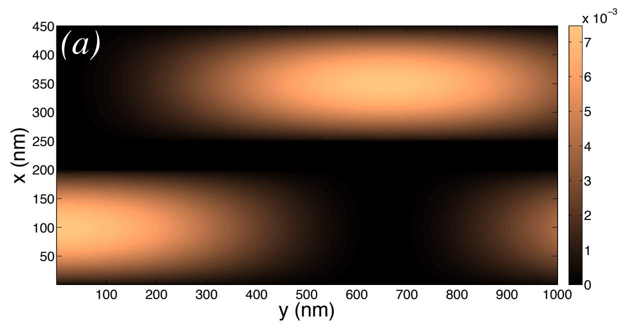

Fig. (2) Electron wavefunction probability for first modes coupling between two graphene waveguides. Like-Rabi oscillations are observed.

These results show that the proposed electron switching device based on graphene electron waveguides has considerable advantages compared to similar devices us- ing the conventional semiconductors materials in terms of operating speed and compactness.

Temporally adjustable polarization entanglement from semiconductor waveguides

K. Laiho[1], B. Pressl[1], A. Schlager[1], T. Günthner[1], H. Suchomel[2],
J. Geßler[2], M. Kamp[2], S. Höfling[2,3], C. Schneider[2] and G. Weihs[1]
[1] *Institut für Experimentalphysik, Universität Innsbruck, Technikerstr. 25, 6020 Innsbruck, Austria*
[2] *Technische Physik, Universität Würzburg, Am Hubland, 97074 Würzburg, Germany*
[3] *School of Physics & Astronomy, University of St Andrews, St Andrews, KY16 9SS, United Kingdom*
kaisa.laiho@uibk.ac.at

Lately, Bragg-reflection waveguides (BRWs) compounded of thin layers of AlGaAs have become compelling emitters of correlated photon pairs. Regarding on-chip quantum optics, sources embedded on semiconductor platforms have the advantage of higher non-linearity and better integrability than the usual non-linear optical materials. The properties of the created photon pairs are determined by the underlying process of parametric down-conversion (PDC). Luckily, the PDC process parameters can easily be extracted from linear transmission measurements and recorded single photon spectra [1].

In comparison to conventional PDC sources BRWs have very low birefringence, which makes them highly attractive for many quantum optics applications. Recently, we have shown that BRWs can produce cross-polarized spectrally indistinguishable photon pairs over tens of nanometers in the telecommunication wavelength range [2]. This is also a requirement for creating polarization entanglement in a simple manner just by splitting the PDC emission at two paths with a dichroic mirror [3,4]. In Fig. 1(a-b) we illustrate the tomographically reconstructed density matrix of our polarization entangled state. Although BRWs work in this scheme even without compensating the relative temporal delay between the created photon pair, our results show an uncompensated phase in the off-diagonal elements of the density matrix, which is caused by the small but non-negligible group index difference between the created photons. We further adjust the coherence of the created states by controlling this relative delay. Fig. 1(c) shows the temporal dependence of the weights of the main off-diagonal elements in the density matrix. Within the time window determined by the spectral band of our photon-pair state we can tune the off-diagonal elements between real and imaginary. To conclude, the phase of the PDC state provides an interesting degree of freedom for engineering the polarization entangled states. Our scheme is easily applicable and can be implemented directly at the PDC source.

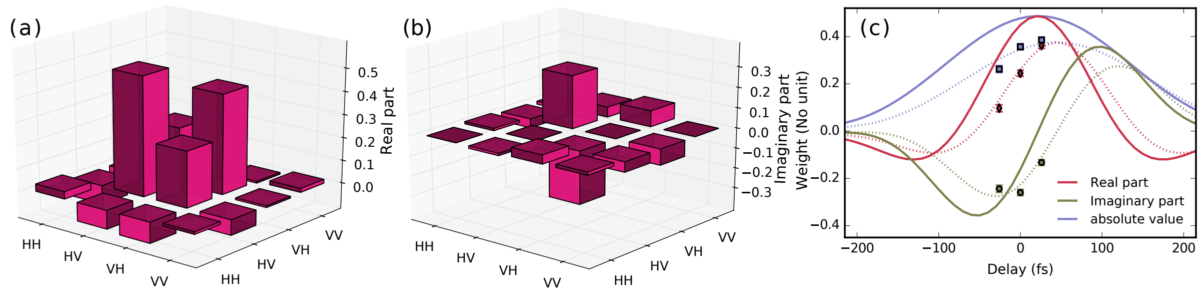

Figure 1: (a) The real and (b) imaginary part of the reconstructed density matrix as well as (c) the temporal dependence of the weights of their main off-diagonal elements together with the theoretical prediction (solid lines) and correction for the experimental imperfections (dashed lines). The measured values for the real and imaginary parts as well as their absolute values are marked with diamonds, circles and squares, respectively.

[1] K. Laiho et al., Uncovering dispersion properties in semiconductor waveguides to study photon-pair generation, Nanotechnology 27, 434003 (2016).
[2] T. Günthner et al., Broadband indistinguishability from bright parametric downconversion in a semiconductor waveguide, J. Opt. 17, 125201 (2015).
[3] R. T. Horn et al., Inherent polarization entanglement generated from a monolithic semiconductor chip, Sci. Rep. 3, 2314 (2013).
[4] A. Schlager et al, Temporally versatile polarization entanglement from Bragg-reflection waveguides, arXiv: 1703.01947 (2017).

Multimode generation of quantum correlated photons with a tunable delay using a crystal

Cyril Laplane, Pierre Jobez, Jean Etesse, Nicolas Gisin and Mikaël Afzelius
Group of Applied Physics, University of Geneva

The ability to generate quantum correlations between photons and excitations in matter is a key resource for quantum repeaters and quantum networks. Photons are ideal carriers of quantum information and matter excitations (eg. spins) can act as long-duration quantum memories to establish heralded entanglement between remote locations. Solid-state devices are gaining interest as potential quantum nodes. These are interesting both from a fundamental point of view and for future large-scale deployment of quantum technologies. A large variety of solid-state systems is currently being investigated, among those single color centers or defects, ensembles of ions and mechanical oscillators.

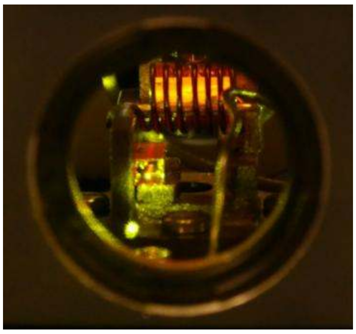

In our work, we investigate ensembles of rare-earth ions doped into crystals (see figure to the right). These have excellent optical properties, and at 4 K or below they can have both long optical and spin coherence times. They also exhibit large inhomogeneous broadening in the optical domain, which can be used for time/frequency multiplexing, provided that the associated inhomogeneous dephasing can be controlled.

We here present an experiment where we can generate quantum correlations between collective spin excitations in a Eu^{3+}:Y_2SiO_5 crystals and single photons at 580 nm, with up to a millisecond quantum storage time of the spin component. The experiment is based on spontaneous Raman scattering generating Stokes photons correlated with spin excitations, as in the DLCZ scheme that is used in laser-cooled gases. It has proven difficult, however, to perform a DLCZ experiment rare-earth crystals, due to the inhomogeneous broadening. To counter this effect we employ inhomogeneous dephasing control on both the optical and the spin transition, using an atomic frequency comb (AFC) and a spin echo sequence, respectively.
In this way, we are also able to produce a stream of time-separated spontaneous Stokes photons, which are time correlated with a corresponding stream of anti-Stokes photons, which demonstrates the multimode capacity of the scheme.

To verify the quantum nature of the correlations we measure both the second-order cross-correlation between the Stokes/anti-Stokes photons (shown below), as well as the second-order auto-correlation of each mode, which violate the Cauchy-Schwarz inequality. This work shows that rare-earth crystals can be used to generate long-lived quantum correlations between spins and single photons, with a unique ability of temporal multiplexing that is important for increasing the speed of future quantum repeaters.

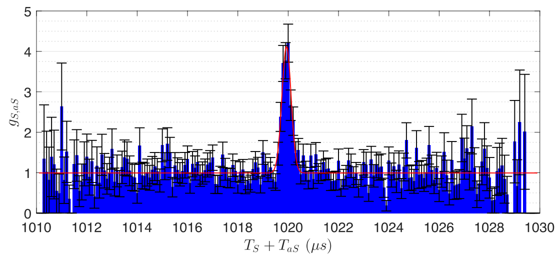

Multipartite nonlocality and random measurements

Anna de Rosier,[1] Jacek Gruca,[1] Fernando Parisio,[2] Tamás Vértesi,[3] and Wiesław Laskowski[1]

[1]*Institute of Theoretical Physics and Astrophysics, University of Gdańsk, Gdańsk, Poland*
[2]*Departamento de Física, Federal University of Pernambuco, Recife, Brazil*
[3]*Institute for Nuclear Research, Hungarian Academy of Sciences, Debrecen, Hungary*

We present an exhaustive numerical analysis of violations of local realism by families of multipartite quantum states. As an indicator of nonclassicality we employ the probability of violation for randomly sampled observables. Surprisingly, it rapidly increases with the number of parties or settings and even for relatively small values local realism is violated for almost all observables. We also present the probability of violation as a witness of genuine multipartite entanglement.

Quantum multiparticle systems do not provide a mere amplification of the nontrivial effects displayed by two-party systems. Rather, they bring about completely new phenomena and applications. On the fundamental level, multipartite systems, e. g., have been employed to illustrate nonlocality without Bell inequalities [1] and, more recently, to show that finite-speed superluminal causal influences would allow for superluminal signalling between spatially separated parties [2]. In what concerns applications, one-way quantum computing [3] and multipartite secret sharing [4] are outstanding examples where complex quantum systems can be employed.

As is the case for multipartite entanglement, the characterization of nonclassical features of multiparticle systems is a hard problem with several open questions [5]. One interesting possibility to analyze the nonclassicality of complex states is to study their correlation properties under random measurements. With this motivation we will be concerned with the following quantity

$$\mathcal{P}_V(\rho) = \int f(\Omega) d\Omega, \tag{1}$$

where the integration variables correspond to all parameters that can be varied within a Bell scenario and, $f = 1$ only for settings that lead to violations in local realism, and vanishes otherwise. Note that, when properly normalized, $\mathcal{P}_V$ can be interpreted as a probability of violation of local realism.

The probability $\mathcal{P}_V$ can be used at different context levels. One can select a particular Bell inequality I and integrate f_I over all possible settings of the corresponding Bell experiment. This was mainly the approach adopted in previous theoretical [6, 7] and experimental [8] works. This is also the case of ref. [9], where the quantity defined in (1) has been considered as a measure of nonlocality and applied in the context of the CGLMP inequality [10, 11]. This procedure, however, would face increasing difficulties as the number of parties grows. For a relatively modest number of qubits, e. g., the corresponding number of inequivalent Bell inequalities with a fixed (say 2) number of settings is already very large and, thus, addressing one inequality at a time would become prohibitive. On a deeper level we can dispense with the choice of a particular inequality and directly consider the space of behaviors (space of joint probabilities), which local polytopes inhabit. In this case, the integration refers to all possible measurements, the only context information required being the number of measurements per party.

In this paper we employed linear programming as a useful tool to analyze the nonclassical properties of quantum states. We checked how many randomly generated sets of observables allow for violation of local realism. It is worth mentioning that the method allows us to reveal nonclassicality even without direct knowledge of Bell inequalities for the given experimental situation. We applied the numerical method to prominent families of quantum states. We calculated the frequencies $\mathcal{P}_V(\rho)$ for an increasing number of different settings per site.

The overall message of the obtained results is that either for many particles or many measurement settings we observe a conflict with local realism for almost any choice of observables ($\mathcal{P}_V(\rho) > 99\%$) for typical families of quantum states.

In addition, we addressed the apparently paradoxical result obtained in [12]. It amounts to the observation, that the products of k-qubit GHZ states and $(N-k)$ pure single qubit states are more nonclassical than the N qubit GHZ state, if we employ the robustness of correlations against white noise admixture as a measure of nonclassicality. Our numerical method shows that $\mathcal{P}_V(\rho)$ for such product states is the same as for k-qubit GHZ state and thus strictly smaller than for the N qubit GHZ state. This suggests that resistance against noise, although relevant, is not a good quantifier of nonclassicality.

We also present the probability of violation $\mathcal{P}_V(\rho)$ as a witness of genuine multipartite entanglement.

[1] D. M. Greenberger, M. A. Horne, and A. Zeilinger, *Bells Theorem, Quantum Theory and Conceptions of the Universe*, edited by M. Kafatos, Vol. 69 (Kluwer Academic, Dordrecht, 1989).
[2] J.-D. Bancal, S. Pironio, A. Acín, Y.-C. Liang, V. Scarani, and N. Gisin, Nature Physics **8**, 867870 (2012).
[3] R. Raussendorf and H. J. Briegel, Phys. Rev. Lett. **86**, 5188 (2001).
[4] Y.-C. Liang, F. J. Curchod, J. Bowles, and N. Gisin, Physical review letters **113**, 130401 (2014).
[5] N. Brunner, D. Cavalcanti, S. Pironio, V. Scarani, and S. Wehner, Rev. Mod. Phys. **86**, 419 (2014).
[6] Y.-C. Liang, N. Harrigan, S. D. Bartlett, and T. Rudolph, Phys. Rev. Lett. **104**, 050401 (2010).
[7] J. J. Wallman, Y.-C. Liang, and S. D. Bartlett, Phys. Rev. A **83**, 022110 (2011).
[8] P. Shadbolt, T. Vértesi, Y.-C. Liang, C. Branciard, N. Brunner, and J. L. O'Brien, Scientific Reports **2** (2012), 10.1038/srep00470.
[9] E. A. Fonseca and F. Parisio, Phys. Rev. A **92**, 030101 (2015).
[10] D. Collins, N. Gisin, N. Linden, S. Massar, and S. Popescu, Phys. Rev. Lett. **88**, 040404 (2002).
[11] A. Acín, T. Durt, N. Gisin, and J. I. Latorre, Phys. Rev. A **65**, 052325 (2002).
[12] W. Laskowski, T. Vértesi, and M. Wieśniak, Journal of Physics A: Mathematical and Theoretical **48**, 465301 (2015).

General bounds for sender-receiver capacities in multipoint quantum communications

Riccardo Laurenza and Stefano Pirandola
Computer Science and York Centre for Quantum Technologies, University of York, York YO10 5GH, UK

Today a huge effort is devoted to the development of robust quantum technologies, inspired by quantum information theory. The most typical communication tasks are quantum key distribution (QKD), reliable transmission of quantum information and distribution of entanglement. The latter allows two parties to implement powerful protocols such as quantum teleportation. Unfortunately, any practical realization of such quantum tasks is affected by decoherence. This is the very reason why the performance of any point-to-point protocol of quantum and private communication, i.e., in the absence of quantum repeaters, suffers from fundamental limitations, which become more severe when the distance is increased.

In this context, an open problem was to find the optimal rates for quantum and private communication that are achievable by two remote parties, say Alice and Bob, assuming the most general strategies allowed by quantum mechanics, i.e., assuming arbitrary local operations (LOs) assisted by unlimited two-way classical communication (CCs), briefly called adaptive LOCCs. These optimal rates are known as two-way (assisted) capacities and their determination has been notoriously difficult. Only recently, after about 20 years [1], Ref. [2] finally addressed this problem and established the two-way capacities at which two remote parties can distribute entanglement (D_2), transmit quantum information (Q_2), and generate secret keys (K) over a number of fundamental quantum channels at both finite and infinite dimension, including erasure channels, dephasing channels, bosonic lossy channels and quantum-limited amplifiers.

For the specific case of a bosonic lossy channel with transmissivity η, Ref. [2] proved that $D_2 = Q_2 = K = -\log_2(1-\eta)$ corresponding to $\simeq 1.44\eta$ bits per channel use at high loss. The latter result completely characterizes the fundamental rate-loss scaling that affects any point-to-point protocol of QKD through a lossy communication line, such as an optical fiber or free-space link. The novel and general methodology that led to these results is based on a suitable combination of quantum teleportation with a LOCC-monotonic functional, such as the relative entropy of entanglement (REE). Thanks to this combination, Ref. [2] was able to upper-bound the two-way capacity $\mathcal{C} = D_2, Q_2, K$ of an arbitrary quantum channel $\mathcal{E}$ with computable single-letter quantities.

The goal of the present paper [3] is to extend such "REE+teleportation" methodology to a more complex communication scenario, in particular that of a single-hop quantum network, where multiple senders and/or receivers are involved. The basic configurations are represented by the quantum broadcast channel where information is broadcast from a single sender to multiple receivers, and the quantum multiple-access channel, where multiple senders communicate with a single receiver. More generally, we also consider the combination of these two cases, where many senders communicate with many receivers in a sort of all-in-all quantum communication or quantum interference channel. In practical implementations, this may represent a quantum bus where quantum information is transmitted among an arbitrary number of qubit registers.

In all these multipoint scenarios, we characterize the most general protocols for entanglement distillation, quantum communication and key generation, assisted by adaptive LOCCs. This leads to the definition of the two-way capacities $\mathcal{C} = D_2, Q_2, K$ between any pair of sender and receiver. We then consider those quantum channels (for broadcasting, multiple-accessing, and all-in-all communication) which are teleportation-covariant. For these channels, we can completely reduce an adaptive protocol into a block form involving a tensor product of Choi matrices. Combining this reduction with the REE, we then bound their two-way capacities by means of the REE of their Choi matrix, therefore extending previous methods [2] to multipoint quantum/private communication.

Our upper bounds applies to both discrete-variable (DV) and continuous-variable (CV) channels. As an example, we consider the specific case of a 1-to-M thermal-loss broadcast channel through a sequence of beamsplitters subject to thermal noise. In particular, we discuss how that the two-way capacities Q_2, D_2 and K between the sender and each receiver are all bounded by the first point-to-point channel in the "multisplitter". This bottleneck result can be extended to other Gaussian broadcast channels. In the specific case of a lossy broadcast channel (without thermal noise), we find a straighforward extension of the fundamental rate-loss scaling, so that any sender-receiver capacity is bounded by $-\log_2(1-\eta)$ with η being the transmissivity of the first beamsplitter.

[1] C. H. Bennett, D. P. DiVincenzo, and J. A. Smolin, Phys. Rev. Lett. **78**, 3217-3220 (1997).
[2] S. Pirandola, R. Laurenza, C. Ottaviani, and L. Banchi, "Fundamental Limits of Repeaterless Quantum Communications," Preprint arXiv:1510.08863 (2015). In press on Nature Communications.
[3] R. Laurenza and S. Pirandola, Preprint arXiv 1603.07262 (2016).

SINGLE-PASS GENERETION OF A DUAL-RAIL CLUSTER STATE

Luca La Volpe[1], **Syamsundar De**[1], **Valentina Parigi**[1], **Claude Fabre**[1] **and Nicolas Treps**[1]

[1] *Laboratoire Kastler Brossel, UPMC-Sorbonne Universités, CNRS, ENS-PSL Research University, Collège de France, 75005 Paris, France*

luca.la-volpe@lkb.upmc.fr

A multimode squeezed state of light can be used as a quantum network in order to accomplish measurement based quantum computing[1] using a continuous variable (CV) approach[2]. Our group has already demonstrated the generation of such quantum state using a synchronously pumped optical parametric oscillator (SPOPO)[3]. Here we present a new quantum source able to produce a multimode squeezed state of light in a single pass configuration as shown in figure 1.

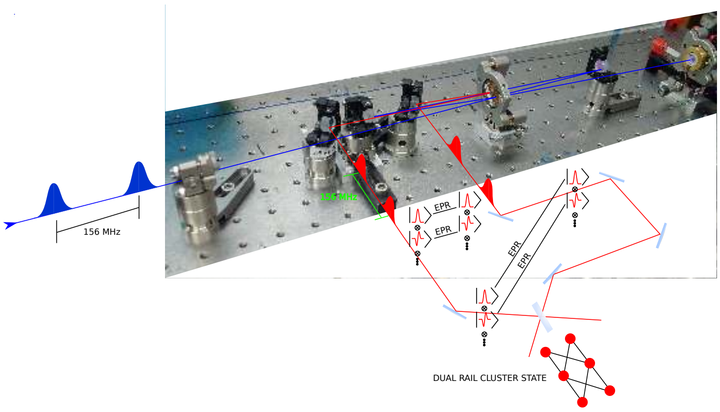

FIGURE 1 : A Ti :Sapphire laser produces a frequency comb centered around 795nm with a full-width-half-maximum (FWHM) of 45nm, these pulses are frequency doubled and all the teeth of the resulting 6nm FWHM frequency comb resonates in an optical cavity with a free spectral range that exactly matches the repetition rate of the laser. A 900μm BBO crystal is positioned where the linear cavity has its waist and is slightly tilted in order to maximize the phase-matching for a non-collinear downconversion.

The source is based on a non-collinear type I parametric downconversion process pumped by a frequency comb. Each pair of pulses produced by this source is predicted to be a quantum state with multipartite entanglement in the frequency domain because of the non-collinear configuration. Furthermore, there is mode basis that diagonalize the interaction Hamiltonian in which each mode is found to be independently squeezed along the phase or the amplitude quadrature. Our theoretical analysis shows that, in this basis, spatial and temporal modes cannot be treated separately.

Exploiting the presence of two separated beams, this source is able to entangle the squeezed supermodes in the time domain. By delaying one of the two multimode pulse by an interpulse delay and combining it with the second pulse on a beam splitter, entanglement between the different time bins can be produced. Since the downconversion process already provides multipartite entanglement between the signal and idler pulses the final quantum state will exhibit entanglement in both time and frequency components. The geometrical structure of the cluster state in the time domain corresponds to a dual rail CV cluster state where the squeezed qumodes exhibit entanglement in time as reported in [4].

[1] R. Raussendorf, H. J. Briegel, *Phys. Rev. Lett.*, 86(22), 5188, (2001).

[2] N. C. Menicucci, P. van Loock, M. Gu, C. Weedbrook, T. C. Ralph, M. A. Nielsen, *Phys. Rev. Lett.*, 97(11), 110501, (2006).

[3] J. Roslund, R. M. de Araújo, S. Jiang, C. Fabre, and N. Treps, *Nature Photonics*, 8, 109112 (2014).

[4] J. Yoshikawa, S. Yokoyama, T. Kaji, C. Sornphiphatphong, Y. Shiozawa, K. Makino and A. Furusawa, *APL Photonics*, 1, 060801 (2016).

A Noiseless Quantum Optical Memory at Room Temperature

P. M. Ledingham[1], K. T. Kaczmarek[1], B. Brecht[1], A. Feizpour[1], G. S. Thekkadath[2], S. E. Thomas[1,3], J. H. D. Munns[1,3], D. J. Saunders[1], J. Nunn[1], I. A. Walmsley[1]

1. Clarendon Laboratory, University of Oxford, Parks Road, Oxford OX1 3PU, UK.

2. National Research Council of Canada, Ottawa, Canada.

3. QOLS, Blackett Laboratory, Imperial College London, London SW7 2BW, UK.

A quantum optical memory (QM) is a device that can store and release quantum states of light on demand. Such a device is capable of synchronising probabilistic events, for example, locally synchronising non-deterministic photon sources for the generation of multi-photon states, or successful quantum gate operations within a quantum computational architecture [1], as well as for globally synchronising the generation of entanglement over long distances within the context of a quantum repeater [2]. Desirable attributes for a QM to be useful for these computational and communicational tasks include high end-to-end transmission (including storage and retrieval efficiency), large storage-time-bandwidth product, room temperature operation for scalability and, of utmost importance, noise free performance for true quantum operation.

Impressive realisations of QMs have materialised based on optical transitions in atomic systems [3-7]. However, several issues remain that prevent these devices from being used within large-scale networks. These include: elaborate cold atom [3,4] or cryogenic [5] experimental setups, complex preparation of the atomic system [5], additional loss through filtering required for noise suppression, and noise photons being induced in the same frequency, spatial or temporal mode as the output thus reducing the quality of the QM readout [3-7].

Here we present a new QM protocol that addresses the above issues, the quantum ladder memory (QLAD). This protocol is based on a two-photon 'ladder' transition between the $6S_{1/2}$ ground state and $6D_{5/2}$ excited state of a caesium (Cs) ensemble at room temperature (see Fig. 1a). We characterise the memory with weak coherent states, storing GHz-band pulses with η=22% storage and retrieval efficiency and a characteristic storage time of τ=5.3ns. We measure the noise at the output to be 8×10^{-6} photons per pulse, giving rise to a noise-to-efficiency ratio of 3.6×10^{-5}, three orders of magnitude better than any memory to date. We generate GHz-band heralded single photons from a spontaneous parametric down conversion source that are matched to the QLAD, coincidence traces seen in Fig. 1b. A heralded second-order autocorrelation function of $g^{(2)}$=0.02±0.005 is measured for the input photon, and true quantum operation is confirmed by storing and retrieving this photon with $g^{(2)}$=0.03±0.01 for a 3.5ns storage time. This result is the lowest $g^{(2)}$ on the output of an on-demand memory to date, and represents a significant step toward large-scale quantum technologies.

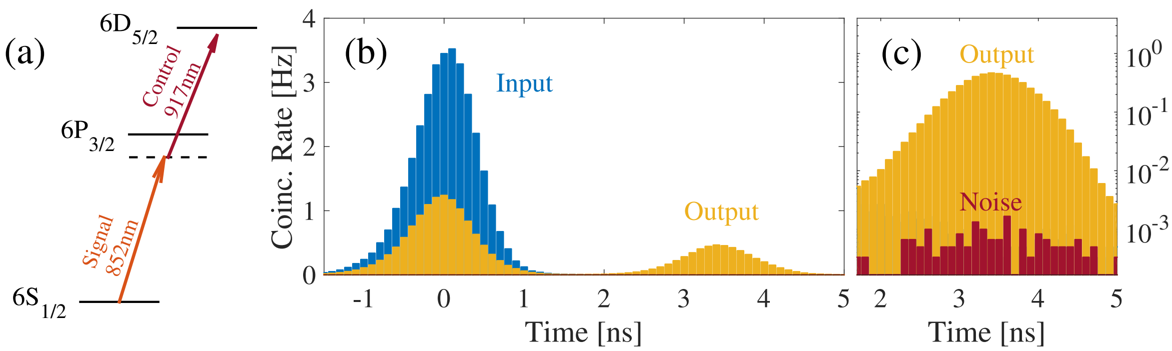

Fig. 1 (a) QLAD protocol in Cs level structure. **(b)** Coincidence histogram of storage and retrieval of heralded single photons. The blue (yellow) histogram represents the memory off (on), labelled Input (Output). **(c)** Log scale with Output and Noise (dark red histogram).

[1] J. Nunn, N. K. Langford, W. S. Kolthammer, T. F. M. Champion, M. R. Sprague, P. S. Michelberger, X.-M. Jin, D. G. England, and I. A. Walmsley "Enhancing Multiphoton Rates with Quantum Memories," Phys. Rev. Lett. **110**, 133601 (2013).
[2] N. Sangouard, C. Simon, H. de Riedmatten, and N. Gisin "Quantum repeaters based on atomic ensembles and linear optics," Rev. Mod. Phys. **83**, 33 (2011)
[3] T. Chanelière, D. N. Matsukevich, S. D. Jenkins, S.-Y. Lan, T. A. B. Kennedy, and A. Kuzmich "Storage and retrieval of single photons transmitted between remote quantum memories," Nature **438**, 833 (2005)
[4] D.-S. Ding, W. Zhang, Z.-Y. Zhou, S. Shi, G.-Y. Xiang, X.-S. Wang, Y.-K. Jiang, B.-S. Shi, and G.-C. Guo "Quantum Storage of Orbital Angular Momentum Entanglement in an Atomic Ensemble," Phys. Rev. Lett. **114**, 050502 (2015)
[5] M. Gündoğan, P. M. Ledingham, K. Kutluer, M. Mazzera, and H. de Riedmatten "Solid State Spin-Wave Quantum Memory for Time-Bin Qubits," Phys. Rev. Lett. **114**, 230501 (2015)
[6] D. G. England, K. A. G. Fisher, J.-P. W. MacLean, P. J. Bustard, R. Lausten, K. J. Resch, and B. J. Sussman "Storage and Retrieval of THz-Bandwidth Single Photons Using a Room-Temperature Diamond Quantum Memory," Phys. Rev. Lett. **114**, 053602 (2015).
[7] M. D. Eisaman, A. André, F. Massou, M. Fleischhauer, A. S. Zibrov, and M. D. Lukin "Electromagnetically induced transparency with tunable single-photon pulses," Nature **438**, 837 (2005)

Quantum state engineering in the near infrared thanks to highly efficient single-photon detectors

H. Le Jeannic[1],[*] A. Cavaillès[1], K. Huang[1,2], V. B. Verma[2], F. Marsili[3], M. D. Shaw[3],
S. W. Nam[2], Y. C. Jeong[1], E Wu[4], H. Zeng[4], R. Filip[5], O. Morin[1], and J. Laurat[1]
[1]*Laboratoire Kastler Brossel, UPMC-Sorbonne Universités, CNRS, ENS-PSL Research University, Collège de France, 4 place Jussieu, 75005 Paris, France*
[2]*National Institute of Standards and Technology, 325 Broadway, Boulder, CO 80305, USA*
[3]*Jet Propulsion Laboratory, California Institute of Technology, 4800 Oak Grove Dr., Pasadena, California 91109, USA*
[4]*State Key Laboratory of Precision Spectroscopy, East China Normal University, Shanghai 200062, China and*
[5]*Department of Optics, Palacký University, 17. listopadu 1192/12, 77146 Olomouc, Czech Republic*

The near-infrared wavelength range has been an important playground for a large community in quantum optics. In particular $\lambda = 1064$ nm has been widely used for high-fidelity quantum state engineering due to the availability of narrow-linewidth and ultra-stable lasers as well as of ultralow-loss optical coatings and photodiodes with close-to-unity efficiency. World record squeezing detection, as well as direct applications, such as teleportation or gravitational wave detection, have been demonstrated at this wavelength. However, detecting efficiently single photons in this range has been a long-standing issue. To generate complex quantum states, with further capabilities, it is often necessary to implement multiple heraldings, in particular in the recent in optical hybrid approach to quantum information where discrete- and continuous-variables states, operations, and toolboxes are combined [1][2]. The scalability of generated states is also often linked to the efficiency of the detection of these probabilistic heraldings. While avalanche photodiodes often suffer from limited quantum efficiencies as well as large dark count rates. Recently, the development of superconducting nanowire single photon detectors (SNSPDs) based on tungsten silicide (WSi) enabled to outperform other infrared single-photon detectors, despite great progress with NbN-based devices.

In this paper, we report on the optimization of WSi SNSPD at $\lambda = 1064$ nm operated at a temperature of 1.8K [3]. A system detection efficiency of $93 \pm 3\%$ is achieved with a dark count rate limited to a few counts per second.

As a first application of the interest of these detectors for quantum state engineering, we show the fast heralding of narrowband single photons, based on a 53-MHz bandwidth optical parametric oscillator (OPO) with a close-to-unity escape efficiency. A heralding efficiency (i.e. the probability of finding a single photon in a given spatio-temporal mode per heralding event) greater than 90% and a heralding rate up to 1 MHz are achieved. This leads to an overall spectral brightness of $\sim 0.6 \times 10^4$ photons/(s·mW·MHz), which is an improvement by more than 15 folds relative to our previous realizations [4]. This result makes our system one of the brightest parametric-down conversion sources to date, due to the combination of an intrinsic narrow bandwidth and a high detection efficiency for the heralding path.

We then demonstrate, using the same source and an additional SNSPD to enable two-photon event detection, the generation of highly pure heralded two-photon Fock states at a rate of 200 Hz, the highest so far. By combining these efficient resources to a method based on the minimization of the non-gaussian experimental costs, we demonstrate the experimental realization of large-amplitude even squeezed Schrödinger cat states $\hat{S}(|\alpha\rangle \pm |-\alpha\rangle)$, with $|\alpha\rangle$ a coherent state, and $\hat{S}$ the squeezing operator. A fidelity as high as 80% with a squeezed cat states of mean photon number $|\alpha|^2 \sim 3$ is obtained [5]. Those free propagating cat states exhibits the highest fidelity reported to date, as well as a rate at least 2 orders of magnitude larger than the ones achieved heretofore in experiments usually based on photon subtraction operated on squeezed light or involving three conditioning steps. This makes them therefore suitable as initial resources for subsequent quantum information protocols.

The demonstrated combination of a high escape efficiency OPO and close-to-unity efficiency SNSPDs makes protocols based on multiple heraldings more accessible, opening the path to a variety of new realizations of quantum states as well as of protocols and operations.

[*] hanna.lejeannic@lkb.upmc.fr

[1] P. van Loock, "Optical hybrid approaches to quantum information", Laser and Photonics Review **5**, 167 (2010).
[2] O. Morin *et al.*, "Remote creation of hybrid entanglement between particle-like and wave-like optical qubits", Nature Photon. **8**, 570-574 (2014).
[3] H. Le Jeannic *et al.*, "High-efficiency WSi superconducting nanowire single-photon detectors for quantum state engineering in the near infrared", Opt. Lett. **41**, 005341 (2016).
[4] O. Morin, V. D'Auria, J. Liu, C. Fabre and J. Laurat, "High-fidelity single-photon source based on a type-II optical parametric oscillator", Opt. Lett. **37**, 3738 (2012).
[5] K. Huang *et al.*, "Optical synthesis of large-amplitude squeezed coherent-state superpositions with minimal resources", PRL **115**, 023602 (2015).

Experimental entanglement diagnostics for quantum relays using nonlinear witnesses

Karel Lemr,[1,*] Karol Bartkiewicz,[2,1,†] Antonín Černoch,[3,‡] and Adam Miranowicz[2,1,§]

[1]RCPTM, Joint Laboratory of Optics of Palacký University and Institute of Physics of Academy of Sciences of the Czech Republic, 17. listopadu 12, 771 46 Olomouc, Czech Republic

[2]Faculty of Physics, Adam Mickiewicz University, PL-61-614 Poznań, Poland

[3]Institute of Physics of Academy of Sciences of the Czech Republic, Joint Laboratory of Optics of PU and IP AS CR, 17. listopadu 50A, 772 07 Olomouc, Czech Republic

Quantum relays and entanglement swapping devices represent a key ingredient for long-distance quantum communications. These devices rely on quality entanglement distribution between communicating nods. Fidelity of ongoing entanglement distribution has to be verified on a regular basis to ensure correct operation. In this contribution, I will discuss two experimental protocols for entanglement diagnostics suitable for the geometry of entanglement swapping devices [1, 2]. Both these protocols make use of nonlinear entanglement witnesses and allow to test entanglement properties more efficiently then quantum state tomography.

Experimental implementation – We have constructed an experimental setup as depicted in Fig. 1 that mimics the geometry of an entanglement swapping device. Two pairs of polarization-entangled photons were generated in a BBO crystal cascade. One photon from each pair interacted on a balanced beam splitter basically performing a teleportation. Only local polarization projective measurements were then performed on the other two photons corresponding to measurements on spatially separated end ports of an entanglement swapping device.

Tested protocols – We have tested two protocols for entanglement diagnostics. The first one is based on the "collectibility" proposed by Rudnicki *et al*. [3]. The second protocol is based on Bell nonlocality and fully entangled fraction [4]. Both these protocols were tested on a set of three typical two-qubit quantum states: maximally entangled Bell state, separable pure state and completely mixed state. Further, Werner states were interpolated using mixtures of Bell state and mixed state. Obtained results are in a good agreement with theoretical predictions. There are several differences between the two tested protocols. While the collectibility requires lower number of local measurements, the Bell nonlocality based protocol on the other hand allows to witness all entangled Werner states.

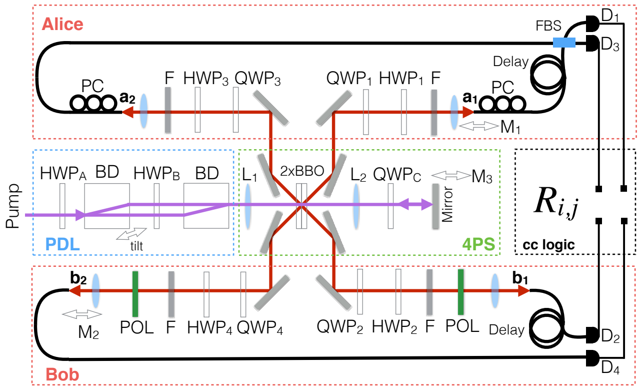

FIG. 1. Schematic drawing of the experimental setup. The components are labeled as follows: M – motorized translation, BBO – nonlinear crystal, HWP – half-wave plate, QWP – quarter-wave plate, PBS – polarizing beam splitter, BD – beam divider, L – lens, P – polarizer, F – interference filter, D – detector.

Acknowledgement — This research is supported by the Czech Science Foundation under the project No. 16-10042Y.

* k.lemr@upol.cz
† bark@amu.edu.pl
‡ acernoch@fzu.cz
§ miran@amu.edu.pl

[1] K. Lemr, K. Bartkiewicz, A. Černoch, Phys. Rev. A **94**, 052334 (2016).
[2] K. Bartkiewicz, K. Lemr, A. Černoch, and A. Miranowicz, Phys. Rev. A **95**, 030102(R) (2017).
[3] Ł. Rudnicki, P. Horodecki, and K. Życzkowski, Phys. Rev. Lett. **107**, 150502 (2011).
[4] K. Bartkiewicz, B. Horst, K. Lemr, and A. Miranowicz, Phys. Rev. A **88**, 052105 (2013).

Quantum enhanced simultaneous measurement of multiple non-commuting observables with SU(1,1) interferometer

Xiaoying Li[1], Yuhong Liu[1], Jiamin Li[1], Nan Huo[1], Z. Y. Ou[2]

1. *College of Precision Instrument and Opto-electronics Engineering, Tianjin University, Key Laboratory of Optoelectronics Information Technology, Ministry of Education, Tianjin, China, 300072,*
2. *Department of Physics, Indiana University-Purdue University Indianapolis, Indianapolis, IN 46202, USA*

Author e-mail address: xiaoyingli@tju.edu.cn

With a comprehensive understanding of quantum concepts, especially quantum entanglement, quantum technologies have been widely applied not only in quantum information and communication, but also in precision measurement for improving the sensitivity beyond what is allowed in classical physics, i.e., the so-called standard quantum limit (SQL) [1]. Sub-shot noise interferometry was the first of such applications utilizing squeezed states [1,2]. So far, most of the studies are concentrated on the phase measurement due to its close relation with precision measurement of a variety of physical quantities such as magnetic field and gravitational field. Because of the Heisenberg uncertainty principle on two non-commuting observables, quantum noise reduction in one observable is inevitably accompanied by the noise increase in the other. By using the squeezed, this noise reduction strategy works fine if we are only interested in measuring one observable. In some applications, on the other hand, different non-commuting observables contain valuable information and need to be measured simultaneously. For example, information about the real and imaginary parts of the linear susceptibility of an optical medium is embedded in the phase and amplitude modulation of a probe optical field passing through the medium. Quantum correlation through entangled quantum states provides us with an approach for simultaneously measuring two non-commuting observables beyond SQL [3]. However, both the schemes of utilizing squeezing and entanglement are based on quantum noise reduction and are in essence similar to the squeezed state interferometry.

Recently, a newly developed SU(1,1) interferometers came into play that are based on different operating principle from the traditional interferometers such as Michelson interferometer [4,5]. The SU(1,1) type interferometer was first proposed by Yurke to have a phase measurement sensitivity approaching the Heisenberg limit. The working principle of the SU(1,1) interferometer for improving the phase measurement sensitivity is fundamentally different from that of squeezed state interferometry. The latter is based on quantum noise reduction whereas the former relies on the noise-free quantum enhancement of the signal with entangled states. Although practical limitation hinders its performance for reaching the Heisenberg limit of phase measurement, it still surpasses the SQL in phase measurement and shows its superiority over the squeezed state interferometry in that it is less sensitive to the losses outside the interferometer such as propagation loss and detection loss [5]. Furthermore, since the working mechanism of the new interferometer is quantum noise cancelation due to destructive quantum interference in an optical parametric amplifier, it applies to all quadrature-phase amplitudes [5,6]. This provides a platform to simultaneously measure all quadrature-phase amplitudes with precision beating SQL.

In this paper, we explore this advantage of the new interferometer for the joint measurement of multiple non-commuting observables such as phase and amplitude as well as arbitrarily rotated quadrature-phase amplitudes. We demonstrate that joint measurement of three non-commuting observables have a sensitivity beating the SQL and approaching Heisenberg limit in the ideal situation. Compared to the joint measurement scheme based on quantum dense coding with Einstein-Podolsky-Rosen (EPR) entangled states in Ref. [3], the current scheme utilizes the merits of the SU(1,1) interferometer and is capable of joint measurement of multiple (more than two) arbitrary non-commuting quadrature-phase amplitudes.

REFERENCES

[1] Caves, "Quantum-mechanical noise in an interferometer," Phys. Rev. D 23, 1693 (1981)
[2] M. Xiao, L. Wu and H. J. Kimble, "Precision measurement beyond the shot-noise limit," Phys. Rev. Lett. 59, 278 (1987).
[3] X. Li, Q. Pan, J. Jing, J. Zhang, C. Xie and K. Peng, "Quantum Dense Coding Exploiting a Bright Einstein-Podolsky-Rosen Beam," Phys. Rev. Lett. 8804790404 (2002).
[4] B. Yurke, S. L. McCall, and J. R. Klauder, \SU(2) and SU(1,1) interferometers," Phys. Rev. A 33, 4033 (1986)..
[5] F. Hudlist, J. Kong, C. Liu, J. Jing, Z. Y. Ou, and W. Zhang, "Quantum metrology with parametric amplifier-based photon correlation interferometers," Nature Comm. 5, 3049 (2014).
[6] X. Guo, X. Li, N. Liu, Z. Y. Ou, "Quantum information tapping using a fiber optical parametric amplifier with noise figure improved by correlated input", Sci. Rep., 6, 30214 (2016)

Spontaneous decay of a two-level system close to a perfectly reflecting sphere

R. P. A. Lima[a], F. N. Lima[b], M. L. Lyra[a]

[a] *GFTC and GISC, Instituto de Física, Universidade Federal de Alagoas, 57072-970, Maceió-AL, Brazil*
[b] *Instituto Federal do Piauí, 64770-000, São Raimundo Nonato-PI, Brazil*

Motivated by experiments showing a pronounced change in the decay rate of atoms trapped in spherical cavities[1], we extend the theoretical model studied by Ford (et al) [2] to the case of an atom placed in the vicinity of a perfectly reflecting spherical surface (see Fig. 1).

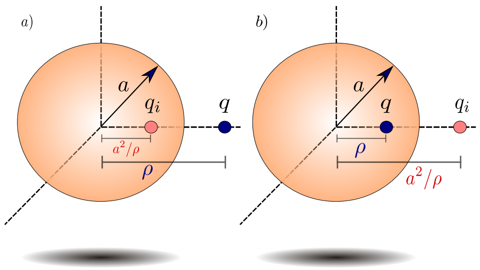

Figure 1: Schematic view of the two-level system (dark blue bullet) and its respective image (clear red bullet) in the vicinity of a perfectly reflecting sphere of radius a. The two-level system is placed at a distance ρ from the center of the sphere. a) Exterior problem; b) Interior problem.

We use a simple theoretical model to investigate the influence of a spherical surface on the spontaneous decay rate process of an excited system. Within a first-order perturbation theory, we provide an analytical expression for the spontaneous decay rate of a two-level monopole coupled to a Hermitian massless scalar field. We demonstrate that both cases of the two-level system placed in the exterior and in the interior of the sphere with a perfectly reflecting surface can be similarly described. For the atom in the exterior region of a sphere, the Wigthman function can be obtained using the method of images and can then be written as

$$G^+(x(\tau), x'(\tau')) = -\frac{1}{4\pi^2}\frac{1}{(\zeta - i\epsilon)^2 + |x - x'|^2} + \frac{1}{4\pi^2}\frac{1}{(\zeta - i\epsilon)^2 + |x - x_i'|^2/q_i}, \quad (1)$$

where x is an arbitrary position in the exterior region, x' is the atom's position, x_i' is the image's position and q_i is the modulus of the image's effective charge. In the case described in Fig. 1 b, it assumes the simpler form

$$G^+(x(\tau), x(\tau')) = -\frac{1}{4\pi^2}\frac{1}{(\zeta - i\epsilon)^2} + \frac{1}{4\pi^2}\frac{1}{(\zeta - i\epsilon)^2 + |\rho - a^2/\rho|^2/(a/\rho)^2}. \quad (2)$$

Using a standard time-dependent firts-order perturbation theory, the asymptotic decay rate assumes de form

$$R(E, \rho, a) = \frac{E}{2\pi}\left(1 - \frac{\sin[(\rho^2/a - a)E]}{(\rho^2/a - a)E}\right). \quad (3)$$

which can be explored to provide a detailed analysis of the dependence of the spontaneous decay rate on the energy of the emitted radiation (or equivalently on its wavelength), the sphere's radius and the emitter's position. In particular, the spontaneous decay rate measured in units of the free space decay rate depicts damped oscillations as a function of either the radiation energy or the emitter's position with simple asymptotic scaling laws. Further, the decay rate in the interior of the sphere is always suppressed in relation to the free space decay in the low energy regime, irrespective to the emitter's position. At higher energies it also develops damped oscillations. The volume averaged relative decay rate shows two distinct regimes: a quadratic vanishing for small energies and a slow convergence to the free space behavior at high energies.

It is worthy emphasizing that the present approach does not capture polarization effects. However, it provides a clear picture of the bare influence of bounding surfaces on the spontaneous emission process caused by the consequent modification of the vacuum field modes near the surface. A deeper understanding of such basic physical mechanism is fundamental in the search of technics to control and tune the radiation process of trapped emitters. It would be interesting to extend the here reported study for the case of emitters trapped in other structures such as cylinders and shells. We hope the present work will stimulate future contributions along these lines.

References

[1] M. J. A. de Dood, L. H. Slooff, A. Polman, A. Moroz, A. van Blaaderen, Applied Physics Letters 79 (2001) 3585.
[2] L. H. Ford, N. F. Svaiter, M. L. Lyra, Physical Review A 49 (1994) 1378–1386.

Email addresses: rodrigo@fis.ufal.br (R. P. A. Lima), nogueira@ifpi.edu.br (F. N. Lima), marcelo@fis.ufal.br (M. L. Lyra)

Shortcuts to adiabaticity for fast operations with trapped ions

I. Lizuain(1), M. Palmero(2), J. G. Muga(2)

(1) Faculty of Engineering, Department of Applied Mathematics, University of the Basque Country, UPV/EHU, Plaza Europa 1, 20018 Donostia-San Sebastian, Spain.

(2) Departamento de Química Física, UPV/EHU, Apdo 644, Bilbao 48080, Spain.

The coherent manipulation of trapped ions for information processing, simulations, or metrology requires sequences of basic operations such as transport, expansions/compressions, separation/merging of ion chains, rotations, or one and two-qubit gates. Shortcuts to adiabaticity (STA) based on dynamical invariants provide fast protocols to perform these operations without final motional excitation. The applications of STA to trapped ions [1, 5] and prospects for further work are reviewed.

[1] M. Palmero et al. “Fast transport of mixed-species ion chains within a Paul trap” Phys. Rev. A 90, 053408 (2014);
[2] M. Palmero et al “Fast expansions and compressions of trapped-ion chains”, Phys. Rev A 91, 053411 (2015);
[3] M. Palmero et al, “Fast separation of two trapped ions”, New J. Phys. 17, 093031 (2015);
[4] M. Palmero et al, “Shortcuts to adiabaticity for an ion in a rotating radially-tight trap”, New J. Phys. 18, 043014 (2016)
[5] I. Lizuain et al, “Dynamical normal modes for time-dependent Hamiltonians in two dimensions”, Phys. Rev. A 95, 022130 (2017)

Quantum optics with extreme time resolution and ultrashort strong pulsed squeezing

Matthias Kizmann, Thiago Lucena de M. Guedes, Andrey S. Moskalenko, Claudius Riek, Philipp Sulzer, Denis V. Seletskiy, Guido Burkard, Alfred Leitenstorfer

Department of Physics and Center for Applied Photonics, University of Konstanz, D-78457 Konstanz, Germany

Recently, considering the time-resolved behavior of the photonic ground state we showed that vacuum fluctuations of its electric field can be directly detected using the linear electro-optic effect [1]. Our theoretical calculations and the corresponding experimental results demonstrated that nonlinear mixing of a femtosecond near-infrared probe pulse with the multi-terahertz (mid-infrared) vacuum field in a thin electro-optic crystal led to an increase of the signal variance with respect to the shot noise level [1,2]. Further, the theory predicted that it should be possible to trace temporal oscillations of the quantum noise of electric field with subcycle resolution [2]. Interestingly, the detection method avoids absorption or amplification of photons of the probed quantum field. This fact is of importance for potential applications in ultrafast quantum spectroscopy and can be discussed in terms of the concept of weak measurements.

A non-classical state of light with dynamics in an ultrashort temporal range can be created by applying another femtosecond pump pulse which interacts with the vacuum in an additional nonlinear optical crystal (GX). In this way we can modify the field being initially in the ground state and generate pulsed squeezed vacuum states [3]. The properties of these states can be explained theoretically via a cascaded $\chi^{(2)}$ process in the GX where at first a coherent mid-infrared field transient $E_{\mathrm{MIR}}(t)$ is created by the pump and then it acts on the vacuum fluctuations distributed around half the carrier frequency via broadband parametric down-conversion [3]. We introduce a time-dependent squeezing factor, which within the cascaded $\chi^{(2)}$ mechanism is proportional to $\partial E_{\mathrm{MIR}}(t)/\partial t$ for low pump intensities, as well as for arbitrary pump intensities at the time moments when $E_{\mathrm{MIR}}(t)$ vanishes. For certain temporal profiles of the generated $E_{\mathrm{MIR}}(t)$ we can find analytical solutions for the complete dynamics of the quantum noise also in the case of the increased pump intensity. We observe an additional broadening of the time segments upon squeezing whereas the segments with anti-squeezing are narrowed. Finally, we theoretically predict a possibility to generate novel pulsed single-cycle-squeezed states of light under realistic conditions of state-of-the-art experiments.

References

[1] C. Riek, D.V. Seletskiy, A.S. Moskalenko, J.F. Schmidt, P. Krauspe, S. Eckart, S. Eggert, G. Burkard, and A. Leitenstorfer, *Science* **350**, 420 (2015).

[2] A.S. Moskalenko, C. Riek, D.V. Seletskiy, G. Burkard, and A. Leitenstorfer, *Phys. Rev. Lett.* **115**, 263601 (2015).

[3] C. Riek , P. Sulzer, M. Seeger, A.S. Moskalenko, G. Burkard, D.V. Seletskiy, and A. Leitenstorfer, *Nature* **541**, 376 (2017).

Coherent states are not classical

Laura Monroy, Carlos Sanchidrián and Alfredo Luis
Departamento de Óptica, Facultad de Ciencias Físicas, Universidad Complutense
28040 Madrid, Spain
alluis@ucm.es

In this work we show that coherent states lead to observed statistics incompatible with classical electromagnetism in a simple eight-port homodyne detector. This result relies on the entanglement between variables present in the observed statistics.

A relevant topic of quantum optics is the discrimination between classical-like and nonclassical field states, revealed by observed statistics incompatible with classical electromagnetism. Nonclassicality cannot be a single-observable property since the statistics of every quantum observable is compatible with classical physics. Therefore, nonclassical properties can only be inferred from the joint measurement of multiple observables. This requires coupling the system with auxiliary degrees of freedom and the measurement must be followed by some kind of inversion procedure to extract the statistics of system variables from the observed statistics in the enlarged space. In classical physics the result of the inversion is always a true joint probability distribution. However, in quantum physics this is not always the case and the result of the inversion can be incompatible with classical electromagnetism.

This is a very general program that includes as particular cases classic demonstrations of nonclassical behavior, such as coincidence detection, quantum tomography, and the failure of Glauber-Sudarshan *P* function to be a true probability density. However the above program provides a much larger and comprehensive approach that can disclose nonclassical properties for light states that otherwise are universally considered as classical light.

Nonclassical light revealed by the joint statistics of simultaneous measurements,
A. Luis, Opt. Lett. 41, 1789-1792 (2016); arXiv:1506.07680 [quant-ph]

All states are nonclassical: entanglement of joint statistics
A. Luis, arXiv:1606.01478 [quant-ph]

The ultimate resolution for quantum and sub-wavelength imaging [1]

Cosmo Lupo, Stefano Pirandola
York Centre for Quantum Technologies (YCQT), University of York, York YO10 5GH, UK

Quantum imaging aims at harnessing quantum features of light to obtain optical images of high resolution beyond the boundaries of classical optics. Its range of potential applications is very broad, from telescopy to microscopy and medical diagnosis, and has motivated a substantial research activity. Typically, quantum imaging is scrutinized to outperform classical imaging in two ways. First, to resolve details below the Rayleigh length $\mathrm{x_R}$ (sub-Rayleigh imaging). Second, to improve the scaling of the resolution with the number of signal photons by exploiting non-classical states of light [2].

We give a complete solution to the problem of finding the ultimate resolution limit of quantum imaging for estimating the linear or angular separation between two point-like monochromatic sources, by using a linear diffraction-limited imaging device in the far-field regime, and within the paraxial approximation.

To achieve this goal, we compute the ultimate error δ_s of any unbiased estimator of the separation s by applying the quantum Cramér-Rao bound

$$\delta_s \geq \frac{1}{\sqrt{\mathrm{QFI}_s}} \,,$$

where QFI_s is the quantum Fisher information (see also [3]).

A linear optical system is characterized by the point-spread function $\psi(x-y)$, giving the field amplitude at coordinate x on the image plane generated by a point-like source located at coordinate y on the object plane. Also, the finite-size pupil introduces losses, quantified by an attenuation parameter η. Therefore, the source operators c_1, $c_1^\dagger$ and c_2, $c_2^\dagger$ are transformed into the image operators a_1, $a_1^\dagger$ and a_2, $a_2^\dagger$ according to a beam splitter-like transformation:

$$c_1 \to \sqrt{\eta}\, a_1 + \sqrt{1-\eta}\, v_1 \,, \;\; c_2 \to \sqrt{\eta}\, a_2 + \sqrt{1-\eta}\, v_2 \,,$$

where v_1, v_2 are vacuum mode operators, and the image modes are defined as $a_1^\dagger = \int dx \psi(x+s/2)\, a_x^\dagger$, $a_2^\dagger = \int dx \psi(x-s/2)\, a_x^\dagger$, with a_x, $a_x^\dagger$ being the canonical field operator at location x on the image plane.

To compute QFI_s we first show that the optical system is equivalent to a pair of beam splitters, whose transmissivities are functions of the separation (see Fig. 1). Thus, we reduce the estimate of the separation to the estimate of the transmissivity of a beam splitter [4]. In this way, not only we are able to compute the quantum Fisher information for any pair of sources but we also determine the optimal sources that saturate the ultimate precision bound.

Our findings show that the separation between sources emitting quantum-correlated light (entangled or discordant) can be super-resolved at the sub-Rayleigh region. In particular, we find the optimal entangled states with this feature (see Fig. 2). Under optimal conditions one can increase the sub-Rayleigh quantum Fisher information by a constant factor with respect to its value for separations much larger than the Rayleigh length. A fundamental consequence of our findings is a no-go theorem: the ultimate accuracy for any linear-optical, far-field imaging system in the paraxial approximation, scales according to the standard quantum limit. While in principle it could still be possible to beat the standard quantum limit, our results show that in order to do so it is necessary to rely on a biased estimator for the source separation, to consider non-point-like sources, or to employ a near-field, non-linear, or non-paraxial imaging system.

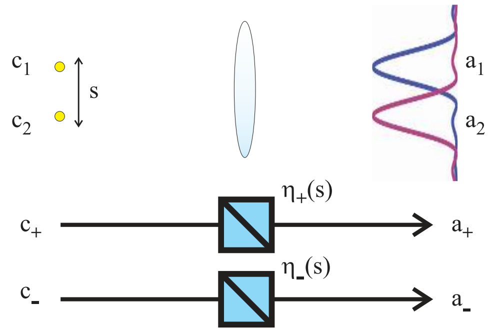

FIG. 1: A linear diffraction-limited imaging system in the paraxial approximation is equivalent to a pair of beam splitters, whose transmissivities are functions of the separation.

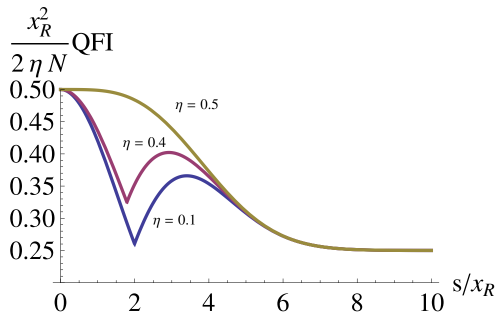

FIG. 2: Normalized QFI_s for the optimal sources of entangled photons emitting N mean photons each. $\mathrm{x_R}$ is the Rayleigh length, and η is the transmissivity of the optical system.

[1] C. Lupo, S. Pirandola, Phys. Rev. Lett. **118**, 100502 (2016).
[2] V. Giovannetti et al. Rev. A **79**, 013827 (2009).
[3] M. Tsang et al. Phys. Rev. X **6**, 031033 (2016).
[4] G. Adesso et al. Phys. Rev. A **79**, 040305(R) (2009).

Composable Security of Measurement-Device-Independent Continuous-Variable Quantum Key Distribution

Cosmo Lupo, Carlo Ottaviani, Panagiotis Papanastasiou, Stefano Pirandola
York Centre for Quantum Technologies (YCQT), University of York, York YO10 5GH, UK

Quantum key distribution (QKD) has been recently extended to a scenario where two honest parties (Alice and Bob) exploit the mediation of an untrusted relay, operated by the eavesdropper (Eve), in order to share a secret-key [1]. The relay applies Bell detection on incoming signals, generating secret correlations in their remote stations (Fig. 1). This type of configuration has been called measurement-device independent (MDI) QKD.

In this work we develop a finite-size security proof of the protocol. We consider a composable framework and collective attacks. The protocol goes as follows: 1) A quantum state is distributed to Alice and Bob, of which Eve holds a purification; 2) Eve measures her share of the quantum system and publicly announces the result Z; 3) Alice and Bob apply local operations conditioned on Z, obtaining a state σ_{ABEZ}; 4) Alice and Bob measure their local states and obtain the state ρ_{XYEZ}, where X and Y denote the results of Alice and Bob measurements; 5) Finally, the raw data are post-processed for parameter estimation, error correction, and privacy amplification.

Since the parties perform local heterodyne detection the cardinality of X and Y is in principle infinite. However, in practice one can always apply an Analog to Digital Conversion algorithm in order to make the variables X and Y discrete and bounded (with cardinality 2^{2d}).

The leftover hash lemma then states that the number of ϵ-secret bits that can be extracted from n i.i.d. instances of ρ_{XYEZ} is bounded by the smooth min-entropy $H^{\epsilon}_{\min}$

$$s^{\epsilon}_n \geq H^{\epsilon}_{\min}(X^n|E^nZ^n)_{\rho^{\otimes n}} - \mathrm{leak}_{\mathrm{EC}}(n, \epsilon_{\mathrm{cor}})\,, \qquad (1)$$

where we have also conditioned on the classical variable Z. According to the Asymptotic Equipartition Property (AEP) the conditional smooth min-entropy in Eq. (1) is given by [2]:

$$H^{\epsilon}_{\min}(X^n|E^nZ^n)_{\rho^{\otimes n}} \geq nH(X|EZ)_{\rho} - \sqrt{n}\,\Delta_{\mathrm{AEP}}(\epsilon, d)\,,$$

where $\Delta_{\mathrm{AEP}}(\epsilon, d) \simeq 4d\sqrt{\log{(2/\epsilon^2)}}$ is a function of the error parameter ϵ and the dimensionality parameter d.

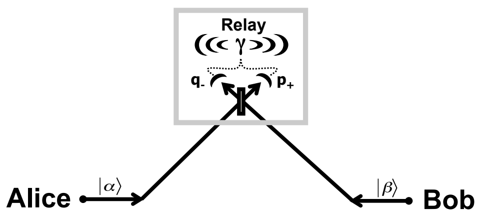

FIG. 1: Alice and Bob sends coherent state to the relay. A trusted relay apply a Bell measurement (entanglement swapping).

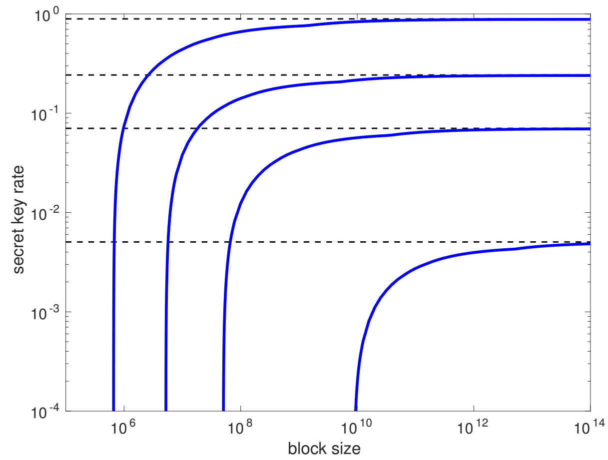

FIG. 2: Finite-size rate (bits per signal) vs block size for Alice being close to the relay. From top to bottom, signals from Bob to the relay are attenuated by $1dB$, $3dB$, $5dB$, $7dB$. Error correction efficiency $\beta = 0.95$, and security parameter $\epsilon = 10^{-21}$.

The assumption that the conditional state $\rho^{\otimes n}$ is a tensor product is justified for collective attacks, but it is no longer guaranteed for a non-zero abort probability $q = 1 - p$ of the error correction routine. Notwithstanding, we are able to show that the secret key rate can still be obtained from Eq. (1) after replacing $\epsilon \to \frac{2}{3}p\epsilon$ and shortening the secret key length by a (very) small amount:

$$\begin{aligned} s^{\epsilon}_n \geq\; & nH(X|EZ)_{\rho} - \mathrm{leak}_{\mathrm{EC}}(n, \epsilon_{\mathrm{cor}}) \\ & - \sqrt{n}\,\Delta_{\mathrm{AEP}}\left(\frac{2}{3}p\epsilon, d\right) + \log\left(p - \frac{2}{3}p\epsilon\right). \end{aligned} \qquad (2)$$

Under the assumption of collective Gaussian attacks, the conditional entropy $H(X|EZ)_{\rho}$ can be estimated from X and Y. Figure 2 show the finite-size secret key rate under collective Gaussian attacks. Applying the Gaussian de Finetti reduction recently introduced in [3], it might be possible to extend the security from collective Gaussian attacks to most general coherent attacks.

[1] S. Pirandola *et al.* Nature Photon. 9, 397-402 (2015).
[2] A. Leverrier, Phys. Rev. Lett. **114**, 070501 (2015).
[3] A. Leverrier, arXiv: 1701.03393 (2017).

Photonic Waveguides for Optical Delivery of 780 nm Laser Light for Quantum Sensors based on Ultra-cold atoms of Rubidium

J.O. Maclean[1], M.T. Greenaway[2] , R.P. Campion[1], M. Wildman[1], T.M. Fromhold[1] and C.J. Mellor[1]

[1] School of Physics and Astronomy, University of Nottingham, University Park, Nottingham, NG7 2RD.

[2] Department of Physics, Loughborough University, Epinal Way, Loughborough, LE11 3TU.

The implementation of portable quantum sensors will greatly widen their application. In quantum sensors based on laser-cooled atomic gases, the laser light must be guided in such a way that it is automatically-aligned and stable in polarisation and phase. An optical waveguide technology which is adapted to this class of sensors is therefore required. Here we describe the design, epitaxy, nanofabrication and measurement of polarisation-maintaining, deep-etched $Al_xGa_{(1-x)}As$ waveguides for near-infra-red 780 nm light. The optical loss was measured to be below 4.3(±0.4) dB cm^{-1} corresponding to an attenuation coefficient, α, of 1.0 (±0.08) cm^{-1} for single mode waveguides and the polarisation extinction ratio was better than -19 (±1) dB for orthogonal polarisations. A literature comparison was made with other reported optical loss values for various Al mole fractions. The ultimate aim of the work is the creation of waveguide-based photonic circuits for compact cold atom sensors based on the D_2 hyperfine transition of ^{87}Rb at 780.24 nm.
We demonstrated and analysed the transmission of low loss, high refractive index $Al_xGa_{(1-x)}As$-based semiconductor waveguides which maintain a single TE polarisation of light at 780 nm. The polarisation-maintaining nature of the waveguides is a significant advantage for applications in compact sensors in which polarisation needs to be controlled and maintained.

Unifying framework for coined quantum walks on irregular and disrupted graphs.

Jan Mareš[1*]
[1]*Department of Physics, Faculty of Nuclear Sciences and Physical Engineering, Czech Technical University in Prague, Břehová 7 11000 Praha 1, Czech Republic*

Quantum walks are now well established in the field of quantum information processing. They were proven equivalent to a universal quantum computer and also specific algorithms for quantum walks were reported. Further, they can be used for simulation of other quantum systems. Some variants of quantum walks have already been realised in various physical systems. Notably, coined quantum walks on a two-dimensional lattice capable of simulating two-particle dynamics have been realised using an optical fiber network. [1]

Coined quantum walks are processes defined on graphs. The Hilbert space of the system is associated with this graph. The state of the quantum walker is given by his position in the graph and by an internal degree of freedom governing the direction of his further movement. Specifically, the time evolution is realised in discrete steps by a subsequent application of two unitary operators : the *coin operator* mixing the internal states separately in every vertex and the *shift operator* moving the walker among vertices.

Alternations of the coin operator were subjected to a rather intense investigation. On the other hand, the shift operator is mostly treated as being obvious, which is probably due to high symmetry of graphs used. The majority of research was done on the line graph with some exceptions of a two-dimensional square lattice or some modification of the line. Already for a honeycomb lattice and even more dramatically for irregular graphs, the choice of the shift operator is far from trivial. In all non-trivial cases, there are multiple possible shift operators leading to dramatically different behaviours of the walk.

We approach the classification of possible shift operators by introducing a framework with the shift operator further separated into two operators. One of the operators realises a pure transport from one vertex to another and the other one is responsible for the choice of the final internal state. This reduces the classification of shift operators to choices of local permutations in vertices.

Our approach allows for for simple definition of quantum walks on irregular graphs and is also useful when dealing with disrupted graphs. In particular, we investigate dynamical bond percolation (randomly chosen edges closed in every step) in quantum walks and search for the asymptotic behaviour of these open quantum systems. (The procedure is based on the previous work reported in [2].) One of the main results is that the asymptotic behaviour is the same for many particular ways of choosing the sets of broken edges. For example, we may have a chance for every edge to be closed independently or we may allow only one edge closed in every step and so on.

The derived theory allows, among other examples, for the investigation of percolated quantum walks on 3-regular graphs (e.g. honeycomb lattice) with various shift operators. For these graphs we show that the choice of the shift operator has a crucial influence on the asymptotic behaviour, for example the asymptotic transfer probability of an excitation.

[1] A. Schreiber, A. Gábris, P. P. Rohde, K. Laiho, M. Štefaňák, V. Potoček, C. Hamilton, I. Jex and C. Silberhorn. "A 2D Quantum Walk Simulation of Two-Particle Dynamics", Science **336** :6077, (2012).

[2] B. Kollár, T. Kiss, J. Novotný and I. Jex. "Asymptotic dynamics of coined quantum walks on percolation graphs", Phys. Rev. Lett. **108** :230505, (2012).

* maresj23@fjfi.cvut.cz

Einstein-Podolsky-Rosen-like correlations for two-mode Gaussian states

Paulina Marian[1,2] and Tudor A. Marian[1]
[1] *Centre for Advanced Quantum Physics, Department of Physics, University of Bucharest, R-077125 Bucharest-Măgurele, Romania and*
[2] *Department of Physical Chemistry, University of Bucharest, R-030018 Bucharest, Romania*

Detecting and measuring quantum entanglement represent one of the goals of quantum information science. In the last two decades, a large amount of work has been invested in writing efficient separability criteria for both discrete- and continuous-variable systems. As shown by Peres [1], a necessary condition of separability for an arbitrary two-party state is the requirement to have a non-negative partially transposed density matrix. In the case of discrete-variable systems, this requirement of positive partial transposition (PPT) is also a sufficient condition of separability only for states on $\mathbb{C}^2 \otimes \mathbb{C}^2$ and $\mathbb{C}^2 \otimes \mathbb{C}^3$ Hilbert spaces [2]. For bipartite states of continuous-variable systems, the PPT condition was first applied by Simon [3]. Specifically, Simon proved that preservation of the non-negativity of the density matrix under partial transposition is not only a necessary, but also a sufficient condition for the separability of two-mode Gaussian states (TMGSs). Moreover, the partial transposition criterion could be expressed in an elegant symplectically invariant form valid for any TMGS [3].

A somewhat parallel method to get general inseparability criteria for two-mode states originates in a practical procedure proposed by Reid for demonstrating the Einstein-Podolsky-Rosen (EPR) paradox [4] in a non-degenerate parametric amplifier [5]. This was done by using two non-local observables linearly built with the canonical quadrature operators of the modes, $\hat{q}_j, \hat{p}_j, (j = 1,2)$ [5]: $\hat{Q}(\lambda) := \hat{q}_1 - \lambda \hat{q}_2, \quad \hat{P}(\mu) := \hat{p}_1 + \mu \hat{p}_2$, where λ and μ are adjustable positive parameters. As a consequence of their commutation relation, $[\hat{Q}(\lambda), \hat{P}(\mu)] = i(1-\lambda\mu)\hat{I}$, we get the weak (Heisenberg) form of the uncertainty principle,

$$\Delta Q(\lambda) \Delta P(\mu) \geqq \frac{1}{2}|1-\lambda\mu|, \tag{1}$$

which has to be fulfilled by any quantum state. Here $(\Delta A)_{\hat{\rho}}$ denotes the standard deviation of the observable $\hat{A}$ in the state $\hat{\rho}$, which is the square root of the variance $[(\Delta A)_{\hat{\rho}}]^2 = \langle \hat{A}^2 \rangle_{\hat{\rho}} - \left(\langle \hat{A} \rangle_{\hat{\rho}} \right)^2$. Unless $\lambda = \mu = 1$, the above operators are not genuine EPR observables since they do not commute. If the two-mode state is separable, i. e., it is a convex combination of product states, $\hat{\rho}_s := \sum_k w_k \hat{\rho}_1^{(k)} \otimes \hat{\rho}_2^{(k)}, \quad (w_k > 0, \quad \sum_k w_k = 1)$, then the product $(\Delta Q)_s (\Delta P)_s$ has a stronger lower bound. We have the following two sets of inequalities:

$$[\Delta Q(\lambda)]_s [\Delta P(\mu)]_s \geqq \frac{1}{2}(1+\lambda\mu),$$
$$\{[\Delta Q(\lambda)]_s\}^2 + \{[\Delta P(\mu)]_s\}^2 \geqq 1 + \lambda\mu \tag{2}$$

In the present work we first evaluate the minimal normalized uncertainty relation (1) for TMGSs. In a very nice way, the extremization of this condition with respect to λ , μ and the local parameters over the set of TMGSs having the same symplectic invariants led us to the result

$$F_m := \min \frac{[\Delta Q(\lambda)]^2 \, [\Delta P(\mu)]^2}{(1-\lambda\mu)^2} = \kappa_-^2,$$

where κ_- is the smallest symplectic eigenvalue of the covariance matrix. Then, we formulate two separability criteria in sum and product forms of normalized EPR-like correlations for TMGSs. To do this we started from Eqs. (2) which are necessary conditions of separability for any state. We evaluate the minimal normalized uncertainty relations (2) for TMGSs and get separability markers which are found to be only dependent on the smallest symplectic eigenvalue of the PT-covariance matrix, being thus consistent to Simon's PPT criterion. As an example, the normalized product of the EPR-variances (2) has the minimal value

$$E_m := \min \frac{[\Delta Q(\lambda)]^2 \, [\Delta P(\mu)]^2}{(1+\lambda\mu)^2} = \left(\kappa_-^{\mathrm{PT}}\right)^2.$$

We can interpret therein the smallest symplectic eigenvalue of the PT-state as a quantifier of the greatest amount of EPR correlations which can be created in a TMGS by means of local operations. Our present approach might stimulate once more a reflection on the central role of the uncertainty relations in quantum mechanics.

[1] A. Peres, Phys. Rev. Lett. **77**, 1413 (1996).
[2] M. Horodecki, P. Horodecki, and R. Horodecki, Phys. Lett. A **223**, 1 (1996).
[3] R. Simon, Phys. Rev. Lett. **84**, 2726 (2000).
[4] A. Einstein, B. Podolsky, and N. Rosen, Phys. Rev. **47**, 777 (1935).
[5] M. D. Reid, Phys. Rev. A **40**, 913 (1989).

Constraints on Downconversion in Atomically Thick Films

Loris Marini[1,2], Luke Helt[3], Benjamin J. Eggleton[1,2], Stefano Palomba[1,2]

1.Institute of Photonics and Optical Science (IPOS), School of Physics, the University of Sydney, NSW 2006, Australia

2. Centre for Ultrahigh Bandwidth Devices for Optical Systems (CUDOS), School of Physics, the University of Sydney, NSW 2006, Australia

3. CUDOS, MQ Photonics Research Centre, Department of Physics and Astronomy, Macquarie University, NSW 2109, Australia

Spontaneous parametric down-conversion (SPDC) sources involve the probabilistic annihilation of individual pump photons into pairs of strongly correlated photons, enabling the selection of non-classical states of light. This process is intrinsically weak as it depends quadratically on the medium second order susceptibility $\chi^{(2)}$, typically limiting the design to structures with long interaction lengths. While atomically thick crystals with unusually large $\chi^{(2)}$ and intrinsic phase-matching have been reported [1,2], the experimental demonstration of SPDC of a photon in a single atomic layer has remained elusive.

Here we aim to uncover physical and experimental constraints to guide the design of an experimental setup for such SPDC. We develop a model for estimating the coincidence-to-accidental ratio (CAR) of photons generated in a free-space SPDC coincidence experiment using data obtained from an appropriate second harmonic generation (SHG) experiment [3,4] (Fig.1 a-b). The geometry consists of a planar monolayer of non-linear medium embedded in a transparent dielectric environment (Fig 1c). We consider a pump photon probabilistically downconverting into signal and idler photons (Fig.1d) which are subsequently collected and guided to a beam splitter for coincidence measurement. Energy and momentum conservation shape the radiation pattern and influence the system loss thereby affecting the CAR. We include the overall system loss and noise as a function of collection optics, illumination angle (Fig. 1e) and detectors efficiency, and the effective medium non-linearity in our model (Fig. 1f).

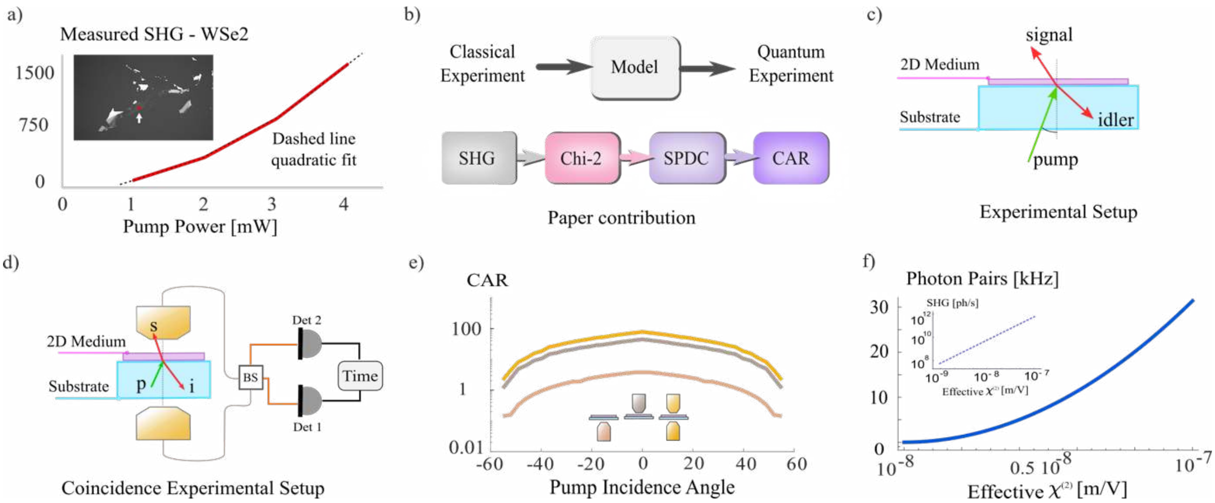

Fig. 1a) Measured second harmonic generation (SHG) on monolayer WSe2. Fig. 1b) The medium effective non-linearity (chi-2) is calculated from SHG. The rate of photon pairs is then estimated and used to simulate the CAR. Fig. 1c) A pump photon (green) interacts over atomic scales with a non-linear crystal and spontaneously downconverts into a signal and a idler photons (red). Fig. 1d) Pairs are collected and their temporal correlation measured with two single photon detectors. Fig. 1e) Calculated CAR dependence on pump angle for 1 SPDC-pair/s. The best performance is predicted for normal illumination and may be improved up to a factor of 20 by collecting light from both sides of the monolayer. Fig. 1f) Calculated rate of SPDC photon-pairs for 1 mW 200 fs pump at 775 nm and its quadratic scaling with the medium nonlinearity.

As a specific example, we focus on study the down-conversion of a visible pump photon into a signal-idler pair at telecom wavelengths in a WSe2 monolayer. SHG measurements of a 1550 nm mode-locked 80 MHz 200 fs laser allow us to calculate $\chi^{(2)}$=12 pm/V. When the same pump is tuned at 775 nm for SPDC, we predict 10^{-3} pairs/s for 1 mW average power. We calculate that the CAR can be increased up to 40 times with normal pumping compared to illuminations with a large numerical aperture and up to 20 times by collecting from both sides of the medium. For monolayer WSe2 and free-running NIR single photon detectors the measurement is noise limited. Detection gating could provide the necessary noise reduction to enable a coincidence measurement.

References:

[1] Y. Li, Y. Rao, K. F. Mak, Y. You, S. Wang, C. R. Dean, and T. F. Heinz, "Probing symmetry properties of few-layer MoS2 and h-BN by optical second-harmonic generation," Nano Lett., vol. 13, no. 7, pp. 3329–3333, 2013.
[2] M. Zhao, Z. Ye, R. Suzuki, Y. Ye, H. Zhu, J. Xiao, Y. Wang, Y. Iwasa, and X. Zhang, "Atomically phase-matched second-harmonic generation in a 2D crystal," Light Sci. Appl., vol. 5, no. 8, p. e16131, 2016.
[3] M. Liscidini and J. E. Sipe, "Stimulated emission tomography," Phys. Rev. Lett., vol. 111, no. 19, pp. 1–5, 2013.
[4] L. G. Helt, M. Liscidini, and J. E. Sipe, "How does it scale? Comparing quantum and classical nonlinear optical processes in integrated devices," vol. 29, no. 8, pp. 2199–2212, 2012.

Gibbs-like asymptotic states of quantum markov processes

Jiří Maryška[1],* Jaroslav Novotný[1], and Igor Jex[1]
[1] *Department of Physics, Faculty of Nuclear Sciences and Physical Engineering, Czech Technical University in Prague, Břehova 7, 115 19 Praha 1 - Staré Město, Czech Republic*

Quantum markov prosesses represent a convenient way of time-evolution description of a general open quantum system. They are divided into two groups - discrete (quantum markov chains) and continuous (e.g. quantum markov dynamical semigroups). Quantum markov processes show a great potential in many areas of quantum theory reaching from its very fundamentals to practical applications, i.e. random quantum walks [2].

Recently, the asymptotic dynamics of a wide class of discrete quantum markov processes (equipped with so-called faithful state) on finite dimensional Hilbert space was studied [1]. It was shown that if the quantum markov proces is equiped with faithful state the asymptotic dynamics can be written by means of so-called attractor space, which can be derived by solving a set of algebraic equations called attractor equations. Analogous results can be derived for continuous quantum markov processes on finite dimensional Hilbert space.

We give the relations between the elements of the attractor space of quantum markov proces and the elements of attractor space of conjugated quantum markov proces. Physically, these are relations which connect the Schrödinger and the Heisenberg picture. This means we are able to derive relations between stationary states and integrals of motion corresponding to such a quantum markov proces. Next, we show that stationary states of such quantum markov proces can be rewritten in a form, which resembles a well known concept of a generalized Gibbs state. These so-called Gibbs-like states follow a principle, which can be regarded as a generalization of maximal entropy principle.

---

[1] J. Phys. A : Math. Theor. 45 (2012) 485301

[2] Eur. Phys. J. Plus (2014) 129 : 103

* maryska.jiri@gmail.com

Quantum State Comparison Amplifier with Feedforward State Correction

Luca Mazzarella[1*], Ross Donaldson[2], Robert Collins[2], Ugo Zanforlin[2], Gerald Buller[2] & John Jeffers[1]
[1] *Department of Physics, University of Strathclyde, John Anderson Building, 107 Rottenrow, Glasgow G4 0NG, U.K.*
[2] *Institute of Photonics and Quantum Sciences, School of Engineering and Physical Sciences, Heriot Watt University, David Brewster Building, Edinburgh EH14 4AS, U.K.* *luca.mazzarella@strath.ac.uk.*

(Dated: April 4, 2017)

Abstract: Here we present a probabilistic amplifier that combines two Quantum State Comparison AMPlifiers (SCAMP) together with a feed-forward state correction strategy. Our system outperform the Unambiguous State Discrimination (USD) based amplifier in terms of the success probability-fidelity product and requires a no more complex experimental setting.

The laws of quantum mechanics pose stringent constraints on the way a quantum signal can be amplified. Deterministic amplification of an unknown quantum state always imply the addition of noise. A perfect amplifier is in principle allowed provided it works only probabilistically [1], [2].

A SCAMP [3] is a probabilistic amplifier that works for a known set of coherent states. Alice picks uniformly at random an input state from the set $\{|+\alpha\rangle, |-\alpha\rangle\}$ and pass it to Bob who has to amplify it.

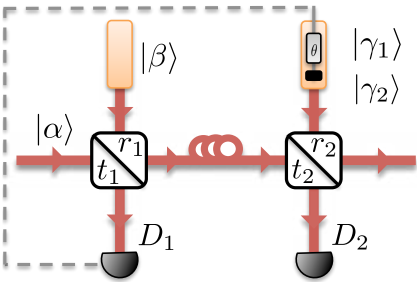

FIG. 1. Device schematics, the lower output of the first beam splitter is send to an APD detector. If the first detector fires, an electrical pulse is sent to the second input and changes the guess from $|\gamma_1\rangle$ to $|\gamma_2\rangle$ in order to correct the output.

Our device is shown in figure 1. Bob mixes Alice's input with two suitable guess coherent states in attempt to achieve destructive interference in both the arms that go to the detectors. The lack of trigger is an imperfect indication that Bob's guess is right (i.e. $|+\beta\rangle = |+\frac{t_1}{r_1}\alpha\rangle$ if Alice pick $|+\alpha\rangle$) and that the output contain the correct amplified state (the indication is imperfect because there could be undetected light due to a wrong guess). On the other hand, if D_1 fires Bob know that his guess was wrong (i.e. $|-\beta\rangle$) but he can still correct the output by changing the input state for the second stage via the amplitude and phase modulator. The overall gain of the system is thus given by $g = \frac{1}{r_1 r_2}$. Since the key working point is this feed-forward State Correction we call this system SCSCAMP.

Bob declares success and postselects the output corresponding to the events $S = \{\{D_1 = 0, D_2 = 0\}, D_1 = 1\}$ (or simply $S = \{\{0,0\},1\}$).

The fidelity of the SCSCAMP is the probability of passing a measurement test on the output comparing it to $|g\alpha\rangle$ and the *success probability-fidelity product* [4] is the joint probability of success and of passing the measurement test:

$$
\begin{aligned}
&P(T,S) = P(T,\{0,0\}) + P(T,1)\\
&= \sum_{\sigma=\pm\beta} \left(P(T|\{0,0\},\sigma)P(\{0,0\}|\sigma) + P(T|1,\sigma)P(1|\sigma)\right) P(\sigma) \qquad (1)\\
&= \frac{1}{2}\left(2 - e^{-4\eta\left(1-\frac{1}{g}\right)\alpha^2} + e^{-4\eta\left(1-\frac{1}{g^2}\right)\alpha^2} e^{-4\left(1-\frac{1}{g}\right)^2\alpha^2}\right) \qquad (2)
\end{aligned}
$$

Where to go from (1) to (2) we used that $P(\pm\beta) = \frac{1}{2}$ and that:

$$
P(\{0,0\}|-\beta) = e^{-4\eta t_1^2\alpha^2} e^{-4\eta t_2^2 r_1^2\alpha^2} \quad P(1|-\beta) = 1 - e^{-4\eta t_1^2\alpha^2},
$$

$$
P(T|\{0,0\},-\beta) = |\langle g\alpha|\tfrac{2r_1^2r_2^2-1}{r_1r_2}\rangle|^2 = e^{-\left|g\alpha - \frac{2r_1^2r_2^2-1}{r_1r_2}\alpha\right|^2}.
$$

Furthermore, we have that $P(\{0,0\}|+\beta) = 1$ and $P(1|+\beta) = 0$. Finally, for simplicity, we have set $r = r_1 = r_2$. Our figures of merit compare favorably with other schemes. In figure 2 we show that success probability-fidelity product of the SCSCAMP is always bigger than the one of USD based amplifier proposed in [2] (and requires no more complex resources) and almost always bigger than the $1 \to 2$ no-cloning limit of 2/3.

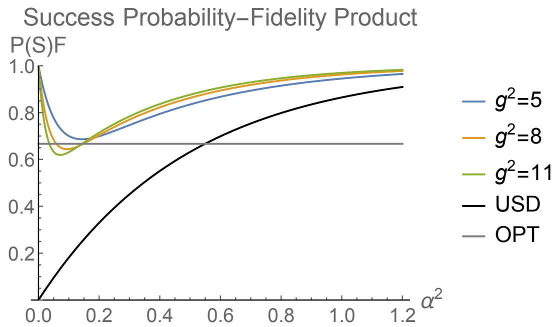

FIG. 2. Success probability-fidelity product for the SCSCAMP with gains of 5 (blue), 8 (green) and 11(yellow), for the unambiguous discrimination (black), and for the no-cloning limit (gray). The detector efficiency are assumed to be equal to 1 for simplicity.

This system can be realized with classical resources (i.e., lasers, linear optics and APD detectors). Similar systems, with no state correction, proved to achieve high-gain, high fidelity and high repetition rates [5], [6] and [7]. The ability to switch between input states on the fly requires delay lines and fast switching but it can still achieved with classical resources.

Due to its simplicity, the system we propose might represent an ideal candidate as a recovery station to counteract quantum signal degradation due to propagation in a lossy fibre or as a quantum receiver to improve the key-rate of quantum communication protocols using weak coherent states. The system is also suitable for on-chip implementation.

The work was supported by the QComm Quantum Communication Hub of the UK Engineering and Physical Sciences Research Council (EP/M013472/1).

[1] T.C. Ralph & A.P. Lund, in *Proceedings of the 9th QCMC Conference*, edited by A. Lvovsky (AIP, Melville, NY, 2009).
[2] V. Dunjko & E. Andersson, Phys. Rev. A 88, 042322 (2012).
[3] E. Eleftheriadou *et al.*, Phys. Rev. Lett. 111, 213601 (2013).
[4] S. Pandey, *et al.*, Phys. Rev. A 88, 033852 (2013).
[5] R. Donaldson *et al.*, Phys. Rev. Lett. 114, 120505 (2015).
[6] M.A. Usuga *et al.*, Nat. Phys. 6, 767 (2010).
[7] R. Donaldson *et al.*, *in preparation*.

Experimental characterization of a non-local convertor for quantum photonic networks

M. Mičuda,[1] R. Stárek,[1] P. Marek,[1] M. Miková,[1] I. Straka,[1] M. Ježek,[1] T. Tashima,[2] Ş. K. Özdemir,[3] and M. Tame[2]

[1] *Department of Optics, Palacký University, 17. listopadu 1192/12, 771 46 Olomouc, Czech Republic*
[2] *School of Chemistry and Physics, University of KwaZulu-Natal, Durban 4001, South Africa*
[3] *Department of Electrical and Systems Engineering, Washington University in St. Louis, St. Louis, MO 63130 USA*

A common problem in quantum networks is that once the entangled resource is shared among the nodes it is fixed and can only be used for a given set of quantum tasks [1, 2]. A different task then requires conversion of the available multipartite entangled state into another state. When the separation between the nodes is large this conversion can employ only local operations and classical communication [3]. Fortunately, in some cases two nodes of the network may be close enough for application of a non-local operation between them. Here we report experimental realization of the two-qubit photonic non-local conversion gate suggested by Tashima *et al.* in [4], see of Fig. 1 (b), with single photons using a linear optical setup [5]. We show its potential for converting a four-qubit linear cluster state into a GHZ state, a Dicke state, and a product of two Bell states. The conversion gate can also be used to generate quantum correlations that are not associated with entanglement, but whose presence is captured by the notion of discord. Furthermore, the conversion gate can be used for 're-wiring' the entanglement connections in a larger graph state network [6].

As shown in Fig. 1 (a), the conversion gate was implemented using a displaced Sagnac interferometer and a single polarizing beam splitter (PBS), where the interferometric phase was controlled by tilting one of the glass plates (GP). This construction provides passive stabilization of the Mach-Zehnder interferometer [7]. $\mathrm{HWP}_1(\theta_1)$ and $\mathrm{HWP}_2(\theta_2)$ were used to configure the conversion gate for its different settings. Outputs from the conversion gate were analyzed using the detection blocks (DB), which consist of a HWP, a QWP, and a PBS followed by an avalanche photodiode (APD). The scheme operated in the coincidence basis and the operation succeeded upon detecting a two-photon coincidence at the output ports.

We have performed a full tomographic reconstruction of the implemented non-local conversion gate based on a tomographically complete set of measurements. For all the considered scenarios where cluster state, a GHZ state, a Dicke state, and a product of two Bell states are generated from four-qubit linear cluster state the purity and process fidelity exceeds 0.91 and 0.94, respectively.

The non-local nature of the gate allows us transform a two-qubit factorized state into a state with non-zero entanglement. By preparing both input states in $(|0\rangle - |1\rangle)/\sqrt{2}$ with gate parameters $\theta_1 = 3\pi/8$ and $\theta_2 = \pi/8$ we are able to transforms them into the entangled Bell state $|\Phi^+\rangle = (|00\rangle + |11\rangle)/\sqrt{2}$.

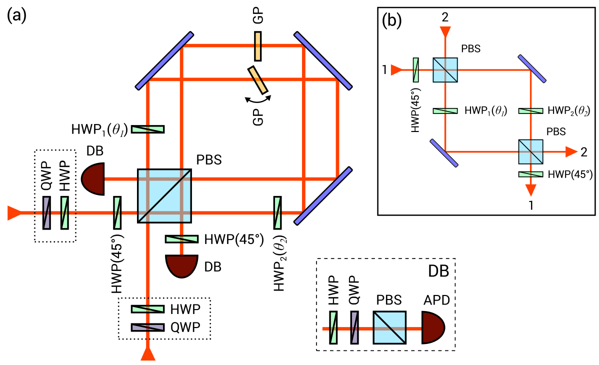

FIG. 1: Experimental setup for the charaterization of the non-local conversion gate. The dotted boxes represent preparation stages for encoding different inputs. See main text for more details.

We also use the conversion gate to prepare a separable state, but with non-zero quantum correlations measured by the discord. To do this, we started with a mixed factorized state $\rho_{in} = \frac{1}{2}\mathbb{I} \otimes |+\rangle\langle+|$ and fed it into the conversion gate with parameters $\theta_1 = \pi/3$ and $\theta_2 = 0$.

Acknowledgments This work was supported by the Czech Science Foundation (GA16-17314S), (GB14-36681G) and South African National Research Foundation and the South African National Institute for Theoretical Physics.

[1] H. J. Kimble, Nature **453**, 1023–1030 (2008).
[2] S. Perseguers, G. J. Lapeyre Jr, D. Cavalcanti, M. Lewenstein and A. Acin, Rep. Prog. Phys. **76**, 096001 (2013).
[3] T. Kobayashi, R. Ikuta, Ş. K. Özdemir, M. S. Tame, T. Yamamoto, M. Koashi, and N. Imoto, New J. Phys. **16**, 023005 (2014).
[4] T. Tashima, M. S. Tame, Ş. K. Özdemir, F. Nori, M. Koashi and H. Weinfurter, Phys. Rev. A **94**, 052309 (2016).
[5] M. Mičuda, R. Stárek, P. Marek, M. Miková, I. Straka, M. Ježek, T. Tashima, Ş. K. Özdemir, and M. Tame, Optics Express **25**, 7839 (2017).
[6] H. J. Briegel, D. E. Browne, W. Dür, R. Raussendorf and M. Van den Nest, Nat. Phys. **5**, 19–26 (2009).
[7] M. Mičuda, E. Doláková, I. Straka, M. Miková, M. Dušek, J. Fiurášek and M. Ježek, Rev. Sci. Instrum. **85**, 083103 (2014).

Evolution of quantum steering of two bosonic modes in a squeezed thermal environment

Tatiana Mihaescu[1,2], Aurelian Isar[1]

[1]Department of Theoretical Physics, National Institute for Physics and Nuclear Engineering, Magurele-Bucharest, Romania
[2]Faculty of Physics, University of Bucharest, Romania

Einstein-Podolsky-Rosen steerability of quantum states is a property that is different from entanglement and Bell nonlocality [1]. We describe the time evolution of a recently introduced measure that quantifies steerability for arbitrary bipartite Gaussian states [2] in a system consisting of two bosonic modes embedded in a common squeezed thermal environment.

We work in the framework of the theory of open systems. If the initial state of the subsystem is taken of Gaussian form, then the evolution under completely positive quantum dynamical semigroups assures the preservation in time of the Gaussian form of the states [3].

In Ref. [4] it was shown that the thermal noise and dissipation introduced by the thermal environment destroy the steerability between the two bosonic modes. In the case of the squeezed thermal bath we show the dependence of the Gaussian steering on the squeezing parameters of the bath and of the initial state of the system. A comparison with other quantum correlations for the same system shows that, unlike Gaussian quantum discord, which is decreasing asymptotically in time, the Gaussian quantum steerability suffers a sudden death behaviour, like quantum entanglement.

Bibliography
[1] S. J. Jones, H. M. Wiseman and A. C. Doherty, Phys. Rev. A **76**, 052116 (2007).
[2] I. Kogias, A. R. Lee, S. Ragy and G. Adesso, Phys. Rev. Lett. **114**, 060403 (2015).
[3] G. Lindblad, Commun. Math. Phys. **48**, 119 (1976).
[4] T. Mihaescu and A. Isar, Romanian J. Phys. **62**, 107 (2017).

Conditional generation of superpositions of photon number states of traveling fields

Gabor Mogyorosi,[1,*] Emese Molnar,[1] and Peter Adam[1,2]

[1]*Institute of Physics, University of Pécs, H-7624 Pécs, Ifjúság útja 6, Hungary*
[2]*Institute for Solid State Physics and Optics, Wigner Research Centre for Physics, Hungarian Academy of Sciences, H-1525 Budapest, P.O. Box 49, Hungary*

The problem of generating various quantum states of light is still an important topic in quantum optics, owing to their numerous applications in quantum information processing, quantum-enhanced metrology, and fundamental tests of quantum mechanics [1–11]. A considerable attention has been devoted also to the idea of quantum state engineering, i.e., to the preparation of several different nonclassical states in a single experimental scheme [5–8]. The generation of nonclassical states of traveling optical modes is often desired in practical application. Conditional preparation is a well-established technique for such a task. This consists in measuring one mode of an entangled state which results in the projection of the other mode to the desired state for certain results of the measurement.

Repeated photon subtraction and addition to a given state are plausible tools to manipulate a quantum state and to prepare various superpositions of photon number states [7–11]. The number of the optical elements in these schemes is usually proportional to the amount of number-states involved in the photon number superposition.

In this communication we show that in the experimental scheme presented in Fig. 1, containing only a beam splitter of transmittance T and a homodyne detector capable of measuring the quadrature X_θ, it is possible to prepare various superpositions of photon number states, albeit with limited number of photons.

The inputs of this scheme are independently prepared squeezed coherent states $|\alpha_i, \zeta_i\rangle$ with complex coherent amplitudes $\alpha_i = |\alpha_i| \exp(\mathrm{i}\phi_i)$ and complex squeezing parameters $\zeta_i = r_i \exp(\mathrm{i}\theta_i)$. The benefit of such inputs is that they can be routinely generated experimentally by standard techniques.

We prove that in this scheme, with the appropriate choice of some of the parameters α_i, ϕ_i, r_i, θ_i of the input states and that of T, the beam splitter transmittance, a prescribed photon number superposition can be prepared on condition that a given measurement result $X_\theta = x$ is obtained by the homodyne detector.

The required parameters can be determined numerically using a genetic algorithm. The objective is that the misfit between the target state and the output state should be minimal while the probability of conditional generation should be maximal. We demonstrate that various superpositions of photon number states of small numbers can be approximately prepared in the proposed scheme at a high accuracy and with large probability.

* mgabor@fizika.ttk.pte.hu

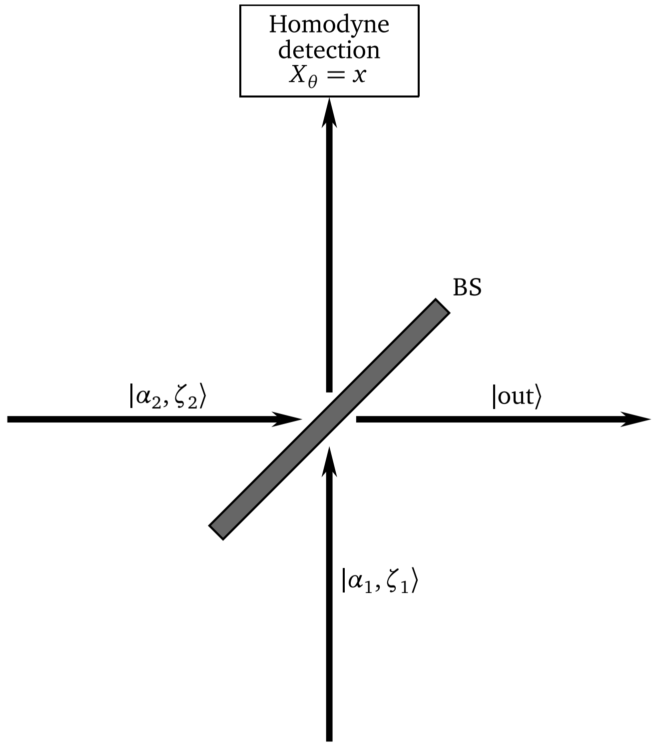

FIG. 1. Experimental scheme for producing various superpositions of a few photon number states.

[1] A. Laghaout, J. S. Neergaard-Nielsen, I. Rigas, C. Kragh, A. Tipsmark, and U. L. Andersen, Phys. Rev. A **87**, 043826 (2013)
[2] K. Huang, H. Le Jeannic, V. B. Verma, M. D. Shaw, F. Marsili, S. W. Nam, E Wu, H. Zeng, O. Morin, and J. Laurat, Phys. Rev. A **93**, 013838 (2016)
[3] P. Adam, T. Kiss, M. Mechler, and Z. Darázs, Phys. Scr. **T140**, 014011 (2010)
[4] H. Jeong, M. S. Kim, T. C. Ralph, and B. S. Ham, Phys. Rev. A **70**, 061801(R) (2004)
[5] S. Szabo, P. Adam, J. Janszky, and P. Domokos, Phys. Rev. A. **53**, 2698 (1996)
[6] P. Adam, E. Molnar, G. Mogyorosi, A. Varga, M. Mechler, and J. Janszky, Phys. Scr. **90**, 074021 (2015)
[7] M. Dakna, J. Clausen, L. Knöll, and D.-G. Welsch, Phys. Rev. A **59**, 1658 (1999)
[8] J. Fiurášek, R. García-Patrón, and N. J. Cerf, Phys. Rev. A **72**, 033822 (2005)
[9] M. S. Kim, J. Phys. B **41**, 133001 (2008)
[10] S.-Y. Lee and H. Nha, Phys. Rev. A **82**, 053812 (2010)
[11] S. Wang, H.-C. Yuan, and X.-F. Xu, Eur. Phys. J. D **67**, 102 (2013)

Nonequilibrium Quantum Critical Phenomena in a Non-Markovian Environment

David Nagy* and Peter Domokos^

Wigner Research Centre for Physics
Hungarian Academy of Sciences

*nagy.david@wigner.mta.hu
^peter.domokos@wigner.mta.hu

Driven dissipative systems opened up a novel research area in the field of quantum criticality. Phase transitions in these systems lie beyond the standard classification of classical dynamical or equilibrium phase transitions and define completely new universality classes. In an open quantum system, the critical behavior appears in the steady state formed by the dynamical equilibrium of the external driving and dissipation processes. The correlation functions at the critical point are determined by nonequilibrium noise rather than thermal or ground-state quantum fluctuations.

We study the open-system realization of the Dicke model, where a bosonic cavity mode couples to a large spin formed by two motional modes of an atomic Bose-Einstein condensate [1-2]. The cavity mode is driven by a high-frequency laser and it decays to a Markovian bath, while the atomic mode

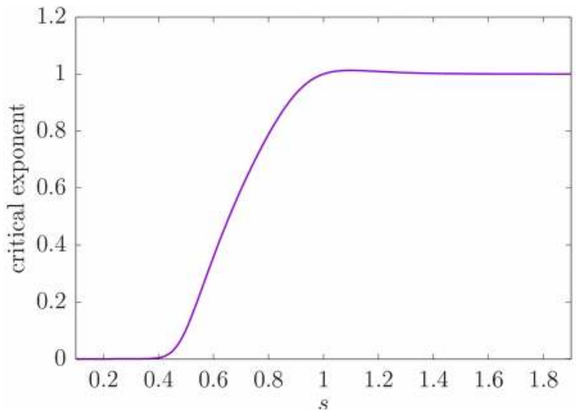

Figure 1: critical exponent as a function of the colored bath exponent s

interacts with a colored bath. We calculate the critical exponent of the superradiant phase transition and identify an inherent relation to the low-frequency spectral density function of the colored bath. Figure 1 explores the critical exponent as a function of the bath exponent s of the colored reservoir, where we assume that the spectral density function of the bath scales as $\rho(\omega) \sim \omega^s$. One observes that for a super-Ohmic bath ($s>1$) the exponent stays constant 1, that corresponds to the exponent of the open-system Dicke model [3]. Conversely, in the sub-Ohmic case ($s<1$) the critical fluctuations are significantly reshaped by the reservoir, and the exponent decreases monotonously with s. Furthermore we show that a finite temperature of the colored bath does not modify qualitatively this dependence.

[1] D. Nagy and P. Domokos, PRL 115, 043601 (2015)
[2] D. Nagy and P. Domokos, PRA 94, 063862 (2016)
[3] D. Nagy, G. Szirmai, and P. Domokos, PRA 84, 043637 (2011)

Exactly solvable time-dependent models of two interacting two-level systems

R. Grimaudo,[1,2] A. Messina,[1,2] and H. Nakazato[3]

[1] Dipartimento di Fisica e Chimica dell'Università di Palermo, Via Archirafi, 36, I-90123 Palermo, Italy.
[2] I.N.F.N., Sezione di Catania, Catania, Italy.
[3] Department of Physics, Waseda University, Tokyo 169-8555, Japan

SUMMARY

Two coupled two-level systems placed under external time-dependent magnetic fields are modelled by a general Hamiltonian endowed with a symmetry that enables us to reduce the total dynamics into two independent two-dimensional sub-dynamics. Each of the sub-dynamics is shown to be brought into an exactly solvable form by appropriately engineering the magnetic fields and thus we obtain an exact time evolution of the compound system. Several physically relevant and interesting quantities are evaluated exactly to disclose intriguing phenomena in such a system.

The simplest coupled spin system we may conceive consists, of course, of two interacting spin 1/2's only in a dimer, isolated from its environment (rest of the sample) degrees of freedom. Some binuclear copper(II) compounds, e.g. [1] [2], provide a possible scenario of this kind and in the previous references the values of the parameters characterizing the spin-spin interaction in such a molecule have been experimentally determined exploiting electron-paramagnetic resonance techniques. Motivations to investigate the emergence of quantum signatures in the behaviour of two coupled spins ($\geq 1/2$) go beyond the area of magnetic materials. Two spin 1/2 Hamiltonians provide indeed experimentally implementable powerful effective models to capture quantum properties of such systems like two coupled semiconductor quantum dots [3] or a pair of two neutral cold atoms each nested into two adjacent sites of an optical lattice made up of an isolated double wells [4]. Spin models provide a successful language to investigate possible manipulations of the qubits aimed at quantum computing purposes and quantum information transfer between two spin-qubits [5], encompassing rather different physical contents like, for example, cavity QED [6] [7], superconductors [8] [9] and trapped ions [10] [11].

In this paper we investigate a Hamiltonian model general enough and not commutating with $\hat{\mathbf{S}}^2$ and $\hat{S}^z$, but such to posses a symmetry property at the origin of significant properties characterizing its quantum dynamics. A peculiar aspect of such a symmetry property is that it displays its usefulness even when we wish to study our physical system in a time-dependent scenario. Exploiting, indeed, the symmetry-induced reduction of the quantum dynamics generated by the time-dependent Hamiltonian we are going to propose to two dynamically invariant proper subspaces of $\mathscr{H}$, we are able to successfully apply a recently reported [12] systematic approach for generating exactly solvable quantum dynamics of a single spin 1/2 subjected to a time-dependent magnetic field. Thus the main result of this paper is twofold. First we report the exact explicit solution of the time-dependent Schrödinger equation of a system of two coupled spin 1/2's described by a time-dependent generalized Heisenberg model. Second, we demonstrate that the method reported in Ref. [12], even as it stands, proves to be a useful tool to treat more complex time-dependent scenarios.

[1] L. M. B. Napolitano, O. R. Nascimento, S. Cabaleiro, J. Castro and R. Calvo, Phys. Rev. B **77**, 214423 (2008).
[2] R. Calvo, J. E. Abud, R. P. Sartoris and R. C. Santana, Phys. Rev. B **84**, 104433 (2011).
[3] M. C. Baldiotti, V. G. Bagrov and D. M. Gitman, Physics of Particles and Nuclei Letters, Vol. **6**, No. 7 (2009).
[4] M. Anderlini, P. J. Lee, B. L. Brown, J. Sebby-Strabley,2, W. D. Phillips and J. V. Porto, Nature **448**, 452-456 (2007).
[5] Van Hieu Nguyen, J. Phys.: Condens. Matter **21** 273201 (2009).
[6] A. Imamoglu, D. D. Awschalom, G. Burkard, D. P. DiVincenzo, D. Loss, M. Sherwin, and A. Small, Phys. Rev. Lett. **83**, 4204 (1999).
[7] Shi-Biao Zheng and Guang-Can Guo, Phys. Rev. Lett. **85**, 2392 (2000).
[8] Xiaoguang Wang, Phys. Rev. A **64**, 012313 (2001).
[9] M. C. Arnesen, S. Bose, and V. Vedral, Phys. Rev. Lett. **87**, 017901 (2001).
[10] X. X. Yi, H. T. Cui, and L. C. Wang, Phys. Rev. A **74**, 054102 (2006).
[11] D. Porras and J. I. Cirac, Phys. Rev. Lett. **92**, 207901 (2004).
[12] A. Messina and H. Nakazato, J. Phys. A: Math. Theor. **47**, 445302 (2014).

Dissipative optomechanical preparation of macroscopic spatial superpositions

C. Navarrete-Benlloch[1], M. Abdi[2], P. Degenfeld-Schonburg[3], M. Sameti[4], and M. J. Hartmann[4]

(1) Max-Planck Institute for the Science of Light, Stadtstrasse 2, 91052 Erlangen, Germany
(2) Institut für Theoretische Physik, Albert-Einstein-Allee 11, Universität Ulm, 89069 Ulm, Germany
(3) Physik Department, Technische Universität München, James-Franck-Strasse 1, 85748 Garching, Germany
(4) Institute of Photonics and Quantum Sciences, Heriot-Watt University, Edinburgh EH14 4AS, United Kingdom

Over the last century, many experiments have proven our ability to create superpositions of mutually exclusive states in the microscopic realm. And yet, this property does not seem to be naturally carried on to our every-day macroscopic world. How to transition from quantum to classical physics remains one of the most relevant open questions in modern science, and experiments aiming at generating spatial superpositions of macroscopic objects hold the promise of shining light onto the matter.

So far, there have been several impressive experiments exploring the regime of low mass but large spatial separation, reaching figures such as 0.3mm for molecules with 10000amu or 0.5m for Rubidium atoms. On the other hand, in the last two decades have brought promising proposals for the exploration of the large-mass regime with opto- and electromechanical systems [1]. These range from the original visionary proposals of Mancini, Man'ko, and Tombesi [2] or Bose, Jacobs, and Knight [3], to the most recent ones of Romero-Isart making use of superconducting levitating spheres rolling down a magnetic skate park [4].

All these proposals are based on coherent dynamics, and try to avoid dissipation as much as possible. The main difference of our proposal is that we tailor dissipation in such a way that the spatial superposition is obtained as a robust steady state [5].

Our proposal [5] makes use of state-of-the-art electromechanical and solid-state technology. As shown in Fig. 1, it consists of a membrane capacitively coupled to a linear superconducting circuit [6]. Typical membranes move in a parabolic potential, but here we show to engineer a double-well potential instead. Then, we show how to use the microwave modes of the circuit to sideband-cool the membrane to its ground state, which is the spatial superposition.

We identify lithium-decorated monolayer graphene sheets, which have become recently available [7], as the most suited candidate for membranes with the required properties (e.g., large Young modulus, zero-point motion, and electrostatic response, and superconducting below 6K). Using realistic parameters available in current labs, we show that it is possible to cool down the 10^8amu membrane to a steady state with 80% of occupation in a large-spatial separation state (6 times the zero-point motion).

Finally, we discuss the prospects of the setup for testing the quantum-to-classical transition through bounds in collapse models, and explain how to probe this via standard population measurements on an additional qubit.

[1] Rev. Mod. Phys. **86**, 1391 (2014); [2] Phys. Rev. A **55**, 3042 (1997); [3] Phys. Rev. A **56**, 4175 (1997); [4] arXiv: 1612.04290; [5] Phys. Rev. Lett. **116**, 233604 (2016); [6] Nature **471**, 204 (2011); [7] J. Electrochem. Soc. **157**, A558 (2010); Nature Physics **8**, 131 (2012); Proc. Natl. Acad. Sci. U.S.A. **112**, 11795 (2015).

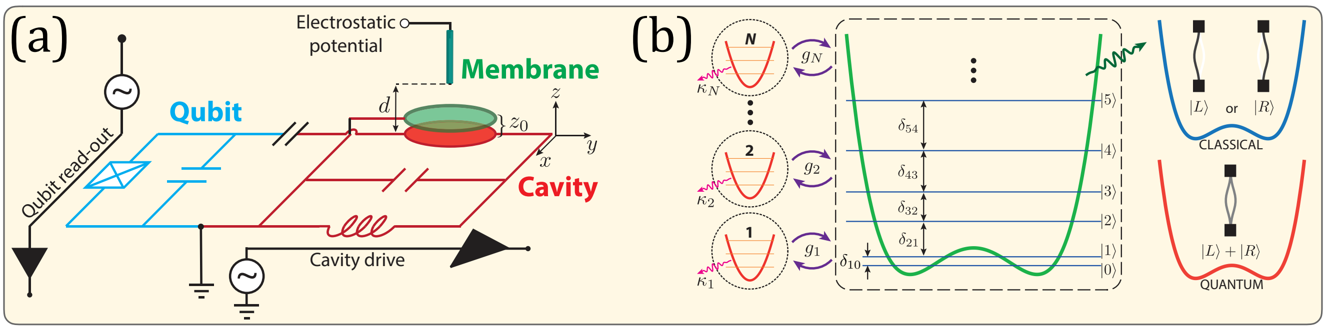

Fig 1. (a) Sketch of the electromechanical proposal. (b) Microwave modes perform sideband cooling of the membrane moving in a double-well potential. For effective temperatures below the gap, the steady state approaches the desired spatial superposition; otherwise, it is a balanced mixture of states localized around the potential minima.

Jaynes' Principle for Quantum Markov Processes

Authors
J. Novotný[1], J. Maryška[1], I. Jex[1]

Affiliation:

1) Department of Physics, FJFI ČVUT vPraze, Břehová 7, 115 19 Praha 1, Czech Republic

Jaynes' principle of maximum entropy has found applications in many different domains of science like e.g. neurobiology, economy, image processing, language processing, computer learning. The truly first motivation came from statistical physics with an effort to relate equilibrium macroscopic properties of complex physical systems to laws governing evolution of its individual constituents. According to Jaynes' principle [1], a macroscopic system evolves towards an equilibrium state which is characterized by the maximum of its entropy under given constrains (usually represented by integrals of motion). Consequently, the corresponding macroscopic equilibrium is described by so-called Gibbs state which surprisingly involve only a few parameters like temperature and number of particles. Recently it has been found that Gibbs states can be employed in the description of equilibrium quantum states also on smaller scales [2].

In which situations, whether at all, or why the maximum entropy principle could be the proper recipe for constructing the quantum equilibrium state remain fairly open questions. In our work we investigate equilibrium states in the context of quantum Markov processes (including both discrete quantum Markov chains and continues quantum dynamical semigroups). For a broad class of homogeneous quantum Markov processes possessing a faithful invariant state we identify their asymptotic states as well as their integrals of motion and show that equilibration within quantum Markov processes follows, in general, different Jaynes' principle which only for a certain subset of quantum Markov processes coincides with the maximum entropy principle. Moreover, taking into account mutual algebraic relationships between their stationary states and integrals of motion, one can show that all resulting equilibrium states can be taken into a generalized Gibbs state form. Remarkably, all well known statistical relations for mean ensemble values of integrals of motion (or their changes) stay untouched.

[1] E. T. Jaynes, *Physical Review. Series II* **106**, 620-630 (1957)
[2] M. Rigol, V. Dunjko, and M. Olshanii, *Nature* **452**, 854-858, (2008)

Quasi-continuous variable quantum computation with collective spins in multi-path interferometers

Tomáš Opatrný, Palacký University, Olomouc, Czech Republic

Collective spins of large atomic samples trapped inside optical resonators can carry quantum information that can be processed in a way similar to quantum computation with continuous variables. It is shown here that by combining the resonators in multi-path interferometers one can realize coupling between different samples, and that polynomial Hamiltonians can be constructed by repeated spin rotations and twisting induced by dispersive interaction of the atoms with light [T. Opatrný, arXiv:1702.03124].

Denoting by X, Y, Z the collective atomic spin operators commuting as $[X, Y] = iZ$, $[Y, Z] = iX$, and $[Z, X] = iY$, it was shown [Schleier-Smith et al., PRA **81,** 021804(R) (2010)] that the scheme in Fig. 1a can generate spin-squeezing Hamiltonian $\propto Z^2$ (for simplicity we use here X, Y, Z rather than the more common notation $J_{x,y,z}$). This is achieved by the ac-Stark shift of the atoms by the resonator field whose intensity is influenced by the atomic state. Here we present a method to construct two-mode quantum non-demolition Hamiltonians (Fig. 1b)

$$H_{\rm QND} = \hbar\chi Z_1 Z_2, \tag{1}$$

as well as a method to construct higher-power Hamiltonians by means of Bloch-sphere rotations and commutators as $e^{-iA\Delta t}e^{-iB\Delta t}e^{iA\Delta t}e^{iB\Delta t} = e^{[A,B]\Delta t^2} + \mathcal{O}(\Delta t^3)$. Thus one can construct, e.g., a cubic Hamiltonian

$$X^3 = \frac{i}{4}\left[(X^2 - Y^2), (YZ + ZY)\right] + \frac{i}{4}\left[(XZ + ZX), (XY + YX)\right] + \frac{1}{4}X, \tag{2}$$

or a two-mode Hamiltonian

$$X_1^3 Z_2 = \frac{1}{4}X_1 Z_2 + \frac{1}{4}\left[(Z_1^2 - Y_1^2), \left[Z_1^2, X_1 Z_2\right]\right] - \frac{1}{4}\left[X_1 Z_1 + Z_1 X_1, \left[X_1^2, Z_1 Z_2\right]\right]. \tag{3}$$

Scaling this up, by employing multi-path interferometers with several optical resonators as in Fig. 1c, one can construct multi-mode Hamiltonians that can realize quantum computation with quasi-continuous variables X_k in a similar way as originally suggested for continuous-variable quantum computation [Lloyd and Braunstein, PRL **82,** 1784 (1999)]. Applications can be expected especially in efficient simulation of quantum systems.

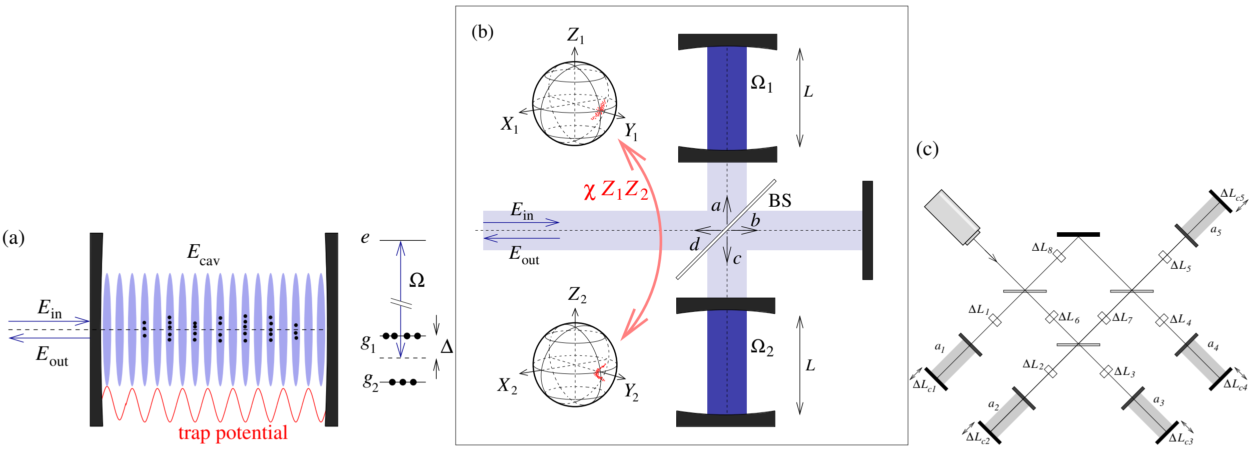

Figure 1: (a) Scheme of the resonator with trapped atoms. (b) Michelson-like interferometer with two resonators. (c) Interferometer with 5 resonators with atomic samples.

Multipartite measurement-device independent quantum conferencing [1]

Carlo Ottaviani, Cosmo Lupo, Stefano Pirandola
Computer Science and York Centre for Quantum Technologies, University of York, York YO10 5GH, UK

Today, much of the effort in quantum key distribution (QKD) protocols is devoted in developing solutions to increase the key rate. At the same time, it is desirable to move towards a full end-to-end network scenario. Continuous variable (CV) systems can offer a solution to both these problems: Using bright coherent states and efficient homodyne detection, one can increase the key rate; then, adopting the configuration of measurement-device independent (MDI) QKD, one can make the first step towards the end-to-end principle. For this reason, CV-MDI-QKD protocols [2, 3] are appealing for quantum networks, especially at the metropolitan distances [4].

In this work we extend CV-MDI-QKD to a multipartite symmetric configuration (star network), where N Bobs send N modulated coherent states to an untrusted relay which performs a multipartite Bell detection. The outcomes γ's are broadcast to the parties. The resulting post-relay N-partite state can then be exploited for private communication, with the trusted parties extracting N keys, that are used to distill a single conference key.

In the fully symmetric configuration the parties are equidistant from the relay and the action of the eavesdropper (Eve) is described by a memory-less thermal channel. The performances of the scheme are quantified in terms of achievable key-rate and distances for fixed number of parties. We perform the security analysis in the entanglement-based representation. Using the Devetak-Winter security criterion, we bound Eve's information by the Holevo function

$$\chi = 2h(\nu) - h(\nu_N), \qquad (1)$$

where $\nu = [\mu\,[\eta + \omega\mu(1-\eta)]\,/\,(\eta\mu + (1-\eta)\omega)]$,

$$h(x) = \frac{x+1}{2}\log_2\frac{x+1}{2} - \frac{x-1}{2}\log_2\frac{x-1}{2}, \qquad (2)$$

and ν_N is a symplectic eigenvalue depending on the number of users N.

From the post-relay CM $\mathbf{V}_{i|\gamma}$, associated with the ith Bob, and from the conditional CM $\mathbf{V}_{i|\gamma\beta_j}$, after heterodyne detection by jth, we obtain the mutual information between two arbitrary Bobs $I_{B_iB_j} = \frac{1}{2}\log\Sigma$, where Σ depends on $\mathbf{V}_{i|\gamma}$ and $\mathbf{V}_{i|\gamma\beta_j}$. We finally get key conference key rate

$$R = \frac{1}{2}\log\Sigma - 2h(\nu) + h(\nu_N). \qquad (3)$$

The figure shows the optimal rate for $N = 2$ (black), 10 (gray), 100 (red) users, assuming no thermal noise (solid lines), 0.01 thermal noise (dashed lines), and 0.1 thermal noise (dotted lines).

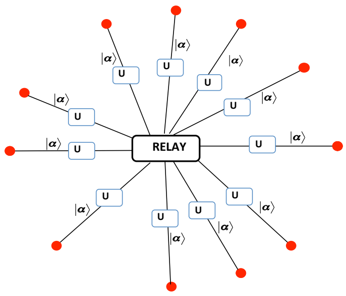

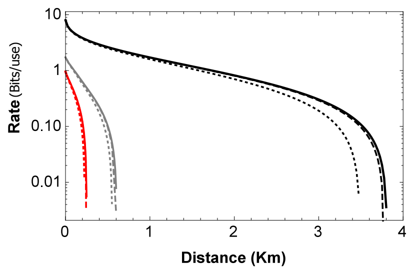

In summary we found that high-rate quantum conference-key-agreement is possible over distances between hundreds of meters and a few kilometers, with a large number of users.

[1] C. Ottaviani, C. Lupo, S. Pirandola, *in preparation.*
[2] S. Pirandola *et al.*, Nature Photon. **9**, 397-402 (2015).
[3] C. Ottaviani *et al.*, Phys. Rev. A **91**, 022320 (2015).
[4] Pirandola S. *et. al.*, Nature Photonics **9**, 773-775 (2015).

Thermal state and CV-MDI-QKD with efficient channel parameter estimation

Panagiotis Papanastasiou, Carlo Ottaviani, and Stefano Pirandola
Department of Computer Science and York Centre for Quantum Technologies, University of York, York YO10 5GH, United Kingdom

(Dated: March 30, 2017)

Quantum cryptography with continuous variables (CV) is rapidly moving towards the implementation in realistic scenarios. For these practical purposes it is important to quantify the performances of the protocols taking into account finite size effects. These emerge when we assume that the parties share a finite number of signals, from which they have to estimate the channel's parameters and prepare the secret key.

In Ref. [1], it has been developed an efficient methodology to accomplish this task, and here we adapt it so as to develop a finite size analysis of one-way thermal and measurement-device independent (MDI) protocols.

The former is when the parties use states with preparation imperfections to encode their variables, which are a result of trusted thermal noise [2, 3]. This noise can be used as a defence against eavesdropping attacks for the direct reconciliation protocols. In addition, using thermal states we can extend the security of the protocol to lower electromagnetic frequencies, e.g. for microwave telecommunications. On the other hand, in MDI protocols [4, 5] the parties, who cannot access a direct link, extract the secret key with the assistance of an intermediate relay operating as a correlator. This configuration can be used as a basis for end-to-end quantum key distribution (QKD) networks, and evolve to protocols for quantum cryptographic conferencing.

For the one-way protocols, we adapted the formula for the secret key rate for finite size effects in the case of thermal states, where we have taken into consideration that part of the signals exchanged were used for the channel parameter estimation. We expressed the rate with respect to the classical modulation V_M, the reconciliation parameter β, the block size number N and the relevant channel parameters transmissivity τ and excess noise variance V_ϵ. For the last two, we defined estimators dependent on the number m of the signals sacrificed.

Then we calculated theoretically their variances and defined confidence intervals. We chose the most pessimistic values from these intervals, so as not to underestimate eavesdropping. This allows us to plot the secret key rate for any block size number by replacing these values into the secret key rate formula. Finally, we optimized over the signals sacrificed for each channel transmissivity. In Fig. 1, we have plotted the finite size key rate for the direct reconciliation no switching protocol in the asymptotic regime (red line) and incorporating finite size effects (black line). By this plot, we are able to quantify the ratio of the finite size effects rate over the asymptotic rate for a given channel loss in dB.

In the MDI protocol, we followed almost the same process. We defined the relevant channel parameters according to the more involved topology of the scheme, which are the two transmissivities and the channel excess noise variances for the two quadratures. For the corresponding plots, for $\tau_A = 0.95$, we calculated the ratio in case of $N = 10^6$ compared with the asymptotic rate. For instance, for channel loss around to $1.2\,dB$ the ratio is roughly around $\simeq \frac{1.5\times10^{-2}}{4\times10^{-2}} = 37.5\%$.

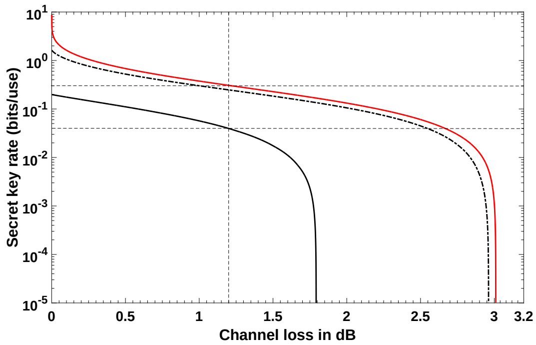

FIG. 1. **The secret key rate with finite size effects for the direct reconciliation protocol without switching in case of a pure loss channel.** We plotted the cases of $N = 10^6$ (black solid line) and $N = 10^9$ (black dashed-dotted line) and optimized over V_M and $r = \frac{m}{N}$ for $\beta = 1$. We also plotted the asymptotic rate for $\beta = 1$ and $V_M = 10^6$ (red line). For example, we calculated the ratio of the $N = 10^6$ case for channel loss around to $1.2\,dB$ to be roughly $\simeq \frac{4\times10^{-2}}{2\times10^{-2}} = 0.8$, which implies that for $N = 10^6$ we can achieve an 80% of the asymptotic rate

[1] L. Ruppert, V. C. Usenko, and R. Filip, Phys. Rev. A **90**, 062310 (2014).
[2] R. Filip, Phys. Rev. A **77**, 022310 (2008).
[3] C. Weedbrook, S. Pirandola, and T. C. Ralph, Phys. Rev. A **86**, 022318 (2012).
[4] S. Prandola, C. Ottaviani, C. Spedalieri, Gaetana ands Weedbrook, S. L. Braunstein, S. Lloyd, T. Gehring, C. S. Jacobsen, and U. L. Andersen, Nat Photon **9**, 397 (2015).
[5] C. Ottaviani, G. Spedalieri, S. L. Braunstein, and S. Pirandola, Phys. Rev. A **91**, 022320 (2015).

Manifesting nonclassicality beyond Gaussian states by observing a single marginal distribution

Jiyong Park,[1,*] Yao Lu,[2] Jaehak Lee,[1] Yangchao Shen,[2] Kuan Zhang,[2] Shuaining Zhang,[2] M. Suhail Zubairy,[3] Kihwan Kim,[2,†] and Hyunchul Nha[1,‡]

[1] *Department of Physics, Texas A&M University at Qatar, Education City, P.O.Box 23874, Doha, Qatar*
[2] *Center for Quantum Information, Institute for Interdisciplinary Information Sciences, Tsinghua University, Beijing 100084, Peoples Republic of China*
[3] *Department of Physics and Institute of Quantum Studies, Texas A&M University, College Station, TX 77843, USA*

We theoretically propose and experimentally demonstrate a method to manifest nonclassicality by observing a single marginal distribution alone [1].

Our method proceeds as follows (See Fig. 1 for illustration). Given a state with its Wigner function $W_\rho(q,p)$, we measure a marginal distribution $M_\rho(x)$ along a certain axis, $x = q\cos\theta + p\sin\theta$. We then construct a fictitious, factorized, Wigner function $W_\rho^{\mathrm{DM}}(x,y)$ either by replicating the obtained distribution as $M_\rho(x)M_\rho(y)$ (DM1) or by multiplying the marginal distribution of a vacuum state as $M_\rho(x)M_{|0\rangle\langle 0|}(y)$ (DM2), with $M_{|0\rangle\langle 0|}(y) = \sqrt{\frac{2}{\pi}}e^{-2y^2}$. We test whether $W_\rho^{\mathrm{DM}}(x,y)$ is a legitimate Wigner function to represent a physical state [2]. As every classical state yields a legitimate Wigner fuctnion under the procedure, we can confirm the nonclassicality of the measured state when the output Wigner fuction $W_\rho^{\mathrm{DM}}(x,y)$ fails to be physical.

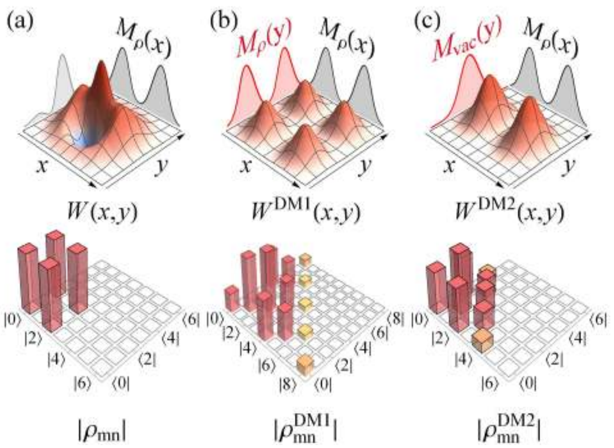

FIG. 1. Illustration of our approach for nonclassicality tests. (a) original Wigner function $W_\rho(x,y)$ of $|\Psi\rangle = \frac{1}{\sqrt{2}}(|0\rangle + |2\rangle)$, with its marginal $M_\rho(x) = \int dy W_\rho(x,y)$ in the backdrop, (b) a fictitious Wigner function $W^{\mathrm{DM1}}(x,y) \equiv M_\rho(x)M_\rho(y)$, with the same distribution $M_\rho(y)$ replicated along the orthogonal axis (red solid curve), and (c) $W^{\mathrm{DM2}}(x,y) \equiv M_\rho(x)M_{|0\rangle\langle 0|}(y)$, with the vacuum-state distribution $M_{|0\rangle\langle 0|}(y)$ used (red solid curve). The second panels show the corresponding density matrix elements. $W^{\mathrm{DM1}}(x,y)$ and $W^{\mathrm{DM2}}(x,y)$ in (b) and (c) do not represent any physical states, confirming the nonclassicality of $|\Psi\rangle$.

Our approach detects a broad class of nonclassical states beyond squeezed states, and also yields a lower bound for entanglement potential, i.e., a measure of entanglement generated using a nonclassical state with a beam splitter setting [3]. Remarkably, our method works regardless of measurement axis for all non-Gaussian states in finite-dimensional Fock space of any size, which also extends to infinite-dimensional states of experimental relevance for CV quantum informatics. We experimentally illustrate the power of our criterion for motional states of a trapped ion confirming their nonclassicality in a measurement-axis independent manner. We also address an extension of our approach combined with phase-shift operations, which leads to a stronger test of nonclassicality, i.e. detection of genuine non-Gaussianity under a CV measurement in contrast to the previously suggested methods [4–6].

* jiyong.park@qatar.tamu.edu
† kimkihwan@mail.tsinghua.edu.cn
‡ hyunchul.nha@qatar.tamu.edu

[1] J. Park, Y. Lu, J. Lee, Y. Shen, K. Zhang, S. Zhang, M. S. Zubairy, K. Kim, and H. Nha, Proc. Natl. Acad. Sci. **114**, 891–896 (2017).
[2] H. Nha, Phys. Rev. A **78**, 012103 (2008).
[3] J. K. Asbóth, J. Calsamiglia, and H. Ritsch, Phys. Rev. Lett. **94**, 173602 (2005).
[4] R. Filip and L. Mišta, Jr., Phys. Rev. Lett. **106**, 200401 (2011); M. Ježek, I. Straka, M. Mičuda, M. Dušek, J. Fiurášek, and R. Filip, *ibid.* **107**, 213602 (2011); I. Straka, A. Predojević, T. Huber, L. Lachman, L. Butschek, M. Miková, M. Mičuda, G. S. Solomon, G. Weihs, M. Ježek, and R. Filip, *ibid.* **113**, 223603 (2014).
[5] M. G. Genoni, M. L. Palma, T. Tufarelli, S. Olivares, M. S. Kim, and M. G. A. Paris, Phys. Rev. A **87**, 062104 (2013); C. Hughes, M. G. Genoni, T. Tufarelli, M. G. A. Paris, and M. S. Kim, *ibid.* **90**, 013810 (2014).
[6] J. Park, J. Zhang, J. Lee, S.-W. Ji, M. Um, D. Lv, K. Kim, and H. Nha, Phys. Rev. Lett. **114**, 190402 (2015); J. Park and H. Nha, Phys. Rev. A **92**, 062134 (2015).

Spatially multimode quantum memories for light based on atomic ensembles

Michał Parniak*, Michał Dąbrowski, Wojciech Wasilewski
Institute of Experimental Physics, Faculty of Physics, University of Warsaw, Pasteura 5, 02-093 Warsaw, Poland
** michal.parniak@fuw.edu.pl*

Spatial degree of freedom becomes increasingly useful in quantum optics and quantum information processing. Raman scattering in atomic ensembles enables generation and delayed retrieval of spatilally multimode quantum states of light [1], although it is more commonly used in the single-mode regime enabling versatile quantum memories [2] and communication with the DLCZ protocol [3].

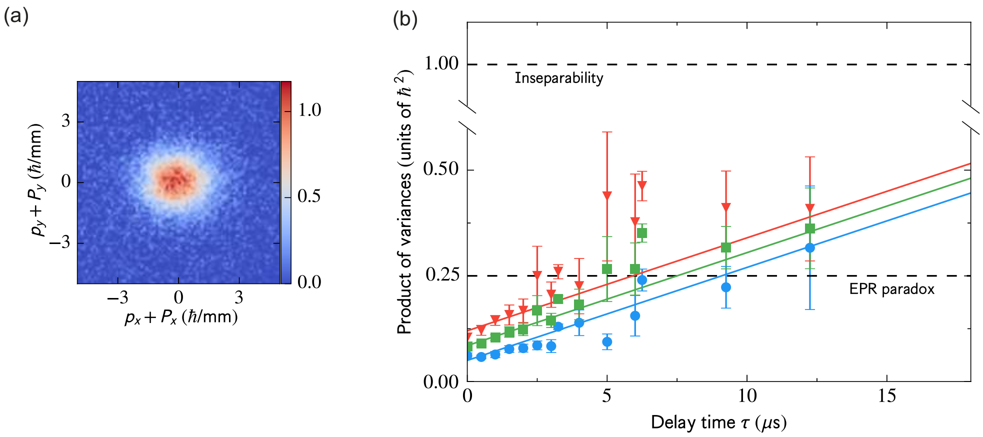

Fig. 1. (a) Exemplary coincidence histogram of momenta of registered photons expressed in terms of composite variables – sum of momenta of a photon and a corresponding collective atomic excitation. (b) Product of variances inferred from coincidence histograms for momenta and positions for a set of quantum memory storage times. The product is well below the classical limit remains in the region in which we witness the EPR paradox for as long as 6 μs.

Here we demonstrate [4] generation of a spatially entangled state of a photon and single collective atomic excitation. We use an ensemble of 10^12 warm Rubidium atoms immersed in Xenon to slow down motional decoherence. A pulse of coherent light drives the squeezing interaction, creating pairs of photons and associated spin-waves. Since the interaction is spatially-multimode, photons will have their momenta anti-correlated with spin-wave spatial trasverse wavevectors. Simultaneously, positions of spin-waves and photons will be correlated.

After a certaion delay time we send another pulse of coherent light to convert the atomic spin-wave excitation to another photon. By measuring photon pairs on the state-of-the-art sCMOS camera equipped with a gated image intensifier we are able to witness spatial entanglement in approximately 12 Schmidt modes. The generated state exhibits the famous Einstein-Podolsky-Rosen (EPR) paradox [5], previously demonstrated in a analgous SPDC sources, without variable delay time [6].

Our results pave the wave towards quantum control of multiple spin-wave excitations in atomic ensembles. In particular, current setup based on a magneto-optical trap allows for storage of many more modes with delay times reaching hundreds of microseconds, thus allowing subtle conditional manipulation of atomic state with the help of external fields.

[1] R. Chrapkiewicz, M. Dąbrowski and W. Wasilewski, "High-Capacity Angularly Multiplexed Holographic Memory Operating at the Single-Photon Level", Phys. Rev. Lett. **118**, 063603 (2017)
[2] M. Hosseini et al. "Coherent optical pulse sequencer for quantum application", Nature **461**, 241-245 (2009)
[3] L. M. Duan et al., "Long-distance quantum communication with atomic ensembles and linear optics", Nature **414**, 413-418 (2001)
[4] M. Dąbrowksi, M. Parniak and W. Wasilewski, "Einstein-Podolsky-Rosen paradox in a hybrid bipartite system", Optica **4**, 272-275 (2017)
[5] A. Einstein, B. Podolsky and N. Rosen, "Can Quantum-Mechanical Description of Physical Reality Be Considered Complete?", Phys. Rev. **47**, 777 (1935)
[6] P.-A. Moreau, F. Devaux and E. Lantz, "Einstein-Podolsky-Rosen Paradox in Twin Images", Phys. Rev. Lett. **113**, 160401 (2014)

Experimental generation of higher-order non-classical states

Jan Peřina Jr.,[1,*] Ievgen Arkhipov,[1] Václav Michálek,[2] and Ondřej Haderka[2]

[1]*RCPTM, Joint Laboratory of Optics of Palacký University and Institute of Physics of the Czech Academy of Sciences, Faculty of Science, Palacký University, 17. listopadu 12, 77146 Olomouc, Czech Republic*

[2]*Institute of Physics of the Czech Academy of Sciences, Joint Laboratory of Optics of Palacký University and Institute of Physics of CAS, 17. listopadu 50a, 772 07 Olomouc, Czech Republic*

Using the postselection method of generating sub-Poissonian states from weak twin beams whose one arm is monitored by a photon-number-resolving detector (iCCD camera) [1] we experimentally generated quantum fields with higher-order non-classicalities observed in different quantities. We have defined suitable quantifiers for higher-order non-classicalities using moments of intensity, photon-number, intensity fluctuation and photon-number fluctuation. Complementary, also individual elements of photocount (photon-number) distributions were used to quantify higher-order non-classicalities via suitable parameters.

The post-selected fields with mean photon numbers varying from 7 to 15 were monitored again by an iCCD camera with quantum detection efficiency better than 20 % and negligible dark counts. Higher-order non-classicalities were investigated both directly for the measured photocount histograms and the reconstructed photon-number distributions reached by the maximum-likelihood reconstruction [2] and also that based on a suitable physically-motivated multi-Gaussian fit [3].

High number of measurement repetitions (1.2 million times) resulted in the very low experimental errors that allowed to observe the higher-order nonclassicalities up to the fifth order in parameters $r_W^{(k)}$ exploiting intensity moments $\langle W^k \rangle$ [4]:

$$r_W^{(k)} \equiv \frac{\langle W^k \rangle}{\langle W \rangle^k} - 1 < 0, \qquad k = 2, \ldots . \tag{1}$$

In parameters $r_p^{(k)}$ defined in terms of the modified photon-number elements $\tilde{p}(k) \equiv k! p(k)/p(0)$ [$p(k)$ denote the usual photon-number elements],

$$r_p^{(k)} \equiv \frac{\tilde{p}(k)}{\tilde{p}(1)^k} - 1 < 1, \qquad k = 2, \ldots , \tag{2}$$

even the ninth-order non-classicality has been experimentally reached directly in the photocount histograms, as documented in Fig. 1. Up to our best knowledge, this is by far the highest order of a non-classical effect observed up to now.

The authors acknowledge support from project No. 15-08971S of the Grant Agency of the Czech Republic.

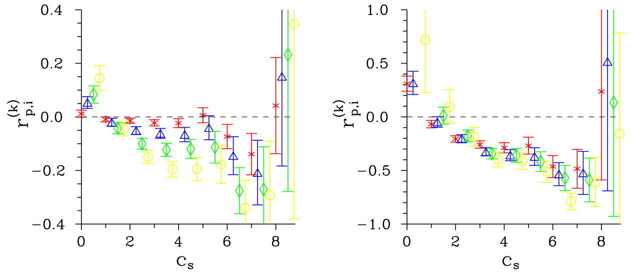

(a) (b)

FIG. 1: [Color online]: Parameters $r_{p,i}^{(k)}$ of the post-selected photocount idler fields for (a) [(b)] $k = 2$ [6] (red $*$), 3 [7] (blue $\triangle$), 4 [8] (green $\diamond$), and 5 [9] (yellow $\circ$) as they depend on signal photocount number c_s.

* Electronic address: jan.perina.jr@upol.cz

[1] J. Peřina Jr., O. Haderka and V. Michálek, Sub-Poissonian-light generation by postselection from twin beams, Opt. Express 21, 19387 (2013).

[2] J. Peřina Jr., O. Haderka, M. Hamar, V. Michálek, Photon-number distributions of twin beams generated in spontaneous parametric down-conversion and measured by an intensified CCD camera, Phys. Rev. A 85, 023816 (2012).

[3] J. Peřina Jr., O. Haderka, V. Michálek and M. Hamar, State reconstruction of a multimode twin beam using photodetection, Phys. Rev. A 87, 022108 (2013).

[4] I. I. Arkhipov, J. Peřina Jr., O. Haderka and V. Michálek, Experimental detection of nonclassicality of single-mode fields via intensity moments, Opt. Express 24, 29496 (2016).

Linear and nonlinear quantum divergence as witnesses of quantum chaotic dynamics – nonlinear Kerr-like oscillator case

Joanna K. Kalaga,[1,*] Wiesław Leoński,[1] and J. Peřina Jr.[2]
[1]*Quantum Optics and Engineering Division, Institute of Physics, University of Zielona Góra, Z. Szafrana 4a, 65-516 Zielona Góra, Poland*
[2]*RCPTM, Joint Laboratory of Optics of Palacký University and Institute of Physics of the Czech Academy of Sciences, Faculty of Science, Palacký University, 17. listopadu 12, 771 46 Olomouc, Czech Republic*

We consider a system involving an anharmonic quantum oscillator driven by a series of ultra-short external pulses [1]. The time-evolution of such system is governed by the following Hamiltonian:

$$\hat{H} = \frac{\chi}{2}\left(\hat{a}^\dagger\right)^2\hat{a}^2 + \epsilon\left(\hat{a}^\dagger + \hat{a}\right)\sum_{k=1}^{\infty}\delta(t - kT)\,, \qquad (1)$$

where the parameter χ is the nonlinearity constant, ϵ describes the strength of the interaction with external field, whereas $\hat{a}$ and $\hat{a}^\dagger$ are boson annihilation and creation operators, respectively. We can model the series of ultrashort pulses by use of Dirac-delta functions $\delta(t - kT)$ where T denotes the time-interval between two subsequent pulses labeled by k.

To detect chaotic behaviour in a quantum system's evolution we apply the Kullback - Leibler (KL) quantum divergence K_{KL} [2–4]

$$K_{KL}[\rho \parallel \sigma] = Tr[\rho(\ln\rho - \ln\sigma)]\,, \qquad (2)$$

where ρ denotes the density matrix corresponding to the situation when external coupling is equal to ϵ, whereas the matrix σ describes the system when external coupling is slightly perturbed, *i.e.* $\epsilon \to \epsilon + \Delta$. Such divergence allows to determine the "distance" between two density matrices ρ and σ and then, the difference between two quantum states.

In our study we do not apply the exact definition of KL quantum divergence. Instead of it we define two new parameters – linear quantum divergence (LQD) and its nonlinear counterpart (NQD). In equation (2) logarithm functions appear and they can be presented in a form of their series expansions

$$\ln\rho - \ln\sigma = \sum_{n=1}^{\infty}(-1)^{n+1}\frac{(\rho-1)^n}{n} - \sum_{n=1}^{\infty}(-1)^{n+1}\frac{(\sigma-1)^n}{n}. \qquad (3)$$

To define LQD we take into account only first (linear) terms of such expansions. Therefore, by replacing the logarithms of σ and ρ by first terms of their expansions, we obtain a formula defining LQD. It can be written as:

$$K_{KL}^{(1)} = Tr\left[\rho\left(\rho - \sigma\right)\right]. \qquad (4)$$

Analogously, we can define the second parameter – NQD. When we take the first two terms of the expansions, the formula defining NQD takes the following form:

$$K_{KL}^{(2)} = Tr\left[\rho\left(\rho - \frac{1}{2}\left(\rho - 1\right)^2 - \sigma + \frac{1}{2}\left(\sigma - 1\right)^2\right)\right], \qquad (5)$$

where the both linear and first nonlinear terms are involved.

In our communication we show that such defined two quantum parameters describing our model's dynamics can behave chaotically in a classical sense. The linear and nonlinear quantum divergences exhibit completely different characteristics for the regions corresponding to the regular and chaotic evolution. In consequence, the parameters proposed here can be applied as indicators of quantum chaotic behavior, allowing for the determination of boundaries between regular and chaotic dynamics of quantum systems.

---

* J.Kalaga@if.uz.zgora.pl

[1] W. Leoński, *Physica A*, 233:365, 1996.
[2] S. Kullback and R. A. Leibler, *Ann. Math. Stat.*, 22:79, 1951.
[3] S. Kullback Information theory and statistics, *John Wiley and Sons*, New York, 1959.
[4] H. Umegaki, *Kodai Math. Sem. Rep.*, 14:59, 1962.

Quantum Interference of Topological Edge States in an Array of Coupled Waveguides

Alberto Peruzzo [1], *Robert J. Chapman* [1], *Jean-Luc Tambasco* [1], *Giacomo Corrielli* [2,3], *Andrea Crespi* [2,3], *Oded Zilberberg* [4], *and Roberto Osellame* [2,3]

1. Quantum Photonics Laboratory and Centre for Quantum Computation and Communication Technology, School of Electrical and Computer Engineering, RMIT University, Melbourne, Victoria 3000, Australia

2. Istituto di Fotonica e Nanotecnologie, Consiglio Nazionale delle Ricerche, Piazza Leonardo da Vinci 32, 20133 Milano, Italy

3. Dipartimento di Fisica, Politecnico di Milano, Piazza Leonardo da Vinci 32, 20133 Milano, Italy

4. Institute for Theoretical Physics, ETH Zurich, 8093 Zurich, Switzerland

Integrated quantum photonics is an attractive platform for quantum information technology, holding great promise for future quantum computing, communication and metrology. However, loss and sensitivity to imperfections are currently a major drawbacks for this technology. Topological photonics offers robustness against inevitable fabrication imperfections [1]; the topological structure offers a method for engineering the band-structure of the material while allowing a single state to cross the structure during the propagation.

Arrays of coupled waveguides are widely used for studying quantum walks and transport in ideal and disordered systems. More recently, these "photonic quasi-crystals" have been used to demonstrate intriguing topological phases in a controlled manner by appropriately modulating the waveguide spacing and thus the implemented Hamiltonian [2, 3]. Edge states are a manifestation of the topology in such a photonic quasi-crystal, where light is confined to the edge of an array of coupled waveguides that follow the Aubry, André and Harper (AAH) model [4, 5]. While photonic topological states have been comprehensively reported [6, 1], the quantum interference of topological single photon states is yet to be explored.

Here, we implement an integrated topological beam splitter and demonstrate quantum interference of two single photon edge states. Our device is an array of coupled waveguides that follow the AAH model, such that we observe topological edge states (see Fig. 1a). We adiabatically transfer the edge states at either side of the device to a central region, where the beam splitter operation is applied. Finally the edge states are adiabatically transferred to the outside of the array again. The device is fabricated by the femtosecond laser written technique [7], and a schematic is shown in Fig. 1a including an experimentally measured intensity profile of the output using laser light to show the beam splitter operation applied to the edge states.

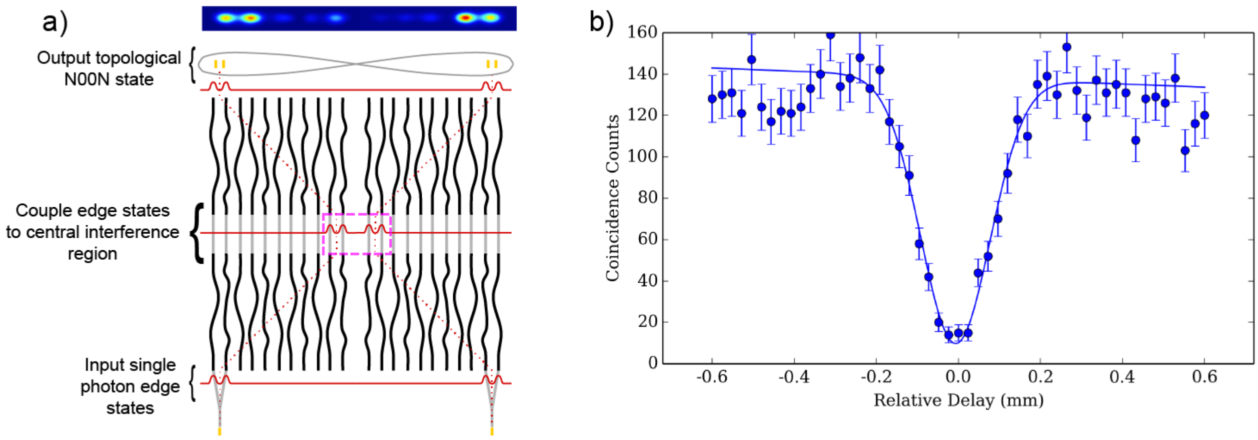

Fig 1 (a) Schematic of the topological beam splitter. The input topological edge states are adiabatically transferred to the centre of the waveguide array where they interfere and bunch. The top image shows the output of laser light injected into the array. (b) Hong-Ou-Mandel type interference of two single photon edge states observed by implementing a time delay and measuring the edge states in the coincidence basis.

We have implemented a 50/50 beamsplitter for topological states in a waveguide array and demonstrated the quantum interference of two single photon edge states, observing characteristic Hong-Ou-Mandel interference, which results in the two photons exiting the beam splitter in the same mode (Fig. 1b).

Our results show that we can utilise the topological structure of a quasi-crystal to engineer its band-structure for single photon experiments, for quantum photonics applications that can benefit from the robust nature of topological systems.

[1] Lu *et al.*, "Topological photonics", *Nat. Photon.* **8**, 821-829 (2014)
[2] Kraus *et al.*, "Topological States and Adiabatic Pumping in Quasicrystals", *Phys. Rev. Lett.* **109**, 106402 (2012)
[3] Rechtsman *et al*., "Photonic Floquet topological insulators", *Nature* **496**, 196–200 (2013)
[4] Aubry and André, "Analyticity breaking and Anderson localization in incommensurate lattices", *Ann. Israel Phys. Soc.* **3**, 133-140 (1980)
[5] Harper, "Single Band Motion of Conduction Electrons in a Uniform Magnetic Field", *Proc. Phys. Soc, Sect. A* **68**, 874 (1955)
[6] Hafezi *et al.*, "Imaging topological edge states in silicon photonics", *Nat. Photon.* **7**, 1001-1005 (2013)
[7] Sansoni *et al.*, "Two-Particle Bosonic-Fermionic Quantum Walk via Integrated Photonics", *Phys. Rev. Lett.* **108**, 010502 (2012)

Observation of localised multi-spatial mode quadrature squeezing

P. G. Petrov, J. H. Hordell, C. Gill, C. S. Embrey, M. T. Turnbull, and V. Boyer

Midlands Ultracold Atom Research Centre, School of Physics and Astronomy, University of Birmingham, Edgbaston, Birmingham B15 2TT, United Kingdom

Optical measurements, including optical imaging, are ultimately limited by the quantum fluctuations of the electromagnetic field. These fluctuations arise from the quantised nature of light and for a coherent state give rise to the so-called quantum noise level (QNL). In quantum optics, light field is described by non-commuting quadrature operators such as amplitude and phase. In this case the QNL for both quadratures is given by their uncertainty relation, which states that there is a minimum uncertainty with which given quadrature can be measured. It is however possible to reduce or squeeze this uncertainty below the QNL on one of the quadratures at the expense of the other, whereby generating quadrature squeezed light. Most of the current optical measurements benefit from employing single-transverse-mode-squeezed light as a means to improve signal-to-noise ratio. In the case of optical imaging applications where the full field-of-view is captured at once, the squeezing must extend to all transverse spatial modes. A special case of such multi-spatial-mode squeezing is realised when the field is squeezed locally at all points of its transverse profile.

In principle, all optical parametric amplifiers, such as nonlinear media supporting parametric down-conversion or four-wave-mixing, can generate local squeezing provided the nonlinearity is strong enough. In parametric down-conversion in a crystal however, the nonlinearity tends to be small and using a cavity to enhance it results in a single spatial mode to resonate and therefore to be squeezed. Here we use resonant four-wave-mixing in an atomic vapour to generate large single-pass gain and realise local squeezing.

The multi-spatial mode (MSM) nature of the generated light is revealed when the quantum field fluctuations are analysed by a narrow local oscillator (LO) homodyne detector arrangement as shown in the figure below.

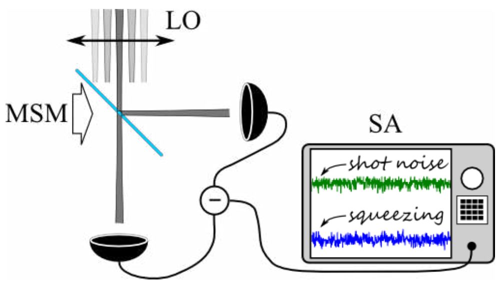

Figure 1. The homodyne detection of the squeezed field results in reduced noise on the balanced photocurrent, as observed by the spectrum analyser (SA). For a MSM state the LO can have any shape or position.

When a MSM squeezed state is analysed a significant level of squeezing is observed for a range of positions of the LO much larger than its waist. More than 75 independently squeezed regions or locales are observed [1]. This type of MSM squeezed light used as illumination in certain super-resolution imaging schemes should lead to improved optical resolution beyond the quantum noise limit.

[1]. C. S. Embrey et al, *Physical Review X*, **5**, 031004, (2015).

Microwave quantum cryptography

Carlo Ottaviani, Cosmo Lupo, Stefano Pirandola
Computer Science and York Centre for Quantum Technologies, University of York, York YO10 5GH, UK

In order to transform quantum key distribution (QKD) into a mature and appealing approach, able to compete with today's conventional cryptographic technology, several problems need yet to be solved. One of these is the implementation at the microwave regime, therefore exploitable in wireless communications. In this context, the appeal of continuous-variable (CV) systems [1] is that they naturally boost the communication rate.

This work investigates free-space thermal QKD at the microwave regime (see top-left and top-right figure), focusing on two distinct approaches. The first consider the Gaussian two-way protocol [2] with thermal states and homodyne detection, used in reverse reconciliation (RR). In this case we find (see bottom-right figure) a positive key rate at the microwave regime even for high loss, not so far from the recently computed secret-key capacity [3] (red line). The thermal variance is $\bar{V} \simeq 5 \times 10^3$, i.e., GHz range at room temperature.

In the second approach we design a novel one-way thermal protocol, with binary encoding and post-selection, which is inspired by the work of Ref. [4], and goes as follows: The sender, Alice, uses two thermal states ρ_u to encode a classical bit of information $u = 0, 1$ with probability $p(u) = 1/2$. The two thermal states have covariance matrix (CM) [1] $\mathbf{V} = 2(n+1)\mathbf{I}$, where $\mathbf{I}$ =diag$(1,1)$ and n the average number of thermal photons. Their first moments x_u are different and separated by a *distance* d. The thermal states travel to the receiver (Bob) through a quantum channel with attenuation $\eta \in [0,1]$ which may come from the ration between the detector's solid angle Ω and 4π (see top-left figure).

We then associate an interval Δx to the arbitrary outcome x and compute Bob's probability of obtaining x conditioned on Alice sending the logical values $u = 0, 1$. This is given by the following expression

$$p(x|u) = \frac{1}{2}\left[\operatorname{erf}\left(\frac{x_u + \Delta}{2\sqrt{2V_b}}\right) - \operatorname{erf}\left(\frac{x_u - \Delta}{2\sqrt{2V_b}}\right)\right], \quad (1)$$

where $x_0 = 2x + \sqrt{\eta}d$, $x_1 = 2x - \sqrt{\eta}d$ and V_b is the variance of the output states received by Bob. From $p(x|u)$, we compute Bob's error probability $p_{err} = [1+\exp(-x\sqrt{\eta}d/V_b)]^{-1}$, and we derive Alice and Bob's mutual information $I_{AB} = 1 - H_2(p_{err})$, where $H_2(p) := -p\log_2 p - (1-p)\log_2(1-p)$. For Eve we compute $I_E = 1 - H_2(p_{eve})$, where $p_{eve} = \frac{1}{2}[1 - \operatorname{erf}(\sqrt{(1-\eta)/(2V_e)}d/2)]$, with V_e being the variance of the states received by Eve. We also bounded Eve's accessible information by using the fidelity and the Pinsker's bound [5].

For all these cases we computed the raw key rate $R_r = I_{AB} - I_{Eve}$ and therefore post-selected key-rate

$$R := \int_{\Sigma} dx\, p(x,d) R_r(x,d), \quad (2)$$

which is integrated over the region Σ such that $R_r > 0$, accounting for the density probability, $p(x,d) = p_\Delta(x,d)/\Delta$ associated with outcome x. The key rates for the binary protocol are summarized in the bottom-left figure. The red curve is obtained the fidelity bound, while the gray curve is obtained by computing the Pinsker's bound.

In conclusion we found that the approaches described above allow us to achieve a high key rate in the presence of remarkable amounts of trusted thermal noise and in very attenuated channels. This may pave the way towards free-space communication at the GHz range.

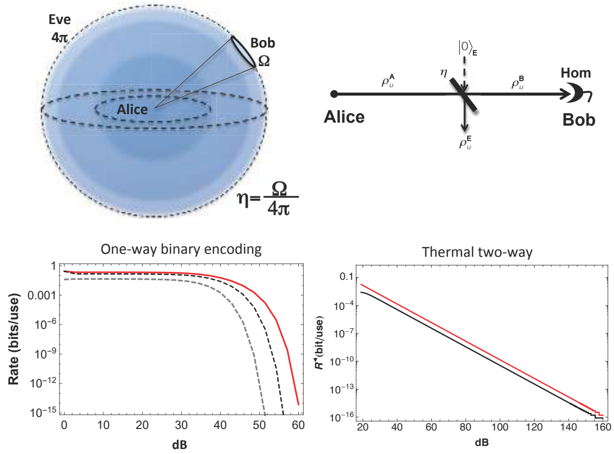

[1] C. Weedbrook *et al.*, Rev. Mod. Phys. **84**, 621 (2012).
[2] C. Weedbrook *et al.*, Phys. Rev. A **89**, 012309 (2014).
[3] S. Pirandola *et al.*, Preprint arXiv:1510.08863 (2015).
[4] Ch. Silberhorn *et al.*, Phys. Rev. Lett. **89**, 167901 (2002).
[5] A. Fedorov, IEEE trans. on Info. Theory **49**, 2003.

An application of quantum Darwinism to a structured environment: redundancy as an indicator of non-Markovianity

Graeme Pleasance[1] and **Barry M. Garraway[1]**

[1] *University of Sussex, Brighton, UK*
E-mail: G.Pleasance@sussex.ac.uk

Quantum Darwinism extends the traditional formalism of decoherence to explain the emergence of classicality in a quantum Universe. In light of recent interest we apply the tools of quantum Darwinism to a qubit interacting with many bosonic sub-environments. We examine the degree to which the same classical information is encoded across collections of: (i) complete sub-environments, and (ii) residual “pseudomode” components of each sub-environment, whose conception provides a dynamical representation of the memory part of the environment. Overall, we find significant redundancy of information and demonstrate that its emergence is suppressed in line with information back flow to the qubit. This effect suggests a direct connection between the accessibility of (classical) information from the environment and the non-Markovianity. Surprisingly, with (ii), it is also discovered that redundant information isn’t necessarily classical—we present an example where purely quantum information, characterized by the quantum discord, is predominant while classical correlations are destroyed over time.

References

[1] W. H. Zurek, Nat. Phys. **5**, 181 (2009)
[2] F. G. S. L. Brandao, M. Piani and P. Horodecki, *et al*, Nat. Commun. **6**, 7908 (2015)
[3] B. M. Garraway, Phys. Rev. A **55**, 2290 (1997)

Generation of non-classical photon pairs from warm atomic vapor using a single driving frequency

L. Podhora, L. Lachman, I. Straka, M. Ježek, L. Slodička
Department of Optics, Palacký University in Olomouc, 17. listopadu 12, 77146 Olomouc, Czech Republic

The scalable quantum-communication protocols based on atom-light interfaces have stimulated development of number of experimental platforms aiming for production of single photons with high purity, efficiency, and frequency linewidth comparable to atomic natural linewidth. Trapped cold atoms [1] have proven to be viable systems for achieving this goal either by employing conditional parametric process or by exploiting the intrinsic purity of single atoms as single photon sources. The high level of isolation from thermal environment in these systems strongly enhances the ability of the generation of photons with narrow linewidths. At the same time, it is the actual isolation what makes these systems bulky and engineering demanding. The recent demonstrations of generation of nonclassical photon pairs in warm atomic ensembles circumvent these demands by employment of several excitation lasers in specially designed optical pumping [3] or ladder-type electronic level schemes [2].

We present further simplification of the presented schemes by experimental demonstration of the generation of nonclassical photon pairs in warm atomic ensembles by the process of spontaneous four wave mixing using the excitation of atoms with single laser frequency. The scheme is based on the counter-propagating laser excitation of ^{87}Rb vapor on D1-line close to F=2→F'=2 transition. Scattered Stokes and anti-Stokes photons are detected at small angle with respect to the excitation beam and the polarizations and frequencies of generated photons are filtered using pairs of Glan-Thompson polarizers and Fabry-Pérot resonators, respectively. The coupling into the opposite single mode fibers directly guarantees proper selection of the phase-matched modes from the atomic emission. The nonlinear interaction is enhanced by focusing the exciting laser beam. Uncorrelated photons coming from the initial population of the F=2 ground state are partially suppressed by the optical pumping mechanism which happens for atoms before they enter the observation area, which is set to be much smaller than the effective laser beam waist.

The non-classical properties of generated light fields are investigated by measuring both Cauchy-Schwarz violation of the correlations between the Stokes and anti-Stokes modes and by measurement of the degree of second-order coherence on the anti-Stokes mode conditioned on the detection of the Stokes photon. The maximal value of cross-correlation function is $g^{(2)}_{\mathrm{S,AS}} = 6.67 \pm 0.02$ and the corresponding conditional $g^{(2)}_{\mathrm{AS,AS}}(0) = 0.48 \pm 0.04$. The measured length of tunable temporal correlations is on the order of few nanoseconds, however, the relatively high biphoton generation rate of more than 5×10^3 pairs/s for 2 ns coincidence window leaves space for further frequency filtration with prospect of linewidths at the order of few MHz and with biphoton rates applicable for interactions with target ensembles. We note, that in our parameter regime, further strong enhancement of both the purity of generated single photons and the generation rate is expected by increasing the power of the excitation laser beam, which has been limited in the presented measurements to 43 mW. The presented results may enable development of quantum communication architectures with spatially small and technically simple single-photon sources.

Reference

[1] Du, S., Kolchin, P., Belthangady, C., Yin et al., Phys. Rev. Lett. **100**, 183603 (2008).

[2] Lee Y. S., Lee S. M., Kim H., Moon H. S., Opt. Express **24**, 28083-28091 (2016).

[3] Shu C., Chen P., Chow T. K. A., Zhu L. et al., Nat. Commun. **7**, 12783 (2016)

Localization of excited states and vortex stability in Bose-Einstein Condensates in the presence of disorder

Marisa Pons[1] and Anna Sanpera[2,3]

[1]Applied Physics Department I, University of the Basque Country, UPV-EHU, Bilbao, Spain
[2]ICREA, Institució Catalana de Recerca i Estudis Avançats, 08010 Barcelona, Spain.
[3] Departament de Física, Universitat Autònoma de Barcelona, UAB, Bellaterra, Spain

We study the onset of localization of excited states of trapped Bose-Einstein Condensates expanding in the presence of Gaussian uncorrelated random disorder. Quantum localization emerges as a consequence of the coherent back scattering that appears when a wave packet spreads in a disordered media [1]. To date, most studies of quantum localization in ultracold gases have exhaustively analyzed the onset of localization for the ground state of a trapped gas expanding freely in a disordered media, see e.g. [2] and references therein. We observe, in 1D systems, that for a fixed ratio between the disorder strength and the initial energy, excited states localize exponentially with a localization length that decreases as the energy of the initial state increases. Moreover, the localized state keeps the shape of the initial state wave function with an exponential tail [3].

In 2D, we analyze the interplay between vorticity and localization by examining the dispersion of a state containing a vortex on it in a disordered media [3]. We find that, if interactions are absent, the vortex superfluid localizes in such media and, moreover, the vortex is resilient to disorder effects. This is a single particle effect. In the presence of interactions, no matter how small they are, the vortex rapidly decays into phase discontinuities although localization is still present. The study of dispersion of a bosonic condensate with vorticity in a disordered media bears similarities with the stability of topological excitations in 2D p-wave fermionic superfluids where the ground state is a Majorana mode that arises in the form of a vortex in the order parameter.

[1] P.W. Anderson, Phys. Rev. **109**, 1492 (1958)

[2] M. Lewenstein, A. Sanpera, V. Ahufinger, Ultracold Atoms in Optical Lattices: mimicking condensed matter and beyond, Oxford University Press, (2012)

[3] M. Pons, A. Sanpera, arXiv:1511.08588, to appear in Phys. Rev. A

The cooperation number in the study of the quantum phase transition of a matter-radiation interaction model

Luis Fernando Quezada and Eduardo Nahmad Achar
Instituto de Ciencias Nucleares, Universidad Nacional Autónoma de México, 04510 Ciudad de México, México.
e-mail: luis.fernando@correo.nucleares.unam.mx

Abstract: We show how the use of variational states to approximate the ground state of a system can be applied to study a matter-radiation interaction model. One of the main contributions of this work is the introduction of a not very commonly used quantity (the *cooperation number*) and the study of its influence over the behavior of the system, paying particular attention to the phase transitions and the accuracy of the used approximations. We also show how these phase transitions affect the dependence of the expectation values of some of the observables relevant to the system and the entropy of entanglement.

Keywords: Matter-radiation interaction, quantum phase transitions, cooperation number, representation theory.

In the study of the Dicke model (and n-level systems), the generators of the Lie algebra of SU(2) (SU(n)) are encountered in the Hamiltonian, thus it is natural to think that the representation theory of SU(2) (SU(n)) can provide some insights into the understanding of the modeling system.

The term *cooperation number* was first introduced by Dicke in his original paper [1], referring to the label "j" of the eigenvalues of the collective spin operator J^2, this label is used in group theory to index the irreducible representations of SU(2).

The effects of the quantum phase transition in the behavior of the system modeled by the Dicke's Hamiltonian have already been studied [2] for the completely symmetric representation of SU(2) and for all the representations indexed by the cooperation number [3].

[1] R. H. Dicke, Phys. Rev. 93, 99 (1954).
[2] E. Nahmad-Achar, S. Cordero, O. Castaños and R. López-Peña, Phys. Scr. 90, 074026 (2015).
[3] L. F. Quezada and E. Nahmad-Achar Phys. Rev. A. 95, 013849 (2017).

Compatibility in Multiparameter Quantum Metrology

Sammy Ragy,[1] Marcin Jarzyna,[2] and Rafał Demkowicz-Dobrzański[2]
[1]*Department of Mathematics, University of York, Heslington, York YO10 5DD, United Kingdom*
[2]*Faculty of Physics, University of Warsaw, ul. Pasteura 5, 02-093 Warszawa, Poland*

The aim of quantum metrology is to estimate the value of some parameters $\vec{\theta} = (\theta_1, \ldots, \theta_k)$ which characterise a quantum channel $\Lambda_{\vec{\theta}}$. This is done as in Figure 1, where a probe state ρ_0 is passed through the channel and then a measurement performed upon the resultant state. In order to get as precise an estimate as possible, it is desirable to optimise over the probe state, measurement and data processing.

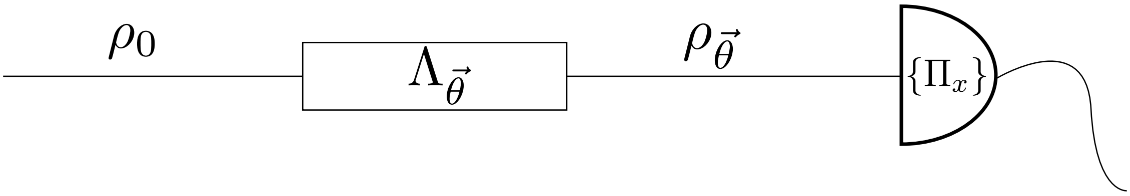

FIG. 1. A depiction of a metrology scheme, with probe, ρ_0, channel, $\Lambda_{\vec{\theta}}$, and measurement, $\{\Pi_x\}$.

In the single parameter case the solution is well-known, and for any (locally unbiased) estimator $\hat{\theta}(x)$, the variance is lower-bounded by $\mathrm{Var}(\hat{\theta}) \geq \min_{\rho_0} \frac{1}{\nu}[QFI(\rho_\theta)]^{-1}$, where $\rho_\theta = \Lambda_\theta(\rho_0)$ and ν represents the number of independent repetitions of the experiment. The quantum Fisher information is defined by $QFI(\rho_\theta) = \mathrm{Tr}(\rho_\theta L_\theta^2)$, where L_θ, the *symmetric logarithmic derivative* (SLD), is implicitly defined by $\frac{\partial \rho_\theta}{\partial \theta} = \frac{1}{2}(L_\theta \rho_\theta + \rho_\theta L_\theta)$. This bound is achievable as $\nu \to \infty$.

In the case of multiple parameters, things are no longer so simple. Although we can define a QFI matrix $QFI(\rho_{\vec{\theta}})_{ij} = \frac{1}{2}\mathrm{Tr}[\rho_{\vec{\theta}}(L_{\theta_i}L_{\theta_j} + L_{\theta_j}L_{\theta_i})]$ and bound on covariance matrix $\mathrm{Cov}(\hat{\theta}) \geq \min_{\rho_0} \frac{1}{\nu}[QFI(\rho_{\vec{\theta}})]^{-1}$, we encounter the following obstacles: 1) it may be that there is no jointly optimal probe state ρ_0, thus invoking a trade-off in estimation precision for different parameters of interest, 2) there may be no jointly optimal measurement, and this will prevent the QFI bound from being achievable, even asymptotically, and 3) if the data is correlated in the parameters to be estimated then they can 'interfere' with each other's estimations (there will be some covariance between them).

We study the regime where these three obstacles are circumvented and the estimation of parameters jointly is no worse for *each* parameter than in a dedicated scheme for that parameter alone. We call this feature *compatibility*. We prove mathematical conditions for compatibility, one of which has been frequently used in the literature but with no previously published proof of which we are aware.

After assembling this mathematical framework, we continue by studying several problems of physical interest. We consider multiparameter unitary operations, and outline when compatibility is achievable. In particular, we find that entanglement can 'unlock' compatibility. We find a two-parameter model where single-qubit probes may not permit any advantage to joint estimation whereas two-qubit probes achieve the Heisenberg limit in both parameters at once. This additionally breaks the equivalence between entangled and sequential estimation which has been observed for single-parameter unitaries on pure states [1].

We also consider the problem of simultaneous estimation of phase and local dephasing, which was first addressed in [2], but for which a solution was only provided for effectively two-dimensional Hilbert spaces, essentially single qubits. We derive a more general solution than this, showing that obstacles 2 and 3 listed above can always be avoided within a large class of states, and providing numerical evidence that a jointly optimal state exists within this class.

[1] Lorenzo Maccone, *Physical Review A* **88** 042109 (2013)
[2] Mihai D. Vidrighin et al., *Nature Communications* **5** 3532 (2014).

Multi-photon scattering tomography with coherent states

Tomás Ramos and Juan José García-Ripoll
Instituto de Física Fundamental IFF-CSIC, Calle Serrano 113b, Madrid 28006, Spain

The achievement of strong coupling between quantum impurities and propagating photons at low dimensions [1–3] has spun a renewed interest in the theory of single- and multi-photon scattering. From earlier developments using wavefunction theory, the field has evolved into sophisticated calculations of one- and two-photon scattering matrices using input-output theory [4], path integral formalism [5], and has been even extended into the ultra-strong coupling regime [6]. Experiments, however, have been mostly constrained to estimates of the single-photon transmission and reflection coefficients [1] or cross-Kerr phases between coherent beams [7].

In this work we develop an experimental framework for determining the multi-photon scattering matrices of an arbitrary and possibly unknown point-like quantum impurity. To this end, we combine tools from scattering theory and homodyne detection in quantum optics, giving rise to an experimentally feasible method which does not require single-photon sources nor single-photon detectors.

In particular, we place the scatterer in a one-dimensional waveguide or channel (see Fig. 1), and we probe it with coherent state inputs of the form,

$$|\Psi_{\rm in}\rangle = |\alpha\rangle_{k_1,\ldots,k_m} = e^{-\frac{|\alpha|^2}{2}} e^{\sum_{\sigma=1}^{m}\alpha_\sigma A^\dagger_{k_\sigma}}|0\rangle, \qquad (1)$$

where $A^\dagger_{k_\sigma}$ are bosonic creation operators of a photon wave-packet centered at different momenta k_σ, with $\sigma = 1,\ldots,m$. In addition, α_σ are the coherent displacement coefficients for each momentum mode, with $|\alpha|^2 = \sum_{\sigma=1}^{m}|\alpha_\sigma|^2$, and $|0\rangle$ denotes the vacuum state. After the interaction with the scatterer, the photonic output state reads, $|\Psi_{\rm out}\rangle = S|\Psi_{\rm in}\rangle$, where the components of the scattering matrix read,

$$S_{p_1\cdots p_n k_1\cdots k_m} = \langle 0|A_{p_1}\cdots A_{p_n} S A^\dagger_{k_1}\cdots A^\dagger_{k_m}|0\rangle. \qquad (2)$$

They describe the probability amplitudes for transitions from m photons with momenta $k_1,\ldots,k_m$ to n photons with momenta $p_1,\ldots,p_n$. Notice that we do not impose any condition on the scattering matrix (besides unitarity $SS^\dagger = S^\dagger S = 1$ and $S|0\rangle = |0\rangle$ which always hold), allowing us to describe any multi-photon process in one-dimension, including the case when the number of photons is not conserved. To perform the detection of photons with different momenta $p_1,\ldots,p_n$, we pass the forwardly scattered photons through a multi-port beam splitter operation $U_{\rm BS}$ (see Fig. 1), which involves A_{p_1} and $n-1$ additional channels $A^2_{p_2},\ldots,A^n_{p_n}$, and thus allows us to measure quadratures of the form,

$$\langle A_{p_1}A^2_{p_2}\ldots A^n_{p_n}\rangle = \langle\Psi_{\rm out}|U^\dagger_{\rm BS}A_{p_1}A^2_{p_2}\ldots A^n_{p_n}U_{\rm BS}|\Psi_{\rm out}\rangle. \qquad (3)$$

Our main result is a relation between the output quadratures moments in Eq. (3) and the general scattering matrix elements in Eq. (2), with an error scaling as $\sim|\alpha|^2$ in the case of highly attenuated coherent state inputs, $|\alpha| \ll 1$, and thus can be made negligibly small.

This allows for the realization of a tomographic protocol to determine the multi-photon scattering matrix elements of an unknown quantum scatterer as shown in detail in our work. An additional feature of the scheme is that the measurement of the quadratures in Eq. (3) is insensitive to vacuum or amplification noise as it involves bosonic fields at independent channels. This is particularly useful for implementations with superconducting circuits as all noise from the amplifiers is canceled out without previous calibration. We close this work with a practical study of the protocol in the case of two- and three-level system scatterers, showing its feasibility under realistic experimental conditions such as losses and dephasing.

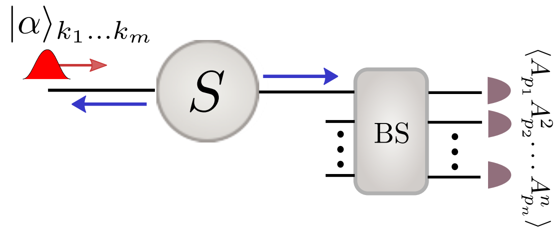

FIG. 1. A one-dimensional waveguide transports incoming photons that are transformed by the quantum impurity into right and left outgoing states, through a unitary transformation S, the scattering matrix. We show that by probing the system with attenuated coherent state wave-packets, $|\alpha| \ll 1$, in combination with homodyne detection at the output, it is possible to reconstruct the multi-photon components of S with negligible errors $\sim|\alpha|^2 \ll 1$.

[1] O. Astafiev *et al.*, Science **327**, 840 (2010).
[2] A. Goban *et al.*, Phys. Rev. Lett. **115**, 063601 (2015).
[3] M. Arcari *et al.*, Phys. Rev. Lett. **113**, 093603 (2014).
[4] S. Fan *et al.*, Phys. Rev. A **82**, 063821 (2010).
[5] T. Shi *et al.*, Phys. Rev. A **92**, 053834 (2015).
[6] T. Shi *et al.*, arXiv:1701.04709.
[7] I.-C. Hoi *et al.*, Phys. Rev. Lett. **111**, 053601 (2013).

Quantum walking down the quantum-number distribution

César Alonso-Lobo, Eugenio Roldán

Departament d'Òptica i d'Optometria i Ciències de la Visió, Universitat de València, Dr. Moliner 50, 46100 Burjassot, Spain

The quantum walk (QW) [1], a quantum analogue of random walks, is a well stablished quantum protocol that allows for the design of efficient quantum algorithms for certain problems [1], as well as constitutes a primitive for quantum computation [2]. Besides, QWs allow the modelling of a number of physical problems, and their physical implementation has been an important goal in the recent past. Here a new physical implementation is proposed whose most relevant feature is that the walking occurs along the number of quanta in the quantum probability distribution of the bosonic field, which could be a light field, a microwave field, or an oscillation mode depending on the specific system chosen for the implementation.

The proposal considers a physical system whose evolution Hamiltonian is such that it can be dynamically tuned to be that of the Jaynes-Cummings model (JCM) or that of the "anti-Jaynes-Cummings" model (aJCM), i.e., the Hamiltonian resulting from the Rabi model when the rotating terms are neglected and the anti-rotating terms are kept. A physical system able of implementing such Hamiltonian is the optically-driven harmonically-trapped ion [3], in which case the quantum field is the quantized oscillation of the ion; however, it could also be implemented with contemporary quantum superconducting circuitry, in which case the quantum field would be a microwave electromagnetic field.

When a two-level ion is harmonically-trapped and driven by a (classical) coherent field, the system implements the JCM or the aJCM depending on whether the coherent driving is tuned, respectively, to the red or blue sidebands of the resonance [3]; hence, by suitably temporally modulating the classical driving, one can alternate between the JCM and aJCM Hamiltonians. If the initial field is initially in a Fock state, a sequence JCM-aJCM can increase or decrease the number of quanta depending on the initial atomic state, a technique already used for generating Fock states from vacuum [4]. Hence, such a sequence implements a displacement operator, which increases/decreases the number of quanta depending on the initial atomic state (excited/fundamental). However, such a system can implement only the trivial QW with $\theta = \pi/2$ in which case one obtains a pure ballistic motion, and taking an initial state of the atom in a superposition between the excited and fundamental levels can be shown not to lead to the standard QW evolution. Nevertheless, when choosing an initial atomic state in a superposition

The approach here for achieving a correct implementation of the QW is two use two parallel versions of the system, one in which the driving sequence starts with JCM (i.e., a sequence JCM-aJCM-JCM-…) while in the other the sequence starts with aJCM; in this way, one of the parts of the system implements an increase in the number of quanta while the other implements the decrease. The coin in this QW consists in the proportion in which the system is driven by one or the other sequence (increase/decrease) and the coin operation consists in mixing them unitarily.

All this can be implemented by using a J=1/2 $\leftrightarrow$ J=1/2 ionic transition, as such a transition can be viewed as two separated two-level systems, one of which is driven by right-circularly polarized light and the other driven by left-circularly polarized light. This allows for the implementation of the two parallel sequences of Hamiltonians (increasing/decreasing). The coin operator could be implemented, e.g., by coherently mixing the populations (after each step of the displacement operation) with the aid of a magnetic or microwave pulse properly tuned to the upper (lower) magnetic sublevels transition. All this will be explained in full detail.

The novel and interesting feature of this new proposal for implementing QWs is that the walk occurs in the number of quanta probability distribution, which has the interest of allowing the use of the capabilities of QWs for transforming an initial distribution into other desired distribution with the aim of synthesizing particular quantum states of the bosonic field. Hence, this QW could be a new tool for the synthesis of quantum states.

References

[1] S.E. Venegas-Andraca, "Quantum walks: a comprehensive review", Quant. Inf. Proc. **11**, 1015 (2012).

[2] A.M. Childs, Phys. Rev. Lett. 102, 18050 (2009) ; N.B. Lovett, S. Cooper, M. Everitt, M. Trevers, and V. Kendon, Phys. Rev. A **81**, 042330 (2010).

[3] D. Leibfried, R. Blatt, C. Monroe, and D.J. Wineland, "Quantum dynamics of single trapped ions", Rev. Mod. Phys. **75**, 281-324 (2003).

[4] D. M. Meekhof, C. Monroe, B. E. King, W. M. Itano, and D. J. Wineland, "Generation of Nonclassical Motional States of a Trapped Atom", Phys. Rev. Lett. **76**, 1796 (1996).

Tests of macrorealism with light polarization measurements

Eugenio Roldán[1,2]***, Johannes Kofler***[2]***, Carlos Navarrete-Benlloch***[3,4]

1. Departament d'Òptica i d'Optometria i Ciències de la Visió, Universitat de València, Dr. Moliner 50, 46100 Burjassot, Spain

2. Max-Planck-Institut für Quantenoptik, Hans-Kopfermann-strasse 1, 85748 Garching, Germany

3. Max-Planck-Institut für die Physik des Lichts, Staudtstrasse 2, 91058 Erlangen, Germany

4. Institute for Theoretical Physics, Erlangen-Nürnberg Universität, Staudtstrasse 7, 91058 Erlangen, Germany

According to macroscopic realism, or macrorealism [1], macroscopic objects are always in a definite state and measurements can be performed without changing these states and the subsequent temporal evolution. If effects of decoherence can be sufficiently suppressed, quantum mechanics is at variance with the predictions of macrorealism. Leggett-Garg inequalities (LGI) can witness a violation of macrorealism by suitably comparing correlations of a dichotomized macroscopic observable that is measured at subsequent different times under different measurement settings. Non-invasive measurability is an essential ingredient for the derivation of LGI: provided that the disturbance of the target system during macroscopic measurements is negligibly small, a violation of LGI would imply the non-existence of well-defined macroscopic properties. An alternative criterion for macrorealism called no-signalling in time NSIT [2] has been recently put forward, which is now known to be in general a stronger and better condition than the LGI [3].

In this work, we try to understand what LGIs and NSIT can tell about light by considering subsequent measurements of the polarization on a well-defined spatiotemporal mode of the light field. In this work we concentrate on linear polarization states with well-defined photon number (states of the form $|N,M\rangle = |N\rangle_x|M\rangle_y$ having N photons with x-polarization and M photons with y-polarization). We pay special attention to the influence and invasiveness of the type of measurements, as we consider measurements consisting in the extraction of a fixed number of photons, but also measurements that average over the number of detected photons, so that our work is a study about the invasiveness of polarization measurements via photon extraction. Our results shed light onto the question under which measurement conditions a violation of LGI and NSIT can be observed.

We consider a quantum-light source that emits a sequence of identical pulses in a well-defined spatiotemporal mode. The light-pulses travel through three identical detection ports in which a small amount of light is extracted and its polarization (that is, the number of photons in two orthogonal polarization modes) is measured. With these measurements the Stokes parameters of the light beam can be determined when measuring along (at least) two different polarization orientations. In order to study LGI, and NSIT, some correlations between the measurements subsequently performed on the same pulses are then extracted and analysed.

Light extraction is made on each measurement port via a beam-splitter of small (polarization-independent) reflectivity r. The small amount of reflected light is then separated into its orthogonal linear polarization components with respect to some θ-oriented reference frame (accomplished, e.g., by a properly oriented calcite crystal), and then each of the two orthogonally polarized beams impinge on ideal photon-counters. The same operation is then repeated on the pulse transmitted by the first measurement port, with a second measurement apparatus differing from the first one only in the orientation of the polarization axes. For the criterion of NSIT, a third measurement is needed.

The detectors are capable of counting photons and will provide outcomes ω_x=0,1,2,... and ω_y=0,1,2,..., where the subindex labels the detector. We consider different strategies to dichotomize the outcomes, all requiring post-selection, and based on some kind of "majority vote", that is, which detector has detected more photons. Specifically, we consider "sharp" measurements (in which only one detector clicks and it does when exactly ω photons impinge on it), "fair" measurements in which the detectors count photons from zero to ω, and "blurred" measurements that are intermediate between the previous two types and allow to pass from one type to the other. Of course this is a very naive description of the photodetection process, just a toy model, whose more obvious defect is the necessity of perfect detection (essential for our wave-vector treatment of the process).

We found that no violation of LGI, nor of NSIT, can occur when the detection process consists in the extraction of a single photon at each measurement port; hence no violation of macrorealism when the detection is fair enough. However, when two-photon detectors are used, LGI and NSIT are always violated by some states with an arbitrarily large number of photons. We discuss in detail how invasiveness leads to violations of macroscopic realism and how coarse-graining of the measurements removes such violations.

References

[1] A. J. Leggett and A. Garg, Phys. Rev. Lett. **54**, 857 (1985)
[2] J. Kofler and C. Brukner, Phys. Rev. A **87**, 052115 (2013)
[3] L. Clemente and J. Kofler, Phys. Rev. Lett. **116**, 150401 (2016)

Delocalization properties of the Husimi function in the vicinity of avoided crossings in Lipkin-Meshkov-Glick type Hamiltonian models

E. Romera[1,2], O. Castaños[2], M. Calixto[1,3], F. Pérez-Bernal[1,4]

(1) Instituto Carlos I de Física Teórina y Computacional, Universidad de Granada, Campus Fuentenueva s/n, 18071 Granada, Spain.
(2) Departamento de Física Atómica, Molecular y Nuclear, Universidad de Granada, Campus Fuentenueva s/n, 18071 Granada, Spain.
(3) Instituto de Ciencias Nucleares, Universidad Nacional Autónoma de México, Apartado Postal 70-543, 04510 Distrito Federal, Mexico
(4) Departamento de Física Aplicada, Facultad de Ciencias Experimentales, Universidad de Huelva, Campus del Carmen, Avenida de las Fuerzas Armadas s/n, 21071 Huelva, Spain

The delocalization properties at isolated avoided crossings in Lipkin-Meshkov-Glick type Hamiltonian models have been studied. This delocalization has been quantified with the Husimi function second moment (related to the inverse participation ratio in phase space) and the Wehrl entropy, for which we have determined analytic expressions for the Dicke states and numerical calculations for arbitrary energy eigenstates. We have also made an analytic study of the monotonicity properties of the Husimi function second moment in the vicinity of exceptional points by using standard perturbation theory [1,2].

[1] O. Castaños, M. Calixto, F. Pérez-Bernal and E. Romera, Phys. Rev. E **92**, 052106 (2015).

[2] E. Romera, O. Castaños, M. Calixto and F. Pérez-Bernal, Journal of Statistical Mechanics, 013101 (2017).

Adaptive interferometry and single-mode measurements do not increase the capacity of coherent-state decoders

Matteo Rosati,[1] Andrea Mari,[1] and Vittorio Giovannetti[1]
[1] *NEST, Scuola Normale Superiore and Istituto Nanoscienze-CNR, I-56127 Pisa, Italy.*

Quantum communication theory is a promising field for the application of quantum technology, since its predictions could be applied in the short-term in several settings of practical relevance. An important example is communication on free-space or optical-fiber links, which are well described theoretically by quantum phase-insensitive Gaussian channels [1–3], e.g., the lossy bosonic channel [4].

The maximum transmission rate of classical information on a quantum channel, known as its capacity, is provided by the Holevo-Schuhmacher-Westmoreland (HSW) theorem [5–9]. In particular for quantum phase-insensitive Gaussian channels the capacity at constrained average input energy can be achieved [10–13] by a simple *separable encoding*, i.e., sending sequences of coherent states [14], each of them constituting a letter for a single use of the channel or communication mode. Unfortunately the detection stage is not as easy, since all known capacity-achieving measurements require *joint decoding* operations [8, 9, 15–26], i.e., reading out entire blocks of letters at once. Such joint quantum measurements are difficult to design with current technology [27–35], so that the quest for an optimal decoder of separable coherent-state codewords that would finally trigger practical applications is still open. Research has then mainly focused on decoding coherent states with the general class of Adaptive Decoders (AD) depicted in Fig. 1a. The latter combines the available *single-mode* technology, e.g., photodetectors and local transformations, with *multi-mode passive* interferometers and *classical feedforward control*. The rationale behind this choice is that introducing correlations between modes during the decoding procedure may increase the transmission rate of simple separable measurements, getting closer to the ultimate capacity of phase-insensitive Gaussian channels.

On the contrary, in this article we prove that the maximum information transmission rate of such channels with coherent-state encoding and AD *is equal to* that obtained with a Separable Decoder (SD) employing the same measurement on each mode, as shown in Fig. 1b. The general idea behind our proof is to map the quantum AD into an effective classical programmable channel with feedback to the encoder. Then we obtain our results by extending Shannon's feedback theorem [36, 37] to this kind of channels.

Our work gives several major contributions: i) it implies the conjecture by Chung *et al.* [38, 39], namely that adaptive passive interactions, single-mode displacements and photodetectors do not increase the optimal transmission rate; ii) if the HSW capacity of phase-insensitive Gaussian channels is achieved only by joint measurements, as the evidence suggests so far, then it cannot be achieved with our AD scheme; iii) it extends the results of Takeoka and Guha [30], who considered only Gaussian measurements; iv) it extends the analysis made by Shor [40] in the context of trine states to coherent states and passive interactions.

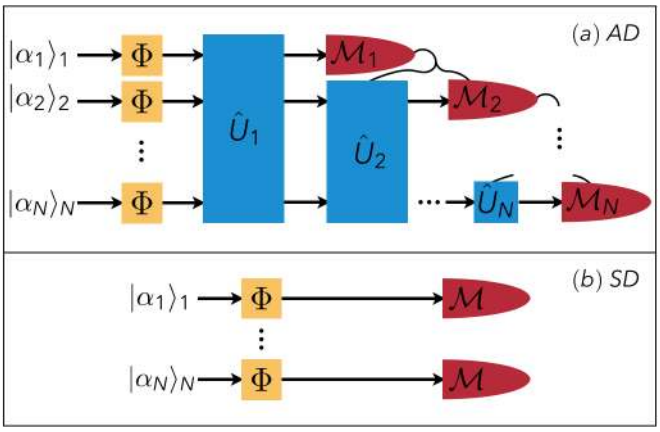

Figure 1. Schematic depiction of the class of (a) Adaptive Decoders (AD) and (b) Separable Decoders (SD) considered, whose maximum information transmission rate is proved to be equal. (a) In the AD case the sender, Alice, encodes the message into separable sequences of coherent states $|\alpha_1\rangle_1 \otimes \cdots \otimes |\alpha_N\rangle_N$ and sends it to the receiver, Bob, with N distinct uses of a quantum phase-insensitive Gaussian channel Φ (yellow/light-gray boxes). Bob's AD comprises multi-mode passive Gaussian interferometers $\hat{U}_j$ (blue/medium-gray boxes) and arbitrary destructive single-mode measurements $\mathcal{M}_j$ (red/dark-gray shapes), adaptively dependent on the measurement results of previous modes and applied successively on the remaining modes. (b) In the SD case Alice uses the same encoding but Bob performs the same measurement $\mathcal{M}$ on each mode and cannot use adaptive procedures.

[1] C. M. Caves and P. D. Drummond, Rev. Mod. Phys. **66**, 481 (1994).
[2] A. S. Holevo, *Quantum Systems, Channels, Information* (de Gruyter Studies in Mathematical Physics, 2012).
[3] A. S. Holevo and V. Giovannetti, Rep. Prog. Phys. **75**, 046001 (2012).
[4] V. Giovannetti, S. Guha, S. Lloyd, L. Maccone, J. H. Shapiro and H. P. Yuen, Phys. Rev. Lett. **92**, 027902 (2004).
[5] A. S. Holevo, Probl. Peredachi Inf. **9**, 3 (1973); Probl. Inf. Transm. (Engl. Transl.) **9**, 110 (1973).
[6] A. S. Holevo, IEEE Trans. Inf. Theory **44**, 269 (1998).
[7] A. S. Holevo, e-print arXiv:quant-ph/9809023 [see also Tamagawa University Research Review, no. 4] (1998).
[8] B. Schumacher and M. D. Westmoreland, Phys. Rev. A **56**, 131 (1997); P. Hausladen, R. Jozsa, B. W. Schumacher, M. Westmoreland, and W. K. Wootters, ibid. **54**, 1869 (1996).
[9] A. Winter, IEEE Trans. Inf. Theory **45**, 2481 (1999).
[10] V. Giovannetti, R. García-Patrón, N. J. Cerf and A. S. Holevo, Nat. Phot. **8**, 796 (2014).
[11] V. Giovannetti, A. S. Holevo and R. García-Patrón, Commun. Math. Phys. **334**, 1553 (2014).
[12] A. Mari, V. Giovannetti and A. S. Holevo, Nature Commun. **5**, 3826 (2014).
[13] V. Giovannetti, A. S. Holevo and A. Mari, Theor. Math. Phys. **182**, 284 (2015).
[14] C. Weedbrook, S. Pirandola, R. García-Patrón, N. J. Cerf, T. C. Ralph, J. H. Shapiro and S. Lloyd, Rev. Mod. Phys. **84**, 621 (2012).
[15] T. Ogawa, Ph.D. dissertation, University of Electro-Communications, Tokyo, Japan, 2000; (in Japanese) T. Ogawa and H. Nagaoka, in *Proceedings of the 2002 IEEE International Symposium on Information Theory*, Lausanne, Switzerland, (IEEE, New, York, 2002), p. 73; T. Ogawa, IEEE Trans. Inf. Theory **45**, 2486 (1999).
[16] T. Ogawa and H. Nagaoka, IEEE Trans. Inf. Theory **53**, 2261 (2007).
[17] M. Hayashi and H. Nagaoka, IEEE Trans. Inf. Theory **49**, 1753 (2003).
[18] M. Hayashi, Phys. Rev. **A** 76, 062301 (2007); Commun. Math. Phys. **289**, 1087 (2009).
[19] P. Hausladen and W. K. Wooters, J. Mod. Opt. **41**, 2385 (1994).
[20] S. Lloyd, V. Giovannetti, L. Maccone, Phys. Rev. Lett. **106**, 250501 (2011).
[21] V. Giovannetti, S. Lloyd and L. Maccone, Phys. Rev. A **85**, 012302 (2012).
[22] P. Sen, e-print arXiv:1109.0802 [quant-ph] (2011).
[23] E. Arikan, IEEE Trans. Inf. Theory **55**, 3051 (2009).
[24] M. M. Wilde, O. Landon-Cardinal and P. Hayden, in *8th Conference on the Theory of Quantum Computation, Communication and Cryptography (TQC 2013)*, Dagstuhl, Germany, 2013 arXiv:1302.0398v1.
[25] M. M. Wilde and S. Guha, IEEE Trans. Inf. Theory **59**, 1175 (2013).
[26] M. Rosati and V. Giovannetti, J. Math. Phys. **57**, 062204 (2016).
[27] M. M. Wilde, S. Guha, *Proceedings of the 2012 International Symposium on Information Theory and its Applications*, 303-307 (2012).
[28] M. M. Wilde, S. Guha, S.-H. Tan, S. Lloyd, *Proceedings of the 2012 IEEE International Symposium on Information Theory* (ISIT 2012, Cambridge, MA, USA), 551-555.
[29] S. Guha, J. L. Habif and M. Takeoka, *2010 IEEE International Symposium on Information Theory*, 2038-2042 (2010).
[30] M. Takeoka and S. Guha, Phys. Rev. A **89**, 042309 (2014).
[31] J. Lee, S.-W. Ji, J. Park and H. Nha, Phys. Rev. A **93**, 050302(R) (2016).
[32] S. Guha, Phys. Rev. Lett. **106**, 240502 (2011).
[33] S. Guha, Z. Dutton and J. H. Shapiro, *IEEE International Symposium on Information Theory (ISIT)*, 274 (2011).
[34] A. Klimek, M. Jachura, W. Wasilewski and K. Banaszek, J. Mod. Opt. **63**, 2074-2080 (2016).
[35] M. Rosati, A. Mari and V. Giovannetti, Phys. Rev. A **94**, 062325 (2016).
[36] C. Shannon, IRE Trans. Inf. Th. **2**, 8 (1956).
[37] T. M. Cover and J. A. Thomas, *Elements of Information Theory* (Wiley-Interscience 2006).
[38] H. W. Chung, S. Guha and L. Zheng, *2011 IEEE International Symposium on Information Theory Proceedings* (St. Petersburg, 2011), 284-288.
[39] H. W. Chung, S. Guha and L. Zheng, e-print arXiv:1610.07578 [quant-ph] (2016).
[40] P. W. Shor, IBM J. Res. Dev. **48**, 115 (2004).

Classical saturability of the Cramér-Rao bound for optimal quantum metrology

Jesús Rubio[1,2], Paul Knott[3] and Jacob Dunningham[1,2]

[1]Sussex Centre for Quantum Technologies, Brighton, UK
[2]Department of Physics and Astronomy, University of Sussex, Brighton, UK
[3]School of Mathematical Sciences, University of Nottingham, UK

(April the 4th, 2017)

Quantum metrology employs quantum resources to study the performance of different schemes that are designed to estimate a physical parameter of interest that cannot be directly measured. Given a particular experimental configuration where $\mathbf{n} = (n_1, n_2, ..., n_\mu)$ are the outcomes of μ observations and θ is the unknown parameter, the precision on average can be defined in terms of the *mean square error*

$$\bar{\epsilon} = \int d\mathbf{n} d\theta p(\mathbf{n}, \theta)(g(\mathbf{n}) - \theta)^2, \tag{1}$$

where $p(\mathbf{n}, \theta)$ is the joint probability density function for the parameter and the outcomes and $g(\mathbf{n})$ is the estimator of the parameter.

In general, this integral cannot be calculated analytically and its optimization is numerically challenging. However, if the probability density is Gaussian, the estimator is unbiased, the probe state is pure, the encoding of the signal is unitary and the quantum measurement is optimal, then Eq. 1 saturates the *Cramér-Rao bound*, that is

$$\bar{\epsilon} = \epsilon_{cr} = \frac{1}{\mu F_Q}, \tag{2}$$

where F_Q is the *quantum Fisher information*.

While the quantum ingredients of the optimization of Eq. 2 have been widely studied, it is generally assumed that, for any strategy, we will end having a Gaussian density function and an unbiased estimator for a large number of observations μ. The aim of our work is to provide a quantitative framework to explicitly specify *how* this asymptotic saturation happens for different states and to show its impact on the overall performance of the scheme when μ is not large enough.

The strategy that we have followed consists of two steps. On the one hand, we have selected several representative states which are employed in optical interferometry and we have performed a numerical calculation of Eq. 1, using an optimal measurement. Since we are interested in the classical contribution to the saturation of the bound, we have also fixed the number of photons $\bar{n}$ per state. This gives us the real precision based on the criterion of the mean square error for any number of observations.

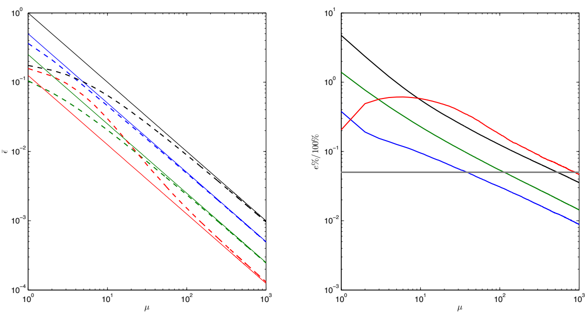

Figure 1: LHS: Cramér-Rao bound (solid line) and mean square error (dashed line) for NOON states of $\bar{n} = 1$ (black line) and $\bar{n} = 2$ (green line) and coherent (blue line) and twin squeezed-vacuum (red line) states of $\bar{n} = 2$; RHS: relative error defined by Eq. 3, with e = 5 (grey line).

On the other hand, by interpreting the Cramér-Rao bound as an asymptotic approximation to the real error of our estimation, we have introduced the relative error

$$\frac{\text{e}\%}{100\%} = \frac{|\bar{\epsilon} - \epsilon_{cr}|}{\bar{\epsilon}}, \tag{3}$$

which informs us about the deviation of the Cramér-Rao bound respect to the exact calculation of Eq. 1.

Our mains results are summarized in Fig. 1. We have found that the classical saturation of the Cramér-Rao bound is state-dependant, and we have provided a method of calculation to quantify how many observations are needed for a given strategy. One consequence is that the relative performance of several states outside the asymptotic regime can be different from the conclusions extracted from the Fisher approach. This has important implications for quantum metrology, in particular for realistic experiments operating outside of the asymptotic regime.

Broadband spontaneous parametric down-conversion unconstrained by phase-matching conditions

M.Yu. Saygin

M.V. Lomonosov Moscow State University, Faculty of Physics, Leninskie gory 1, Moscow 119991, Russian Federation

Nowadays, the process of spontaneous parametric down-conversion (SPDC) is widely exploited as a source of light with useful spectral and non-classical characteristics. In order to implement this process quadratic nonlinear crystals are usually used to make a strong pump field decaying into pairs of low-frequency modes. For this, the fulfillment of proper phase-matching conditions is required, due to constructive interference of the waves participating in SPDC. Namely, the combined mismatch comprising the pump wavevector, $\vec{k}_P$, and those of the generated pairs, $\vec{k}_1$ and $\vec{k}_2$, has to be compensated: $\Delta\vec{k} = \vec{k}_P - \vec{k}_1 - \vec{k}_2 = 0$, in case of the compensation by birefringence or $\Delta\vec{k} = \vec{k}_P - \vec{k}_1 - \vec{k}_2 = \vec{G}$, when the periodic structure is used, with $\vec{G}$ being the lattice wavevector. Because of this stringent three-wave conditions, the generated parametric fields are narrow band in space.

In this work, we consider the SPDC process under more relaxed conditions, namely, we study the case of $\vec{k}_P = \vec{G}$. As a result, the condition that is left to fulfill for the pair of generated modes wavevectors ($\vec{k}_1 + \vec{k}_2 = 0$) is met automatically, so that the parametric emission can be potentially broadband in space. Previously, the condition of complete compensation of pump wavevector has been investigated in the context of backward-propagating waves in SPDC [1]. However, to our knowledge, the possibility to use it as a way for generation of broadband parametric fields has not been reported yet. In contrast to the traditional three-wave phase-matching scenario, the field distribution in this broadband regime is largely defined by the orientational dependencies of the quadratic nonlinear tensor and refractive index of the crystal, and it is more sensitive to the pump beam profile. Here, we analyze the efficacy of SPDC in this broadband regime.

References

1. A. Gatti, T. Corti and E. Brambilla, Temporal coherence and correlation of counterpropagating twin photons // Phys. Rev. A, 92, 053809 (2015).
2. C.-S. Chuu and S. E. Harris, Ultrabright backward-wave biphoton source // Phys. Rev. A, 83, 061803 (2011).

Experimental cavity optomechanics with multi-membrane systems

Clemens Schäfermeier,[1] João P. Moura,[1] and Simon Gröblacher[1]

[1]*Kavli Institute of Nanoscience, Delft University of Technology, 2628 CJ Delft, The Netherlands**

A major aim in the field of quantum optomechanics is the enhancement of opto-mechanical coupling, eventually to enter a regime where the interaction with a single photon establishes non-classical effects. This so-called single-photon-strong-coupling regime establishes quantum electro-dynamical effects such as normal mode splitting and lays the foundation for light matter interaction at the single-quanta level. Such a system can, for instance, be used for information purposes where opto-mechanical cavities are thought of as nodes in a quantum network or for quantum sensing applications. Commonly, the opto-mechanical coupling is improved by decreasing the optical and mechanical dissipation or by engineering systems which increase the overlap between the mechanical and optical modes.

Here, we present experimental and theoretical progress to improve the opto-mechanical coupling by exploiting the effect of multiple mechanical resonators embedded in an optical cavity. Theoretical studies suggested that even with available well-known opto-mechanical systems, the coupling can be greatly increased by using multiple mechanical resonators [1, 2, 4, 5]. Our aim is to experimentally show the working concept of system with two individual membranes which are widely movable to assess a large parameter space. Experiments are conducted at 1550 nm to exploit the optical properties of silicon-based membranes [3].

* c.schaefermeier@tudelft.nl

[1] M. Bhattacharya and P. Meytre. Multiple membrane cavity optomechanics. *Phys. Rev. A*, 78:041801, 10 2008.

[2] C. Genes and A. Dantan. Light-matter interactions in multi-element resonators. *arXiv*, 1 2017.

[3] R. A. Norte, J. P. Moura, and S. Gröblacher. Mechanical resonators for quantum optomechanics experiments at room temperature. *Phys. Rev. Lett.*, 116:147202, 4 2016.

[4] A. Xuereb, C. Genes, and A. Dantan. Collectively enhanced optomechanical coupling in periodic arrays of scatterers. *Phys. Rev. A*, 88:053803, 11 2013.

[5] A. Xuereb, C. Genes, G. Pupillo, M. Paternostro, and A. Dantan. Reconfigurable long-range phonon dynamics in optomechanical arrays. *Phys. Rev. Lett.*, 112:133604, 4 2014.

Generating Squeezed Thermal States via Parametric Down Conversion in Lossy Cavities

***Hossein Seifoory*[1], *Marc. M. Dignam*[1], *and J. E. Sipe*[2]**

1. *Department of Physics, Engineering Physics and Astronomy, Queen's University, Kingston, ON K7L 3N6, Canada*
2. *Department of Physics and Institute for Optical Sciences, University of Toronto, Toronto, ON, M5S 1A7, Canada*

Squeezed states have long been of interest for interferometric measurements. More recently, they have attracted attention for use as continuous variable entangled systems in quantum information processing [1]. Chip-based squeezing greatly enhances the scalability and efficiency of squeezing, and can be implemented in microring resonators and photonic crystal cavities. However, the scattering loss that is inherent in these nanoscopic devices can degrade their performance. In this work, we show that the states created in lossy cavities via parametric down conversion are squeezed thermal states. We examine the effects of loss on the squeezing parameter and thermal photon number, as a function of both time and pump intensity.

We consider a cavity with one leaky signal mode, and consider a classical pump at twice the frequency of the signal mode. The problem then reduces to determining the photon dynamics of an optical parametric oscillator (OPO) with the pump light treated classically. In the past this has been treated either by determining and solving the dynamical equations for the operator correlation functions using the Heisenberg-Langevin equations [2] (or their equivalent), or by solving for the density matrix numerically by, say, expanding it in a basis of number states [3]. However, in our approach we show that the exact solution for the Lindblad master equation for an OPO is the density matrix of a *squeezed thermal state*: $\rho(t) = S(u,\phi)\rho_{th}(n_{th})S^{\dagger}(u,\phi)$. The problem is therefore reduced to solving the three coupled differential equations for u, ϕ, and n_{th}, which are respectively the squeezing amplitude, the squeezing phase, and the thermal photon number in the thermal state that is being squeezed. We solve these equations to yield the time-dependent and steady-state solutions for the quadrature noise, thermal photon number, squeezing parameter, total photon number, and second order correlation function under different pumping regimes.

In Fig. 1, we plot the quadrature uncertainties, thermal photon number, average photon number, and squeezing parameter in the strong pumping regime, where the pumping strength dominates over the loss. As can be seen, the squeezing amplitude and the thermal photon number increase with time and never saturate to reach a steady state value. Note that for a pure squeezed state, $\Delta X \Delta Y = 1$, so the derivation from 1 is a measure of departure from a pure squeezed state. The squeezing in X rapidly reaches a steady state while ΔY grows exponentially. Thus, the price that one pays for an increased squeezing in X is an increase in ΔY.

The key advantage of our approach is that even without solving the dynamic equations, the nature of the state is known and one can calculate higher-order correlation functions as analytic expressions of for u, ϕ, and n_{th}, which can easily be calculated numerically. In this talk, we prove that the OPO state is a squeezed thermal state and we examine the key dependence of these parameters on pumping conditions and present the results for some higher-order correlation functions.

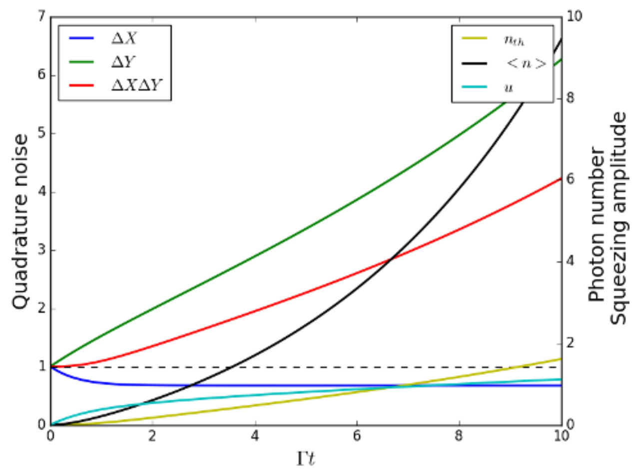

Fig. 1 The quadrature noise, squeezing amplitude, thermal photon number and, average photon number as a function of time for strong pumping regime. The dashed at line at ΔXΔY=1 represent the pure squeezed limit.

References

[1] J. Fiurášek, "Continuous-variable quantum process tomography with squeezed-state probes," Phys. Rev. A. **92**, 022101 (2015)
[2] M. O. Scully and M. S. Zubairy, *Quantum optics* (Cambridge university press, 1997).
[3] J. Johansson, P. Nation, and F. Nori, Computer Physics Communications **184**, 1234 (2013).

Partition formalism employed to get new inequalities for indivisible quantum systems

V. I. Man'ko[1,2], **Z. Seilov** [1,*]

[1] *Moscow Institute of Physics and Technology (State University), Institutskii per. 9, Dolgoprudnyi, Moscow Region 141700, Russia*

[2] *Lebedev Physical Institute, Russian Academy of Sciences, Leninskii Prospect 53, Moscow 119991, Russia*

*e-mail: *seilov@live.ru*

Correlations in quantum system play essential role in quantum communication and quantum computation. Recently in works [1, 2] the notion of hidden quantum correlations was introduced. These correlations are defined for indivisible N-level quantum system (qudit) can be presented as entropic inequalities analogous to the properties of of composite quantum systems, such as subadditivity condition and strong subadditivity condition.

In our work using constructed bijective map between integers $y = 1, \dots, N$ and set of variables $x_i = 1, \dots, X_i$, where $N = \prod_{i=1}^{n} X_i$, we obtain [3] the partition of indivisible N-level system into n subsystems. Such approach allows employing the properties of composite system (bipartite, tripartite) of n subsystems to any indivisible N-level quantum system. This approach can be employed to any partition of multilevel system into "virtual" subsystems.

Using obtained functions detecting the hidden correlations in the system, we found new inequalities for special functions that determine the matrix elements of the SU(2)-group irreducible representation and the Clebsch-Gordan coefficients for quantum angular momentum. In this approach we used representation of squares of Clebsch-Gordan coefficients as probabilities the same way as we did it in our previous work [4]. For example, subadditivity condition for considered case has the following form

$$\begin{aligned}
&- \sum_{m_2=-j_2}^{j_2} f(y(m_1, m_2)) \log \sum_{m_2=-j_2}^{j_2} f(y(m_1, m_2)) - \\
&- \sum_{m_1=-j_1}^{j_1} f(y(m_1, m_2)) \log \sum_{m_1=-j_1}^{j_1} f(y(m_1, m_2)) \\
&\geq - \sum_{y=0}^{N} f(y(m_1, m_2)) \log \sum_{y=0}^{N} f(y(m_1, m_2)), \qquad (1)
\end{aligned}$$

where $f(y(m_1, m_2))$ is a square of Clebsch-Gordan coefficient $\langle j_1, j_2 |\, j, m\rangle$.

Same technique can be applied to any set of real numbers, which can be associated with a set of probabilities according to the formula $p(y) = \dfrac{|s_y|}{\sum_{y'=1}^{N} |s_{y'}|}$, where $p(y)$ is the probability associated with a real number s_y, and y takes integer values from 1 to the number N of elements in the set of considered real numbers.

[1] M. A. Man'ko and V. I. Man'ko, J. Russ. Laser Res. **34**, 203 (2013).

[2] V. N. Chernega, O. V. Man'ko, Phys. Scr. **90**, (2015).

[3] V. I. Man'ko, Z. Seilov, J. Russ. Laser Res. **38**, 50 (2017).

[4] V. N. Chernega, O. V. Man'ko, V. I. Man'ko, and Z. Seilov, Theor. Math. Phys. (to be published) [accepted for publication].

Continuous-variable quantum teleportation on a photonic chip

Takahiro Serikawa,[1] Naoto Takanashi,[1] Yohei Sakamaki,[2] Kenta Takata,[2]
Toshikazu Hashimoto,[2] Dylan H. Mahler,[3] Jeremy L. O'Brien,[3] Jun-ichi Yoshikawa,[1] and Akira Furusawa[1]

[1]*Department of Applied Physics and Quantum-phase Electronics Center, School of Engineering, The University of Tokyo*
[2]*Device Technology Laboratories, NTT Basic Research Laboratories*
[3]*Centre for Quantum Photonics, H. H. Wills Physics Laboratory & Department of Electrical and Electronic Engineering, University of Bristol*

Scalable implementation of photonic circuits is demanded for sophisticated applications of quantum optics, such as error correction and quantum computation. An integrated waveguide chip exhibits smaller size, higher stability, and better reproducibility, than the traditional free-space optics. Bulky mode-matching equipments such as lenses and adjustable mirrors are not needed for a waveguide optics because it is single-mode, and this feature enables tuning-less construction.

Recently Carolan *et al.* demonstrated a single-photon interferometer system with a reprogrammable optical waveguide chip [1]. In this experiment, 15 Mach-Zehnder interferometers (MZI) compose a beamsplitter network which works as a six mode universal linear optics. In contrast, in many-photon regime, the scale is relatively limited such as two sequential interferometers [2]. The difference comes from the sensitivities to the optical loss. In a discrete-variable (DV) system, the loss does not appear on the output state because each event is post-selected by the photon-clicks as a trigger. On the other hand, a continuous-variable (CV) system is usually unconditional, and the loss is included as an error in the output. However, this does not mean that CV systems are specially fragile to losses and DV systems do not suffers from them, since the waiting time increases exponentially with the mode-number in a DV system without error correction. Therefore, veryfing the process in CV regime is an explicit benchmark of on-chip optics, and technical improvements are still requied for a complex CV system.

Here, we developped an application specific photonic integrated circuit to realize low-loss implementation of CV quantum teleportation, which demonstrates the essential components of CV operations including feedforwarding. It contains 8 interferometers dedicated to the linear optical part of CV teleportation, that is, entanglement generation, displacement, and homodyne detection. Each of these variable MZI beamsplitters is controlled by a heater and has 20dB of extinction ratio, enabling the fine tuning of split ratio and giving the degree of freedom to temporally switch the path during the verificaiton.

Figure 1. shows the schematic of the experimental setup. The ancilla squeezed light beams are generated in the optical parametric oscillators (OPO) and coupled to optical fibers. Input state beam, feedforward beams, and local oscillator beams for homodyne detection are also fiber-coupled. All these light beams enter the waveguide via a fiber array, where the coupling efficiency is measured to be 85%. On the teleportation chip, an EPR beam pair is generated with one beamsplitter, and distributed to “Alice” and “Bob” parts both on the chip. In Alice, CV Bell-measurement is done on the input state beam and the one part of EPR beams. For this, three beam splitters are tuned to 50:50 split ratio and the light signal is measured by external photodetectors. The teleportation is completed by displacement operation by the external electronics and Bob’s two sequential 98:2 beamsplitters. The output state is analyzed by homodyne-tomography also with an on-chip beamsplitter and off-chip photodetectors. The total losses on the chip is estimated at 6% for Alice’s paths and 10% for Bob’s path.

We prepared the input state as a coherent state and one example of the Wigner functions of the input / output states is shown in Fig.2. From the quadrature-variance of the output state, the fidelity of the output state is estimated at 0.62, which is above the classical limit of 0.5 [3].

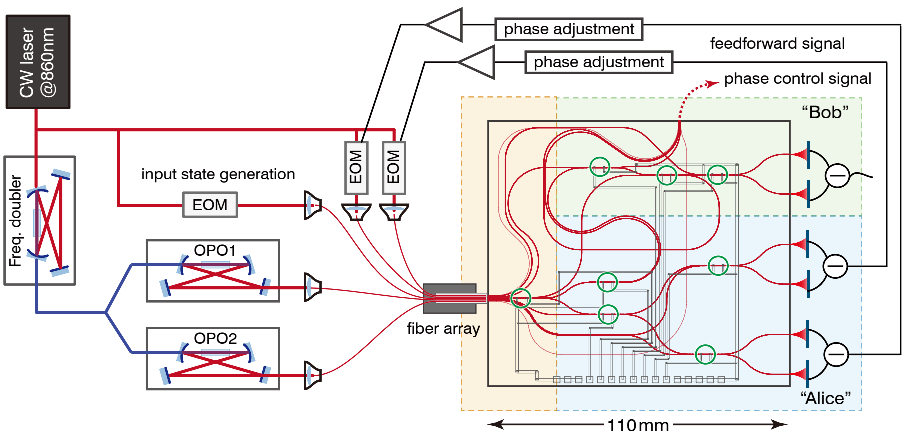

Figure 1. schematic of the experimental setup. Optical pathes are depicted as red lines on the chip. Green circles indicates the place of variable beamsplitters.

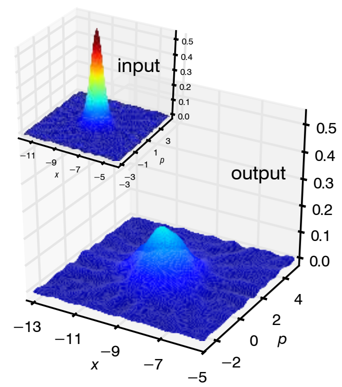

Figure 2. Wigner functions of the input / output states. $\hbar = 1/2$.

[1] J. Carolan *et al.*, Universal linear optics, Science **14**, 711-716 (2015).
[2] G. Masada *et al.*, Continuous-variable entanglement on a chip, Nature Photonics **9**, 316–319 (2015).
[3] A. Furusawa *et al.*, Unconditional Quantum Teleportation, Science **23**, 706-709 (1998).

Witnessing Quantum Squeezing via Binary Homodyne Detection

Christian R. Müller, Kaushik P. Seshadreesan, Christian Peuntinger, Gerd Leuchs, Christoph Marquardt
Max Planck Institute for the Science of Light, Staudtstraße 2, D-91058 Erlangen, Germany
Department of Physics, Friedrich Alexander University Erlangen-Nürnberg (FAU), Staudtstraße 7/B2, D-91058 Erlangen, Germany

Homodyne detection [1] is the most prominent measurement scheme in continuous-variable quantum optics. A homodyne detector performs a projective measurement along a quadrature of the electromagnetic field mode, yielding continuously distributed outcomes. The outcome distribution is the marginal of the Wigner function of the quantum state. Homodyne detection also forms the basis of heterodyne, or ``dual homodyne" detection, which corresponds to measuring the Q function of the state.

While homodyne detection in principle provides continuously distributed quadrature observables, the observables are often discretized in practice. In the extreme case, the discretization is binary, yielding "quadrature parity" observables that simply distinguish positive quadrature values from the negative. Such projections are used, e.g., in continuous-variable Bell tests, binary phase shift keying (BPSK) optical communication and binary modulated continuous variable quantum key distribution (QKD) [2]. In some practical systems, the binary discretization is implemented by direct saturated amplification right after photodetection, which renders the continuous values completely inaccessible. In any system, at the very least, there is always some unavoidable discretization due to Analog-to-Digital (AD) conversion.

We investigate the implications of discretizing homodyne measurements. We consider the extreme case of quadrature parity binary homodyne detection. We show that despite the one-bit resolution quadrature squeezing [3] can be witnessed efficiently with such a scheme when augmented with displacements in phase space. We treat the task as binary hypothesis testing between a coherent state and a squeezed state and determine the *a posteriori* probabilities and the minimum average error probability. We complement our theoretical analysis with an experimental verification. To this end, we witness both a coherent state and a weakly squeezed state via binary homodyne detection and compare the results to homodyne detection with a continuous spectrum. We show that the ratio between the required sizes of the data set to achieve the same average *a posteriori* probability as ideal homodyne detection is merely 3.3. We stress that this value, as it applies to the extreme discretization into binary outcomes, is indeed an upper bound for the required samples overhead for arbitrarily discretized homodyne detection.

Our results bear implications on the feasibility of detecting quantum squeezing in optical satellite communication systems, where the detectors intrinsically implement binary homodyne detection by design. We show that these detectors operating at state-of-the-art bandwidths (gigahertz range) can detect a squeezed vacuum beam even after substantial channel attenuation. For example, a moderately squeezed vacuum beam (6 dB below shot noise) can be detected within a few seconds even after about 45 dB loss, which corresponds to low Earth orbit (LEO)-scale distances for typical aperture sizes of the optics used.

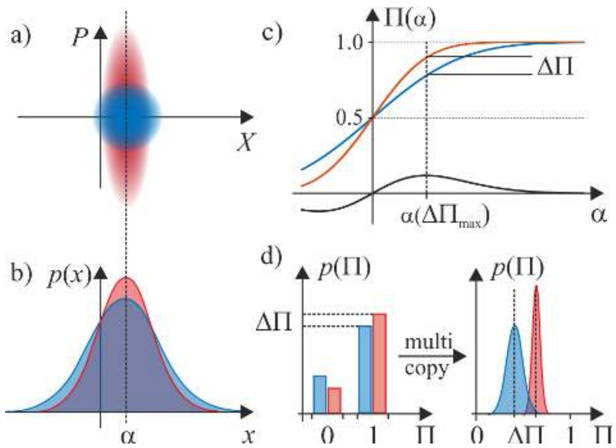

Fig. 1 a) Illustration of a displaced vacuum (blue) and a displaced squeezed vacuum state (red) in phase space. b) Marginal distributions as obtained via (high-resolution) homodyne detection along the squeezed quadrature x. c) Expectation value of the quadrature parity of the displaced states and their difference $\Delta\Pi(\alpha)$ (black curve) as a function of the displacement amplitude α. d) The uncertainty of the individual measurement outcomes and the mutual overlap of the associated statistical distributions is reduced by accumulating measurement statistics.

References

[1] H. P. Yuen and V. W. S. Chan., "Noise in homodyne and heterodyne detection," Opt. Lett. **8**, 177–179 (1983).

[2] C. Weedbrook, S. Pirandola, R. Garcia-Patron, N. J. Cerf, T. C. Ralph, J. H. Shapiro, S. Lloyd, "Gaussian Quantum Information", Rev. Mod. Phys. **84**, 621 (2012).

[3] U. L. Andersen, T. Gehring, C. Marquardt, and G. Leuchs, "30 years of squeezed light generation," Phys. Scripta **91**, 053001 (2016).

Effects of multimode dynamics through quantum model of electro-optic light modulation

V Sheremetev[1], A Trifanov[1], Alexei D. Kiselev[1], G Miroshnichenko[1]
[1]Department of Mathematics, ITMO University, Kronverksky Ave. 49, 197101 St. Petersburg, Russia

Rapidly developing quantum communication systems require efficient tools to control and manipulate single-photon states in waveguides. In classical optics, there is a class of such tools known as light modulators that use electro-optic effects to modulate light waves both in space and time. An algebraic approach to electro-optic modulation (EOM) of quantum light developed in [1] resolves difficulties of previous quantum theories and provides exactly solvable EOM model where the modulator can be regarded as a multiport device. In this paper we use this approach for investigation into the effects of multimode dynamics in systems of both technological and fundamental interest.

We have generalized the model presented in [1] to take into account polarization states of interacting frequency modes. Polarization dependent dynamics of the resulting multimode system is studied to perform analysis of temporal evolution of Stokes operators. We discuss a number of effects related to the state of polarization of different modes depending on the input polarization state and the characteristics of the modulator.

In our second problem, which is closely related to famous Bell's theorem, we study three-photon entangled states. There are several known approaches to demonstrate violation of Bell's inequality in the bipartite case . For example, two frequency-entangled photons generated in spontaneous down conversion process were used in [2,3]. It was found that in observed violation of CH74 inequality the exact quantum boundary was not reached. In our tripartite setup, the source emits three photons sent to the three observers: Alice, Bob and Charlie that are equipped with their waveguides, modulators, filters and detectors. Parameters of the modulators could be chosen independently by the owners (no information exchange between parties is allowed). We present analytical results on the Mermin inequality and perform numerical analysis of the related optimization problem. The results confirm the statement of nonlocality and provide further insight into the Bell inequality problem.

Our third problem concerns logical gates in quantum schemes. We show how to built NS-gate in the frequency domain using quantum electro-optic modulators rather than traditional polarization and dual-rail coding. This result is of importance as it can be used to construct the key CNOT quantum element.

References

[1] Miroshnichenko G P, Kiselev A D, Trifanov A I, Gleim A V 2016 arXiv:1605.05770v1
[2] Brunner N, Cavalcanti D, Pironio S, Scarani V, Wehner3 S 2014 arXiv:1303.
[3] Olislager L, Cussey J, Nguyen A T, Emplit P, Massar S, Merolla J M and Phan Huy K 2010 Phys. Rev. A **82** 013804
[4] Olislager L, Mbodji I, Woodhead E, Cussey J, Furfaro L, Emplit P, Massar S, Phan Huy K, Merolla J-M 2012 New J. Phys. **14** 043015

Random Numbers From Vacuum Fluctuations

Yicheng Shi , Brenda Chng , Christian Kurtsiefer

March 31, 2017

Abstract

We implement a quantum random number generator (QRNG) based on a balanced homodyne measurement of vacuum fluctuations of the electromagnetic field. Using a polarising beam splitter we split a local oscillator laser source into two beams with equal power and illuminate them on two fast photodiodes. The fluctuation of the photocurrent difference is measured and shows a white noise over a large bandwidth.

The noise signal is recorded and digitized with a high speed ADC unit and is directly processed with a fast randomness extraction scheme based on a linear feedback shift register. The random bit stream is continuously read into a computer at a rate of about 480 Mbit/s and passes an extended test suite for random numbers.

The above implementation is published on: Appl. Phys. Lett. 109, 041101 (2016); doi: http://dx.doi.org/10.1063/1.4959887

More recent work of ours includes building a even more simplified version of the above QRNG implementation. By shining an elliptical laser beam spot direct onto a pair of segmented photodiodes (wave front splitting) instead of using a beam splitter (amplitude splitting) we manage to significantly shrink the size of the device while maintaining the same performance. A manuscript of this work is under preparation.

On-chip plasmonic cavity-enhanced quantum emitters

Hamidreza Siampour, Shailesh Kumar, and Sergey I. Bozhevolnyi*

Centre for Nano Optics, University of Southern Denmark, Campusvej 55, DK-5230 Odense M, Denmark

**hasa@mci.sdu.dk*

Abstract: Nanofabrication of quantum cavities based on dielectric-loaded-plasmonic waveguides using Bragg gratings is presented. The cavities are deterministically positioned around the diamond-based emitters using lithographic patterning of electron-beam resist on silver. We observe a modulation of emission spectrum for the coupled emitter and a 6-fold enhancement in the total decay rate.

Keywords: Nanofabrication, quantum cavity, nitrogen-vacancy center, dielectric-loaded plasmonic waveguides, integrated quantum optics, quantum optical networks.

Strongly confined surface plasmons can be utilized to enhance the light-matter interaction for individual quantum emitters [1, 2]. Dielectric loaded surface plasmon polariton waveguide (DLSPPW) has been proposed as a waveguide which support confined modes at relatively lower loss compared with other metallic plasmonic structures [3]. Here, we employ the method of top-down fabrication [4] to make a compact cavity based on DLSPPWs which exploits filtering abilities of Bragg reflecting gratings [5] to form a cavity, which also leads to an emission rate enhancement (Fig. 1).

In the experiment, a silicon sample is coated with a silver film, on which gold coordinate markers are made, and subsequently, nanodiamonds are spin coated. The sample is then characterized by scanning in a fluorescence confocal microscope and lifetime, spectrum and autocorrelation measurements are taken for the nanodiamonds. DLSPPW-based cavities are fabricated by lithographic patterning of hydrogen silsesquioxane (HSQ) electron beam resist onto the NV-centers containing nanodiamonds (Fig.1-a (top)). Postfabrication camera image shows the coupling of the NV emitter to the cavity, and subsequent emission from the tapered gratings at the two ends of the waveguide (Fig.1-a (down)). A reduction in lifetime (from ~9 ns to ~3 ns) is observed for the coupled NV center (Fig.1-b). On average the lifetime of NV-centers decreased by a factor of 2 due to a silver plane surface, from ~18 ns on fused silica substrate to ~9 ns on silver surface. This gives a ~6-fold enhancement in total decay of the quantum emitter indicating strong mode confinement. Spectrum taken from the uncoupled NV (blue), coupled NV (red), and outcoupled ends A (dark green), and B (light green) shows an improved spectral purity (selective narrow band) for the outcoupled ends (Fig.1-c). Considering the average mode index of ~1.3, and the roundtrip length of ~13.5 µm for the cavity, the free spectral range (FSR) of the cavity is calculated to be ~25 nm at around 700 nm free space wavelength that is almost agreed with the experimental results shown in Fig1-c for the outcoupled ends A and B.

In conclusion, we have presented a DLSPPW-based cavity coupled to a diamond-based NV emitter. The integrated structure with enhanced total decay rate and improved spectral purity of the coupled NV emitter potentially can be applied for on-chip realization of quantum-optical networks.

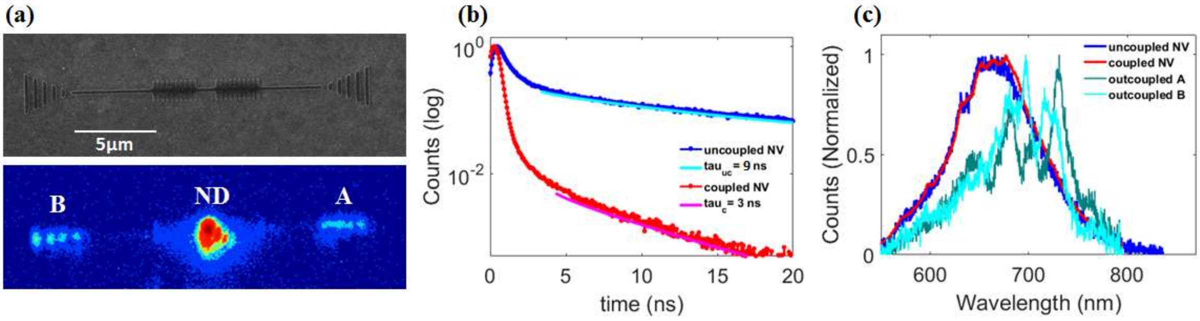

Fig. 1 (a) Scanning electron micrograph of a HSQ DLSSPW-based cavity, fabricated on silver film (top). The DLSPPW ridge has dimensions of 250 nm in width and 180 nm in height. The transverse ridges of the Bragg reflecting gratings are 1.25 µm in length, 130 nm in width and repeated with a period of Λ=275 nm. This gives an average refractive index of 1.3 for the effective DLSSPW mode. The gap distance between the two Bragg reflecting mirrors is 2.32 µm.. The periodicity of the tapered gratings at the two ends of the DLSSPW is 550 nm. Charge coupled device (CCD) camera image of the whole structure where the nanodiamond is excited at the center of the cavity and a fluorescence image of the focal plane is taken, is presented (down). (b) Lifetime of the NV center before (blue) and after coupling to the cavity. (c) Spectrum taken from the uncoupled NV (blue), coupled NV (red), and outcoupled ends A (dark green), and B (light green).

References

[1] M.S. Tame et al., Nat Phys, 9 (2013) 329-340.
[2] N.P. de Leon et. al, Physical Review Letters, 108 (2012) 226803.
[3] R.M. Briggs et al., Nano Letters, 10 (2010) 4851-4857.
[4] W. Pfaff et al., Journal of Applied Physics, 113 (2013) 024310.
[5] G. Biagi et. al, Opt. Letters, 40 (2015) 2429-2432.

Quantum metrology of spatial deformation using arrays of classical and quantum light emitters

Jasminder S. Sidhu[1,*] and Pieter Kok[1,†]

[1]Department of Physics and Astronomy, The University of Sheffield, Sheffield, S3 7RH, UK.

Quantum mechanics has established physical limitations to precision bounds in myriad applications in parameter estimation. Approaching these limitations through high precision measurements is one of the principal objectives in quantum metrology. These efforts have historically predicated the development of fundamental theories across science. An immediate example is the use of squeezed light for sensitivity enhancements of large gravitational wave interferometers such as LIGO [1]. Performance enhancements have also been fruitfully demonstrated in clocks, sensing, and thermometry.

Quantum metrology is rooted in the theory of quantum parameter estimation. The quantum Cramér-Rao bound (QCRB) has become a standard tool to lower bound the variance of an unbiased estimator that maps measured data from quantum measurements to parameter estimations. Quantum resources have demonstrated improvements to the estimation sensitivities of physical parameters. A large proportion of metrological protocols can be reduced to that of phase estimations [2]. Extensive studies have thus estimated Hamiltonian parameters, given their enhancement to phase and frequency sensitivities [3]. The study of direct spatial measurements remains largely unexplored.

In this work [4], we focus on estimating the distances between neighbouring light sources along an array. We evaluate how changing the nature of the light sources and array deformations can impact the estimation precision. This motivates the first construction of a generator of translations in source distances for the detection of arbitrary spatial deformations. By considering some general deformation ξ introduced to an array of light sources, we derive the generator $\hat{\mathcal{G}}$ responsible for changes in the source separation distance d. We find that

$$\hat{\mathcal{G}}(\xi) = -\xi \sum_{j=1}^{N} \mu_j' \int dk_j \; k_j \, \hat{n}_j(k_j), \tag{1}$$

where $\mu_j' = \partial_d \mu_j$ defines the derivative of the initial j^{th} source position and $\hat{n}_j(k_j)$ the number operator for source j in mode k_j. This generator characterises the dynamical property of the parameterisation process of the state on ϑ due to homogenous deformations and its Hermiticity follows from the number operator. It has units of momentum which is expected since the array sources undergo spatial translations according to the homogeneous transformation ξ. For the unitary process $\rho(\vartheta) = \hat{U}(\vartheta)\rho(0)\hat{U}^\dagger(\vartheta)$, we show that the unitary may be written as $\hat{U}(\xi) = \exp\left[-id\hat{\mathcal{G}}(\xi)\right]$. This establishes the quantum Fisher information (QFI) as the variance of our generator [5]. For some stretching ξ_s of the array, we compare the performance of single photon emitters, coherent, thermal, and entangled sources of light. Consistent with the work of Giovannetti *et al.* [6], we find the entangled state related to the generator provides the best performance. Photon number counting is an optimal measurement which saturates the QCRB since its classical Fisher information is shown to become identical to the QFI. We also report on the first occurrence of a second optimal estimator for the same metrological problem. We demonstrate that this second estimator satisfies all of the necessary criteria for optimally unbiased estimators.

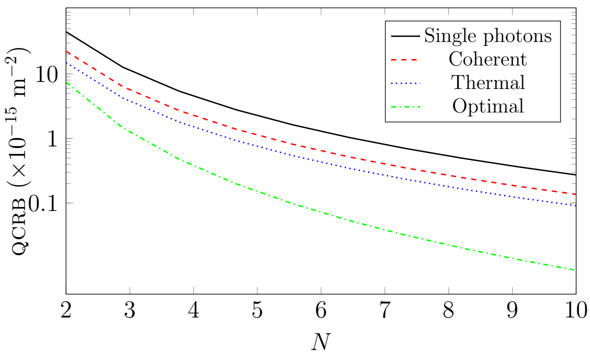

FIG. 1: The QCRB scaling with number of sources N for SPEs, coherent, thermal states and the optimally entangled state with $s = 300$ nm and $\xi_s = 2$. The higher mode occupancy of thermal states permits better estimation performance when compared with the quantum SPEs. However, the entangled state constructed from the eigenvectors corresponding to the minimum and maximum eigenvalues of the generator $\hat{\mathcal{G}}$ remains optimal.

Our work permits the precise evaluation of deformed coordinates of light emitters and allows for corrective measures to negate their effects. This would find applications in evaluating stresses and strains to prevent material fractures and imaging of tagged DNA molecules [7].

This research was funded by the DSTL Quantum 2.0 Technologies Programme. The authors thank Mark Pearce for useful discussions.

* Electronic address: jsidhu1@sheffield.ac.uk
† Electronic address: p.kok@sheffield.ac.uk

[1] A. J. *et al.*, Nature Photonics **7**, 613 (2013).
[2] V. Giovannetti, S. Lloyd, and L. Maccone, Science **306**, 1330 (2004).
[3] S. Pang and T. A. Brun, Phys. Rev. A **90**, 022117 (2014).
[4] J. Sidhu and P. Kok, (2017), arXiv:1610.00497v2 [quant-ph] .
[5] S. L. Braunstein, C. M. Caves, and G. Milburn, Annals of Physics **247**, 135 (1996).
[6] V. Giovannetti, S. Lloyd, and L. Maccone, Phys. Rev. Lett. **96**, 010401 (2006).
[7] M. Tsang, Optica **2**, 646 (2015).

Reconfigurable & Modular Quantum Optics On-chip

P. L. Mennea[1], W. Clements[2], M. T. Posner[1], R. H. S. Bannerman[1], D. H. Smith[1], J. Renema[2], J. C. Gates[1], W. S. Kolthammer[2], I. A. Walmsley[2], P. G. R. Smith[1]
1. Optoelectronics Research Centre, University of Southampton, Southampton, UK
2. Clarendon Laboratory, University of Oxford, Oxford, UK

Quantum optical experiments are increasingly taking an integrated format to enhance scalability and phase stability. Silica is an advantageous material for this purpose due to low propagation loss and high-efficiency coupling to optical fibre; a number of key on-chip experiments have already been carried out with up to four photons using this material [1]. Fabrication imperfections create a number of difficulties in moving to more complex setups since the classical characteristics of the network must be found before an analysis of its quantum properties can be carried out, and this process becomes combinatorially difficult as the circuit size grows.

We have therefore developed a system of reconfigurable linear optical modules which may be tested as units and then combined to make up *any* desired network. The ability to test and select subunits improves yield compared with those of monolithic devices, as well as improving uniformity across units. Each of these modules contains ten parallel Mach-Zehnder interferometers (MZIs), each combined with two thermo-optic phase shifters in the arrangement depicted in figure **??**, permitting modulation of both reflectivity and relative phase–each MZI thus acts as an arbitrarily configurable beamsplitter.

Modules are fabricated via direct UV writing of a photosensitive germanosilicate glass layer in deposited on a silica-on-silicon substrate by flame hydrolysis deposition. Waveguide dimensions are selected to provide mode-matching to optical fibre for improved coupling efficiency. Out-of-band first-order Bragg gratings are co-patterned with the waveguides in the network using a two-beam Direct Grating Writing (DGW) approach in order to further simplify the characterisation process, permitting values such as propagation losses and coupling coefficients to be extracted precisely. The thermo optic phase shifters are patterned via lift-off of an e-beam evaporated nichrome layer before polishing and mounting to produce the final devices shown in figure **??**.

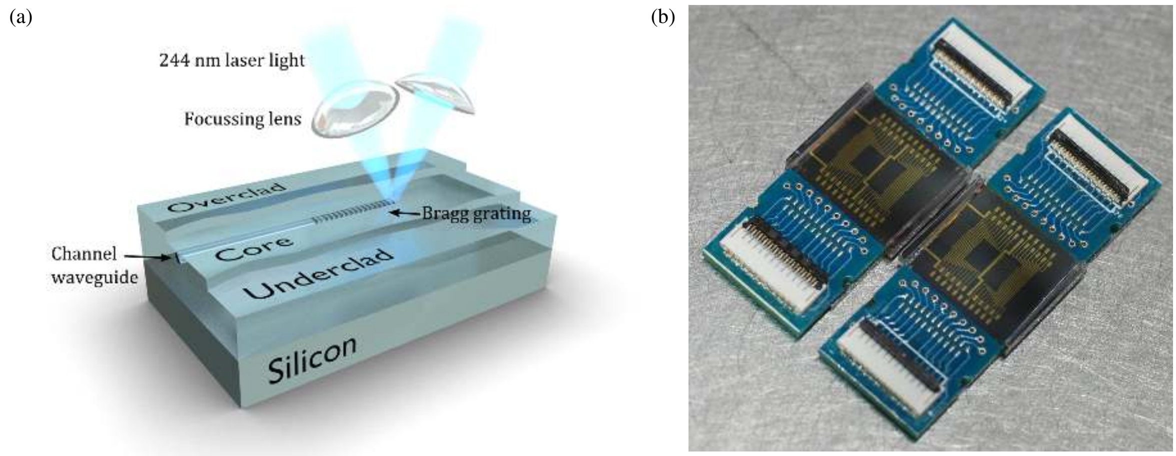

Fig. 1 ?? Diagram of the direct grating writing system used to pattern waveguides and Bragg gratings in photsensitive glass layers. **??** A pair of mounted modular chips ready to be coupled together.

We will report on the design, fabrication and characterisation of these modules, as well as on initial results from quantum experiments making use of this system.

References

[1] J. B. Spring, P. Salter, P. Mennea, B. Metcalf, P. C. Humphreys, M. Moore, J. C. Gates, N. Thomsa-Peter, M. Barbieri, X.-M. Jin, N. K. Langford, S. W. Kolthammer, P. G. Smith, M. Booth, B. J. Smith, and I. A. Walmsley, "Quantum interference of multiple on-chip heralded sources of pure single photons," in Research in Optical Sciences, Optical Society of America, QW1B.6 (2014).
[2] B. J. Metcalf, J. B. Spring, P. C. Humphreys, N. Thomas-Peter, M. Barbieri, W. S. Kolthammer, X.-M. Jin, N. K. Langford, D. Kundys, J. C. Gates, B. J. Smith, P. G. R. Smith, and I. A. Walmsley, "Quantum teleportation on a photonic chip," Nat. Photonics **8**, 770–774 (2014).

Nanodiamond on integrated waveguides as a spin-photon interface

Joe Smith,* J Kennard, A Young, P Jiang, F Huerta, S Knauer, J Pugh, M Cryan, and J Rarity

Quantum Engineering Centre for Doctoral Training and QET Labs, University of Bristol, Tyndall Avenue, Bristol, BS8 1FD, United Kingdom.

Linear optical quantum circuits (LOQC) are a powerful platform for quantum optical experiments. With the addition of high-fidelity photon sources, feed-forward, and efficient photon detection, LOQC forms a core component of proposed quantum enhanced technologies [1].

Atom-like colour centres in diamond are addressable two level systems that look promising as a single photon source [2]. Strong emission from a nanodiamond alleviates the need for processing bulk diamond. Additionally, in low strain, the NV centre is capable of producing pairs of photons entangled to the long-lived spin state of the system [3]. It has been demonstrated that by evanescently converting the dipole emission into the propagating mode of a fibre, this can be converted to spin-path entanglement [4].

We use FDTD simulations to merit a proposal to generate spin-path entangled photons by depositing a nanodiamond on the c-line of a high index suspended waveguide and illustrate a method to reduce the strain in nanodiamonds using a local array of electrodes. We present recent experimental results of nanodiamond-coupled devices fabricated in-house using electron beam lithography, metallisation, and plasma etching.

[1] J. L. O'Brien, A. Furusawa, and J. Vučković, Nature Photonics **3**, 687 (2009).

[2] I. Aharonovich and E. Neu, Advanced Optical Materials **2**, 911 (2014).

[3] E. Togan, Y. Chu, A. Trifonov, L. Jiang, J. Maze, L. Childress, M. G. Dutt, A. S. Sørensen, P. Hemmer, A. Zibrov, *et al.*, Nature **466**, 730 (2010).

[4] R. Mitsch, C. Sayrin, B. Albrecht, P. Schneeweiss, and A. Rauschenbeutel, Nature Communications **5** (2014).

* j.smith@bristol.ac.uk

Spectral manipulation of quantum light by space-time duality methods

Filip Sośnicki, Michał Karpiński

Faculty of Physics, University of Warsaw

A promising approach towards large scale quantum information processing is via a hybrid quantum network which uses disparate quantum systems such as single photon sources, quantum memories or quantum qubit gates, interconnected with photonic links. However these systems typically have vastly different spectral-temporal characteristic: for example the bandwidths of systems exhibiting single-photon nonlinearity lie in the single MHz range, whereas typical single-photon and optical communication channel bandwidths approach tens to hundreds of GHz. Efficient optical interfacing of these systems requires devices capable of low-loss coherent bandwidth compression or expansion of single-photon light pulses.

A feasible approach towards bandwidth compression stems from the concept of space-time duality [1], which enables finding temporal equivalents of spatial optical phenomena. Dispersive temporal broadening of an optical pulse corresponds to diffractive propagation of a beam in space. By applying a time-varying quadratic phase a temporal lens may be realized, enabling modification of spectral and temporal bandwidths. Direct electro-optic phase modulation enables guided-wave realization of time lenses in a deterministic and noise-free manner, meeting the key requirements for spectral manipulation of quantum light pulses [2]. However standard electro-optic time lenses, driven by single-tone electronic signals, enable only limited compression factors, due to material limitations on achievable phase modulation depth.

Large-scale spectral modifications of quantum light pulses, including single photons and entangled photon pairs, may be realized by utilizing the temporal analogue of the Fresnel lens concept, where application of a quadratic phase modulo 2π enables bypassing the phase modulation depth limitations. Such complex phase modulation patterns require the use of electronic arbitrary waveform generators (AWG). By numerical simulations we analyze the performance of realistic bandwidth conversion devices, including important AWG characteristics such frequency response, resolution and noise. The use of graphical processing unit platform enabled efficient realization of multiple Fourier transforms on very large samples, necessary to accurately probe spectral and temporal scales spanning up to 6 orders of magnitude.

We show that a bandwidth converter based on an electro-optic time lens can perform low-loss compression of spectral width of single photons from hundreds of GHz to tens of MHz, prospectively enabling efficient interfacing of media exhibiting single-photon nonlinearity with optical communication channels. We foresee the feasibility of an initial experimental demonstration, especially given the ongoing development of fast electro-optic phase modulation techniques. Our results indicate that electro-optic bandwidth converters may become an enabling tool for the development of hybrid quantum networks.

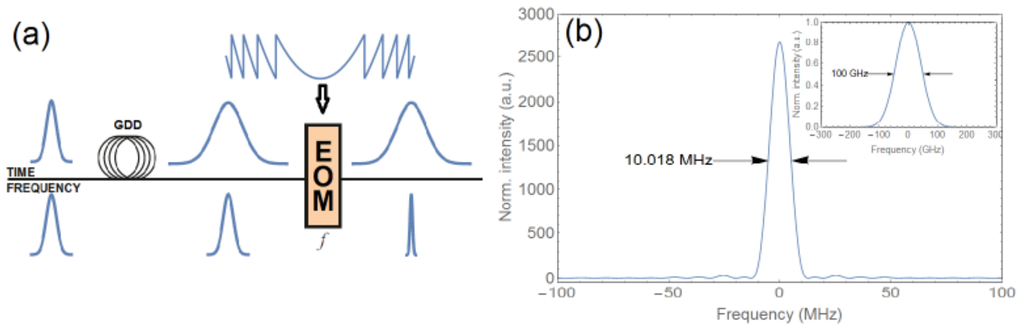

Figure 1: (a) Conceptual schematic of electro-optic bandwidth compression. (b) Spectral intensities of initial (inset) and spectrally compressed wavepackets.

References

[1] B. H. Kolner, *Space-Time Duality and the Theory of Temporal Imaging*, IEEE J. Quant. Electron. **30**, 1951–1963 (1994).

[2] M. Karpiński, M. Jachura, L. J. Wright, and B. J. Smith, *Bandwidth manipulation of quantum light by an electro-optic time lens*, Nat. Photon. **11**, 53–57 (2017).

Narrow-bandwidth sensing of high-frequency fields with continuous dynamical decoupling

Alexander Stark,[1,2] Nati Aharon,[3] Thomas Unden,[2] Daniel Louzon,[2,3] Alexander Huck,[1] Alex Retzker,[3] Ulrik Lund Andersen[1] and Fedor Jelezko[2,4]

[1]Department of Physics, Technical University of Denmark, Fysikvej, Kongens Lyngby 2800, Denmark
[2]Institute for Quantum Optics, Ulm University, Albert-Einstein-Allee 11, Ulm 89081, Germany
[3]Racah Institute of Physics, The Hebrew University of Jerusalem, Jerusalem 91904, Israel
[4]Center for Integrated Quantum Science and Technology (IQst), Ulm University, 89081 Germany

Weak oscillating signals are typically out of reach for ordinary detection schemes making dynamical decoupling the method of choice to succeed this task. State of the art decoupling sequences, however, are limited to detect signals in the kHz to MHz frequency range. We present a general scheme that relaxes this limitation and allows for the detection of high frequency signals. The implementation can be performed with any two-level system (TLS) with an energy separation matching the signal's frequency. Our scheme is based on continuous driving of the TLS (cf. Fig. 1b), thereby effectively decoupling the system from external noise fields. Further concatenation of driving fields reduce the impact of inherent power fluctuations and hence, robustness to both external and controller noise is achieved (cf. Fig. 1c), resulting in a significantly enhanced coherence time (cf. Fig. 1d) enabling narrow bandwidth sensing. While our scheme is general and suitable to a variety of atomic and solid-state systems, we experimentally demonstrated it with the Nitrogen Vacancy (NV) center in diamond, utilizing its ground sub-states as a two-level system (cf. Fig. 1a). For a diamond with natural abundance of ^{13}C we achieved coherence times up to 1.43 ms (cf. Fig. 1d) resulting in a smallest detectable magnetic field strength of 4 nT at 1.6 GHz. Attributed to the inherent nature of our scheme, we observed an additional increase in coherence time due to the signal itself.

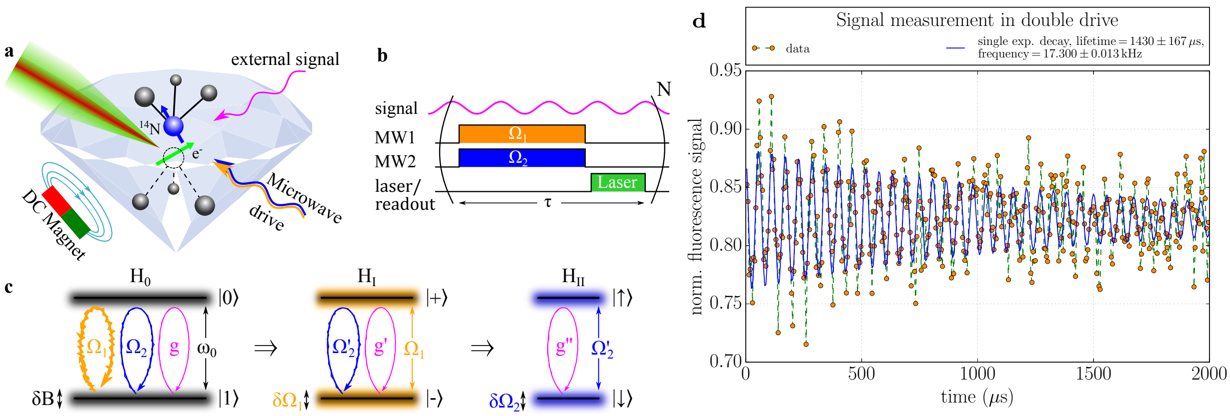

Figure 1: Schematic representation of our setup: (a) The NV center probes an external signal while it is being manipulated by the control fields. (b) Schematic representation of the sequence applied in this work. (c) The protected TLS: The bare system, H_0, is subjected to strong environmental noise δB. Applying a strong drive, Ω_1, opens a protected gap, now subjected mainly to drive fluctuations $\delta\Omega_1$. A second drive, Ω_2, is then applied to protect the TLS, H_I , from these fluctuations, resulting in a TLS, H_{II} , on resonance with the signal, $g'' = g/4$, with noise mainly from the second weak drive $\delta\Omega_2 \ll \delta\Omega_1$. (d) Measurements of an external high frequency signal of strength g. By the application of two drive fields with $\Omega_1/2\pi = 3.363$ MHz and $\Omega_2/2\pi = 505$ kHz, we record a signal $g'' = \frac{g}{4}$ and increase the coherence time of the sensor by one order of magnitude with respect to the case of $g = 0$.

Two-photon interference from two blinking quantum emitters

Klaus D. Jöns[1], Katarina Stensson[1], Marcus Reind[2], Marcin Swillo[1], Yongheng Huo[3,2,4], Val Zwiller[1], Armando Rastelli[2], Rinaldo Trotta[2], and Gunnar Björk[1]
[1]Department of Applied Physics, Royal Institute of Technology (KTH), AlbaNova University Center, SE - 106 91 Stockholm, Sweden
[2]Institute of Semiconductor and Solid State Physics, Johannes Kepler University Linz, 4040, Austria
[3]Institute for Integrative Nanosciences, IFW Dresden, 01069, Germany
[4]Hefei National Laboratory for Physical Sciences at Microscale, University of Science and Technology Shanghai, 201315, China
stenss@kth.se

We investigate the effect of blinking on the two-photon interference measurement quantifying the indistinguishability of two independent quantum emitters. We find that blinking significantly alters the statistics in the second order intensity correlation function $g^{(2)}(\tau)$ and the outcome of two-photon interference measurements performed with independent quantum emitters. We demonstrate that the presence of blinking can be experimentally recognized by a deviation towards zero of the ratio $g^{(2)}(0)\ /g^{(2)}(\tau) = 0.5$ when distinguishable photons impinge on a beam splitter (Fig. 1). In general, such a deviation would indicate partial indistinguishability, but with blinking present, even completely distinguishable photons will give this result. Our findings explain the significant differences between linear losses and blinking for correlation measurements between independent sources. Through an "induced blinking" measurement, where we control blinking properties and linear loss, we show that the contribution to $g^{(2)}(\tau)$ originating in photons entering the beam splitter through the same port scales linearly with blinking on-state probability and quadratic with linear loss (fig. 2). This results in arbitrarily low values of $g^{(2)}(0)\ /g^{(2)}(\tau)$ for emitters with low on-state probabilities. Our results show that blinking imposes a mandatory cross-check measurement with distinguishable photons at $\tau = 0$ to correctly estimate the degree of indistinguishability of photons emitted by independent quantum emitters.

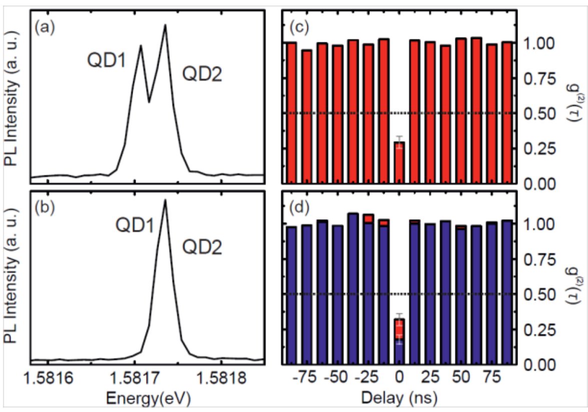

Fig 1. *(a) Photoluminescence spectrum from two remote QDs. Distinguishable. (b) Same as a) but with QD1 and QD2 tuned in resonance. (c) measured $g^{(2)}(\tau)$ for photons from (a). (d) $g^{(2)}(\tau)$ for photons from (b). Data from photons in parallel polarization (blue, indistinguishable) and perpendicular polarization (red, distinguishable).*

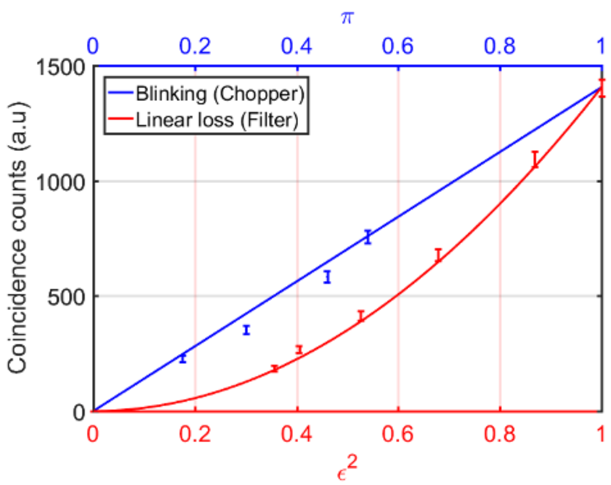

Fig 2. The contribution to $g^{(2)}(\tau)$ from photons entering the BS through the same port, at time delay τ=300 ns, as a function of induced blinking on-state probability π (blue) and filter transmission ε^2 (linear loss, red). Error bars represent statistical errors.

References

[1] K. D. Jöns *et al.*, ArXiv 1702.03278 (2017).

Adaptive Measurements in Experimental Quantum Process Tomography

I.A.Pogorelov, G.I.Struchalin, S.S.Straupe, K.S.Kravtsov, I.V.Radchenko, I.V.Dyakonov, S.P.Kulik

M.V.Lomonosov Moscow State University, Faculty of Physics,
119991, Russia, Moscow, Vorobjevy Gory, 1, MSU

Keywords:
adaptive quantum tomography
bayesian inference

We discuss experimental quantum process tomography based on adaptive Bayesian inference.

We have implemented an adaptive measurement scheme for the reconstruction of the action of arbitrary quantum channels on single qubits encoded in polarization of photons. Both trace-preserving and lossy processes are realized and reconstructed. We demonstrate a qualitative improvement in estimation precision in comparison with ordinary tomographic protocols. The advantage of the adaptive protocol is most significant for unitary and close to unitary processes.

An important point is that adaptive tomography is less sensitive to instrumental errors. We have studied the tomography performance in the case of artificially introduced noise and instrumental errors and have observed that the 'noise floor' for the adaptive protocol is lower. We have proposed and tested validation criteria, allowing an experimentalist to detect the presence of instrumental errors in measurements and to quantify the maximal achievable precision for the tomographic reconstruction of a quantum process. We outline further steps towards a general paradigm for the implementation of self-learning measurement apparatus which is able to avoid noisy measurements and to choose an optimal estimation strategy at the same time.

We also discuss the application of adaptive machine-learning algorithms to characterization of integrated-optical devices. We experimentally demonstrate fast techniques for calibration of actively tunable complex integrated interferometers fabricated by femtosecond laser writing. We further outliner the path towards implementing adaptive self-learning measurements in a fully integrated optical framework.

Quantum Information Resources in two-mode Gaussian Open Systems

Serban Suciu* and **Aurelian Isar***

*National Institute of Physics and Nuclear Engineering, P.O.Box MG-6, Bucharest-Magurele, Romania

Progress in the development of quantum information theory came from a resource theory approach to quantum entanglement. When restricted to local operations and classical communication (LOCC), entanglement can be regarded as a resource for quantum information processing tasks. An active field of research is the extension of this framework to general quantum correlations such as discord and coherence. Most work however is restricted to the discrete case, leaving out continuous variable systems necessary for quantum optics.

Recently, a framework for analyzing resource theories was developed, based on so called resource destroying maps. This class of maps leave resource-free states unchanged but erase the resource stored in all other states. They can be used to define a class of simple resource measures that can be calculated without optimization, and that are monotone non-increasing under operations that commute with the resource destroying map.

In this sense, we apply the theory of resource destroying maps to the dynamics of two-mode Gaussian open systems, described by the Gorini-Kossakowski-Lindblad-Sudarshan (GKLS) quantum master equation. Based on the theory of completely positive quantum dynamical semi-groups, GKLS gives a fully analytically solvable description of the irreversible time evolution of an open system.

Using measures that require no optimization, we compute the evolution of quantum discord and coherence for a system consisting of two non-interacting and non-resonant bosonic modes, embedded in a thermal environment. Depending on the choice of resource destroying map and the geometry of the resource-free set, different measures for quantum information resources can be defined.

Entangled Virtual State Spectroscopy Based on Intense Twin-Beams

Jiří Svozilík[1,2], Jan Peřina Jr.[2], Roberto de J. León-Montiel[3]
[1] *Quantum Optics Laboratory, Universidad de los Andes, A.A. 4976, Bogotá D.C., Colombia*
[2] *RCPTM, Joint Laboratory of Optics of Palacký University and Institute of Physics of AS CR, 17. listopadu 12, 771 46 Olomouc, Czech Republic and*
[3] *Instituto de Ciencias Nucleares, Universidad Nacional Autónoma de México, Apartado Postal 70-543, 04510 Cd. Mx., México*

Spectroscopic methods represent pivotal tools in the determination of an unknown chemical material. In addition, time-resolved methods, such as the pump-probe spectroscopy, allow to measure the excitation dynamics inside examined materials [1]. In recent years, a large attention has been devoted to optical methods based on the quantum (non-classical) features of light permitting to increase the detection resolution and also efficiently increase the interaction of samples with a probing light [2]. Among various approaches, the virtual state spectroscopy [3, 4] offers the possibility of resolving intermediate levels in the process of two-photon absorption.

Usual approach based on the solution of the Schrödinger equation describes an ideal case of only one photon pair interacting with the sample. This requires to maintain a low photon flux. Recent advances in both theoretical and experimental domains in the generation of intense entangled photon beams (twin beams) in the nonlinear process of spontaneous parametric down-conversion (SPDC) [5] enable to boost the atom-light interaction meanwhile quantum features of light persist. For that reason, we focus our study on effects occurring in the scenario when many (entangled) photons interact with the sample [6]. However, this implies the existence of contributions in the detected signal originating also from non-entangled correlations between participating photons. Additionally, we put our attention also to spectral properties of such intense beams with respect to the pump power and changes in detected spectra if photon fluxes are raised above a certain level.

For our theoretical study, we considered a simple atom with transitions between the ground state $|g\rangle$, three intermediate states $|k\rangle$, and the final state $|f\rangle$. The energy of the final state is chosen such that $E_f - E_g = hc/\lambda_{p0}$, where λ_{p0} nm is the central wavelength of the pump pulse with time duration τ_p and power P_p, that interacts with a nonlinear crystal of length L. Photon pairs are generated in the SPDC process in a nonlinear crystal with the central wavelengths $\lambda_{s0} = \lambda_{i0} = 2\lambda_{p0}$. Among generated photons a time-delay τ between them is introduced. Information about virtual transitions is then obtained by monitoring the two-photon absorption rate as a function of τ. The studied experimental arrangement is shown in Figure 1.

In Figure 2, changes of the detected absorption spectrum with an increasing photon flux (quantified via the signal-beam photon numbers N_s) are presented. As it can be seen, higher photon fluxes of the twin beams result in reduction of Schmidt's modes and this leads to the loss of the spectrum-resolving capabilities.

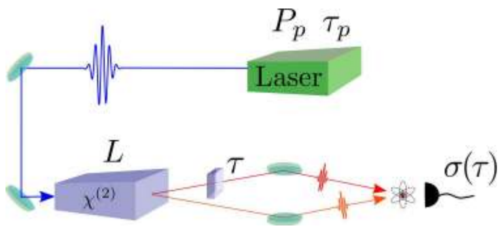

FIG. 1: Sketch of the experimental setup.

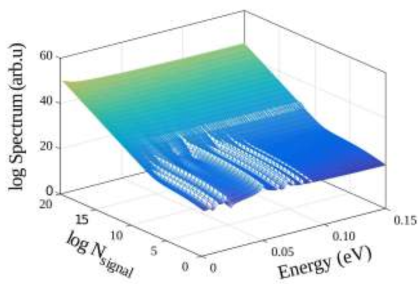

FIG. 2: Resolved energy spectrum as it depends on the pump power.

[1] C. Minhaeng,"Two-dimensional optical spectroscopy," CRC press, 2009.
[2] K. E. Dorfman, F. Schlawin, S. Mukamel, Rev. Mod. Phys., 88, 045008 (2016).
[3] B. E. A. Saleh, B. M. Jost, H.-B. Fei, M. C. Teich, Phys. Rev. Lett. 80, 3483 (1998).
[4] R. de J. Len-Montiel, J. Svozilik, L. J. Salazar-Serrano, and J. P. Torres, New J. Phys. 15, 053023 (2013).
[5] R. Machulka, O. Haderka, J. Peřina Jr., M. Lamperti, A. Allevi, M. Bondani, Opt. Exp. 22, 13374 (2014).
[6] J. Svozilík, J. Peřina Jr., and R. de J. León-Montiel, arXiv:1608.07326.

Quantum enhanced holometer

Siva Pradyumna[1,2], I. Ruo berchera[1], I. P. Degiovanni[1], E. Losero[1,2], P.Traina[1], M.Zucco[1], M.Genovese[1], Tobias Gehring[3], Christian S. Jacobsen[3], Ulrik L. Andersen[3]

1. INRIM Strada Della Cacce 91, Torino ,Italy
2. Politecnico di Torino, Torino, Italy
3. Danmark Tekniske Universitet(DTU), Kongens Lyngby, Denmark

The dream of building a theory unifying general relativity and quantum mechanics, the so called quantum gravity (QG), has pushed theoretical physics research for decades. However, for many years no testable prediction emerged from these studies. Several QG theories predict non-commutativity of position variables at Planck scale inducing a slight random wandering of transverse position (called “holographic noise”).

The first results of the Fermilab Holometer, a pair of ultra-sensitive coupled 40-m-long Michelson interferometers built to measure the possible presence of the "holographic noise", while obtaining sensitivity to cross-correlated signals far exceeding any previous measurement in a broad frequency band, exclude the existence of this exotic noise to a 4.6σ significance [1].

On the other hand, a sub-shot-noise phase measurement in a **single** interferometer (e.g. gravitational wave detector) exploiting squeezed light was suggested [2,3] and recently realized [4], ultimately leading to the groundbreaking detection of gravitational waves [5].

Here we discuss the advantages [6] of introducing the use of quantum light by injecting it into a pair of Power recycled Michelson interferometers on a table-top scale and measuring the cross correlations at the output of the interferometers. Prompted by these considerations we present the efforts to realize an analogous system with the aim of reaching, in a foreseeable future, a phase sensitivity almost comparable with the one obtained at Fermilab.

[1] Chou et al., arxiv: 1512.01216;

*[2] Caves, PRD **23**, 1693 (1981);*

*[3] Kimble et al., PRD **65**, 022002 (2001);*

*[4] Ligo, Nature Phys. **7**, 962 (2011);*

*[5] Abbott et al., Phys. Rev. Lett. **116**, 061102 (2016);*

*[6] Ruo-Berchera et al., Phys. Rev. A **92**, 053821 (2015).*

Quadratic fermionic dynamics with dissipation

A.E.Teretenkov*
*Dept. of Physics, Moscow State University; e-mail: taemsu@mail.ru

We consider the Lindblad equation with a generator which is quadratic in fermionic creation and annihilation operators. In the general n-modal case this equation can be represented in the form

$$\dot{\rho}(t) = -i\left[\frac{1}{2}c^T Hc, \rho(t)\right] + c^T \rho(t)\Gamma c - \frac{1}{2}c^T \Gamma^T c\rho(t) - \frac{1}{2}\rho(t)c^T \Gamma^T c, \qquad (1)$$

where $c = (c_1, ..., c_n, c_1^+, ..., c_n^+)^T$ is a vector entries of which are creation and annihilation operators acting in 2^n-dimensional linear space, Γ and H are complex-valued $2n \times 2n$-matrices meeting the conditions $\Gamma^T = \tilde{\Gamma}$, $\Gamma E \geq 0$, $H = \tilde{H}$. The involutive operation ~ over $2n \times 2n$-matrix is defined by the formula $\tilde{X} = E\overline{X}E$, where E is a block $2n \times 2n$-matrix with zero $n \times n$-matrices at the diagonal and identity $n \times n$-matrices at the anti-diagonal. Canonical anti-commutation relations (CAR) take the form

$$\{c, c^T\} = E$$

in such notation.

We set the Gaussian initial conditions in the exponential form

$$\rho(0) = e^{\frac{1}{2}c^T K(0)c + s(0)}, \qquad (2)$$

where $K(0) = -K(0)^T = -\tilde{K}(0)$ and $c(0) = \overline{c}(0)$ such that $Tr\rho(0) = 1$.

Thus, (1) and (2) set a Cauchy problem, the solution of which is the main result of this report. It could be formulated in the following form:

Theorem. *The solution of equation (1) with initial condition (2) has the form* $\rho(t) = e^{\frac{1}{2}c^T K(t)c + s(t)}$, *where matrix* $K(t) = -K^T(t)$ *is uniquely defined by the equation* $e^{K(t)E} = -I + 1/Z(t)$, *where* $Z(t)$ satisfies the linear differential equation

$$\frac{d}{dt}Z(t) = \left(iH - \frac{\Gamma + \Gamma^T}{2}\right)EZ(t) + Z(t)\left(-iH - \frac{\Gamma + \Gamma^T}{2}\right)E + \Gamma^T E \qquad (4)$$

and the evolution of the normalizing factor is defined by the formula (consisting with the normalization condition)

$$s(t) = s(0) - \frac{1}{2}\ln\det Z(0) + \frac{1}{2}\ln\det Z(t). \qquad (5)$$

Thus, the quadratic completely positive dynamics for Gaussian states of form (2) is calculated in terms of purely algebraic operations with matrices. The dimensions of these matrices are linear in n while initial equation (1) is for matrices with dimensions exponentially depending on n.

---

1. F. A. Berezin, The Method of Second Quantization (Academic Press, New York, 1966).
2. V. V. Dodonov and V. I. Man'ko, Invariants and the Evolution of Nonstationary Quantum Systems," in Proceedings of the Lebedev Physics Institute, Vol. 183 (Nova Science, Commack, N.Y., 1989).
3. A. S. Holevo, Quantum systems, channels, information (Walter de Gruyter GmbH, Berlin/Boston, 2013)
4. A. M. Chebotarev and A. E. Teretenkov, Math. Notes 92 (5-6), 837 (2012)
5. A. E. Teretenkov, Math. Notes 100 (4), 642 (2016)
6. A. E. Teretenkov, Quadratic Dissipative Evolution of Gaussian States with Drift, Math. Notes, 101:2 (2017), 341–351
7. A. E. Teretenkov, Quadratic Fermionic Dynamics with Dissipation, Math. Notes (to be published)

Gigahertz quantum signatures compatible with telecommunication technologies

Matthew Thornton,[1] Callum Croal,[1] Imran Khan,[2, 3] Christoph Marquardt,[2, 3] Gerd Leuchs,[2, 3] and Natalia Korolkova[1]

[1]*School of Physics and Astronomy, University of St. Andrews, North Haugh, St. Andrews, Fife, KY16 9SS, Scotland*
[2]*Max Planck Institute for the Science of Light, Günther-Scharowsky-Str. 1/Bldg. 24, Erlangen, Germany*
[3]*Institute of Optics, Information and Photonics, University of Erlangen-Nuremberg, Staudtstraße 7/B2, Erlangen, Germany*

Modern cryptography covers much more than encryption of messages in order to keep them secret. Many other cryptographic primitives exist, and it is important to consider how the security of these will be affected in a quantum future. Digital Signatures are a widely used cryptographic primitive, found eg. in e-mail, e-commerce and digital banking, and they form the basis for larger protocols. A signature σ_m appended to a classical message m ensures the authenticity and transferability of the message, whilst preventing forgery and repudiation. By employing quantum mechanics to distribute the σ_m between recipients, unconditionally secure signature schemes can be constructed [1–4].

As the development of quantum security progresses, one must consider how to implement these schemes using currently existing technology. To this end, we present a continuous-variable quantum signature scheme with an emphasis on compatibility with existing telecommunication technologies. Our scheme is information-theoretically secure against repudiation attacks and collective forging attacks, and can be implemented even when some QKD-based signature protocols fail. We note that this is the first implemented continous-variable quantum signature scheme which does not require secure quantum channels between participants, though discrete-variable protocols have been proposed and will soon be implemented [5].

In the simplest scenario, quantum digital signature (QDS) schemes involve three parties: Alice, who wishes to sign m, and two recipients, Bob and Charlie. In a Distribution stage, Alice forms sequences of quantum states, ρ_B^m and ρ_C^m, and sends them to Bob and Charlie, who measure the states and record their outcomes. The quantum states can be thought of as Alice's "public key". Her corresponding "private key", containing classical information about which states she sent, is used as the signature σ_m. Crucially, since a QDS scheme relies on quantum measurement, recipients gain only partial information about σ_m. Later, in an entirely classical Messaging stage Alice sends (m, σ_m). Bob and Charlie compare σ_m to their measurement results, and accept or reject m accordingly.

We have implemented our scheme by distributing an alphabet of phase-modulated coherent states over a 20 km optical fiber, and have devised the corresponding security proof. In particular, we prove that a dishonest forger who interacts with the quantum states cannot then declare some σ'_m which will be accepted by honest recipients, except with negligible probability (security against forging). The probability of successful forgery is related to the smooth min-entropy, which can be interpreted as the uncertainty that an eavesdropper has about an honest participant's measurement outcomes [6]. Hence, by estimating a lower bound for the smooth min-entropy we prove security of our protocol, taking into account the finite-size effects intrinsic to signatures. As tighter bounds are developed these can readily be incorporated. Furthermore, Bob's and Charlie's measurement outcomes are symmetrised with respect to Alice, which makes it unlikely that a dishonest Alice can find some σ''_m which Bob will accept but that she can later deny sending (security against repudiation).

Our system is built from telecom components running at a wavelength of 1553.33 nm and is completely fiber-integrated. The coherent states are distributed by Alice at a rate of 10 GHz and are measured using homodyne detection at Bob/Charlie. With our security proof the signature lengths are of the order of 10^6 to sign m with a 0.01% chance of failure, meaning a 1 bit message can be signed in 0.1 ms. This opens up the possibiliy of efficiently distributing quantum signatures on a large scale with minimal installation cost, and makes our scheme competitive in a landscape where both practicality and security are important.

[1] D. Gottesman and I. Chuang, "Quantum Digital Signatures," 0105032 [quant-ph] .
[2] R. J. Collins, R. J. Donaldson, V. Dunjko, P. Wallden, P. J. Clarke, E. Andersson, J. Jeffers, and G. S. Buller, Phys. Rev. Lett. **113**, 040502 (2014).
[3] V. Dunjko, P. Wallden, and E. Andersson, Phys. Rev. Lett. **112**, 040502 (2014).
[4] C. Croal, C. Peuntinger, B. Heim, I. Khan, C. Marquardt, G. Leuchs, P. Wallden, E. Andersson, and N. Korolkova, Phys. Rev. Lett. **117**, 100503 (2016).
[5] R. Amiri, P. Wallden, A. Kent, and E. Andersson, Phys. Rev. A **93**, 032325 (2016).
[6] R. König, R. Renner, and C. Schaffner, IEEE Trans. Inf. Theory **55**, 4337 (2009).

Multimode quantum model of electro-optic phase modulator: Applications in quantum information science

Trifanov A.I.,[1,*] Kiselev A.D.,[1] and Miroshnichenko G.P.[1]
[1] *ITMO University*
197101, Kronverksky avenue 49, Saint Petersburg, Russia

The linear electro-optic effect (EOE) is known to underline the mode of operation of light modulators widely used in modern optical communication systems. The penetration of quantum technologies and protocols into the telecommunication area makes these devices particularly attractive for use as tools for manipulation few-photon signals. A straightforward translation of the well-known classical EOE theory into the quantum domain of single photon states faces with a number of problems related to non-unitary evolution caused by the unbounded frequency spectrum of uniformly interacting modes [1].

An alternative approach to quantization of EOE model based on effective Hamiltonian of parametric interaction between radio-frequency (RF) modulation field and finite number of optical modes in $LiNbO_3$ crystal of length L is suggested in our paper [2]. The microwave mode is characterized by the wavenumber $k = \frac{2\pi}{L}$ and the frequency $\Omega_{MW} = kv_{MW}$, where v_{MW} is the phase velocity. For optical modes, the longitudinal wavenumber takes the quantized values $k_m = mk$, $m \in \mathbb{Z}$ and the frequency of the central (carrier) optical mode, which is typically excited by the laser pulse, is given by $\omega_{opt} = \Omega m_{opt}$, where $\Omega = kv_{opt}$, v_{opt} is the phase velocity and m_{opt} stands for the mode number.

The parametric interaction between the modes inside the crystal is governed by the Hamiltonian of the following form:

$$H = \Omega A_0 + \gamma \left(A_+ e^{-i\theta(t)} + A_- e^{i\theta(t)} \right),$$

where $\theta(t) = \Omega_{MW} t + \varphi$, γ is the intermode coupling constant, $A_- = A_+^\dagger$ and

$$A_0 = \sum_m m a_m^\dagger a_m, \quad A_+ = \sum_m f(m) a_{m+1}^\dagger a_m,$$

a_m is the annihilation operator of k-th mode and $f(m)$ is the normalized function describing mode number dependence of the intermode interaction strength. We assume that the mode number of interacting modes is defined by the inequality $m_{min} < m \leq m_{max}$ and the intermode interaction is modeled through the function

$$f(m) = 2\sqrt{(m - m_{min})(m_{max} - m)}/(2S + 1),$$

where $2S + 1 = m_{max} - m_{min}$ is the total number of interacting modes.

Then the Hamiltonian generators A_0, A_+, A_- obey the $SU(2)$ commutation relations and the spectral problem is exactly solvable. In particular, temporal evolution of the mode annihilation operators is given by

$$a_\mu(t) = e^{-i(\omega_{opt} + \mu\Omega_{MW})t} \sum_{\nu=-S}^{S} (-1)^\nu e^{-i(\mu+\nu)\alpha} d_{\mu\nu}^S(\beta) e^{i(\mu-\nu)\varphi} a_\nu,$$

where $d_{\mu\nu}^S(\beta)$ is the Wigner d-function and the angles α and β depend on the parameters of the modulator. Note that in the large S limit, where $S \to \infty$ and asymptotic behavior of the Wigner d-functions is given by the Mehler-Heine formula, the well-known classical phase factor describing the effect of light modulation can be recovered.

Now we briefly describe some of the problems in quantum information science where using our exactly solvable model turned out to be useful. First, we have generalized our model to analyze the quantum dynamics of polarization states inside the crystal taking into account the interaction between differently polarized modes.

Second, following [3], we have estimated the quantum bound for the bipartite case and suggested the tripartite Bell inequality that simulate experiment with GHZ-like states. In this case, the quantum theory predicts dramatic violation of the classical bound 2 up to the algebraic value of 4.

Finally, in analogy with linear optical quantum computations that use the polarization and dual-rail coding, we have considered the phase modulator as a multiport quantum scheme realizing quantum logical operations for frequency-bin coding qubits. In particular, we have proposed the algorithm of realizing NS-gate [4] in the frequency domain:

$$a\,|0\rangle + b\,|1\rangle + c\,|2\rangle \to a\,|0\rangle + b\,|1\rangle - c\,|2\rangle$$

which is required for universal CNOT-gate.

* Electronic address: alextrifanov@gmail.com

[1] J. Capmany, C. R. Fernandez-Pousa, Laser Photonics Rev. **5**, No.6, 750-772 (2011)
[2] G. P. Miroshnichenko et. al, arXiv:1605.05770v1
[3] L. Olislager et al, New Journal of Physics, **14** 043015 (2012)
[4] R. Okamoto et al, arXiv:1006.4743v1

Continuous-Wave Single-Photon Transistor with Rydberg Atoms

Iason Tsiamis, Oleksandr Kyriienko, and Anders Søndberg Sørensen

The Niels Bohr Institute, University of Copenhagen, Blegdamsvej 17, DK-2100 Copenhagen, Denmark

The rapid evolution of the quantum technologies during the past years triggered the development of efficient tools — quantum gates — to control and route quantum signals. These devices commonly rely on the optical and microwave signals, serving similar role to control voltages in conventional electronics, and are largely inspired by the preceding classical electrical circuits. One of the devices from this family is an optical quantum transistor, being the analog of a classical field effect transistor. Similar to its electronic counterpart, it is a device where a weak optical control field is used to switch on and off the propagation of an optical probe field via a nonlinear optical interaction. The fundamental limiting case of an optical quantum transistor is a single-photon transistor, where the presence or absence of a single photon in the gate field controls the propagation of the probe field.

In this work we study a single-photon transistor model, which consists of an ensemble of Rydberg atoms located inside a single-sided optical cavity, which is driven by two classical fields. A *probe* field incident on the ensemble can be reflected or lost, conditioned by the absence or presence of a *control* field that is mapped to a collective Rydberg excitation, which leads to the Rydberg blockade. The main advantage of the current proposal, compared to previous models, is that the driving fields are continuously turned on throughout the entire protocol, leading to the continuous wave version of the single-photon transistor.

The protocol consists of three steps. Initially, all atoms of the ensemble are in the ground state and the resonant multiphoton coherent probe field Ω_1 that couples to the $|g\rangle \leftrightarrow |e\rangle$ transition is fully reflected under EIT conditions, due to the resonant driving field Ω_2 which couples to the $|e\rangle \leftrightarrow |r\rangle$ transition. We then send the *control* single photon field to the atomic ensemble, which transfers the atoms from the ground state $|g\rangle$ to the collective Rydberg state $|r'\rangle$ through an impedance matching mechanism.

Subsequently, the presence of the excitation $|r'\rangle$ leads to an energy shift for the $|r\rangle$ state, due to the interaction between Rydberg collective states $|r\rangle$ and $|r'\rangle$. Therefore, the probing coherent field Ω_1 incident on the cavity is no longer reflected with unity probability, since the EIT condition is broken by the energy mismatch. We find the optimal conditions for zero reflectance, meaning that the incoming probe field will be mapped to the excited state $|e\rangle$ and decay to the environment with rate γ_e with unity probability.

Finally, the last part of the protocol describes the enhancement of the lifetime for the $|r'\rangle$ excitation as a result of a localization process due to Rydberg induced dephasing. The first photon of the incoming multiphoton probe field arrives into the excited state $|e\rangle$ and decays as described in the previous step. The l-th atom that decays from $|e\rangle$ to $|g\rangle$, induces an effective dephasing to the $|r'\rangle$ collective state. This localizes the collective excitation, initially shared over all N_A atoms of the ensemble, into superposition of the N atoms located inside the sphere with center at the l-th atom and radius the Rydberg blockade radius R_b. Then the lifetime of the excitation $|r'\rangle$ is enhanced by a factor $\frac{N_A}{N}$, as the decay rate of the $|r'\rangle$ is proportional to the number of atoms participating in the excitation. Subsequently, the next photon of the probe field leads to the decay of the $l'-$th atom, which localizes the collective excitation $|r'\rangle$ on the superposition of the N' atoms located inside the intersection of the two spheres with same radius R_b, and centers at the l-th and the l'-th atom, leading to an extra enhancement of the lifetime. This continuous localization process results in long lifetime of the collective excitation $|r'\rangle$ and large gain of the transistor.

The continuous wave version of the transistor largely simplifies its operating protocol and possible experimental realization. Noteworthy, the proposed device could be alternatively used as an optical single-photon detector. In this case the protocol allows for the detection of a presence or absence of the single photon control field by measuring the reflected probe field. The large gain is enabled by the long lifetime of the Rydberg excitation, potentially leading to the detection with high signal-to-noise ratio.

Figure 1: a) Schematic representation of the atomic ensemble inside a single-sided cavity. b) Energy level diagram of the atoms.

An efficient quantum spin-photon interface in diamond for a quantum network

S.B. van Dam[1], S. Bogdanovic[1], C. Bonato[1], W.J. Westerveld[1], M.T. Ruf[1], M.J. Degen[1], S.L.N. Hermans[1], L.C. Coenen[1], A.M.J. Zwerver[1], B. Hensen[1], M. S. Z. Liddy[2], M. Eschen[3], T. Fink[4], A. Reiserer[1], M. Lonçar[5] and R. Hanson[1]

[1]QuTech, Delft University of Technology, PO Box 5046, 2600 GA Delft, The Netherlands

[2]Insitute for Quantum Computing, University of Waterloo, Waterloo, ON, N2L3G1, Canada

[3]Netherlands Organisation for Applied Scientific Research (TNO), PO Box 155, 2600 AD Delft, The Netherlands

[4]Institute of Quantum Electronics, ETH, CH-8093 Zürich, Switzerland

[5]John A. Paulson School of Engineering and Applied Sciences, Harvard University, Cambridge, Massachusetts 02138, USA

In a future quantum network distant parties will be connected via long-distance entanglement. Nitrogen-vacancy (NV) centers in diamond have developed into a building block for such a network. The current success probability of heralded entanglement generation over 1.3 km is approximately 10^{-8} [1], limited by the probability that the NV center emits a photon in the zero-phonon line, as well as by the photon collection efficiency from the diamond. We can address both by embedding the NV in a Fabry-Perot cavity at cryogenic temperatures, benefitting from Purcell enhancement and an improved collection efficiency. Here we present the design and low-temperature characterization of a tunable fiber-based microcavity containing a thin diamond membrane [2]. We observe cavity finesse between 4,000 and 15,000 and find sub-nanometer cavity length stability. Coupling nitrogen-vacancies to these cavities could lead to a three orders of magnitude increase in the remote NV-NV entanglement success rate. We show our most recent results aimed at observing and exploiting such efficient NV-cavity coupling. With such an efficient spin-photon interface a quantum network can be extended over multiple nodes and longer distance.

[1] Nature 526, 682 (2015)
[2] arXiv:1612.02164 (2016)

Two-dimensional quantum repeater architectures based on atomic ensembles

V. Kuzmin[1], D.V. Vasilyev[1], C. Muschik[1,2], N. Sangouard[3], W. Dür[2] and P. Zoller[1,2]
[1] *Institute for Quantum Optics and Quantum Information of the Austrian Academy of Sciences, 6020 Innsbruck, Austria*
[2] *Institut für Theoretische Physik, Universität Innsbruck, Technikerstr. 21a, A-6020 Innsbruck, Austria*
[3] *Department of Physics, University of Basel, Klingelbergstrasse 82, 4056 Basel, Switzerland*

Quantum networks is a fast-growing research area driven by such applications as secure communication and distributed quantum computing. Recently, it was proposed [PRA 94, 052307] to use two-dimensional quantum repeater schemes for creation of high fidelity entangled states to be applied in multi-user networks for performing quantum protocols. Possible applications include distributed quantum computation, secret voting and secret sharing, clock synchronisation, remote sensing. The scheme uses fractal-like multi-partite entangled structures at growing scale which take advantage of entanglement swapping and multi-party entanglement purification for creation of high fidelity entangled states.

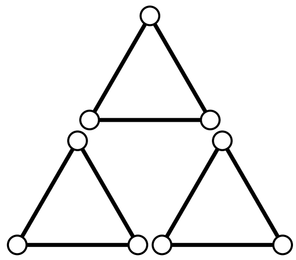

FIG. 1. 2D repeater

In this work, we study 2D repeater architectures based on thermal atomic ensembles — a simple and scalable resource, currently available experimentally. The networks (building blocks are shown in Fig. 1) allow for direct generation of three-partite Greenberger-Horne-Zeilinger (GHZ) states. We estimate performance of the networks at a metropolitan and national scales taking into account realistic imperfections such as optical fibre losses, inefficiency and dark counts of the detectors, finite coherence time of the quantum memory. Analytical description together with quantum Monte Carlo simulation of the network are used to evaluate fidelities and generation rates of the entangled states. It is shown that the 2D repeater scheme based on atomic ensembles including imperfections of network elements outperforms analogous schemes (combined of 1D repeater lines) generating corresponding GHZ states. Build-in entanglement purification steps of the 2D scheme lead to higher error resilience. The native 2D protocol shows better fidelity scaling with growth of the memory coherence time which allows to build large scale networks.

Atmospheric quantum-light channels

D. Vasylyev, A. A. Semenov, and W. Vogel
Institut für Physik, Universität Rostock, Albert-Einstein-str. 23, D-18059 Rostock, Germany

Many fundamental and applied experiments in quantum optics require transferring nonclassical states of light through large distances. In this context the free-space channels are a very promising alternative to optical fibers as they are mobile and enable establishing communications with moving objects, using satellites for global quantum links. For such channels the atmospheric turbulence is the main disturbing factor.

During the propagation through the atmosphere, optical beams undergo random broadening and deformation as well as stochastic deflections as a whole, due to perturbations by refractive index fluctuations. This results into fluctuating losses on the receiver site, since only a part of the beam is transferred through the receiver aperture. Recently we have proposed two models for the probability distribution of transmittance for the atmospheric quantum channels. One model describes nonclassical light under conditions when the atmospheric turbulence results in beam wandering only [1]. Another model, cf. Ref. [2], considers also random fluctuations of the beam shape. We discuss the applicability of both models for conditions of weak and strong turbulence, for different propagation distances, and for different designs of optical experiments. We discuss the nonclassical properties of the transmitted light in the case of discrete-variable, cf. Ref. [3], and continuous-variable, cf. Ref. [2], protocols. The obtained results are compared with the corresponding experiments, cf. Refs. [4, 5, 6].

References

[1] D. Yu. Vasylyev, A. A. Semenov, and W. Vogel, Phys. Rev. Lett. **108**, 220501 (2012).

[2] D. Vasylyev, A. A. Semenov, and W. Vogel, Phys. Rev. Lett. **117**, 090501 (2016).

[3] M. O. Gumberidze, A. A. Semenov, D. Vasylyev, and W. Vogel, Phys. Rev. A **94**, 053801 (2016).

[4] A. Fedrizzi, R. Ursin, T. Herbst, M. Nespoli, R. Prevedel, T. Scheidl, F. Tiefenbacher, T. Jennewein, and A. Zeilinger, Nature Phys. **5**, 389 (2009).

[5] C. Peuntinger, B. Heim, Ch. Müller, Ch. Gabriel, Ch. Marquardt, and G. Leuchs, Phys. Rev. Lett. **113**, 060502 (2014).

[6] C. Croal, C. Peuntinger, B. Heim, I. Khan, Ch. Marquardt, G. Leuchs, P. Wallden, E. Anderson, and N. Korolkova, Phys. Rev. Lett. **117**, 100503 (2016).

Wide-field imaging of magnetic fields using nitrogen-vacancy centers in diamond

Adam M. Wojciechowski[1], Louise F. Frellsen[1], Mürsel Karadas[2], Sepehr Ahmadi[1], Haitham El-Ella[1], Axel Thielscher[2,3], Fedor Jelezko[4], Jan Meijer[5], Alexander Huck[1] and Ulrik L. Andersen[1]

[1]Department of Physics, Technical University of Denmark, 2800 Kgs. Lyngby, Denmark
[2]Department of Electrical Engineering, Technical University of Denmark, 2800 Kgs. Lyngby, Denmark
[3]Danish Research Center for Magnetic Resonance, Copenhagen University Hospital Hvidovre, 2650 Hvidovre, Denmark
[4]Institute for Quantum Optics, Ulm University, Albert-Einstein-Allee 11, 89081 Ulm, Germany
[5]Felix Bloch Institute of Solid State Physics, Leipzig University, Linnéstraße 5, 04103 Leipzig, Germany

We present our work on wide-field imaging of magnetic field using negatively charged nitrogen-vacancy (NV) centers in diamond, aiming towards studies of biological systems with high spatial and temporal resolution.

At the heart of our microscope is a carefully engineered ultra-pure diamond substrate, with a top micrometer-thin layer grown with >99.99% of ^{12}C isotope and rich in ^{15}NV centers (~1-10 ppm). Fluorescence light from the NV layer is collected with a high numerical aperture objective and imaged on a camera. In our setup, we use a high-speed, large-well-capacity sensor capable of in-pixel lock-in demodulation. This allows us to record small relative changes of the NVs fluorescence level, $\Delta F/F \sim 10^{-4}$, in the optically detected magnetic resonance spectra. Together with the narrow (~600 kHz) resonance linewidths observable in our diamond sample, this results in a sub-microtesla magnetic field sensitivity per single pixel and frame (exposure), while maintaining a video framerate of over 50 fps and image resolution of 300x300 pixels.

We are aiming at magnetic imaging of micro particles such as beads commonly used for biological tagging, with a focus on both static images and particle-flow videos. Additionally, we have carried out electromagnetic modelling of complex neurological systems. The simulation results indicate magnetic signals on micrometer length-scales, from single neurons to a brain tissue. In case of evoked activity in the brain tissue, the numerical results show the generation of magnetic fields with a magnitude of a few nanotesla, with most of the time-information contained within the DC-50 Hz bandwidth. Such signals are expected to be measurable using our current experimental setup.

Theoretical study of photon subtraction improved by filtering

Jun-ichi Yoshikawa*[1,2], Warit Asavanant[1], and Akira Furusawa[1]

[1] *Department of Applied Physics, School of Engineering, The University of Tokyo, 7-3-1 Hongo, Bunkyo-ku, Tokyo 113-8656, Japan*
[2] *Quantum-Phase Electronics Center, School of Engineering, The University of Tokyo, 7-3-1 Hongo, Bunkyo-ku, Tokyo 113-8656, Japan*

Pure non-Gaussian quantum states are indispensable resources in continuous-variable quantum information processing. Among them, Schrödinger cat states, defined as superposition of coherent states $|\alpha\rangle + e^{i\theta}|-\alpha\rangle$, are of great importance, partly because of their application to quantum computation as generalized qubits [1]. Although it is currently difficult to create arbitrary cat states, it was shown that photon-subtracted squeezed vacuum states in quantum optics well approximate plus or minus cat states $|\alpha\rangle \pm |-\alpha\rangle$ when the amplitude $|\alpha|$ is small [2, 3]. Generation of cat states have been experimentally demonstrated with this scheme, both in pulsed [4] and continuous-wave (CW) [5, 6] regimes. We are especially interested in the CW regime because highly pure cat states have been reported with CW setups.

Photon subtraction is a conditional, nonunitary operation, achieved by tapping a small portion of the initial state with an asymmetric beamsplitter and measuring it with a photon detector. When a photon is detected, the photon subtraction is succeeded, and the heralded photon-subtracted state exists in some wavepacket, localized in the time domain around the heralding signal.

However, here we pay attention to the fact that the initial squeezed vacuum state in such a wavepacket is generally in a mixed state, owing to the nonflat spectrum of squeezing produced by an optical parametric oscillator (OPO). The squeezing and antisqueezing spectra from an OPO are, in the ideal case of no optical losses [7],

$$V^{(\pm)}(\omega) = \frac{(\gamma/2 \pm \epsilon)^2 + \omega^2}{(\gamma/2 \mp \epsilon)^2 + \omega^2}, \tag{1}$$

where $V^{(-)}(\omega)$ is the squeezing spectrum and $V^{(+)}(\omega)$ is the antisqueezing spectrum, ω denoting relative angular frequency, and $\epsilon \geq 0$ and $\gamma > 0$ denoting the pump strength and the cavity decay rate, respectively [7]. Although squeezed states in narrow sidebands are pure, satisfying the minimum uncertainty $V^{(-)}(\omega)V^{(+)}(\omega) = 1$ for all ω, those in wavepackets $\phi(t) = \int \tilde{\phi}(\omega)e^{-i\omega t}d\omega$ are generally impure, $[\int |\tilde{\phi}(\omega)|^2 V^{(-)}(\omega)d\omega][\int |\tilde{\phi}(\omega)|^2 V^{(+)}(\omega)d\omega] \geq 1$. This impurity of initial squeezed states would remain as impurity of the heralded cat states.

We have theoretically found that the above mechanism indeed causes some inefficiency of heralded cat states in the ordinary CW methods. Furthermore, we have also found that this inherent inefficiency can be arbitrarily suppressed by inserting a filter to limit the bandwidth before the photon detection. Note that previous demonstrations of photon subtraction in the CW regime are already using filter cavities, but their bandwidths are wider than those of OPOs, in order to utilize the raw correlations of photons produced by the OPO cavities as the wavepackets of heralded cat states. However, our calculations show that it is more advantageous to engineer the wavepackets of heralded cat states by filtering the subtraction path.

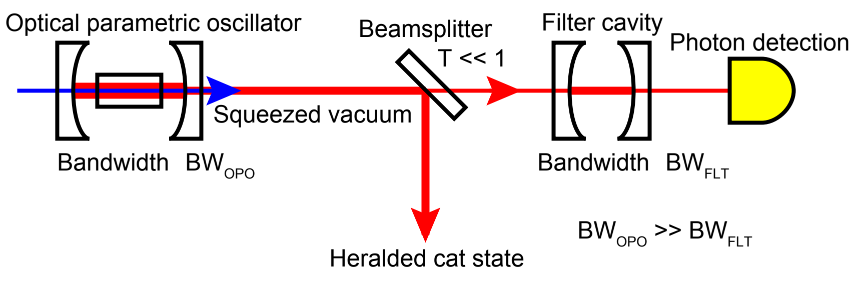

Figure 1: Photon subtraction with a filter cavity inserted before the photon detection.

References

[1] T. C. Ralph, A. Gilchris, G. J. Milburn, W. J. Munro, and S. Glancy, Phys. Rev. A **68**, 042319 (2003).
[2] M. Dakna, T. Anhut, T. Opatmý, L. Knöll, and D.-G. Welsch, Phys. Rev. A **55**, 3184 (1997).
[3] A. P. Lund, H. Jeong, T. C. Ralph, and M. S. Kim, Phys. Rev. A **70**, 020101(R) (2004).
[4] A. Ourjoumtsev, R. Tualle-Brouri, J. Laurat, P. Grangier, Science **312**, 83 (2006).
[5] J. S. Neergaard-Nielsen, B. Melholt Nielsen, C. Hettich, K. Molmer, and E. S. Polzik, Phys. Rev. Lett. **97**, 083604 (2006).
[6] K. Wakui, H. Takahashi, A. Furusawa, and M. Sasaki, Opt. Express **15**, 3568 (2007).
[7] M. J. Collett and C. W. Gardiner, Phys. Rev. A **30**, 1386 (1984).

*yoshikawa@ap.t.u-tokyo.ac.jp

Progress report on on-demand scalable room-temperature heralded photon source with long memory time

Michael Zugenmaier,[1,*] Karsten Dideriksen,[1] Boris Albrecht,[1]
Johannes Borregaard,[2] Anders S. Sørensen,[1] and Eugene S. Polzik[1]

[1] *The Niels Bohr Institute, University of Copenhagen, Blegdamsvej 17, Copenhagen DK-2100, Denmark*

[2] *Department of Physics, Harvard University, Cambridge, Massachusetts 02138, USA*

Building large scale quantum photonic networks will enable distributed quantum computing and secure communications over long distances using quantum key distribution, but still remains challenging. Even though photons are regarded as the ideal carriers of information small losses in optical fibers make direct long range quantum communication impractical. In order to circumvent these losses quantum repeater protocols like the DLCZ protocol employing atomic ensembles have been established [2] and experimentally implemented using ensembles of cold atoms. However cold atoms require an extended cooling apparatus, which makes the scalability of such a system challenging. On the other hand room temperature vapor cells have been shown to work as efficient quantum interfaces, combining easy scalability, fast re-initialization as well as technological simplicity. Typically the coherence times of these systems are limited due to the atomic motion. As opposed to previous ensemble-based experiments, which typically rely on performing operations sufficiently fast that the atoms remain inside the laser beam [3], we employ motional averaging where atoms move in and out of the beam several times during the interaction while maintaining the phase information for much longer than the interaction time [1].

In our experiment we use cesium atoms at room temperature trapped in microcells with spin-protecting coating in combination with a cavity around the microcell to enhance the light-matter interaction. By suitable spectral filtering we erase the "which atom" information and obtain an efficient and homogenous coupling between all atoms and the light. Photon-heralded single excitations can be created and stored as collective spinwaves on a timescale given by the spin coherence time of a few ms. The excitation can then be read out producing coherent single photons in a scalable fashion. We have experimentally confirmed the necessity of narrow spectral filtering for high efficiencies of the heralding step and characterized our setup varying write and read powers and delays. Numerical simulations show that the readout process can be very efficient (approx. 95 %) [1]. Currently the main contribution prohibiting the read out of single photons is four wave mixing noise. Here the read pulse produces more atomic excitations which then lead to an enhanced photon number in the read out. With experimental modifications we are confident to reduce the four wave mixing noise significantly and reach high single photon fidelities in the near future.

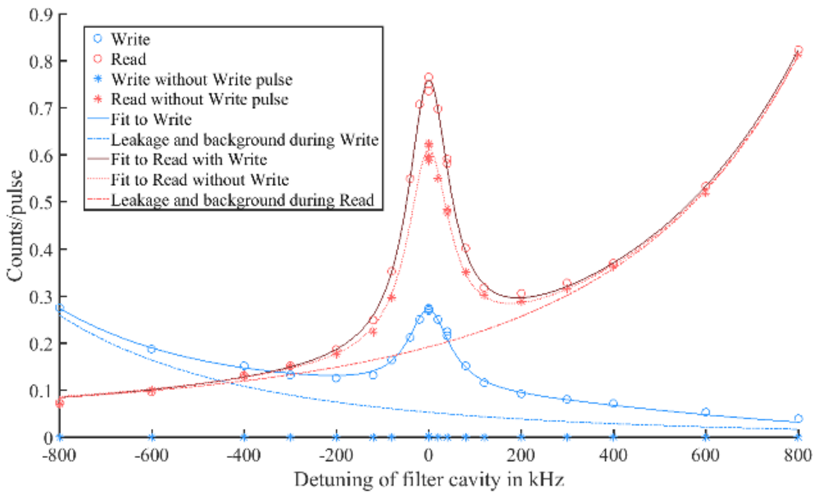

FIG. 1. Counts at the detector during write (blue) and read (red) process when detuning the spectral filtering. Photons scattered by the atoms peak clearly above the dashed leakage tails. The main contribution in the read process comes from four wave mixing (dotted line)

[1] J. Borregaard *et al.*, Nature communications **7**, 11356 (2016).
[2] L.-M. Duan *et al.*, Nature **414**, 413-418 (2001).
[3] P. S. Michelberger *et al.*, New Journal of Physics, **17**, (2015)

* zugenmaier@nbi.ku.dk; http://quantop.nbi.ku.dk/

Approach to description of light-matter interaction in dispersive dissipative structures

Alexander A. Zyablovsky[1,2], Evgeny S. Andrianov[1,2], Igor A. Nechepurenko[1,2], Alexander A. Dorofeenko[1,2,3], Alexander A. Pukhov[1,2,3], Alexey P. Vinogradov[1,2,3]

[1]*Dukhov Research Institute of Automatics (VNIIA), 22 Sushchevskaya, Moscow, 127055, Russia*
[2]*Moscow Institute of Physics and Technology, 9 Institutskiy per., Moscow, 141700, Russia*
[3]*Institute for Theoretical and Applied Electromagnetics, 13 Izhorskaya, Moscow, 125412, Russia*

The study of the interaction between light and matter is a key problem in physics [1]. Progress in nanotechnologies [2] has made it possible to control light-matter interaction at the nanoscale by means of engineering of the local density of states [3]. For example, a high local density of states in photonic and plasmonic structures results in increase the rate of spontaneous and stimulated emission [3, 4]. The local density of states is inverse proportional to group velocity of the electromagnetic waves [5]. As a result the rate of spontaneous and stimulated emission is higher at a low group velocity. The ratio group velocity to speed of light in nanostructures may be less than 10^{-4} [6]. So the propagation time along these system may be many more than the mode or atom relaxations times [7]. Thus for description light-matter interaction in the such structures it is necessary take into account both the spontaneous emission and the finiteness of propagation speed.

Consistent consideration of the dynamics of electromagnetic fields and atoms is based on quantum electrodynamics. The quantum properties of light arise in theory after the procedure of field quantization, which implies that the electromagnetic field is expanded in a series of system eigenmodes [3, 8]. With excitation of the mode, the electromagnetic field appears in the entire mode volume. Thus, if it is essential to consider the temporal evolution of the electromagnetic field then it is necessary to take into account the infinite number of modes with an appropriate phase relation [3, 8].

In a full quantum mechanical consideration, the increase of both the number of modes and the number of atoms leads to the exponential increase of the number of degrees of freedom [9]. As a result, a first-principles consideration of the multimode lasers with a large number of atoms is impossible. In this work we develop approach to description of light-matter interaction in multimode lasers, taking into account the process of spontaneous emission, dissipation and the finiteness of the propagation speed of electromagnetic fields in the plasmonic structures. For this purpose we had been obtained based on the master equation for density matrix [9] the equations on the expectation values of the operators of the number of photons and the population inversion as well as the operators that describe the interaction between the photons and the atoms and the operators that describe the interference between the electromagnetic waves of the different modes. We show that in our approach electromagnetic pulses propagates with the group velocity and the electromagnetic pulse that is spontaneously emitted by an atom takes the form of a delta function at initial time. The number of equations in the developed approach is a quadratic function of the number of the modes and linear function of the number of the atoms. It makes possible the study of the multimode structures with a large number of the atoms.

[1] S. Haroche, Review of Modern Physics, 85, 1083 (2013).
[2] S. A. Maier, Plasmonics: Fundamentals and Applications (Springer, New York, 2007).
[3] M. S. Tame et al., Nature Physics, 9, 329 (2013).
[4] W. Zhou et al., Nature Nanotech., 8, 506 (2013).
[5] V. S. C. Manga Rao and S. Hughes, Phys. Rev. Lett., 99, 193901 (2007).
[6] T. Pickering et al., Nature Commun., 5, 4972 (2014).
[7] M. T. Hill, and M. C. Gather, Nature Photon., 8, 908 (2014).
[8] V. B. Berestetskii, E. M. Lifshitz, and L. P. Pitaevskii, Quantum electodynamics, Course of Theoretical Physics, Vol. 4 (Pergamon press, Oxford, 1980).
[9] H. Carmichael, An open systems approach to quantum optics (Springer-Verlag, Berlin, 1991).

List of Authors